DRAWER 29
FILE 2

SANDIA REPORT

SAND90—2491 • UC—814
Unlimited Release
Printed January 1992

Yucca Mountain Site Characterization Project

Summary and Evaluation of Existing Geological and Geophysical Data Near Prospective Surface Facilities in Midway Valley, Yucca Mountain Project, Nye County, Nevada

J. D. Gibson, F. H. Swan, J. R. Wesling, T. F. Bullard,
R. C. Perman, M. M. Angell, L. A. DiSilvestro

Prepared by
Sandia National Laboratories
Albuquerque, New Mexico 87185 and Livermore, California 94550
for the United States Department of Energy
under Contract DE-AC04-76DP00789

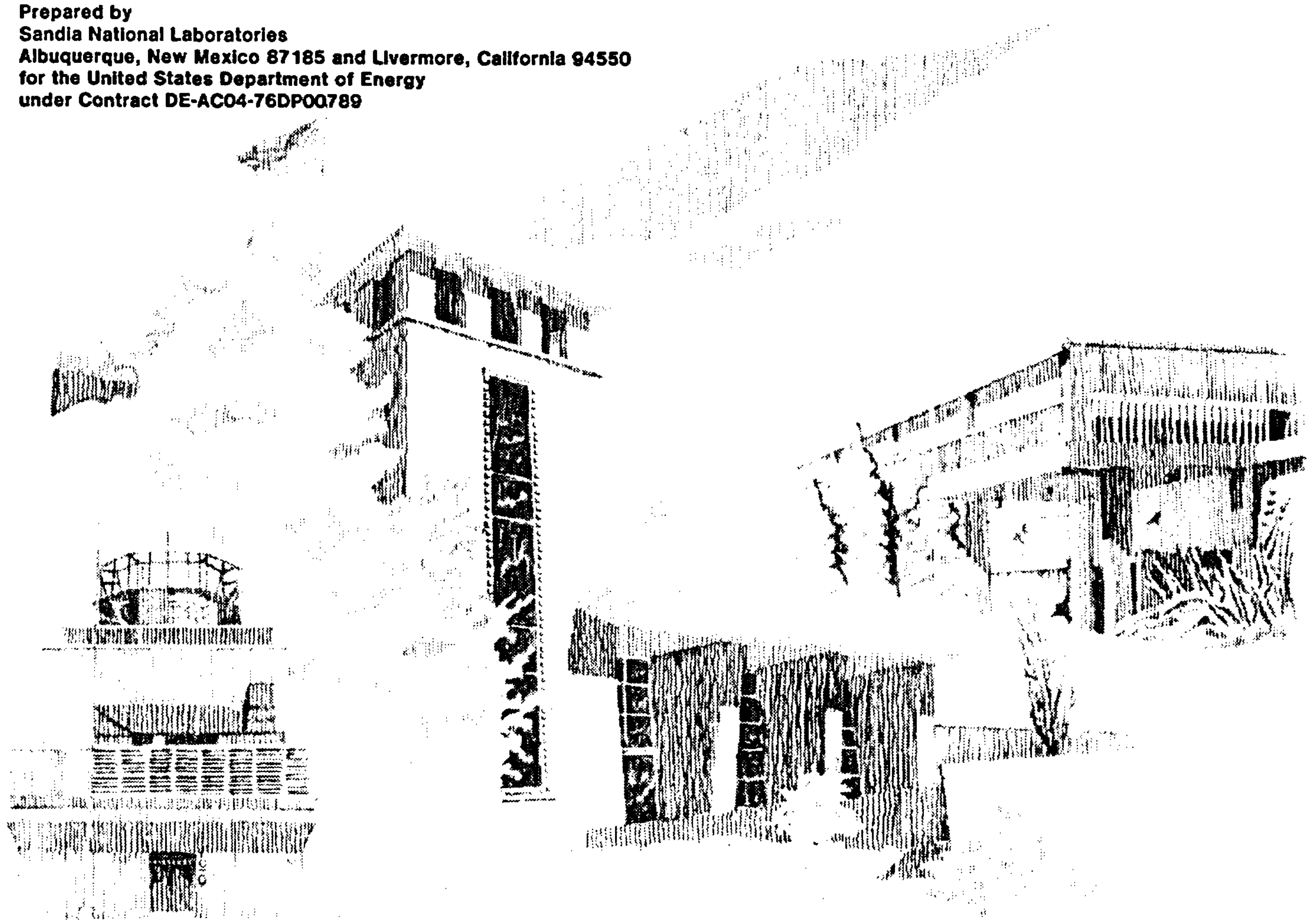

SF2900Q(8-81)

"Prepared by Yucca Mountain Site Characterization Project (YMSCP) participants as part of the Civilian Radioactive Waste Management Program (CRWM). The YMSCP is managed by the Yucca Mountain Project Office of the U.S. Department of Energy, DOE Field Office, Nevada (DOE/NV). YMSCP work is sponsored by the Office of Geologic Repositories (OGR) of the DOE Office of Civilian Radioactive Waste Management (OCRWM)."

Issued by Sandia National Laboratories, operated for the United States Department of Energy by Sandia Corporation.

Available to DOE and DOE contractors from
Office of Scientific and Technical Information
PO Box 62
Oak Ridge, TN 37831

Prices available from (615) 576-8401, FTS 626-8401

Available to the public from
National Technical Information Service
US Department of Commerce
5285 Port Royal Rd
Springfield, VA 22161

NTIS price codes
Printed copy: A09
Microfiche copy: A01

SAND90-2491
Unlimited Release
Printed January 1992

Distribution
Category UC-814

SUMMARY AND EVALUATION OF EXISTING GEOLOGICAL AND GEOPHYSICAL DATA NEAR PROSPECTIVE SURFACE FACILITIES IN MIDWAY VALLEY, YUCCA MOUNTAIN PROJECT, NYE COUNTY, NEVADA

by

J.D. Gibson
Sandia National Laboratories
Albuquerque, NM 87185

F.H. Swan, J.R. Wesling, T.F. Bullard,
R.C. Perman, M.M. Angell, and L.A. DiSilvestro
Geomatrix Consultants, Inc.
100 Pine Street, Suite 1000
San Francisco, CA 94111

ABSTRACT

Midway Valley, located at the eastern base of Yucca Mountain in southwestern Nevada, is the preferred location of the surface facilities for the potential high-level nuclear waste repository at Yucca Mountain. One goal in siting these surface facilities is to avoid faults that could produce relative displacements in excess of 5 cm in the foundations of the waste-handling buildings. This study reviews existing geologic and geophysical data that can be used to assess the potential for surface fault rupture within Midway Valley.

Dominant tectonic features in Midway Valley are north-trending, westward-dipping normal faults along the margins of the valley: the Bow Ridge fault to the west and the Paintbrush Canyon fault to the east. Both faults displace Quaternary sediments. Published estimates of average Quaternary slip rates for these faults are very low ($\approx 10^{-3}$ mm/yr), but the age of most recent displacement and the amount of displacement per event are largely unknown. Surface mapping and interpretive cross sections, based on limited drillhole and geophysical data, suggest that additional normal faults, including the postulated Midway Valley fault, may exist beneath the Quaternary/Tertiary fill within the valley. Existing data, however, are inadequate to determine the location, recency, and geometry of this faulting.

To confidently assess the potential for significant Quaternary faulting in Midway Valley, additional data are needed that define the stratigraphy and structure of the strata beneath the valley, characterize the Quaternary soils and surfaces, and establish the age of faulting. The use of new and improved geophysical techniques, combined with a drilling program, offers the greatest potential for resolving subsurface structure in the valley. Mapping of surficial geologic units and logging of soil pits and trenches within these units must be completed, using accepted state-of-the-art practices supported by multiple quantitative numerical and relative age-dating techniques.

This report was prepared under WBS number 1.2.3.2.8.4.2.

TABLE OF CONTENTS

	Page
TABLE OF CONTENTS	i
LIST OF FIGURES	iii
LIST OF PLATES	iv
LIST OF TABLES	v
1.0 INTRODUCTION	1
1.1 Purpose	1
1.2 Scope of Work	1
1.3 Siting Criteria	3
1.4 Location and Regional Geologic Setting	3
1.5 Acknowledgements	5
2.0 OVERVIEW OF PREVIOUS GEOLOGIC INVESTIGATIONS	7
2.1 Geologic Mapping	7
2.2 Borehole Information	10
2.3 Geophysical Surveys	11
2.4 Photolineaments	11
3.0 QUATERNARY GEOLOGY AND AGE-DATING	14
3.1 Quaternary Studies Outside the Yucca Mountain Region	15
3.2 Studies of Hoover et al. (1981) and Hoover (1989)	17
3.3 Soil-Geomorphology Studies in Crater Flat (Peterson, 1988)	23
3.4 Soils-Geomorphic Relationships Along Yucca and Fortymile Washes (Taylor, 1986)	27
3.5 Dating Methods Used in the Yucca Mountain Region	34

TABLE OF CONTENTS (cont'd)

		Page
4.0	FAULTING IN THE MIDWAY VALLEY AREA	37
4.1	Tectonic Setting	37
4.2	Geologic Structure of the Midway Valley Area	44
4.3	Displacement History and Slip Rates on the Paintbrush Canyon and Bow Ridge Faults	70
5.0	SUMMARY AND RECOMMENDATIONS	73
5.1	Location and Geometry of Faults	74
5.2	Quaternary Geologic Studies	75
5.3	Concluding Remarks	78
6.0	REFERENCES	79

APPENDIX A - Structural Model for Western Midway Valley Based on RF Drillhole Data and Bedrock Outcrops

APPENDIX B - Geophysical Surveys in the Midway Valley Study Area

APPENDIX C - Aerial Photographs That Include Midway Valley Area

APPENDIX D - Soil Data of Taylor (1986)

APPENDIX E - Description of Tertiary Stratigraphic Units in the Midway Valley Area

APPENDIX F - Relevant Yucca Mountain Project Data and Information Bases

LIST OF FIGURES

		Page
Figure 1-1 -	Generalized map of the Midway Valley area	2
Figure 3-1 -	Quaternary geologic map of Midway Valley and surrounding area showing locations of soil trenches (after Taylor, 1986)	29
Figure 4-1 -	Regional tectonic setting	38
Figure 4-2 -	Tectonic setting of southwest Nevada and adjacent California showing relation of study area to the southern Walker Lane belt	39
Figure 4-3 -	Schematic log of trench 14 as presented by Swadley et al. (1984, p. 34)	50
Figure 4-4 -	Schematic log of trench A1 as presented by Swadley et al. (1984, p. 38)	54
Figure 4-5 -	Schematic log of trench A2 as presented by Swadley et al. (1984, p. 39)	55
Figure 4-6 -	Schematic log of trench 17 as presented by Swadley et al. (1984, p. 37)	56
Figure 4-7 -	Schematic log of trench 16 as presented by Swadley et al. (1984, p. 35)	57
Figure 4-8 -	Schematic log of trench 16B as presented by Swadley et al. (1984, p. 36)	58
Figure 4-9 -	Locations of cross sections shown in Figures 4-10 to 4-12	62
Figure 4-10 -	Part of geologic cross section A-A' from Scott and Bonk (1984)	63
Figure 4-11 -	Part of geologic cross section B-B' from Scott and Bonk (1984)	66
Figure 4-12 -	Geologic cross section from Neal (1986)	67
Figure 4-13 -	Graph showing displacement versus age of displacement unit for the Paintbrush Canyon and Bow Ridge faults	71

LIST OF PLATES

Plate 1 - Preliminary Geologic Map of the Midway Valley Area from Scott and Bonk, 1984.

Plate 2 - Surficial Deposits in the Midway Valley Area from Swadley, Hoover, and Rosholt, 1984.

Plate 3 - Drillhole and Trench Locations in the Midway Valley Area from Holmes and Narver, 1988.

Plate 4 - Geophysical Lines and Features Interpreted from Geophysical Data in Midway Valley.

LIST OF TABLES

		Page
Table 2-1	- Major volcanic units of southwestern Nevada volcanic field	8
Table 2-2	- Summary of available information on boreholes in Midway Valley	12
Table 3-1	- Classification of Quaternary geomorphic surfaces of the Vidal Region (modified from Bull and Ku, 1975 and Ku et al., 1979)	16
Table 3-2	- Correlation characteristics of surficial deposits (from Hoover et al., 1981 and Hoover, 1989)	19
Table 3-3	- Age and characteristics of stratigraphic units of Hoover et al. (1981) and Hoover (1989)	21
Table 3-4	- Geomorphic surfaces and ages on the piedmont slopes in Crater Flat (modified from Peterson, 1988)	24
Table 3-5	- Map units of the Yucca and Fortymile washes (summarized from Taylor, 1986)	30
Table 3-6	- Characteristics of pedogenic silica stages (Taylor, 1986, p. 31)	33
Table 4-1	- Preliminary displacement data for the Paintbrush Canyon and Bow Ridge faults	46
Table 4-2	- Stratigraphic dip separation on the Bow Ridge, Midway Valley, and Paintbrush Canyon faults, calculated from the cross sections of Scott and Bonk (1984), Neal (1986), and Carr (1984)	48

1.0 INTRODUCTION

1.1 PURPOSE

This report presents a summary and evaluation of the geologic and geophysical data available for the area of the prospective surface facilities associated with the proposed high-level radioactive waste repository at Yucca Mountain, Nevada. This report was prepared as part of Site Characterization Plan (SCP) Study 8.3.1.17.4.2, "Evaluating the Location and Recency of Faulting Near Prospective Surface Facilities" (DOE, 1988; Gibson et al., 1990). The primary objective of SCP Study 8.3.1.17.4.2 is to acquire surface and near-surface geologic data needed to evaluate the potential for surface-fault rupture in Midway Valley, the proposed location of the prospective surface facilities. The data obtained during this study will be used in conjunction with other site characterization activities to support: (1) the siting of the surface facilities, and (2) an assessment of the potential effects of surface faulting on the design of the surface facilities.

1.2 SCOPE OF WORK

The scope of work for this task includes a review of available published and unpublished literature, maps, and data that are relevant to evaluation of the stratigraphy, structure, and tectonics of the Midway Valley area. Emphasis was placed on: (1) information pertaining to the nature and ages of the Quaternary deposits, soils, and geomorphic surfaces in the Midway Valley area; and (2) the nature and timing of late Cenozoic faulting in the region. It is expected that additional information may be found during this investigation and that new data will be obtained during related SCP activities. Consequently, data compilation and review are expected to continue throughout the study. The following summary and evaluation were prepared to facilitate the planning and implementation of detailed field investigations in Midway Valley for SCP Study 8.3.1.17.4.2. The location of Midway Valley is shown on Figure 1-1.

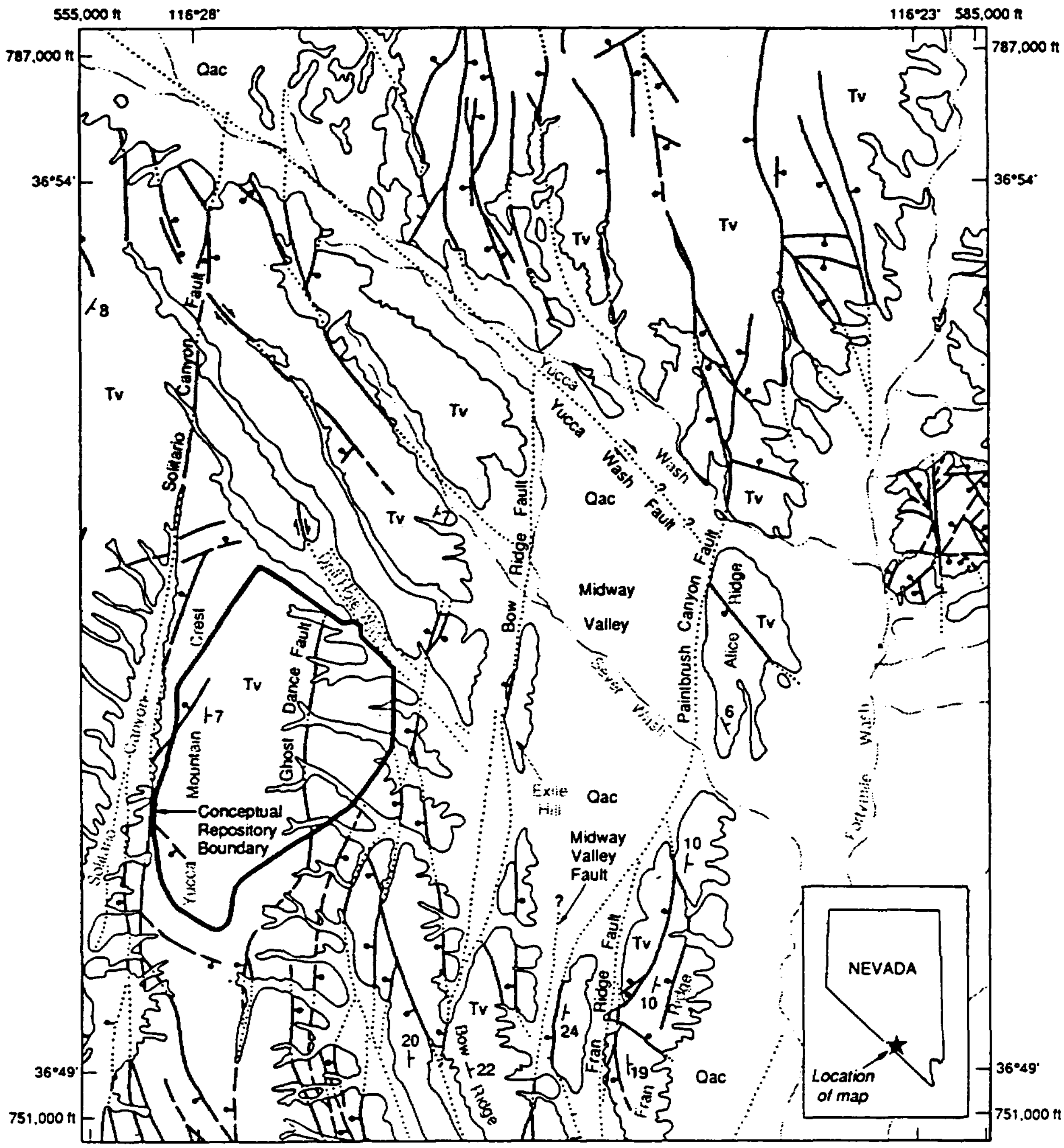

Geology compiled from Scott and Bonk (1984), Maldonado (1985), and Swadley and Parrish (1988); conceptual repository boundary from Holmes and Narver (1988).

EXPLANATION

Fault: dotted where concealed; queried where inferred; ball and bar on downthrown side; arrows indicate relative movement

17 Strike and dip of bedding or foliation

Qac Quaternary alluvium and colluvium

Tv Tertiary volcanic rocks

0 1 Mile

0 2 Kilometers

Figure 1-1. Generalized map of the Midway Valley area.

By reviewing these data, we are not implying that the data will be qualified for licensing. If appropriate, some of the data may be qualified for licensing during later phases of this investigation or as part of other SCP activities.

1.3 SITING CRITERIA

To accomplish the study plan objectives, this investigation emphasizes identifying and evaluating significant late Quaternary (less than 100,000 years old) faults in Midway Valley. "Significant late Quaternary faults," as defined for this study (DOE, 1988, SCP Section 8.3.1.17), are faults that have had a slip rate greater than 0.001 mm per year during the past 100,000 years. The goal in siting the prospective surface facilities is to avoid faults that could produce relative displacements in excess of 5 cm in the foundations of facilities important to safety (FITS), such as the waste handling building (DOE, 1988).

1.4 LOCATION AND REGIONAL GEOLOGIC SETTING

Yucca Mountain and Midway Valley are located along the southwestern edge of the Great Basin, which is part of the Basin and Range structural/physiographic province. Quaternary faulting in the Yucca Mountain region exhibits characteristics of both the Walker Lane belt, which is dominated by northwest-trending, right-lateral strike-slip faults, and the Basin and Range province, which is dominated by north-trending normal faults (see Section 4.1). The Quaternary faulting also may be influenced by pre-existing structures related to silicic volcanism during the Miocene and by structures in the underlying pre-Tertiary units. Some evidence suggests that Yucca Mountain may lie within the upper plate of a regional subhorizontal detachment fault (Scott and Rosenbaum, 1986; Scott and Whitney, 1987).

Yucca Mountain and Midway Valley lie within an extensive Tertiary silicic volcanic field. The Tertiary volcanic rocks consist primarily of high-silica rhyolitic to quartz-latitic air-fall and ash-flow tuffs. Silicic volcanism was most voluminous between about 13 and 14 million years ago (Ma) and ended more than 5 Ma (Carr, 1984). Basaltic volcanism, which began about 11 Ma, has continued at a low rate into the Quaternary (Crowe and Carr, 1980; Carr, 1984; Wells et al., 1990a). Various coalesced eruptive centers have been identified in the Yucca Mountain area (Byers et al., 1976, 1989; Christiansen et al., 1977). The Timber Mountain-Oasis Valley caldera complex, located about 6 km north of Midway Valley, was the source of most of the tuffs that crop out in the Yucca Mountain region (Byers et al., 1976). The Paintbrush Tuff contains two of the welded tuffs that are exposed in the Midway Valley area: the Topopah Spring Member and the Tiva Canyon Member (Plate 1). Additionally, the Pah Canyon Member of the Paintbrush Tuff, the Rainier Mesa Member of the Timber Mountain Tuff, and the rhyolites of Fortymile Canyon crop out in the Midway Valley area. At Yucca Mountain, approximately 1000 to 3000 m of volcanic rocks overlie the pre-Tertiary sequence (Gibson et al., 1990), which consists of a thick section of Proterozoic and Paleozoic sedimentary rocks locally intruded by granitic bodies of Mesozoic age. The upper Tertiary and Quaternary sediments that fill Midway Valley consist mostly of alluvial fan deposits (fluvial and debris flow sediments) and some thin eolian deposits.

Midway Valley is an alluvium-filled structural and topographic valley that lies between Yucca Mountain to the west and Fran Ridge and Alice Ridge to the east (Figure 1-1). Two major drainages, Sever Wash and Yucca Wash, flow southeast across the valley. The Midway Valley area contains a system of north-trending normal faults (Scott and Bonk, 1984). The two largest are the Paintbrush Canyon fault on the east side of Midway Valley and the Bow Ridge fault on the west side. Where exposed in bedrock, both faults dip steeply toward the west and have down-on-the-west displacement (Scott and Bonk, 1984). The Bow Ridge and Paintbrush Canyon faults converge south of Midway Valley near Busted Butte (Scott and Bonk, 1984). Some short northwest-trending faults within and to the north of Drill Hole Wash are interpreted to have a component of right-lateral strike-slip displacement (Scott and Bonk, 1984).

Based on geometric constraints imposed by limited surface and drillhole data, Scott and Bonk (1984) infer that a series of small-displacement, north-trending, west-dipping normal faults underlie Midway Valley between the Bow Ridge and Paintbrush Canyon faults. These inferred, unmapped faults are reported to displace Tertiary volcanic rocks but not the Quaternary/Tertiary alluvial deposits that fill Midway Valley. Existing data, however, are insufficient to preclude faulting of the older alluvial deposits within Midway Valley. Based primarily on geophysical data, a linear, north-trending feature that lies in the center of the southern part of Midway Valley has been interpreted as a fault zone by Scott and Bonk (1984); it is informally called the "Midway Valley Fault (Zone)" by Neal (1986, his Figure 3). A concealed fault that coincides with the postulated Midway Valley fault initially was mapped by Lipman and McKay (1965).

Most of the displacement along the Paintbrush Canyon and Bow Ridge faults, as well as along parallel faults elsewhere at Yucca Mountain, occurred during the Miocene (Carr, 1984), more or less synchronously with a period of extensive silicic volcanism in this region. Both faults apparently have been active during the Quaternary. Quaternary geologic units, however, exhibit markedly lower apparent offset rates than do Tertiary units (Gibson et al., 1990).

1.5 ACKNOWLEDGEMENTS

This summary and evaluation of existing geologic and geophysical data for the area of the prospective surface facilities were prepared by the individuals listed below.

SANDIA NATIONAL LABORATORIES, Albuquerque, New Mexico:

J. Duane Gibson	Task Leader and Principal Investigator
Wilfred J. Carr (Appendix A)	Consultant to SNL -- Tertiary stratigraphy and structural geology

GEOMATRIX CONSULTANTS, INC., San Francisco, California:

F. H. Swan	Project Manager
John R. Wesling	Quaternary geology and geomorphology
Thomas F. Bullard	Quaternary geology and geomorphology
Roseanne C. Perman	Geology and geophysics
Michael Angell	Structural geology and regional tectonics
Laurel A. DiSilvestro	Geophysics

Technical review of this report was provided by Francis B. Nimick, Christopher A. Rautman, and Les E. Shephard of SNL. Further improvement to the manuscript was provided by Kent Anderson, Moya Melody, and Catherine A. Hensley.

2.0 OVERVIEW OF PREVIOUS GEOLOGIC INVESTIGATIONS

2.1 GEOLOGIC MAPPING

The bedrock geology of the Yucca Mountain region has been mapped on 1:24,000-scale USGS quadrangle maps by Christiansen and Lipman (1965), Lipman and McKay (1965), McKay and Sargent (1970), and Orkild and O'Connor (1970). Scott and Bonk (1984) mapped the geology of Midway Valley and vicinity at a scale of 1:12,000 (Plate 1). Maldonado (1985) compiled a geologic map of the Jackass Flats area, which includes Midway Valley, at a scale of 1:48,000; his data for the Midway Valley area were obtained from Lipman and McKay (1965). A geologic map of the Nevada Test Site (NTS) at a scale of 1:100,000 was compiled by Frizzell and Shulters (1990); their data for the Midway Valley area were derived from Scott and Bonk (1984).

The Yucca Mountain region contains four major groups of rocks: Precambrian crystalline rocks; Proterozoic (upper Precambrian) and Paleozoic sedimentary rocks; Tertiary volcanic rocks; and upper Tertiary and Quaternary alluvial and colluvial sediments and basaltic extrusives. Only Tertiary and Quaternary units are exposed in the Midway Valley area. Plate 1 shows the geology of the area as mapped by Scott and Bonk (1984).

Descriptions of the stratigraphy of the volcanic bedrock units in the Yucca Mountain region have been published by Christiansen and Lipman (1965), Lipman and McKay (1965), Orkild (1965), Marvin et al. (1970), Byers et al. (1976), Scott and Bonk (1984), Carr et al. (1986), and Byers et al. (1989). The volcanic rocks in several deep drillholes were described by Spengler et al. (1979, 1981), Maldonado and Koether (1983), Scott and Castellanos (1984), and Spengler and Chornack (1984). The stratigraphic sequence of volcanic rocks in the Southwestern Nevada Volcanic Field (Byers et al., 1989), which includes the Midway Valley area, is summarized in Table 2-1. Stratigraphic units found in the Midway Valley area are described in Appendix E.

TABLE 2-1

MAJOR VOLCANIC UNITS OF SOUTHWESTERN NEVADA VOLCANIC FIELD SOURCE: BYERS ET AL. (1989, p. 5910)

Formation	Member	Volcanic Center	Approximate Age,[1] Ma
Alluvium			0-11
Basalts[2]			0-13
Stonewall Flat Tuff	Civet Cat Canyon	Both members from Stonewall	6.5
	Spreadhead	Mountain caldera complex	6.5
Thirsty Canyon Tuff	Gold Flat	All members from Black	7.5
	Trail Ridge	Mountain caldera	7.5
	Pahute Mesa		7.5
	Rocket Wash		7.5
Rhyolite of Shoshone Mountain		Shoshone Mountain	9.0
Mafic lavas		Moat of Timber Mountain caldera	9-10
Timber Mountain Tuff[2]	Ammonia Tanks	Both members from Timber	11.5
	Rainier Mesa	Mountain-Oasis Valley caldera complex	11.5
Rhyolite lavas of Fortymile Canyon[2,3]		Timber Mountain caldera	11-13[3]
Paintbrush Tuff[2]	Tiva Canyon	Claim Canyon cauldron	
	Yucca Mountain	All other members from	13
	Pah Canyon	Timber Mountain-Oasis	13
	Topopah Spring	Valley caldera complex	13
Wahmonie and Salyer formations		Wahmonie area	13.5
Crater Flat Tuff[2]	Prow Pass	All members from Crater	13.5
	Bullfrog	Flat-Prospector Pass	13.5
	Tram	caldera complex	13.5
Belted Range Tuff	Grouse Canyon	Both members from Silent	14
	Tub Spring	Canyon caldera	14
Dacite lavas and breccias[2]		Periphery of Crater Flat	14
Lithic Ridge Tuff[2]		Uncertain	14
Rhyolite of Kawich Valley		Silent Canyon caldera	15
"Older" tuffs		Uncertain	15
Sanidine-rich tuff		Uncertain	15
Tuff of Yucca Flat		Uncertain	15
Redrock Valley Tuff		Uncertain	16

[1] Ages are given to nearest 0.5 m.y. and corrected for modern constants. A few ages are inferred from stratigraphic position with respect to dated units. Sources are Kistler (1968), Marvin et al. (1970), Carr et al. (1986), Noble et al. (1984, 1988), and Warren et al. (1988).
[2] Volcanic units of the Yucca Mountain area.
[3] A few rhyolite lavas of Fortymile Canyon postdate the Timber Mountain Tuff (Warren et al., 1988).

The Topopah Spring SW quadrangle (renamed the Busted Butte quadrangle), mapped by Lipman and McKay (1965), includes Midway Valley south of Yucca Wash. Three major unnamed faults that trend north and are down-on-the west are mapped in Midway Valley: (1) a fault along the western edge of the valley, west of Exile Hill; (2) a fault along the eastern edge of the valley; and (3) a fault in the central part of the valley. The faults are concealed by alluvium within Midway Valley, but each of the structures is mapped in the bedrock exposed at the south end of the valley. In addition, the easternmost fault, the Paintbrush Canyon fault, is exposed in bedrock outcrops north of Yucca Wash.

Scott and Bonk (1984) mapped the geology of the Midway Valley area in greater detail than did Lipman and McKay (1965) (Plate 1). They divided the members of the Paintbrush Tuff into several mapping units. Scott and Bonk also used geophysical (aeromagnetic and electromagnetic) data to constrain the locations of the larger faults concealed by alluvial sediments within the valley. Two concealed faults are mapped on the west and east sides of Midway Valley; they are named the Bow Ridge fault and the Paintbrush Canyon fault, respectively. These faults are approximately coincident with the concealed faults mapped along the margins of the valley by Lipman and McKay (1965). Where concealed, faults along Yucca Wash and Drill Hole Wash (Yucca Wash fault and Drill Hole Wash fault) also were delineated by Scott and Bonk largely from aeromagnetic anomalies and electromagnetic survey results, respectively. An unnamed, concealed fault that is mapped for approximately 2 km beneath the valley alluvium is associated with exposed bedrock faults within Bow Ridge along the south-central margin of Midway Valley. The bedrock faults also were mapped by Lipman and McKay (1965), who connected them to a concealed fault more than 6 km long that was mapped through the central part of Midway Valley; this central fault subsequently was named the Midway Valley fault by Neal (1986).

Hoover et al. (1981) defined the stratigraphy of Quaternary/Tertiary surficial deposits and described the correlation characteristics in the NTS area, which includes Midway Valley. The three principal stratigraphic units defined were similar to the QTa, Q2, and Q1 deposits first described in the Syncline Ridge area of western Yucca Flat by Hoover and Morrison (1980). The surficial deposits mapped on the Topopah Spring 15-minute quadrangle by Swadley et al. (1984), a part of which is shown on Plate 2, were based on the stratigraphy of Hoover et al. (1981). Fault-trench studies by Swadley and Hoover (1983) and Swadley et al. (1984) in and around Midway Valley also relied on the stratigraphy of Hoover et al. (1981). Maps of Quaternary deposits in the area west and south of Yucca Mountain include the Lathrop Wells quadrangle (Swadley, 1983); the Big Dune quadrangle (Swadley and Carr, 1987); and the Bare Mountain quadrangle (Swadley and Parrish, 1988). These maps also follow the stratigraphy of Hoover et al. (1981).

2.2 BOREHOLE INFORMATION

Boreholes have been drilled in the Midway Valley area to characterize the geologic, geophysical, and hydrologic setting. The locations of boreholes in the Midway Valley area were complied by Holmes and Narver (1988); borehole locations are shown on Plate 3. Information on stratigraphy, structure, engineering and physical properties, groundwater depth, thickness of alluvium, and other subsurface properties has been obtained from these boreholes. Some boreholes have been used for geophysical survey shot holes, and various geophysical logs (including acoustic, resistivity, gamma ray, and density) have been acquired from most of the boreholes. Table 2-2 lists location, surface elevation, and selected geologic information for the boreholes.

To provide detailed subsurface information on Midway Valley, exploratory boreholes UE-25 RF #1 through #8 were drilled between January and July 1984; boreholes UE-25 RF #3B, #9, #10, and #11 were drilled in July and August 1985. Borehole depths range from 16 to 94 m (51 to 306 ft) (customary units shown in parenthesis are reported in feet in the original references). Lithologic logs and partial cores of these boreholes provide data on thicknesses of alluvium and underlying volcanic rock units, which are useful in assessing the subsurface structure of Midway Valley (see Section 4.2). Interpretations of this stratigraphic information by Carr (Appendix A, this report) and Neal (1985, 1986) are indicated in Table 2-2.

2.3 GEOPHYSICAL SURVEYS

Several types of geophysical surveys have been used to characterize the subsurface geology of the Midway Valley area. The objectives of these surveys have included evaluation of geologic structure, stratigraphic correlation between boreholes, and assessment of engineering properties. Appendix B contains descriptions of the surveys conducted in Midway Valley: seismic reflection surveys, seismic refraction surveys, resistivity/geoelectric surveys, and magnetic surveys. Survey lines and features interpreted from geophysical data are shown on Plate 4.

The resistivity/geoelectric surveys have detected variations in lateral resistivity that correlate with the Bow Ridge and Paintbrush Canyon faults; evidence for the postulated Midway Valley fault is equivocal. To date, the seismic reflection and refraction surveys conducted in Midway Valley have produced no reliable data (see Appendix B).

2.4 PHOTOLINEAMENTS

Aerial photographs of the Yucca Mountain region have been taken by the Nevada Bureau of Mines and Geology, U.S. Geological Survey, U.S. Department of Energy, and Sandia National Laboratories. These photographs, which include black and white, color, and false color infrared photographs, were taken under various lighting conditions and at different scales. Index maps that show the locations of these photographs within the area of investigation are provided in Appendix C.

TABLE 2-2

SUMMARY OF AVAILABLE INFORMATION ON BOREHOLES IN MIDWAY VALLEY

Borehole Designation	Surface Elevation (ft)[1]	Total Depth (ft)[1]	Thickness of Alluvium (ft)[1]	Depth to Rainier Mesa Member (ft)[1]	Depth to Tiva Canyon Member (ft)[1]	No. of Geophysical Logs Run	Nevada Plane Coordinates North (ft)[1]	Nevada Plane Coordinates East (ft)[1]
UE-25 RF #1	3688.5	145[2] 145[3]	120[2] 115[3]	N.P.[3] N.P.[3]	120[2] 115[3]	-	762190	570890
UE-25 RF #2	3656.8	51[2] 52[3]	35[2] 34[3]	N.P.[2] N.P.[3]	35[2] 34[3]	-	758800	570335
UE-25 RF #3	3657.7	301[2] 301[3,4]	90[2] 90[3,4]	N.P.[2] N.P.[3,6]	265[2] 264[4]	-	765575	571100
UE-25 RF #3B	3661.1	111[2]	105[2]	>111[6]	>111[6]	-	765695	571066
UE-25 RF #4	3636.8	306[2] 306[3]	150[2] 155[3]	N.P.[2] 155[3]	265[2] 276[3]	-	762091	572063
UE-25 RF #5	3813.7	122[2] 122[3]	103[2] 102[3]	>122[6] 102[3]	>122[6] >122[3,6]	-	759199	568098
UE-25 RF #7a	3755.9	153[2] 153[3]	>153[2] >153[3]	>153[6] >153[3,6]	>153[6] >153[3,6]	-	768768	570269
UE-25 RF-#7	3756.1	150[2] 150[3]	>150[2] >150[3]	>150[6] >150[3,6]	>150[6] >150[3,6]	-	768804	568790
UE-25 RF #8	3787.9	128[2] 128[3]	45[2] 45[3]	N.P.[2] 45[3]	100[2] 108[3]	-	765631	568790
UE-25 RF #9	3674.0	106[2] 106[4]	65[2] 65[4]	N.P.[2] N.P.[4]	65[2] 65[4]	-	765945	570643
UE-25 RF #10	3669.7	60[2] 60[4]	36[2] 35[4]	N.P.[2] N.P.[4]	36[2] 35[4]	-	765308	570230
UE-25 RF #11	3665.4	77[2] 77[4]	40[2] 38[4]	N.P.[2] N.P.[4]	40[2] 38[4]	-	765622	570435
UE-25 WT #4 **	3829.0	1580	-	-	-	13	768512	568040
UE-25 WT #5 **	3559.0	1330	-	-	-	-	761826	574250
UE-25 WT #14	3529.9	1310	-	-	-	10	761651	575210
UE-25 WT #16	3971.4	1710	-	-	-	9	774420	570395
UE-25 UZN #13	3821.3	65	-	-	-	-	768025	568255
UE-25 UZN #14	3823.9	55	-	-	-	-	767967	568233
UE-25 UZN #50	3892.1	35	-	-	-	-	759757	566567
UE-25c #1	3709.0	3000	-	-	-	34	757096	569680
UE-25c #2	3714.1	3000	-	-	-	29	756849	569634
UE-25c #3	3714.2	3000	-	-	-	24	756910	569555

TABLE 2-2

SUMMARY OF AVAILABLE INFORMATION ON BOREHOLES IN MIDWAY VALLEY

Borehole Designation		Surface Elevation (ft)[1]	Total Depth (ft)[1]	Thickness of Alluvium (ft)[1]	Depth to Rainier Mesa Member (ft)[1]	Depth to Tiva Canyon Member (ft)[1]	No. of Geophysical Logs Run	Nevada Plane Coordinates North (ft)[1]	East (ft)[1]
UE-25p #1	**	3564.0	5923	128[7]	128[7]	180[7]	>33	756171	571485
US-25 #2		4316.0	53	-	-	-	-	762403	566427
US-25 #3		3620.0	52	-	-	-	-	762075	572454
US-25 #4		3800.0	50	-	-	-	-	762458	567853
US-25 #5		3799.0	52	-	-	-	-	762432	567853
US-25 #6		3782.0	52	-	-	-	-	762377	568551
US-25 #7		3783.0	52	-	-	-	-	762354	568551
US-25 #8		3757.0	52	-	-	-	-	762317	569332
US-25 #9		3755.0	50	-	-	-	-	762285	569329
US-25 #10		3724.0	50	-	-	-	-	762251	570112
US-25 #11		3724.0	52	-	-	-	-	762226	570111
US-25 #12		3688.0	52	-	-	-	-	762198	570894
US-25 #13		3688.0	52	-	-	-	-	762168	570891
US-25 #14		3653.0	50	-	-	-	-	762137	571675
US-25 #15		3654.0	50	-	-	-	-	762106	571670
US-25 #16		3620.0	50	-	-	-	-	762046	572453
US-25 #17		3576.0	50	-	-	-	-	761986	573627
US-25 #18		3545.0	50	-	-	-	-	761895	574709

Sources: Surface elevations, Nevada plane coordinates, and number of geophysical logs run from Holmes and Narver, Inc., 1988; other values indicated in footnotes.

[1] To convert feet to meters, multiply by 0.3048.
[2] W. Carr (Appendix A, this report).
[3] Neal (1985)
[4] Neal (1986)
[5] N.P. = not present
[6] Not encountered but possibly present at depths greater than total depth.
[7] Muller and Kibler (1984)

- No information available or no survey.
* Dirt pad elevation.
** Casing elevation.

Note: Locations shown on Plate 3

3.0 QUATERNARY GEOLOGY AND AGE-DATING

The foundation and reference point for Quaternary geologic studies of the Yucca Mountain region are studies by Bull (1984), Bull and Ku (1975), and Ku et al. (1979). These studies describe the Quaternary stratigraphy and chronology of the Parker-Vidal area, approximately 240 km south of Las Vegas. Their chronology is based primarily on the ^{230}Th-^{234}U dating of pedogenic carbonate.

Wells et al. (1984), Dohrenwend et al. (1986), and McFadden et al. (1984, 1987) conducted studies of the Quaternary geology, geomorphology, and soils in the Cima volcanic field and Silver Lake playa southwest of Las Vegas. Through these soils-geomorphic studies and by dating Pleistocene volcanic events, paleolake levels, and geomorphic surfaces, these researchers develop a temporally constrained late Quaternary chronology that has increased understanding of the area's dominant desert geomorphic processes and geomorphic responses to climatic change. McFadden et al. (1987) provide new insights and models to describe the influence of atmospheric dust and pedogenic processes on the development of desert pavements. Dorn and Oberlander (1981a, 1981b, 1982), Dorn (1983), and Dorn et al. (1986), building on work by Potter and Rossman (1977, 1979) concerning origins of desert varnish, developed new techniques for dating the nearly ubiquitous desert varnish that coats the clasts that compose desert pavements.

Hoover and Morrison (1980) initially defined three basic Quaternary/Tertiary stratigraphic units (QTa, Q2, and Q1) in the NTS area near Yucca Flats. Hoover et al. (1981) and Hoover (1989) expanded on this stratigraphy to develop a Quaternary/Tertiary stratigraphy and correlation characteristics for surficial deposits in the NTS area. Swadley and Hoover (1983) and Swadley et al. (1984) describe trench stratigraphy for fault studies in the NTS area and at Crater Flats while retaining the stratigraphy of Hoover et al. (1981). Swadley (1983), Swadley et al. (1984), Swadley and Carr (1987), and Swadley and Parrish (1988) published geologic maps of the Yucca Mountain region that incorporate the Quaternary stratigraphy of Hoover et al. (1981). More recently, Whitney et al. (1986) and Harrington and Whitney (1987) address neotectonics and age-dating in the Crater Flats region adjacent to Yucca Mountain, and Crowe (1986), Crowe et al. (1989), and Wells et al. (1990a) utilize soils and geomorphic methods and techniques to investigate volcanic risks associated with volcanic centers in Crater Flats. No detailed Quaternary geologic studies have been performed within Midway Valley itself, although Taylor (1986) characterizes the soils on fluvial terrace sequences along Yucca and Fortymile washes, immediately north and east, respectively, of Midway Valley. Ho et al. (1986) provide limited data on the engineering properties of the near-surface materials in Midway Valley. Recent studies directed by the State of Nevada address their concerns regarding siting of the Yucca Mountain repository (e.g., Peterson, 1988; Dorn, 1988; Forman, 1988; and Ku, 1988).

The following sections review Quaternary geologic studies relevant to the Midway Valley area. Nomenclature for pedogenic soils used in the following text and tables generally follows that of Birkeland (1974, 1984) and Soil Survey Staff (1975). Dating methods used in the Yucca Mountain region also are discussed.

3.1 QUATERNARY STUDIES OUTSIDE THE YUCCA MOUNTAIN REGION

Quaternary geologic studies by Bull and Ku (1975), Ku et al. (1979), and Bull (1984) in the Parker-Vidal region south of Las Vegas focus on neotectonics, stratigraphy, and radiometric dating of Quaternary deposits by Th^{230}-U^{234} methods. Units were mapped based on the concept that a geomorphic surface is "a mappable landform, formed during a given time span and having distinctive topographic, pedologic, and stratigraphic-sedimentologic characteristics" (Ku et al., 1979). The work of Bull and Ku (1975) and Bull (1984) emphasizes the radiometric dating of geomorphic surfaces. Table 3-1 summarizes the stratigraphy of Bull and Ku (1975) and Ku et al. (1979) and presents their age assignments of the seven geomorphic surfaces identified and mapped in the Vidal region. Bull and Ku (1975) and Ku et al. (1979) suggest that these geomorphic surfaces were formed as complex

TABLE 3-1

CLASSIFICATION OF QUATERNARY GEOMORPHIC SURFACES OF THE VIDAL REGION (MODIFIED FROM BULL AND KU, 1975, AND KU ET AL., 1979)

Geomorphic Surface		Age (ka)	Characteristics and basis for age determinations
Bull and Ku (1975)	Ku et al. (1979)		
Q4b	Q4b	0 - < 2	Active wash. Unvarnished bar-and-swale topography and stream channels. Age based on lack of desert varnish; about 2 ka is required to form incipient varnish.
Q4a	Q4a		Surfaces infrequently flooded, so that riparian trees are not present or are dead.
Q3	Q3	2 - 10	Varnished bar-and-swale topography containing A and Ck horizons but lacking B horizons. Q3 age based on desert varnish (lower limit), ^{14}C, and U-Th dating of pedogenic carbonate and soil profile characteristics (upper limit) that indicate soil has not been subjected to climate wetter than Holocene.
Q2b	Q2c	10 - 70	Q2c and Q2b (Ku et al., 1979) have desert pavements underlain by argillic and calcic soil horizons. Pedogenic carbonate in soils of Q2a and Q2b (Bull and Ku, 1975) were dated by U-Th methods. ^{14}C methods were used to assess degree of illuviation of pedogenic calcium carbonate.
Q2a	Q2b	70 - 96	
Period of net erosion of alluvium			
Q1b	Q2a	400 - 800	Highly dissected ridges or terraces containing remnants of desert pavement that are underlain by argillic soil horizons. Age assignment based on soil-geomorphic relationships. Pedogenic carbonate dated by U-Th method gave maximum age of 176 $\pm$ 2.5 ka, but sample was considered contaminated and yielded a much younger age than the age required by soil-geomorphic relationships. ^{14}C methods were used to assess degree of illuviation of pedogenic calcium carbonate.
Period of net erosion of alluvium			
		1,200	Maximum age of Grand Canyon basalt flows (K-Ar dated) that are represented in gravel of younger terraces of the Colorado River, but not the Q1 river terraces.
Q1a	Q1	>1,200	Post-Miocene alluvium that is so old and dissected that planar surfaces, pavements, and remnants of original soil horizons are no longer present on most piedmonts. U-Th method dates pedogenic carbonate at >300 ka.

geomorphic responses to changes in climate and regional base level. Climatic changes during the Quaternary produced many base-level changes in the Colorado River that influenced piedmont fluvial systems in the Vidal region. These regional and local base-level changes, together with climate-controlled changes in piedmont fluvial systems, produced distinct geomorphic surfaces in the Vidal region (Bull and Ku, 1975; Ku et al., 1979).

Bull and Ku (1975) initially estimated the ages of geomorphic surfaces based on diagnostic pedogenic carbonate morphology after the classification of Gile et al. (1966). Bull and Ku also assumed that the rates of calcium carbonate accumulation in the Vidal region are about the same as in southern New Mexico, where Gile et al. (1966) conducted their work. Bull and Ku (1975) compared the thicknesses of calcium carbonate rinds on clasts from Holocene geomorphic surfaces in the Vidal area with rind thicknesses from surfaces of similar age in New Mexico. They concluded that the rates of accumulation probably were slower in the relatively drier Vidal region than along the moister Rio Grande Valley of New Mexico. Consequently, ages assigned on this basis may be significantly less than the actual age of the surface. Ku et al. (1979) subsequently dated outer and inner layers of carbonate rinds on clasts in the alluvium to establish rates of carbonate accumulation in the Vidal area. The ages of geomorphic surfaces listed in Table 3-1 are based on data from both Bull and Ku (1975) and Ku et al. (1979).

3.2 STUDIES OF HOOVER ET AL. (1981) AND HOOVER (1989)

Hoover et al. (1981), building on work by Bull and Ku (1975), as well as on regional works by Morrison (1967) and Hoover and Morrison (1980), summarizes the Quaternary stratigraphy of the Yucca Mountain region based on the concept of "correlation characteristics." Hoover (1989) elaborates on the work of Hoover et al. (1981), retaining the established stratigraphy while improving on the assigned ages of stratigraphic units proposed by Swadley et al. (1984).

The work of Hoover et al. (1981) proposes three major late Cenozoic stratigraphic units for the NTS region. Their basis for differentiating units is the concept of correlation characteristics, which relies on physical and morphologic characteristics of landscape elements, including landform, drainage network, soils, topographic position, desert pavement, desert varnish, depositional environment, and lithology. The correlation characteristics of Hoover et al. (1981) and Hoover (1989) are presented in Table 3-2.

The concept of correlation characteristics provides a useful basis both for reconnaissance-level mapping of large areas based primarily on photogeologic interpretations and for detailed mapping; however, Hoover et al. (1981) and Hoover (1989) present few data to support the stratigraphic framework and conclusions of their studies. The application of correlation characteristics in these studies appears to be qualitative and may allow other investigators to interpret map units differently. Additionally, soil-geomorphic relationships presented by Birkeland (1974, 1984) and the state factor approach to soil formation of Jenny (1980) are not reflected consistently in the correlation characteristics of Hoover et al. (1981). Recent research on the genesis of desert soils (Birkeland, 1984; McFadden et al., 1987); development of desert pavements (McFadden et al., 1987); and origin of parallel, transverse stripes on desert pavements (Wells and Dohrenwend, 1985; Wells et al., 1990b) is not reflected in Hoover (1989).

The three major Quaternary/Tertiary geologic units of Hoover et al. (1981) in the NTS region are subdivided into several subunits. The oldest surficial unit, QTa, is Quaternary and/or Tertiary in age. Units Q2 and Q1 represent older and younger Quaternary deposits, respectively. QTa is underlain by the lake deposits of the Amargosa Desert, which comprise a fourth unit that is lacking in the Midway Valley area. The lake deposits contain a Pliocene ash bed. A total of 10 subunits of Q1 and Q2, and possibly "three additional subunits of uncertain age that may belong in unit Q2" (Hoover et al., 1981, p. 8), are mappable in the NTS region. The stratigraphy of the NTS area as defined by Hoover et al. (1981) and Hoover (1989) is summarized in Table 3-3.

TABLE 3-2

CORRELATION CHARACTERISTICS OF SURFICIAL DEPOSITS (FROM HOOVER ET AL., 1981, AND HOOVER, 1989)

I.	Topography[1] A. Macrotopography (300 m along contour) B. Microrelief (10- to 20-m radius)
II.	Drainage[2] A. Direction of pattern development B. Cross-sectional shape C. Depth
III.	Topographic relationships[3]
IV.	Soils[4] A. A and B horizons 1. Color 2. Clay, carbonate, and silica content B. Pedogenic caliche (C or K horizons) 1. Stage 2. Thickness
V.	Desert pavement[5] A. Packaging of clast lithologies B. Maximum fragment size C. Varnish color and luster
VI.	Depositional environment
VII.	Lithology A. Ratio of clast lithologies B. Maximum fragment size and frequency C. Sand and clay content D. Color

TABLE 3-2

CORRELATION CHARACTERISTICS OF SURFICIAL DEPOSITS (FROM HOOVER ET AL., 1981 AND HOOVER, 1989) (concluded)

Notes:

[1] Topography as a correlation characteristic relates to the curvature of topographic contour lines in planimetric view, implying that topographic curvature is a direct result of geomorphic processes. Qualitative descriptors of macrotopography include flat, slightly convex, convex, and highly convex or well rounded. Microrelief refers to the visible relief on the ground within a 10- to 20-m radius of the viewer. Excluded from microrelief are *slope relief* (an undefined term), boulders, and recent eolian accumulations around vegetation. Microrelief is classified as less than 0.2 m, 0.2 to 0.5 m, and greater than 0.5 m. Hoover et al. (1981) attribute microrelief to postdepositional modification of original constructional or erosional landforms. They apply the criteria of microrelief to identifying the youngest alluvial deposits in the study region.

[2] Drainage is used as a correlation characteristic to relate drainage characteristics to the age of surficial deposits. However, Hoover et al. (1981) do not differentiate drainage developed following deposition from that developed during deposition. Characteristics of drainage include drainage patterns, direction of pattern development, shape of the drainage cross section, and depth of drainage. The relationship between drainage form and age of deposits is not assessed quantitatively and does not include consideration of sediment transport in arid environments. Hoover et al. (1981) interpret depth of drainage as reflecting tectonic activity in the area but do not address other factors that might affect depth of drainage, such as climate change, complex response, or base-level changes.

[3] Topographic relationships are used to differentiate surficial deposits. Hoover et al. (1981) explain in detail that topographic relationships are not always straightforward or consistent.

[4] Soils typically play an integral part in the correlation of surficial deposits in Quaternary geologic studies. Hoover et al. (1981) use soils qualitatively as a correlation tool and as an indicator of relative age of surficial deposits. Characteristics they utilize include color, clay content, and silica content of A and B horizons, stage and thickness of pedogenic calcium carbonate, and morphologic characteristics of the A and B horizons. The descriptions by Hoover et al. (1981) of some key diagnostic properties are not always consistent with established methods of soil description as presented by the Soil Survey Staff (1975), Gile et al. (1966), and Birkeland (1974, 1984).

[5] Desert pavements in the study region are characterized qualitatively by the degree of packing or interlocking and the size and sorting of clasts based on visual estimates. The measure of desert varnish on clasts is visual; qualitative colors range from brown to black and from dull to shiny. Thicknesses of the films are also assigned. Hoover et al. (1981) also make clear the inherent variability in desert pavements and varnish due to geomorphic processes.

TABLE 3-3

AGE AND CHARACTERISTICS OF STRATIGRAPHIC UNITS OF HOOVER ET AL. (1981) AND HOOVER (1989)

Depositional Unit	Age (ka)	Age and characteristics of depositional units
Q1a	< 0.15	Active wash. Some debris flow deposits. Bar-and-swale topography. No desert pavement or desert varnish. Age based on Antevs' (1955) postulated arroyo incision throughout the southwest U.S. beginning about 1840.
Q1b	< 3.0	Low terraces 0.5 to 2.0 m above Q1a. Topography and drainage distinguish Q1b from Q1c. No evidence of calcium carbonate accumulation. Stratigraphic relationships suggest Q1b is younger than the oldest period of Q1e deposition (5.3 to 3.0 ka).
Q1e	5.3-3.0, 2.0-1.0, 0.2-0	Dunes and remnants of sandsheets represent two depositional periods. Differences based on soil profile development. Three eolian periods based on ^{14}C dates. Weakly developed soils having possible Stage I to II calcium carbonate accumulation in upper 0.5 m. Desert pavements consist of deflation pavements associated with underlying Q1b. Older Q1e overlies Q1c or older units; younger Q1e deposits cover Q1b at lower altitudes.
Q1s	> 5.3	Sandsheets derived from older deposits before deposition of Q1b. Soil development consists of leached calcium carbonate a few cm below the surface and films on particles in a layer a few cm thick in the upper 0.5 m. Desert pavements are deflation pavements.
Q1c	5.3 - 8.3	Dominantly fluvial in origin; alluvial fans and sheetwash deposits containing < 10 percent debris flow. Soil development consists of Stage I calcium carbonate morphology on clasts; slight darkening of A horizon in sandy deposits. No pavement developed. Desert varnish on clasts is light brown and thin.
Regional Unconformity		
Q2a, Q2a(?)	31±10 - 55±20	Debris flow deposits. Soil development consists of vesicular A horizon, cambic B horizon, and Stage I calcic horizon. Desert pavement is loosely packed and poorly sorted. Desert varnish is patchy, dull, brown to dark brown. Q2a(?) differs from Q2a in deposit color, lithology, and sedimentology; otherwise they are the same. Ages shown are for Q2a(?). Subunit Q2a has not been dated.

TABLE 3-3

AGE AND CHARACTERISTIC OF STRATIGRAPHIC UNITS OF HOOVER ET AL. (1981) AND HOOVER (1989)

Depositional Unit	Age (ka)	Age and characteristics of depositional units
Q2b	145 ±25 - 200 ±80	Terrace deposits and thin sheets of alluvial fan deposits. Soil development consists of vesicular A horizon, cambic B horizon (5YR), and Stage I calcic horizon. Desert pavement is similar to Q2c but less densely packed. Desert varnish is duller and less complete than Q2c.
Q2s	160 ±90	Fluvial sand sheet derived from Q2e. Soil development consists of vesicular A horizon and 5R B horizon with "noticeable" clay films. Desert pavement is loosely to densely packed, moderately to well sorted. Desert varnish is a very dark brown to blackish brown, dull to shiny film.
Q2e		Sand sheets and sand ramps form lithofacies of Q2c. Interfinger with Q2c. Soils typically eroded to the calcic horizon. Most soils consist of < 20-cm-thick vesicular A horizon, 0.5- to 1.0-m-thick Stage II to IV calcic horizon, and locally cambic B horizons < 0.5 m thick. Bishop ash found at or near base of Q2e.
Q2c	< 128 - > 128 240 ±50 - 480 ±90 > 738	Fluvial and debris flow deposits of three ages. Interfinger with Q2e and Q2s. May be as much as 100 m thick. Soil development (from oldest to youngest) consists of: 0.3- to 0.7-m-thick, 10R argillic horizon engulfed by the K horizon and silicified and a 1- to 2-m-thick Stage IV K horizon; 0.5-m-thick, 10R to 5YR argillic horizon and Stage III to IV K horizon; and < 0.5-m-thick, 5YR cambic B horizon and a Stage II to III K horizon. Desert pavements are densely packed, moderately to well sorted. Desert varnish is a blackish brown, dull to shiny coating. Pavements display "patterned ground" consisting of lineations or arcs. Bishop ash found at or near base of Q2e.
Regional Unconformity		
QTa	900 - 1,100	Alluvium and debris flow deposits. Broad interfluves form concordant summits termed "ballenas," or whalebacks. Boulders as much as 10 m in diameter at surface may be evidence of erosion of 25 to 100 m of QTa. Soil development consists of a 10- to 40-cm-thick vesicular A horizon, a 50-cm-thick argillic horizon engulfed by Stage IV K horizon, opaline silica lenses up to 5 cm thick, and Stage IV K horizons 2 to 3 m thick. Desert pavement is very densely packed and poorly to moderately sorted. Desert varnish is shiny brownish black to black, 0.5 to 2 mm thick, and continuous.

3.3 SOIL-GEOMORPHOLOGY STUDIES IN CRATER FLAT (PETERSON, 1988)

Peterson (1988) evaluates geomorphic relationships and soils in the Crater Flat area, which is less than 5 km west of Midway Valley. The purposes of Peterson's study were to (1) delineate the major geomorphic surfaces in Crater Flat, (2) describe soils on geomorphic surfaces to identify taxonomic and soil features that may define a surface, and (3) resolve how the surficial mapping of Swadley et al. (1984) relates to geomorphic surfaces and soils. Peterson's study was part of a much larger effort by the State of Nevada to evaluate the geology and seismotectonic stability of the Yucca Mountain area.

Taking advantage of the near-ubiquitous desert varnish that coats surficial clasts on fan surfaces, Peterson assigns ages to geomorphic surfaces. He utilizes ^{14}C-dating techniques for basal rock varnish and the varnish cation ratio (VCR) method applied by Dorn (1988). Potential problems with rock varnish dating are discussed in Section 3.5. The following discussion of Peterson (1988) is divided into three topics: geomorphic surfaces, soils data, and conclusions of Peterson.

Geomorphic Surfaces

The geomorphic surfaces in Crater Flat were not mapped formally by Peterson (1988); however, he examined the mapping of Swadley et al. (1984) in the field and checked boundaries of geomorphic surfaces on 1:24,000-scale aerial photographs. From these Peterson (1988) defines five major geomorphic surfaces. From youngest to oldest, these are: Crater Flat, late Holocene (less than 7.3 thousand years old [ka]); Little Cones, early Holocene or late Pleistocene (more than 7.3 ka but less than 19 ka); Black Cone, late to mid-Pleistocene (more than 19 ka but less than 360 ka); Yucca, mid-Pleistocene (more than 360 ka but less than 660 ka); and Solitario, mid- to early-Pleistocene (more than 660 ka). Table 3-4 summarizes the ages and characteristics of the geomorphic surfaces. As indicated in the table, ages are based on radiocarbon dating of rock varnish, VCR dating, and stratigraphic position.

TABLE 3-4

GEOMORPHIC SURFACES AND AGES ON THE PIEDMONT SLOPES IN CRATER FLAT (MODIFIED FROM PETERSON, 1988).

Geomorphic Surface	Age (ka)	Characteristics
Crater Flat	<< 7.3[1]	Active recently active washes, inset fans, and fan skirts. May have open, poorly sorted, "proto-desert-pavement" development. Soils are classified as Typic Torriorthents. Very slight accumulation of carbonate on pebble bottoms but no secondary opaline silica accumulation. Microtopography is best for age distinctions within this surface.
Little Cones	> 7.3[2], << 19[3]	One large fan skirt remnant surrounding Little Cones. Geomorphic position demonstrates relative age. Slightly varnished desert pavement. Soils are classified as Typic Camborthids and Camborthidic Torriorthents. Thin Av, Bk to Bwk, Stage I carbonate morphology.
Black Cone (three subunits)	> 19[2], << 360[4]	Fan piedmont remnants. Two ages of surfaces: Late Black Cone and Early Black Cone.
• Late Black Cone (mixed limestone and volcanic alluvium)	28.3[2]	Lower fan piedmont remnants. Pavement well sorted and closely spaced. Limestone clasts deeply etched; volcanic pebbles darkly varnished. Soil are classified as Typic Calciorthids. Soils have Av, Avk, Bwk (Stage II to III). .
• Late Black Cone (volcanic alluvium)	19[2] - 33.4[2]	Lower fan piedmont remnant. Well-sorted pavement development with thinly varnished clasts (some darkly varnished). Soils are classified as Haplic Durargids and Typic Haplargids. Soil have Av, Ak, minimal argillic, and haplic duripan. Parts of Bt are noncalcareous.

TABLE 3-4

GEOMORPHIC SURFACES AND AGES ON THE PIEDMONT SLOPES IN CRATER FLAT (MODIFIED FROM PETERSON, 1988)

Geomorphic Surface	Age (ka)	Characteristics
• Early Black Cone (volcanic alluvium)	128[5], 137[5]	Mid-fan piedmont remnants. Pavement clasts commonly are darkly varnished. Soils are classified as Typic Durargids. Soils have Av, Avk, 7.5YR argillic horizon with secondary opaline silica and carbonate accumulations.
Yucca	> 360[5], < 660[6]	Deeply dissected upper-fan piedmont remnants. Pavement and varnish variable. Cobbles and pebbles may be darkly varnished. Stone spalling results in clasts that are not darkly varnished. Soils are classified as Typic Durargids. Soils have Av, Avk, partly noncalcareous argillic horizon, strongly cemented duripan up to 0.5 m thick.
Solitario	>> 660[5]	Single ballena. Volcanic clasts are darkly varnished. Gravel-sized chips of duripan laminae are on surface. There is no Solitario surface soil; the soils consist of a complex of younger soils over a duripan stripped of the original Av and Bt horizons. Soils are classified as Typic Durorthids and Typic Durargids in small areas on the ballena.

[1] Age based on stratigraphic relations to the Little Cones surface.
[2] Age based on ^{14}C-date of rock varnish.
[3] Age based on stratigraphic relations to the Black Cone surface.
[4] Age based on stratigraphic relations to Yucca surface.
[5] Age based on VCR date.
[6] Age based on stratigraphic relations to the Solitario surface.

Peterson's work indicates that one or more map units of Swadley and Hoover (1983) and Swadley et al. (1984) comprise a given geomorphic surface. Units Q1a, Q1b, and Q1c of Swadley and Hoover (1983) are correlated with the Crater Flat surface. The Little Cones surface is shown to be Q1 by Swadley et al. (1984). The Black Cone surface was mapped as Q2b and Q2c by Swadley and Hoover (1983). The Yucca and Solitario surfaces are correlated with QTa, but the Yucca surface also is mapped partly as Q2bc. Similar correlations were made to the stratigraphy of Taylor (1986).

Soils Data

Peterson (1988) describes the alluvium of Crater Flat as extremely gravelly, cobbly, or stony sand to sandy loam. The alluvium exposed in excavations was composed entirely of either volcanic clasts or a mixture of limestone, volcanic and metamorphic rocks.

Peterson (1988) found that soils developed on different geomorphic surfaces are distinctly different and reflect the age of the surface. Characteristics of these soils are summarized in Table 3-4. Peterson (1988) presents detailed soil descriptions in his Appendix II (his pp. 26-49). Estimates of the volume percent of particles >2 mm and of weight percent of sand, silt, and clay are presented with soil descriptions. Detailed site descriptions are included with each soil description.

Conclusions of Peterson

In the Crater Flat area, Peterson (1988) identified five geomorphic surfaces and assigned ages to them based on radiocarbon dating of desert varnish, VCR dating, relative geomorphic position, and soil development. This work forms the basis for his criticisms of the work of Hoover et al. (1981), Swadley et al. (1984), and Taylor (1986).

Peterson (1988) criticizes this previous work on several bases. He questions their use of the Av horizon as the major criterion for distinguishing Pleistocene from Holocene surfaces. Peterson states that the criterion could be effective if the Av horizon were "operationally" defined and if the time required for dust accumulation sufficient to form the Av horizon could be determined.

Peterson (1988) also criticizes Hoover et al. (1981) for treating pedogenic soil horizons as if they date the surficial deposit in which the horizon occurs rather than dating the onset of long-term stability of the surface developed on the deposit. Peterson also claims that Hoover et al. (1981) do not recognize that pedogenic soil horizons can contain features that are "age-related to younger geomorphic surfaces formed on top of them, or to changed environments operating on the initial or younger geomorphic surface and the horizons under it" (Peterson, 1988, p. 3).

Peterson (1988) believes that Swadley and Hoover (1983) and Swadley et al. (1984) failed to distinguish three separate geomorphic surfaces and the related soils in their QTa unit in Crater Flat (Peterson's Black Cone, Yucca, and Solitario surfaces), and that their Q2 unit included two separate geomorphic surfaces (Peterson's Little Cone and Black Cone surfaces). Peterson states that "geomorphic surfaces, defined and mapped in terms of soils and stratigraphic relations, should be used as the geomorphic dating tool for neotectonic studies" (1988, p. 23).

3.4 SOILS-GEOMORPHIC RELATIONSHIPS ALONG YUCCA AND FORTYMILE WASHES (TAYLOR, 1986)

Taylor (1986) mapped fluvial, debris flow, eolian, and sheetwash deposits along Yucca and Fortymile washes to (1) assess the influence of time and climate on soil development, and (2) model calcic horizon development to quantify the variability in past Quaternary climates in the area. The study, which was part of a much larger effort by the U.S. Geological Survey to reconstruct the paleoclimate of the Quaternary, emphasized the past 45 ka (Winograd and Doty, 1980; Winograd, 1981; Spaulding, 1985). The following discussion of Taylor (1986) is divided into three topics: map units, soils data, and changes in soil properties with time.

Map Units

Taylor (1986) adopts the Quaternary stratigraphic framework of the NTS region that was developed by Hoover et al. (1981) and Swadley (1983) (see Section 3.2). Stratigraphic units were identified on the basis of geomorphic position, surface morphology, degree of desert pavement development, desert varnish, and soil profile development. Table 3-5 summarizes the ages and diagnostic characteristics of these map units. Twenty backhoe trenches were excavated on the stable parts of fluvial terraces and alluvial fan surfaces. The locations of these trenches are shown on Figure 3-1 and Plate 3.

Taylor (1986) maps six Tertiary to Quaternary geologic units along Yucca and Fortymile washes. Figure 3-1 shows Taylor's geologic map of Quaternary/Tertiary deposits and Tertiary bedrock in the Midway Valley area. QTa is the most areally extensive surficial unit in the area. Large areas north and south of Yucca Wash are underlain by QTa, which is present from the headwaters southeastward to near the confluence of Yucca and Fortymile washes.

Units younger than QTa, except for unit Q2c below the confluence of Yucca and Fortymile washes, are laterally discontinuous at this map scale (Figure 3-1). Fluvial units along Fortymile Wash are more widespread and laterally continuous than the same units along Yucca Wash. The small scale (~ 1:59,000) of the map in Taylor (1986), however, makes it difficult to discern relations between map units along washes.

As summarized in Table 3-5, Taylor (1986) recognizes fluvial, debris flow, sheetwash, and eolian deposits. Fluvial deposits are poorly to moderately sorted, are poorly to well bedded, and contain angular to subrounded clasts. All fluvial terraces are interpreted to be fill terraces, although Taylor (1986) presents few data to support this conclusion. Debris flow deposits are reported to be matrix-supported, poorly sorted, and massive; clasts are angular to subrounded. Sheetwash deposits are moderately well sorted and may be thinly bedded. Eolian deposits include moderately sorted to well-sorted sand and silt.

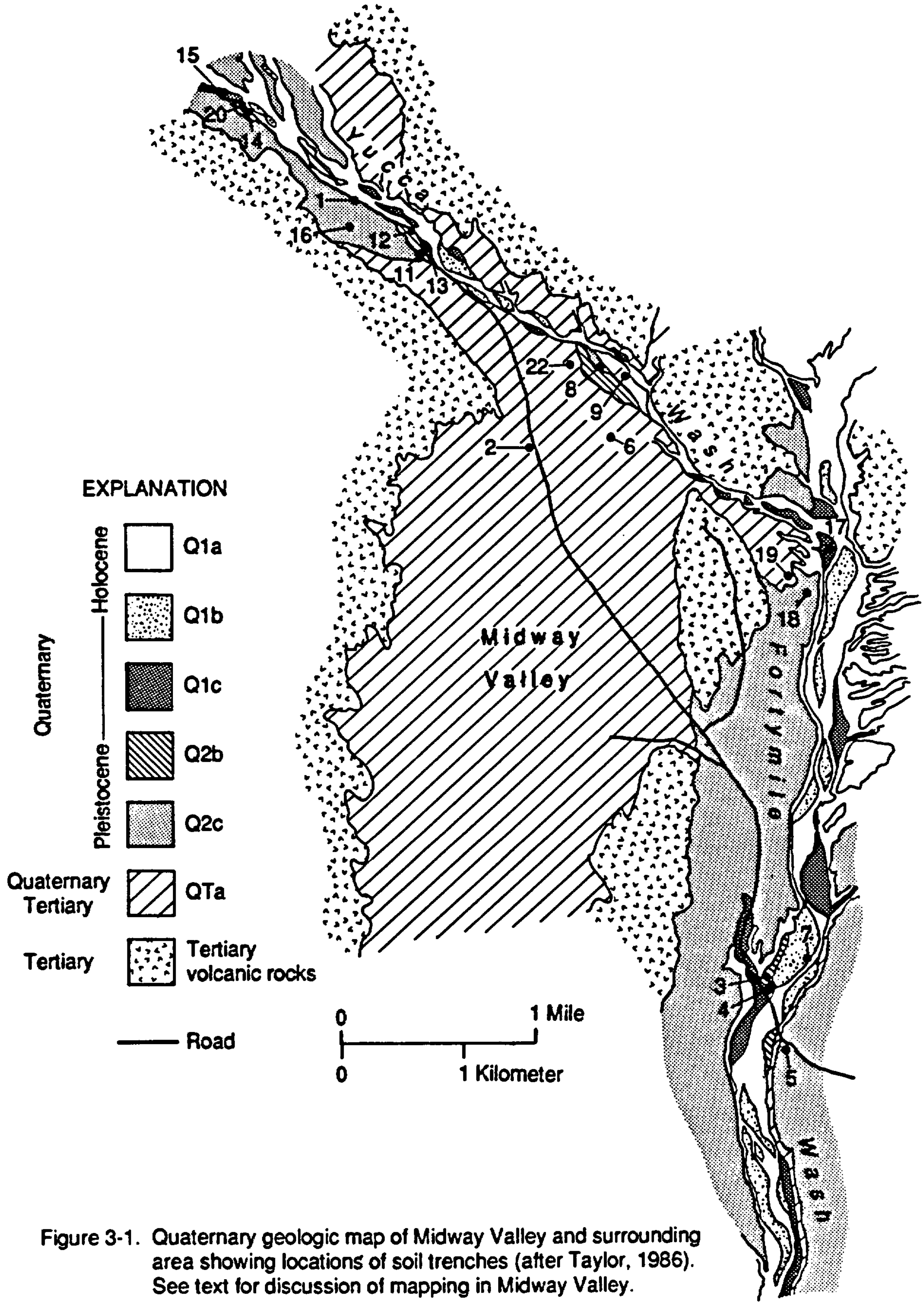

Figure 3-1. Quaternary geologic map of Midway Valley and surrounding area showing locations of soil trenches (after Taylor, 1986). See text for discussion of mapping in Midway Valley.

TABLE 3-5

MAP UNITS OF THE YUCCA AND FORTYMILE WASHES (SUMMARIZED FROM TAYLOR, 1986)

Depositional Unit	Age (ka)	Characteristics
Q1a	0	Active wash. No soil development.
Q1e	0	Eolian sand in active dunes. No soil development.
Q1b	<0.14	Fluvial deposits 0.5 to 2 m above active wash. Bar-and-swale topography preserved; no desert pavement development. Soil profiles have thin A and C (Cox, Cuk, and/or Cu) horizons and Stage I (locally Stage II) carbonate morphology.
Q1s	3.3-7	Slope wash or sandsheets. Dissected near active channels. Soils have A and B (Bw, Bkj, Btj, and/or Bqj) horizons, Stage I to II carbonate morphology, and Stage I silica morphology.
Q1c	~10	Fluvial terraces 1 to 2 m above active wash (may include fan, colluvium, or sheetwash deposits). Lacks bar-and-swale topography; incipient desert pavement development and little to no varnish. Soils have A and B (Bw, Bkj, Btj, and/or Bqj) horizons, Stage I to II carbonate morphology, and Stage I silica morphology.
Q2a	30-47	Sandy slope wash containing <25% gravel; lacks topographic expression. Soils have Av and B (Bt and/or Bk) horizons and Stage I carbonate morphology.
Q2b	145-160	Fluvial gravel on strath terraces 5 to 12 m above active channels and debris flow fans. Desert pavement is well sorted and tightly packed. Clasts are darkly varnished. Soils have Av and B (Bw, Bt, Bqm, and/or Bk) horizons, Stage I to II carbonate morphology, and/or Stage II to III silica morphology.

TABLE 3-5

MAP UNITS OF THE YUCCA AND FORTYMILE WASHES (SUMMARIZED FROM TAYLOR, 1986)

Depositional Unit	Age (ka)	Characteristics
Q2c	270-430	Fluvial gravel and debris flow deposits. Fluvial gravels underlie terrace 10 to 21 m above active channel. Desert pavement is well sorted and tightly packed. Clasts are darkly varnished. Soils have Av and B (Bt, Bqm, and/or B/K) and K (Kqm) horizons, Stage III to IV carbonate morphology, and/or Stage III silica morphology.
n Q2e	<738	Eolian sand in dunes and sand ramps. Desert pavement is well sorted and tightly packed. Clasts are darkly varnished. Soils have Av, B (Bk, Bkq, and/or B/K), and K horizons; Stage III to IV carbonate morphology; and/or Stage III to IV silica morphology.
Q2s	<738	Slope wash or sand sheets derived from sand ramps. Lacks desert pavement. Soils have A, B (Bk, Bkq, and/or Bk), and K horizons, Stage III to IV carbonate morphology, and Stage III to IV silica morphology.
QTa	1100-2000	Eroded alluvial fans 20 to 30 m above active channels. Desert pavement is well sorted and tightly packed; contains opaline silica platelets. Clasts have continuous dark varnish. Soils have A (or Av), B (Bt, Bqm, and/or B/K), and K (Kqm and/or Kmq) horizons; Stage III to IV carbonate morphology; and Stage III to IV silica morphology.

The aged ages of map units presented in Table 3-5 were assigned based on an inferred correlation with the stratigraphy and dates of Hoover et al. (1981), Szabo et al. (1981), and Swadley and Hoover (1983). The ages in these latter studies are assigned primarily on the basis of uranium-trend dating of deposits from trenches excavated to evaluate fault activity and not from exposures specifically chosen to date the deposits. (Age-dating of Quaternary stratigraphic units is an objective of future site characterization activities.) The estimated age of channel incision, radiocarbon ages, and correlation of volcanic ashes also were used to estimate the ages of deposits. Further discussion of age-dating is presented in Section 3.5.

Soils Data

Soils were described by Taylor (1986) using the terminology of the Soil Survey Staff (1951) and Birkeland (1984). In addition, Taylor (1986) developed a methodology for describing secondary silica morphology that is similar to the carbonate morphology nomenclature of Gile et al. (1965, 1966, 1979), because secondary "silica accumulation produces a unique morphology that varies with age" (Taylor, 1986, p. 30). Table 3-6 presents the general characteristics of pedogenic silica morphology as defined by Taylor (1986). This terminology, however, is untested in other areas and must be applied with caution.

Soil descriptions of Taylor (1986) are presented in Table D-1 in Appendix D of this report. From these data, Taylor calculated the profile development index (PDI) of Harden (1982) using a spreadsheet template developed by Nelson and Taylor (1985a) and Taylor (1988).

Taylor (1986) analyzed selected soil samples for particle size, bulk density, carbonate content, soluble salt content, gypsum content, organic carbon content, loss on ignition, pH, secondary silica content, clay mineralogy, dithionite extractable iron content, and oxalate extractable iron content. The methods for these laboratory analyses are discussed in Appendix C of Taylor (1986, her pp. 161-164). The results of these analyses are presented in Tables D-2 and D-3 in Appendix D of this report.

TABLE 3-6

CHARACTERISTICS OF PEDOGENIC SILICA STAGES (TAYLOR, 1986, P. 31).

Stage I	"White, yellow, or pinkish scale-like coatings <2 mm thick on the undersides of gravel clasts. Found in soils on Q1c deposits; may occur at depths on older deposits."
Stage II	"Stalactitic or pendant features 2-4 mm long extending downward from a coat on the undersides of gravel clasts. Found in soils on Q2b deposits; may occur at depths on older deposits."
Stage III	"Opaline SiO_2 cemented horizon, extremely hard when dry. Peds do not slake in water or a weak solution of HCl. The color is 7.5YR, probably due to clay particles in the silica cement. Found in soils on Q2b, Q2c and QTa deposits; maximum accumulations tend to form in horizons of maximum $CaCO_3$ accumulation. Frequently in the field stage III appears to be forming above the maximum accumulation of $CaCO_3$ because the whiteness of the $CaCO_3$ masks the precipitated SiO_2."
Stage IV	"Stage III morphology with laminar, indurated opaline SiO_2 platelets, 4-10 mm thick, in the upper part. Maximum $CaCO_3$ accumulation is below maximum opaline SiO_2 induration. Commonly calcareous ooids are precipitated above platelets. Found in soil on Q2c (infrequently and thin) and QTa deposits."

Changes in Soil Properties with Time

Taylor (1986) identifies distinctive trends that relate deposit age to soil morphologic development and accumulation of secondary silica, carbonate, and clay. Soil morphologic properties were quantified by calculating normalized properties and the profile development index (PDI) of Harden (1982). Quantified properties include dry consistence, color lightening, rubification, structure, texture, clay films, and total PDI, all of which increase logarithmically as a function of deposit age. No relationship between Av thickness and age was observed for soils of the Midway Valley area. Secondary carbonate, clay, silt, and opaline silica appear to accumulate at logarithmic rates, and soils of latest Pleistocene to Holocene age appear to be accumulating "at a higher average rate than the older soils" (Taylor, 1986, p. 87). Taylor (1986) notes that climate and the availability of eolian material on the surface may control accumulation rates.

Taylor (1986) relates the relative abundance and type of clay minerals in the soils to climate but detects little change in clay mineralogy with age of the deposit. The overall clay content increases with age of the soil.

3.5 DATING METHODS USED IN THE YUCCA MOUNTAIN REGION

Dating methods used in Quaternary geologic studies in the Yucca Mountain region include uranium-series, uranium-trend (i.e., uranium-series disequilibrium), radiocarbon (^{14}C), and, more recently, ^{14}C-dating of desert varnish, varnish cation ratio (VCR), and thermoluminescence (TL). Other techniques for evaluating relative ages of geomorphic surfaces include rock weathering, surface morphology, desert varnish development, cosmogenic radionuclides, and soil profile development.

Ku (1988) provides a concise review of the uranium-series method of dating Quaternary surficial deposits and a review of work in the Yucca Mountain area that utilizes this method. Uranium-series dating was first applied to pedogenic carbonate by Bull and Ku (1975) and Ku et al. (1979) in the Vidal area. In Midway Valley, Szabo et al. (1981) dated carbonate and silica by the uranium-series method. The loosely constrained results obtained by Szabo et al. were attributed to the assumption that the carbonate/silica chemical system is a closed one. Muhs et al. (1990) applied a uranium-series disequilibrium method to calcium carbonate deposits exposed in trenches in Midway Valley. Uranium-trend methods assume an open system and therefore may be more applicable to the soil system. The uranium-trend method has been used most extensively by Swadley et al. (1984) for fault trench studies in and around Midway Valley.

Radiocarbon (^{14}C) dating in the Yucca Mountain region has been of limited value because of the generally oxidizing desert environment, resultant destruction of organic materials, and paucity of preserved samples. Radiometric dating of packrat middens and organic material in marsh deposits (Haynes, 1967; Quade and Pratt, 1989) has provided some age control for Holocene deposits in the region.

Advances have been made since the early attempts by Knauss and Ku (1980) to apply uranium-series methods to desert varnish. Varnish cation-ratio (VCR) dating and ^{14}C-dating of desert varnish were conducted in Crater Flat adjacent to Yucca Mountain by Harrington and Whitney (1987) and by Dorn (1988). However, the methods and approaches to varnish dating are controversial (Harrington and Whitney, 1987; Dorn, 1988; Bierman and Gillespie, 1990; Harrington et al., 1990; Krier et al., 1990). Bierman and Gillespie (1990) question the precision of measured VCR and the resulting ages. They note that a small error in precision can translate into large errors in age. Harrington et al. (1990) and Krier et al. (1990) discuss problems with the construction of VCR dating curves in areas of young volcanism; cation ratios apparently correlated better to a site's proximity to the volcanic center than to age because titanum-rich volcanic ash is incorporated into the varnish. VCR dating appears promising, but the data derived should be confirmed independently whenever possible as there are potential problems with the analytical procedures, the precision of the technique, and sampling methods.

Thermoluminescence (TL) is a relatively new technique for dating Quaternary deposits. Forman (1988) briefly reviews the technique and summarizes its application at Yucca Mountain. Most research that utilizes TL-dating methods has been applied to fault studies in Utah. More recently, Whitney et al. (1986) applied TL to trench studies in Crater Flat and dated the Av horizon in trenches CF-2 and CF-3. The Av horizon, which was displaced less than 10 cm by faulting, yielded a TL date of 3 to 6.5 ka. The study focuses on the processes involved in development of the Av horizon rather than on the methodology.

Other relative age-dating techniques are applicable to Quaternary geologic studies in desert regions. McFadden et al. (1989) review the use of multiparameter relative-age methods for age estimation and correlation of alluvial fan surfaces in the Silver Lake region south of Death Valley. Some of the relative-age parameters of McFadden et al. (1989) include particle size, relative abundances of lithologies of surface particles, surface pitting of clasts, varnish, rubification, roundness, weathering rind thickness, grain relief on clasts, and hammer-blow/ring ratios.

4.0 FAULTING IN THE MIDWAY VALLEY AREA

4.1 TECTONIC SETTING

Midway Valley is situated within the Walker Lane belt, which is a major tectonic element of the North American/Pacific plate boundary (Figure 4-1). The Walker Lane belt is a northwest-trending zone of strike-slip and extensional deformation that separates a regime of right-lateral transpression, centered on the San Andreas fault to the west and south, from a regime of crustal extension in the Basin and Range province to the north and east (Stewart, 1980; Carr, 1984). The transition zone between these tectonic regimes has existed since at least the early Miocene and has produced a complex overprinting of structural styles in the Yucca Mountain area (DOE, 1988; Fox and Carr, 1989).

Post-Miocene upper-crustal deformation within the southern part of the Walker Lane belt is characterized by four primary structural elements: north- to north-northeast-trending normal faults (Lipman and McKay, 1965; Carr, 1984; Scott and Bonk, 1984); northwest-trending, right-lateral strike-slip faults (Carr, 1984; Scott, 1984; Scott and Bonk, 1984); northeast-trending, left-lateral strike-slip faults (Carr, 1984); and clockwise, rigid block rotations about a vertical axis (Scott and Rosenbaum, 1986). In addition, some amount of the horizontal displacement associated with these structural elements probably is accommodated at depth by slip on one or more low-angle detachment faults that do not crop out in the Midway Valley area (Scott, 1988; DOE, 1988; Maldonado, 1990). Seismicity data from historical and instrumental records, as well as results from several studies on the magnitude and orientation of principal stress directions in the area (DOE, 1988), are consistent with the observed style of deformation in the southern Walker Lane belt.

North-trending Normal Faults. North- to north-northeast-trending normal faults are a prominent tectonic feature within the southern part of the Walker Lane belt (Figure 4-2) (DOE, 1988). Displacement on these faults accommodates west-northwest regional extension, producing the tilted fault blocks of the Midway Valley area that are characteristic

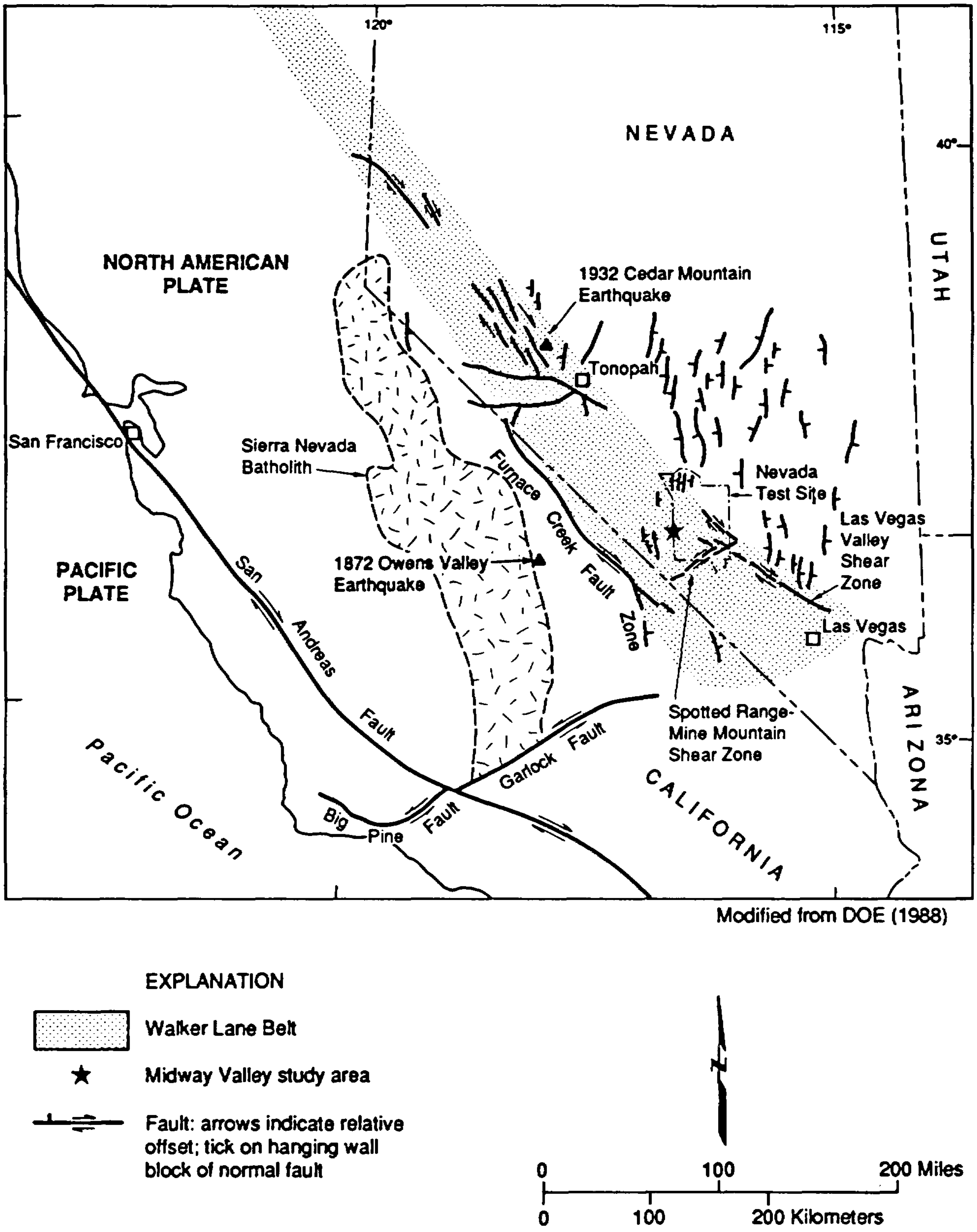

Figure 4-1. Regional tectonic setting.

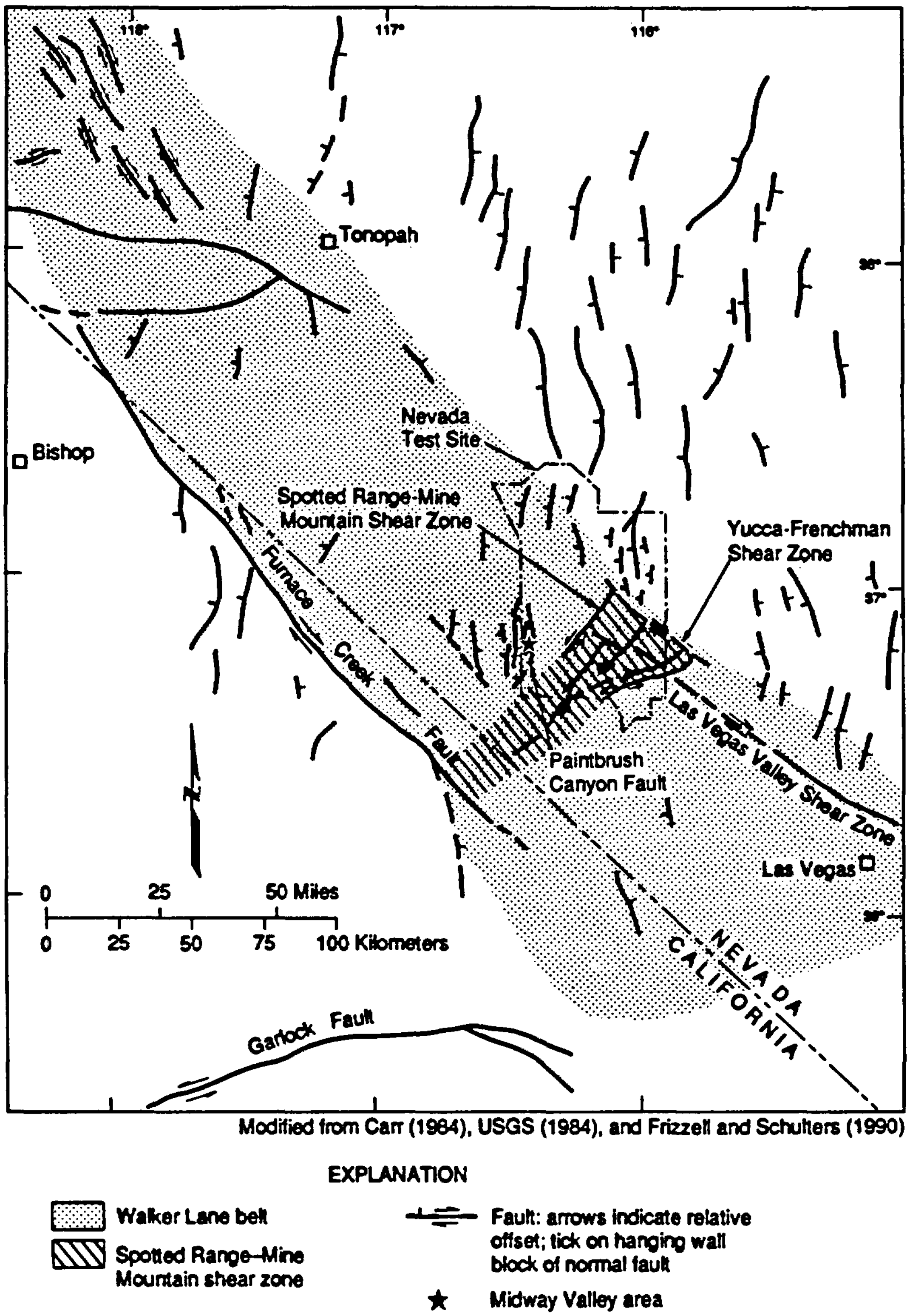

Figure 4-2. Tectonic setting of southwest Nevada and adjacent California showing relation of study area to the southern Walker Lane belt.

of the Basin and Range province (Lipman and McKay, 1965; Scott and Bonk, 1984; Carr, 1984). Although the timing of displacements on these faults is not known precisely, their geomorphic expression as range-front faults and limited data from trenches excavated across them in the Midway Valley area indicate that they have experienced very low slip rates during the Quaternary (see Section 4.3). The north to north-northeast trend of these faults in the Midway Valley area relative to the north to north-northwest trend of similar faults in the southern Basin and Range province to the north may reflect distributed right-lateral shear and/or block rotation in the southern Walker Lane belt.

Northwest-trending, Right-lateral Strike-slip Faults. The northeast and southwest boundaries of the southern Walker Lane belt, and to a lesser extent the interior of the belt, are marked by discontinuous, northwest-trending, right-lateral strike-slip faults (Figures 4-1 and 4-2) (DOE, 1988). The overall right-lateral shear associated with the Walker Lane belt is indicated by a deflection of the regional structural grain from slightly west of north in the southern Basin and Range province to slightly east of north within the Walker Lane belt. Estimates of the total displacement along the Walker Lane belt associated with this deflection range from 70 km (Fleck, 1970) to 190 km (Stewart et al., 1968). Albers (1967) reports that northwest-trending strike-slip faults locally displace deposits of Quaternary age; however, the rate and magnitude of slip associated with these displacements are not well defined.

The Las Vegas Valley shear zone is a northwest-trending, right-lateral shear zone within the southern Walker Lane belt (Figures 4-1 and 4-2) (Carr, 1984). A lack of geomorphic evidence for Quaternary activity suggests that Quaternary slip rates within this zone may be extremely low or that it may be inactive (DOE, 1988). Movements more recent than 17 Ma on the Las Vegas Valley shear zone are reported by Burchfiel (1965) and Ekren (1968). According to Fleck (1970), most of this movement took place before 10.7 Ma. Burchfiel (1965) and Ekren (1968) suggest that the Las Vegas Valley shear zone may extend northwest at depth beneath the Yucca Mountain region and that its expression at the surface may be subtle. In this interpretation, northwest-trending, right-lateral strike-slip faults observed in the Midway Valley area (e.g., Yucca Wash, Sever Wash, Pagany Wash, and Drill Hole Wash faults) are the result of slip at depth on the Las Vegas Valley shear zone.

Data from the Cedar Mountain earthquake of 1932, which occurred about 200 km northwest of Yucca Mountain (Figure 4-1), are consistent with the interpreted sense of displacement on the Las Vegas Valley shear zone. Seismicity data from the estimated Richter magnitude (M) 7.2 to 7.3 Cedar Mountain earthquake suggest that the rupture occurred on a steeply dipping, northwest-trending structure and that slip was predominantly right lateral (Molinari, 1984). Surface deformation was expressed as a 60-km-long system of ruptures attributed to slip on northwest-trending, en echelon strike-slip faults in the upper crust (Gianella and Callaghan, 1934).

Northeast-trending, Left-lateral Strike-slip Faults. Northeast-trending, left-lateral strike-slip faults also occur in the southern Walker Lane belt. The largest of these faults proximal to the Midway Valley area lie within the Spotted Range/Mine Mountain shear zone, a 26- to 40-km-wide zone of discontinuous faults having displacements as great as 1 to 2 km (Figure 4-2) (Carr, 1984). Several of these faults displace Quaternary lithologic units and appear to be associated with a northeast-trending belt of seismicity (Nevada Test Site Paleoseismic Zone of Carr, 1984) located approximately 25 km east of the Midway Valley area. The Spotted Range/Mine Mountain shear zone appears to terminate to the northeast against the northwest-trending Yucca/Frenchman shear zone, a zone of right-lateral strike-slip faults that is subparallel to the Las Vegas Valley shear zone (Figure 4-2) (Carr, 1984).

Vertical Axis Block Rotations. In the Yucca Mountain region, paleomagnetic data from the Tiva Canyon Member of the Paintbrush Tuff indicate that vertical axis block rotations of up to 30 degrees have occurred since approximately 13 Ma (Scott and Rosenbaum, 1986; Rosenbaum et al., in press). Although the distribution of these rotations within the Midway Valley area is not well constrained, the data suggest an overall southward increase in amount of rotation. The age of the inferred rotations indicates that this style of deformation coincides with post-mid-Miocene to Quaternary activity on the regional fault systems described above.

Seismicity. Historical and instrumental seismicity data are important for understanding the present tectonic character of the Midway Valley area (DOE, 1988). The Walker Lane belt, as characterized by its seismicity, is a transition zone between predominantly normal focal mechanisms to the north and east and predominantly strike-slip focal mechanisms to the south and west. The area surrounding Yucca Mountain is characterized by few hypocenters and a low density of seismic energy, indicating local quiescence. Earthquake focal depths range from less than 1 km to 17 km; most earthquakes occur at depths of 0 to 2 km and 5 to 8 km. Focal mechanisms from 29 earthquakes in the NTS region evaluated by Rogers et al. (1987) indicate that the direction of minimum horizontal stress is between N50°W and N70°W; the magnitudes of the vertical stress and the maximum horizontal stress appear to be approximately equal. This stress configuration favors normal slip on northeast-striking faults, right-lateral strike slip on north-striking faults, and left-lateral strike slip on east-northeast-striking faults (DOE, 1988).

The seismicity data of Rogers et al. (1983, 1987) suggest that in this area north- to east-northeast-striking faults are more active than faults of other orientations. This finding is corroborated by Vetter (1990), who notes that the small to moderate earthquakes that have occurred in the western Great Basin during the past 30 years, as well as the 1872 Owens Valley earthquake (Figure 4-1), estimated to have a body wave magnitude (M_b) of 8.25 and the 1932 Cedar Mountain earthquake, estimated to be M 7.2 to 7.3, show a dominance of strike-slip displacement over vertical displacement. The 1872 Owens Valley earthquake, which occurred about 150 km west of Yucca Mountain, is the nearest major historical earthquake. Most of the major faults in the region exhibit a large component of normal displacement; the predominance of strike-slip displacement in the historical seismicity is not well understood. Vetter (1990) states that the recent small to moderate earthquakes may be unrepresentative of larger future earthquakes, which are expected to have normal displacements.

Depolo et al. (1990) examined historical earthquake data from the Basin and Range province to estimate the maximum background, or random, earthquake (i.e., the largest event that could occur without primary surface rupture) in the Yucca Mountain region. Data compiled from 38 historical earthquakes of about magnitude 6 and greater suggest that the maximum background earthquake for the Basin and Range province is at least M 6.3 and may be as high as M 6.8 (Depolo et al., 1990).

Stress Regime. The Basin and Range province appears to be characterized by a least horizontal principal stress direction that is oriented west-northwest (Zoback and Zoback, 1980). In the region of the Nevada Test Site, studies based on a variety of geologic data, earthquake focal mechanisms, and in situ stress measurements indicate either normal or strike-slip faulting and least horizontal principal stress orientations of N50°W to N70°W (e.g., Carr, 1984; Rogers et al., 1983 and 1987; Stock et al., 1985; Frizzell and Zoback, 1987; and Stock and Healy, 1988).

Frizzell and Zoback (1987) used fault-slip data obtained from the southern part of the Nevada Test Site to estimate principal stress orientations. The fault-slip data indicate nearly pure strike-slip and pure normal dip-slip faults, suggesting that both normal and strike-slip faulting may be compatible with deformation in the current stress regime (Frizzell and Zoback, 1987).

Based on stress measurements from hydraulic fracturing in four drillholes in the Yucca Mountain area, Stock and Healy (1988) found the orientation of the least horizontal stress axis to be between N60°W and N65°W. Calculated values of the greatest horizontal stress (S_H) are intermediate between the least horizontal stress (S_h) and the vertical stress (S_v, which is assumed to be vertical because no shear stress can be applied across the free face of the earth/atmosphere interface). These reported stress magnitudes suggest a normal-faulting stress regime.

4.2 GEOLOGIC STRUCTURE OF THE MIDWAY VALLEY AREA

Two of the three principal styles of faulting that occur within the southern Walker Lane belt are mapped in the Midway Valley area: north- to north-northeast-trending normal faults and northwest-trending, right-lateral strike-slip faults. Northeast-trending, left-lateral strike-slip faults have not been mapped in the Midway Valley area. A series of north-trending structural blocks, bounded by major north-trending, predominantly normal, faults is the most prominent structural feature in the Yucca Mountain area. These normal faults generally dip steeply toward the west and have vertical displacements of hundreds of meters. Scott (1984) postulates that some blocks bounded by major normal faults typically have an internal structure that ranges from simple on the west to complex on the east. The eastern parts of the blocks commonly contain abundant west-dipping normal faults having vertical displacements that generally are less than three meters ("imbricate zone" of Scott and Bonk, 1984). The downthrown sides of the major normal faults typically contain chaotic brecciated fault zones as much as 500 m wide. Several northwest-trending, right-lateral strike-slip faults are mapped in bedrock exposures at Yucca Mountain north of Drillhole Wash (Plate 1) (Scott and Bonk, 1984). The mapped faults are closely associated with a group of well-developed northwest-trending washes, suggesting that development of the washes may be structurally controlled. Scott and Bonk (1984) and Frizzell and Shulters (1990) map the northwest-trending Yucca Wash fault as projecting across Midway Valley from Yucca Wash to just west of the Paintbrush Canyon fault at the base of Alice Ridge.

Local Faults. Three normal faults have been identified in Midway Valley near the prospective surface facilities: the Bow Ridge fault, the Paintbrush Canyon fault, and the postulated Midway Valley fault (Figure 1-2; Plate 1). The Bow Ridge and Paintbrush Canyon faults are exposed locally in bedrock outcrops on the southern end of Midway Valley and along the sides of the valley (Scott and Bonk, 1984). The postulated Midway

Valley fault is exposed in bedrock at the southern end of Midway Valley; evidence that the fault extends north beneath the valley alluvium is equivocal.

The Yucca Wash fault is mapped along the northwest-trending Yucca Wash at the northern end of Midway Valley. The fault, which is concealed by alluvium, is interpreted as a right-lateral strike-slip fault (Scott and Bonk, 1984; Carr, 1984).

Mapped sections of the Bow Ridge, Paintbrush Canyon, Midway Valley, and Yucca Wash faults that are obscured by alluvium are correlated with anomalies observed in geophysical survey data (Scott and Bonk, 1984) (see Appendix B). Although many of the anomalies detected by geophysical methods can be interpreted as faults, these data are insufficient to provide unequivocal characterization. Downhole logging of lithologic contacts and dip attitudes in drillholes provide some structural information, but these data lack adequate control of strike orientation.

Estimates of vertical displacement on the Bow Ridge, Paintbrush Canyon, and postulated Midway Valley faults vary considerably among published reports (USGS, 1984; Carr, 1984; Scott and Bonk, 1984; Neal, 1986; DOE, 1988). In many cases, the locations of the reported displacements along the trace of the fault are not given; in some cases the name and age of the major stratigraphic unit used to estimate displacement also are not provided. Given the available information, it is difficult to characterize activity on these faults.

The most recent tabulation of vertical separation on the Paintbrush Canyon and Bow Ridge faults, which is provided by Gibson et al. (1990), is summarized in Table 4-1. Observed vertical separation of stratigraphic units and the most recently calculated ages of these units are correlated to assess the displacement history of the two faults (see Section 4.3). The locations of these displacements, however, are not given.

TABLE 4-1

PRELIMINARY DISPLACEMENT DATA FOR THE PAINTBRUSH CANYON AND BOW RIDGE FAULTS
Source: Gibson et al. (1990)

Unit	Age of Displaced Unit (Ma)	Vertical Separation (m)	Source
	Paintbrush Canyon Fault		
Tiva Canyon Member, Paintbrush Tuff	12.9 ± 1.1[a]	200	Primarily Carr (1984) In addition, USGS (1984) and DOE (1988).
Waterpipe Butte rhyolite[e]	9.6[b,c]	90	
Dome Mountain basalt[e]	9.6-9.3[c]	70	
Thirsty Canyon tuff[e]	7.5 ± 0.6[a]	45	
Alluvium (Q2e)	0.5[d] (Carr, 1984) <0.7[g] (DOE, 1988)	4.1	
Present surface	0.0	0.0	
	Bow Ridge Fault		
Topopah Spring Member, Paintbrush Tuff	13.1 ± 0.8[a]	220	USGS (1984) Marvin et al. (1970)
Tiva Canyon Member, Paintbrush Tuff	12.5 ± 1.1[a,f]	120	
Fractures in Q2s	0.27-0.038[d]	0.0	

[a] Age based on potassium-argon analysis.
[b] No error or age range was presented in the cited references.
[c] Age based on stratigraphic relationships with dated units.
[d] Age based on uranium-trend analysis.
[e] Recent work by Warren et al. (1988) supports an older age than cited by Carr (1984), Marvin et al. (1970), and Kistler (1968).
[f] Age listed in USGS (1984) differs from that cited by Carr (1984), Marvin and et al. (1970), and Kistler (1968).
[g] Age based on correlation of volcanic ash in Q2e deposits with Bishop ash.

Estimates of vertical displacement on the postulated Midway Valley fault are speculative; neither the fault nor the bedrock structure near the inferred location of the fault is exposed within the alluvium in Midway Valley. Projection of bedrock structure from Fran Ridge and Exile Hill suggests significant vertical displacement across the valley, but the rate, style, and location of this deformation are unknown. Scott and Bonk (1984) and Neal (1986) attempt to estimate the distribution and magnitude of vertical displacement across a wide fault zone concealed by alluvium in Midway Valley. Although these efforts are a significant step toward understanding the possible nature of the Midway Valley fault, the available data are insufficient, and the authors' techniques too interpretive, to yield definitive results.

Table 4-2 gives the apparent dip separations on the Bow Ridge, Midway Valley, and Paintbrush Canyon faults as measured from the cross sections of Scott and Bonk (1984), Carr (Appendix A, this report), and Neal (1986). Although these data are preliminary and are not rigorously defined, they provide estimates based on the most recent geologic mapping, drillhole data, and constrained locations of displacements.

Bow Ridge Fault. The Bow Ridge fault is a north-trending, west-dipping normal fault that extends along the western side of Midway Valley as a marginal fault to the Exile Hill and Bow Ridge bedrock/topographic highs (Figure 1-2; Plate 1). As mapped by Scott and Bonk (1984), the fault is more than 9 km long, extending from Yucca Wash on the north to south of Bow Ridge. The regional geologic maps of Maldonado (1985) and Frizzell and Shulters (1990) show the total length of the Bow Ridge fault to be about 9 to 10 km. Along most of its length, the fault is concealed beneath alluvium, but on the western edge of Bow Ridge, it is exposed in bedrock. At this exposure, 4 km south of Exile Hill, the fault dips west about 75 degrees (Scott and Bonk, 1984). South of this location, it intersects several other faults and, as mapped by Scott and Bonk (1984), bends abruptly southeast, following Bow Ridge (Figure 1-2; Plate 1). North of Exile Hill, the Bow Ridge fault is interpreted to

TABLE 4-2

STRATIGRAPHIC DIP SEPARATIONS ON THE BOW RIDGE, MIDWAY VALLEY, AND PAINTBRUSH CANYON FAULTS CALCULATED FROM THE CROSS SECTIONS OF SCOTT AND BONK (1984), NEAL (1986), AND CARR (APPENDIX A, THIS REPORT)

	Bow Ridge Fault	Midway Valley Fault	Paintbrush Canyon Fault
Neal (1986); Figure 4-12, this report. Marker Horizon: Top upper cliff unit, Topopah Spring Member, Paintbrush Tuff	145 ± 5 m	50 ± 5 m[1]	---
Carr (Appendix A); Figure 4-13, this report. Marker Horizon: Top Topopah Spring Member, Paintbrush Tuff	115 ± 5 m	50 ± 5 m[2]	---
Scott & Bonk (1984)[3]; Figure 4-11, this report. Marker Horizon: Top Topopah Spring Member, Paintbrush Tuff	145 ± 5 m	105 ± 5 m	515 ± 5 m
Scott & Bonk (1984)[3]; Figure 4-10, this report. Marker Horizon: Top Topopah Spring Member, Paintbrush Tuff	220 ± 5 m	---	220 ± 5 m

[1] Total apparent dip separation of upper cliff caprock, Tiva Canyon Member, Paintbrush Tuff, between drillhole RF #3 and outcrop on Exile Hill: values may not reflect total separation across the Midway Valley fault zone.

[2] Total apparent dip separation between Exile Hill and Midway Valley fault (six faults).

[3] Displacements do not include offsets in the inferred "imbricate zones." Apparent dip separations are measured across the primary fault and associated breccia zone only.

extend toward an oblique intersection with the poorly constrained Yucca Wash fault. The character of this fault intersection is unknown.

In areas where the Bow Ridge fault is concealed, Scott and Bonk (1984) located the fault through aeromagnetic anomalies and, locally, from electromagnetic survey data (Plate 1). Faults interpreted from anomalies in resistivity/geoelectric data were identified by Flanigan (1981), Senterfit et al. (1982), and Smith and Ross (1982). Reynolds and Associates (1985) presented seismic reflection and refraction data that suggest a down-on-the-west normal fault (Plate 4). However, confidence in these data is low (see Appendix B). Plate 4 shows the locations of these anomalies.

No displacement of alluvial surfaces has been identified along the mapped trace of the Bow Ridge fault. Trench 14 (Plate 3), excavated on the northwest side of Exile Hill, however, exposed a fault in Tertiary volcanic rocks and fractures in unconsolidated Quaternary/ Tertiary alluvium or colluvium (Swadley et al., 1984; DOE, 1988). Figure 4-3 reproduces the schematic log of Trench 14 presented by Swadley et al. (1984). The primary fault zone, exposed near the east end of the trench, appears to be nearly vertical, although the dip of the fault at depth is unknown. The fault consists of a zone of shearing several meters wide that contains breccia and blocks of Tertiary volcanic rocks. In addition, colluvium and breccia in the fault zone have "abundant laminar opaline carbonate Laminae (sic)" parallel to fractures, soil horizons, and surfaces of blocks of rock (Swadley et al., 1984). Although not addressed specifically in this log, the Tiva Canyon Member of the Paintbrush Tuff on the upthrown (eastern) block of the fault probably is juxtaposed against the Rainier Mesa Member of the Timber Mountain Tuff on the downthrown (western) block, because Scott and Bonk (1984) and Maldonado (1985) map these bedrock relationships near Trench 14.

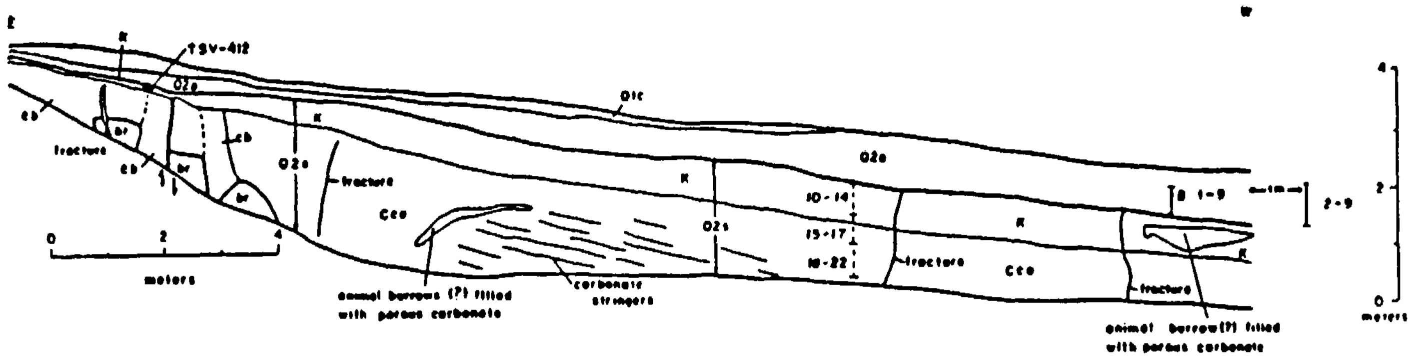

Diagram of south wall of trench 14. Trench trends east-west across the trace at fault C. Mapped in May 1982 by Swadley, L. D. Parrish, and H. E. Huckins. Fault offsets blocks of Tertiary volcanic rocks. Fractures cut Q2s and its soil but not the overlying Q2a. The K horizon that developed in Q2s extends across the fault without offset but is fractured (fractures too small to show on this figure) and fracture surfaces are coated with secondary carbonate immediately above fault. Animal burrow 5 m west of the main fault may have been dug along a fracture in Q2s. Sample locations for uranium-trend age determinations shown by bar; bar is dashed where location is projected from north wall. Sample location for uranium-series age determinations (sample TSV-412) shown by cross.

Unit	Description
Q1c	Sand, gravelly, unconsolidated
Q2a	Sand, gravelly, slightly indurated with clay
Q2s	Sand, gravelly. Exposed soil horizons developed in unit consist of K and Cca horizons
K	K horizon--sand, gravelly, stage III to IV carbonate development
Cca	Cca horizon--sand, gravelly, stage I to II carbonate development; carbonate stringers along bedding(?) surfaces
cb	Colluvium and breccia with abundant laminar opaline carbonate Laminae parallel fractures, soil horizons, and surfaces of large blocks in underlying breccia
br	Breccia and blocks of Tertiary volcanic rocks

Radiometric Ages

Sample No.	Unit	Age (in 10^3 yr)
YM 14-2 thru 9	Q2a	90 ± 50
YM 14-10 thru 14	Q2s	270 ± 90
YM 14-15 thru 17	Q2s	420 ± 50
YM 14-18 thru 22	Q2s	480 ± 90
YM 14 B-1 thru 9	Q2a	38 ± 10
TSV-412-1	Q2s K horizon	>400 and >350
TSV-412-3	Q2s K horizon	>550
TSV-412-7	Q2s K horizon	>400

Figure 4-3. Schematic log of trench 14 as presented by Swadley et al (1984, p. 34). See Plate 3 for location of trench.

The K horizon developed on unit Q2s is fractured but not significantly displaced (Figure 4-3) (Swadley et al., 1984; Taylor and Huckins, 1986; DOE, 1988). Taylor and Huckins (1986) suggest that fractures are found as far as 50 m from the primary fault zone.

Sand deposits of units Q2a and Q1c, which overlie unit Q2s, are unfaulted and unfractured (see Section 3.0 for a discussion of the Quaternary deposits of the region).

From uranium-series and uranium-trend age analyses of samples from Trench 14, Swadley et al. (1984) and DOE (1988) infer the age of the last movement on the Bow Ridge fault to be between 278 ± 90 ka and 38 ± 10 ka. However, a number of inconsistencies are apparent. Uranium-series dates of the K horizon developed on Q2s, for example, range from >350 to >550 ka; the uranium-trend date for this same horizon is 270 ± 90 ka. Also, two uranium-trend analyses of Q2a deposits from similar depths but laterally separated by approximately two meters yielded ages of 38 ± 10 ka and 90 ± 50 ka.

More recently, Taylor and Huckins (1986) correlate basaltic ash in the fault zone in Trench 14 to ash from Crater Flat, which was dated as 1.2 and 0.27 Ma. They interpret the ash to record the most recent faulting event in the trench. As part of on-going USGS investigations, five additional trenches have been excavated near Trench 14 (Plate 3). Data from these trenches are not available. Trench 15 was excavated across the Bow Ridge fault on the southwest side of Bow Ridge. Swadley et al. (1984) show this trench on their map but do not present or discuss trench logs.

Paintbrush Canyon Fault. The Paintbrush Canyon fault is a west-dipping normal fault that strikes generally north along the eastern margin of Midway Valley (Figure 1-2; Plate 1). The Paintbrush Canyon fault is the frontal fault to the north-trending Alice Ridge/Fran Ridge topographic high. Total fault length is approximately 25 km, according to Maldonado (1985) and Frizzell and Shulters (1990). Frizzell and Shulters (1990) indicate that the bedrock exposure of the Paintbrush Canyon fault extends north beyond

Yucca Wash for approximately 11 km. South of Yucca Wash, the fault is concealed by alluvium and colluvium for about 5 km. The fault is exposed along the western edge of the bedrock high between Bow Ridge and Fran Ridge and is concealed by alluvium and queried for 2 km south of Midway Valley.

At the southern end of Midway Valley, several secondary faults splay off the primary strand of the Paintbrush Canyon fault (Figure 1-2; Plate 1). One of these splays, the Fran Ridge fault, is exposed in bedrock on the west side of Fran Ridge (Plate 1) (Scott and Bonk, 1984). The Fran Ridge fault probably was intersected in drillhole UE-25p #1 at a depth of about 1200 m (Scott and Bonk, 1984; Carr et al., 1986, p. 24 and his Figure 12); displacement along the Fran Ridge fault and other probable associated faults in this area totals about 300 m. The dip of the Fran Ridge fault is about 65 degrees to the west, if the subsurface correlation is correct. The Fran Ridge and Paintbrush Canyon faults may rejoin farther to the south in the Dune Wash area (Frizzell and Shulters, 1990).

Where the Paintbrush Canyon and Fran Ridge faults are obscured by alluvium, Scott and Bonk (1984) map their locations based on geophysical anomalies detected on aeromagnetic and electromagnetic surveys (Plate 1). Anomalies from resistivity/geoelectric data were interpreted as faults by Flanigan (1981), Hoover et al. (1982), Frischknecht and Raab (1984), and Fitterman (1982) (see Appendix B and Plate 4).

No displaced alluvial surfaces have been identified along the mapped trace of the Paintbrush Canyon fault (Plate 1). The fault, however, is exposed in gullies in sand ramps immediately west of Busted Butte. The sand ramps and soils developed in them are separated vertically 4.1 m by a possible southern continuation of the Paintbrush Canyon fault (DOE, 1988). The Bishop ash, present at or near the base of these deposits, is faulted. The Bishop ash is dated at 740 ka (Izett, 1982; Izett and Naeser, 1976), indicating that faulting occurred after 740 ka. The sand ramps are mapped by Swadley et al. (1984) as Q2, implying an age of middle to late Quaternary (see Section 3.0).

Trenches A1 and A2 (Plates 2 and 3) were excavated across the mapped trace of the Paintbrush Canyon fault at the northern end of Alice Ridge in material mapped as Q2 by Swadley et al. (1984). Generalized trench logs presented by Swadley et al. (1984) are shown on Figures 4-4 and 4-5. Trench A1 exposed fractures that cut eolian sand (Q2e) and the soil developed in it but not the overlying colluvium and slope wash deposits (Q2b) (Figure 4-4). In Trench A2, fractures cut unit Q2c but neither the soil developed in those deposits nor the overlying Q2b deposits (Figure 4-5). The amount of displacement along fractures is difficult to assess, because bedding features are scarce in the fractured deposits of both trenches (Swadley et al., 1984). Swadley et al. (1984) conclude that the displacement along these fractures probably is less than a few centimeters. Through correlation of stratigraphic units in these trenches, Swadley et al. (1984) and DOE (1988) infer that the most recent displacement on the Paintbrush Canyon fault occurred between 270 and 700 ka.

Trench 17 was excavated across the Paintbrush Canyon fault at the south end of Midway Valley (Plate 3). The log of Swadley et al. (1984) is shown on Figure 4-6. The trench exposed unfaulted eolian sediments (Q2e), indicating no fault movement after 700 ka (Swadley et al., 1984; DOE, 1988).

Trenches 16 and 16B were excavated immediately south of Midway Valley across the mapped trace of the Fran Ridge fault (Plate 3). No faults or fractures were observed in eolian deposits (Q2e) of Trench 16 (Swadley et al., 1984; Figure 4-7). Carbonate-coated fractures that strike N25°E and dip 75°SW in Trench 16B cut eolian deposits (Q2e) but not the overlying slope wash and colluvium (Q2s) (Figure 4-8). Swadley et al. (1984) interpret these fractures to indicate minor movement on the Fran Ridge fault in bedrock but little or no movement ("no visible offset") in the eolian sediments of Q2e. The fault is exposed in welded tuff about 100 m south of the trench. Through correlation of Quaternary stratigraphic units in Trench 16B, Swadley et al. (1984) and DOE (1988) infer the age of the latest movement of the fault to be between 270 and 700 ka.

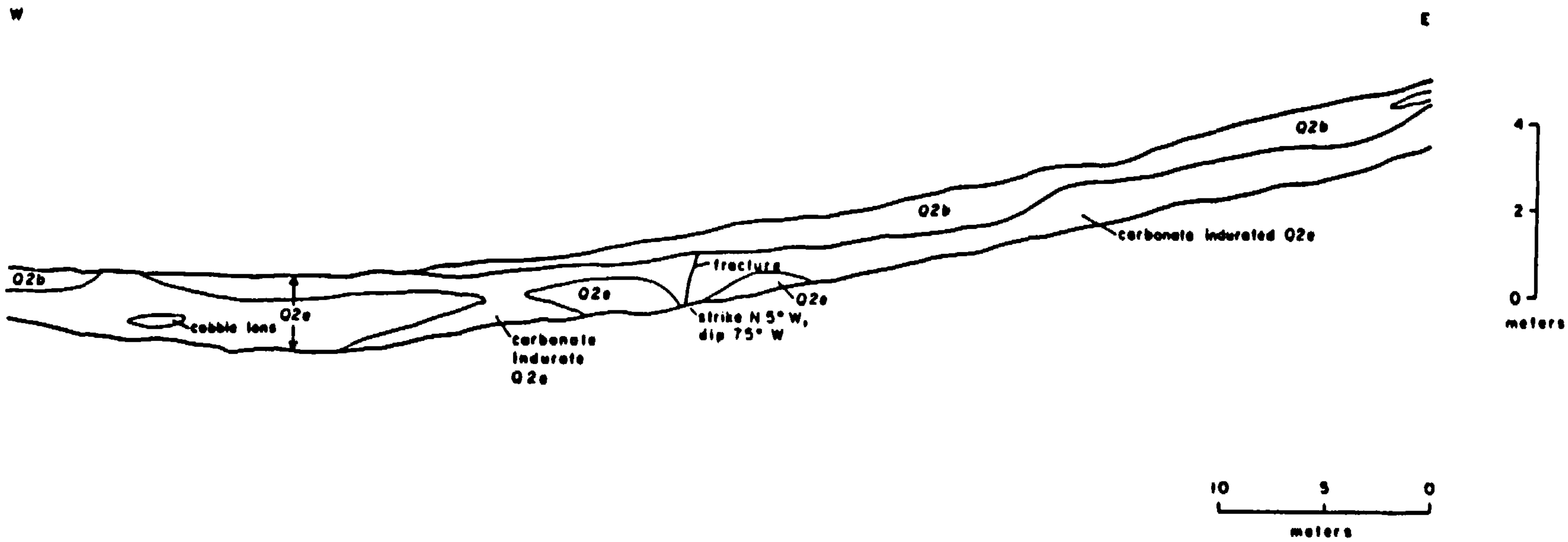

Diagram of north wall of trench A1, Paintbrush fault. Trench trends east-west. Mapped in 1979 by A. J. Gordon (F&S) and L. D. Parrish (F&S). Fractures cut unit Q2e and its soil but not the overlying Q2b.

Unit	Description
Q2b	Gravelly sand, probably a mixture of colluvium and slope wash. Soil horizons (not mapped) consist of light-brown cambic B horizon and stage II Cca horizon
Q2e	Eolian sand, well sorted locally includes pebbles and cobbles (colluvium). Root casts common. Sand is commonly moderately indurated with patchy areas of nonpedogenic carbonate (shown by stipple pattern). Soil development consists of thin stage III K horizon (not mapped)

Figure 4-4. Schematic log of trench A1 as presented by Swadley et al. (1984, p 38). See Plate 3 for location of trench.

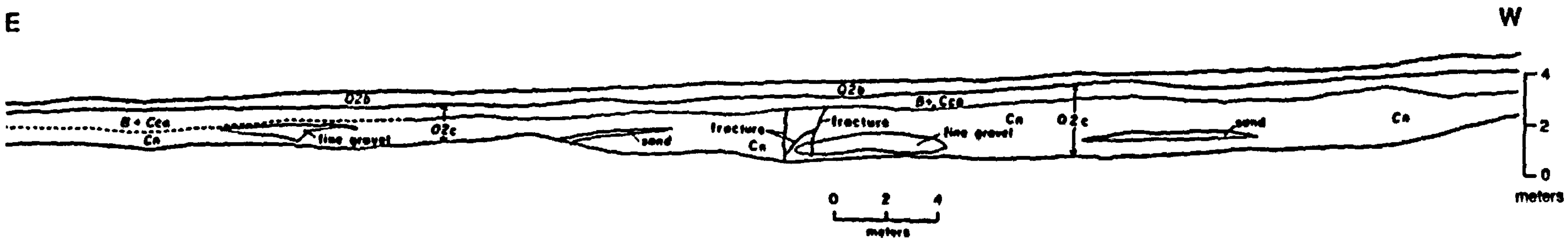

Diagram of south wall of trench A2, Paintbrush Canyon fault. Trench trends N. 85° E. Mapped in July 1983 by Swadley and L. D. Parrish. Fractures cut unit Q2c but not its soil or the overlying Q2b.

Unit	Description
Q2b	Sandy gravel, probably a mixture of slope wash and colluvium Soil (not mapped) consists of a weak cambic B horizon and a stage I Cca horizon
Q2c	Gravel, sandy, poorly sorted, poorly bedded
B+Cca	B and Cca soil horizons undivided: B horizon is light brown, cambic; developed in sandy gravel; Cca horizon, stage II carbonate development in sandy gravel
Cn	Gravel, very sandy, poorly sorted, poorly bedded; coarse, with scattered boulders; well indurated; includes lenses of sand and fine gravel

Figure 4-5. Schematic log of trench A2 as presented by Swadley et al. (1984, p. 39). See Plate 3 for location of trench.

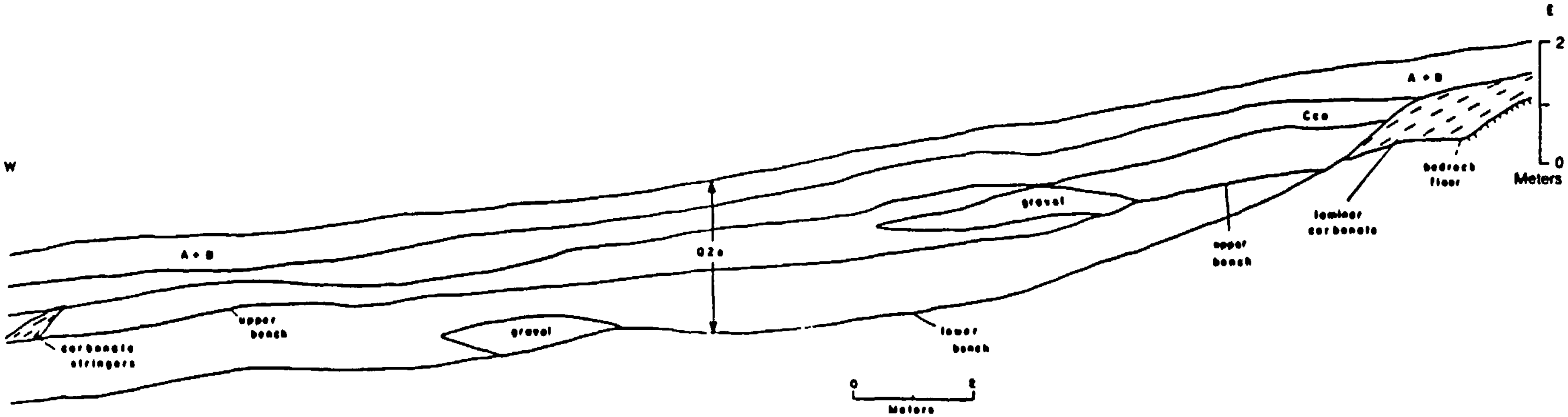

Diagram of north wall of trench 17. Trench trends N. 55° W. across a projection of a branch of Paintbrush Canyon fault. Cut on two levels, upper bench is 1-2 m wide. Mapped in July 1983 by Swadley and L. D. Parrish.

Unit	Description
Q2e	Eolian sand, moderately well to well sorted, poorly consolidated, nonbedded; includes scattered clasts and lenses of colluvial gravel. Root casts locally common. Soil developed in unit consists of A, B, and Cca horizons
A+B	A and B horizons, undivided. A horizon is light-gray silt and clay; vesicular, preserved locally. B horizon is light brown, cambic
Cca	Cca horizon--stage II carbonate development in fine well-sorted sand

Figure 4-6. Schematic log of trench 17 as presented by Swadley et al. (1984, p. 37). See Plate 3 for location of trench.

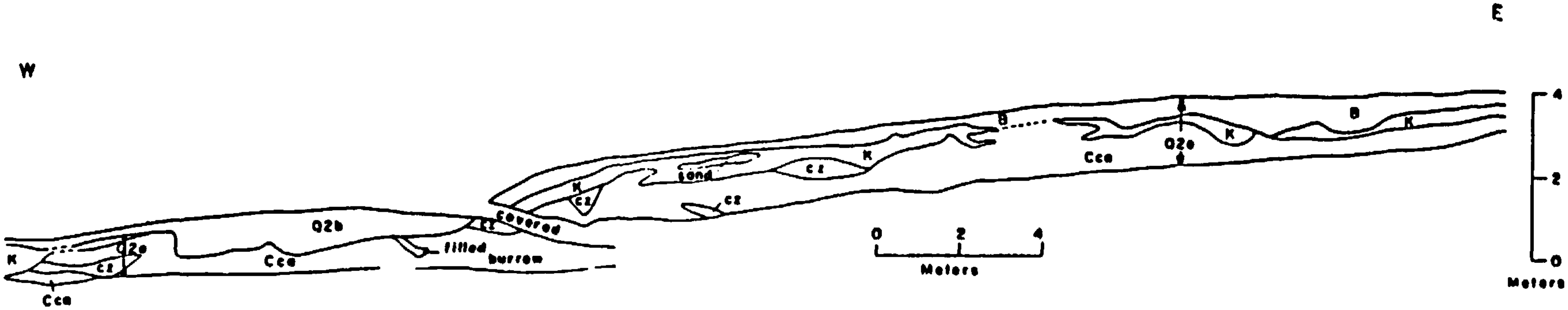

Diagram of north wall of trench 16. Trench trends N. 75° W. across a projection of the Paintbrush Canyon fault. Mapped in June 1982 by Swadley and H. E. Huckins.

Unit	Description
Q2b	Sand, poorly bedded, moderately well sorted; locally cemented with carbonate at base. Unit channels into underlying Q2e
Q2e	Eolian sand, fine, well sorted, nonbedded. Soil development consists of B, K, and Cca horizons
B	B horizon--light-brown, cambic, developed in well sorted fine sand
K	K horizon--stage III carbonate development in well sorted sand. Horizon is discontinuous, probably disrupted by burrows
Cca	Cca horizon--well sorted sand with stage I to II carbonate development. Root casts common to abundant. Includes local zones of carbonate enrichment (cz) that may be nonpedogenic

Figure 4-7. Schematic log of trench 16 as presented by Swadley et al. (1984, p. 35). See Plate 3 for location of trench.

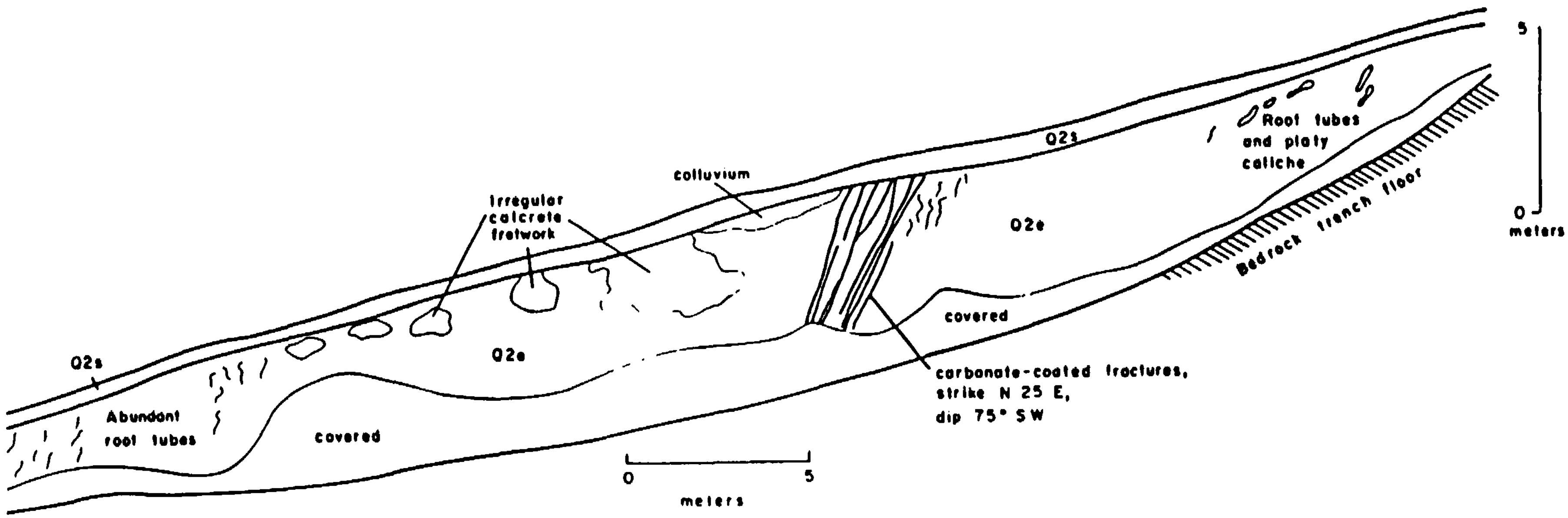

Diagram of north wall of trench 16B, located near the southern end of the Paintbrush Canyon fault. Mapped in February 1983 by W. J. Carr (USGS). Fractures cut unit Q2e but not overlying Q2s.

Unit	Description
Q2s	Sand, light-grayish-brown, and angular gravel. Probably a mixture of slope wash and colluvium
Q2e	Sand, eolian, well sorted, nonbedded; includes scattered clasts and lenses of colluvial gravel; root tubes and secondary carbonate deposits common. Q2e soil not preserved

Figure 4-8. Schematic log of trench 16B as presented by Swadley et al. (1984, p. 36). See Plate 3 for location of trench.

Midway Valley Fault. The postulated Midway Valley fault, named by Neal (1986), is mapped by Lipman and McKay (1965) as an unnamed and concealed fault that extends north-northeast for more than 6 km through the center of Midway Valley. The concealed fault is connected to a west-dipping normal fault exposed in bedrock at the southern end of Bow Ridge. Scott and Bonk (1984) map the same bedrock fault in Bow Ridge south of Midway Valley but connect it to a concealed, queried fault that extends only about 2 km into the valley beneath alluvium (Figure 1-2; Plate 1). A cross section prepared by Scott and Bonk (1984) that crosses Midway Valley near Exile Hill shows a zone of complex faulting near the center of Midway Valley (see discussion on cross sections below). The data used to interpret this faulting are not specified; however, a general statement is made that aeromagnetic, gravity, refraction seismology, and electromagnetic data were used "to project structures beneath alluvium" (Sheet 2 of Scott and Bonk, 1984).

Bedrock units offset across Midway Valley provide geologic evidence of significant net vertical displacement on buried faults within the valley (Carr, 1984; Scott and Bonk, 1984; Neal, 1986). This displacement could be accommodated on a limited number of faults that have relatively large offsets, or on a large number of faults that have much smaller offsets. Scott and Bonk (1984), who prefer the latter scenario, invoke the relationship between their "imbricate zones" on the eastern margins of fault blocks and the major range-front normal faults/breccia zones farther south to infer the presence of many small-displacement faults beneath the alluvium in Midway Valley.

Geophysical surveys provide equivocal evidence of the postulated Midway Valley fault (Appendix B; Plate 4). Frischknecht and Raab (1984) used short-offset time-domain electromagnetic (TDEM) soundings to obtain data that suggest the central Midway Valley area contains "a major fault or fault zone ... which displaces the lower conductive layer about 400 m downward on the west side" (p. 987). Based on personal communications with other researchers, Frischknecht and Raab (1984) cite other evidence of the postulated Midway Valley fault, including a low-velocity zone at depth on a seismic refraction profile and a sharp, prominent gravity feature. They also suggest that there is weak aeromagnetic evidence for faults at this location. Other resistivity/geoelectric surveys by Fitterman (1982), Senterfit et al. (1982), and Smith and Ross (1982) reveal anomalies within Midway Valley that could be attributed to faulting. However, these anomalies are distributed widely across the valley (Plate 3). Seismic reflection and refraction surveys described by Pankrantz (1982), McGovern (1983), and Reynolds and Associates (1985) do not provide reliable data. Reynolds and Associates (1985) identified three principal faults in central Midway Valley (Plate 3); however, confidence in these data is low (see Appendix B).

To date, no trenches have been excavated across the projected trace of the Midway Valley fault. No surface displacement has been reported along the mapped trace of the fault.

Yucca Wash Fault. On the basis of aeromagnetic anomalies and contrasting bedrock across Yucca Wash, Scott and Bonk (1984) and Frizzell and Shulters (1990) show a northwest-trending, right-lateral strike-slip fault along Yucca Wash. The fault, as mapped, is concealed beneath alluvium and is about 8.5 to 9.0 km long, extending from the headwaters area of Yucca Wash to near the northern end of Alice Ridge.

Maldonado (1985) shows a northwest-trending, 10-km-long "fault lineament" along this general trend. The "fault lineament" is shown trending along Yucca Wash from a northwest-dipping normal fault exposed in bedrock in the headwaters reach, through the water gap at the northern end of Alice Ridge, to a position northeast of the ridge. No relative sense of displacement across the "fault lineament" is shown.

No trenches have been excavated across the projected trace of the Yucca Wash fault. Additionally, no displaced Quaternary deposits are reported along the fault.

Cross Sections. Cross sections that portray the near-surface geologic structure beneath Midway Valley have been constructed by various workers, most notably Scott and Bonk

(1984) and Neal (1986). These cross sections are reviewed below. A cross section constructed by W.J. Carr near Exile Hill is presented in Appendix A of this report. Lipman and McKay (1965) and Frizzell and Shulters (1990) also present cross sections that include the Midway Valley area. These are the product of regional geologic mapping and compilation, however, and do not provide details of the structure of Midway Valley. URS/John A. Blume & Associates (1986) present four geologic cross sections through Midway Valley that were prepared to help appraise the effects of alluvial materials on potential ground motions and are "not intended for any other purpose" (URS/John A. Blume & Associates, 1986, p. 4).

Scott and Bonk (1984) present two geologic cross sections to illustrate the possible shallow subsurface structure of Midway Valley. The cross sections, which trend northwest, incorporate outcrop data and limited borehole data (Figure 4-9; Plate 1). Two categories of faults are indicated on the cross sections: those that have major or minor dip-slip displacements and a "position known or concealed at surface," and "unmapped and inferred faults of small displacement required by geometric constraints in surface exposures and drill holes" (Plate 1 of this report; Sheet 2 of Scott and Bonk, 1984). The latter category represents faults of the imbricate zones that are at the eastern margins of the fault blocks, adjacent to the major normal faults. Scott and Bonk's (1984) cross section A-A' crosses the southern end of Midway Valley (Figure 4-10). This cross section shows the Bow Ridge and Paintbrush Canyon faults and the west-dipping imbricate zones and fault breccia that lie just west of them. An unnamed fault having "major dip-slip displacement" that is mapped in Midway Valley between the Bow Ridge and Paintbrush Canyon faults is approximately coincident with the inferred Midway Valley fault (Neal, 1986; Lipman and McKay, 1965). The volcanic rocks are inferred to be down-dropped to the west between the postulated Midway Valley fault and Bow Ridge. This evidence has been used to infer the presence of three or more intervening normal faults (Scott and Bonk, 1984; Neal, 1986). A complex zone of faulting is inferred between the postulated Midway Valley fault and the Paintbrush Canyon fault on the east.

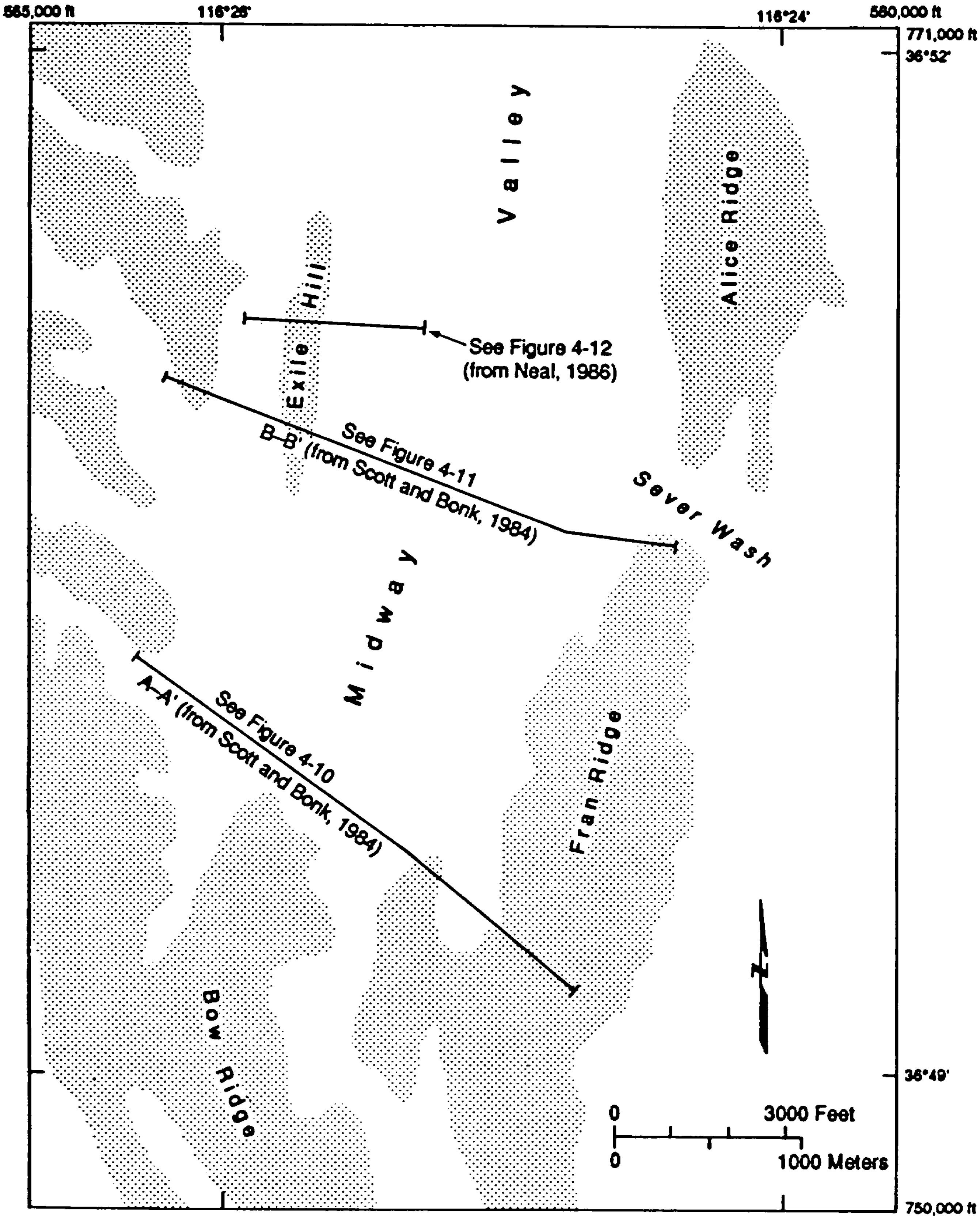

Figure 4-9. Locations of cross sections shown in Figures 4-10 to 4-12. Screened areas indicate the location of Tertiary silicic volcanic rocks. Unscreened areas indicate the location of Tertiary to Quaternary alluvial, fluvial, and eolian sediments.

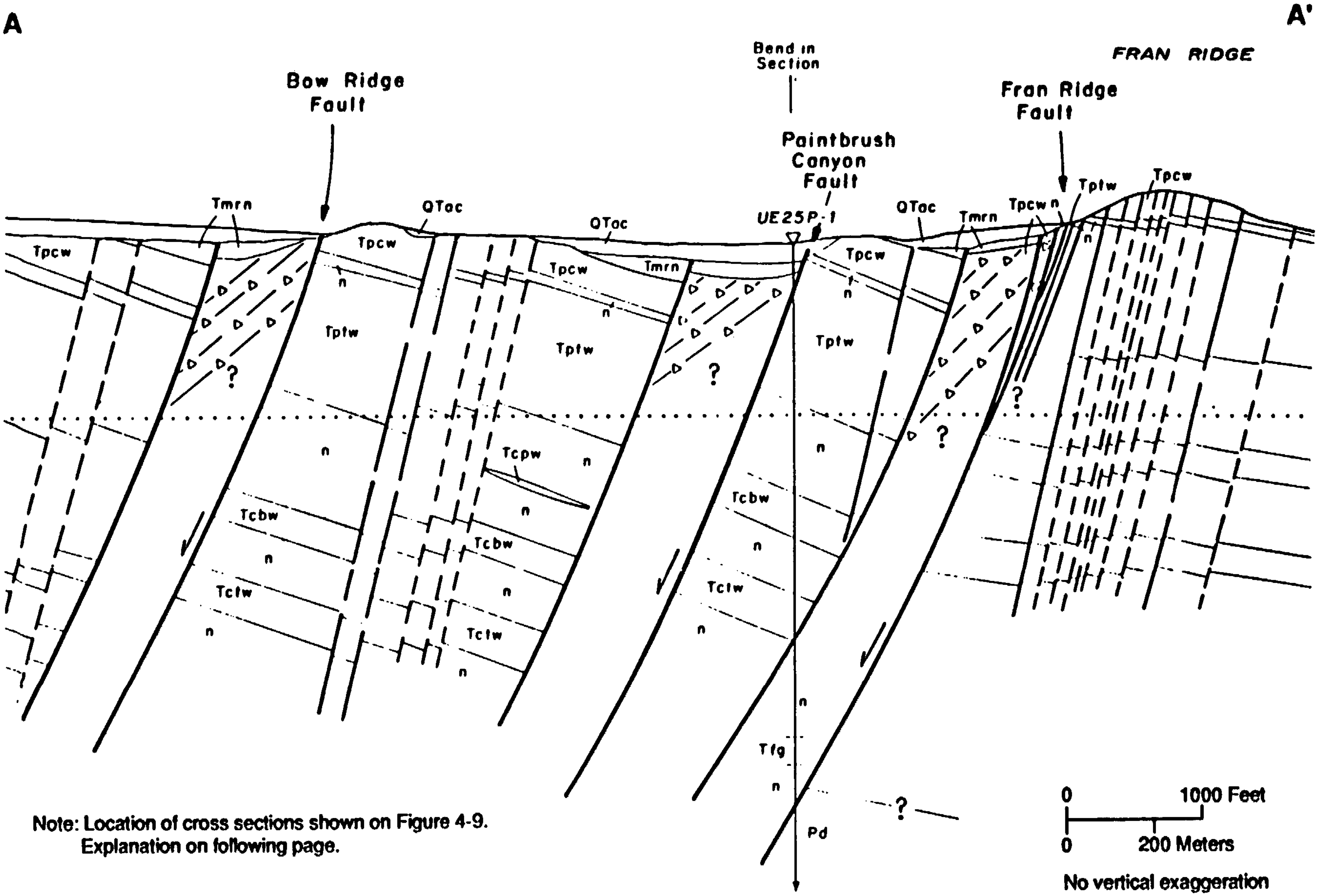

Note: Location of cross sections shown on Figure 4-9.
Explanation on following page.

Figure 4-10. Part of geologic cross section A-A' from Scott and Bonk (1984).

EXPLANATION

———— ? Contact; queried where inferred

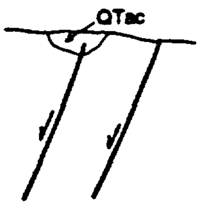

Fault with major dip-slip displacement, position known or concealed at surface; arrows show direction of relative displacement. Average dip of fault planes at surface is 70° and subsurface drill hole data suggest a decrease to about 60° below 1 km depth. Some faults cut older QTac but do not cut younger Quaternary deposits shown by partial penetration of fault through QTac to surface

Faults with minor dip-slip displacements, positions known or concealed at surface; no evidence to suggest a decrease in dip with depth; average dip is 76° at surface and in drill holes

Unmapped and inferred faults of small displacement required by geometric constraints in surface exposures and drill holes

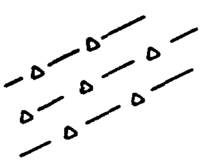

Zone of west-dipping strata containing abundant breccia and faults too complex to draw individually; stratigraphic units shown only near surface

.... Static water level; queried where extended beyond drill hole data control; measured prior to December 1983

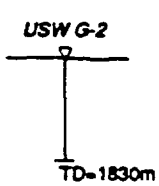

Drill hole showing total depth

Physical-Property Stratigraphic Units

QTac	Alluvium and colluvium (Quaternary and Tertiary)
Tmrw/Tmrn	Rainier Mesa Member of Timber Mountain tuff, w - welded, n - nonwelded
n	Nonwelded tuff
Tpcw	Tiva Canyon Member of Paintbrush tuff, welded
n	Nonwelded tuff
Tptw	Tonopah Spring Member of Paintbrush tuff, welded
n	Nonwelded tuff
Tcpw	Prow Pass Member of Crater Flat tuff, welded
n	Nonwelded tuff
Tcbw	Bullfrog Member of Crater Flat tuff, welded
n	Nonwelded tuff
Tctw	Tram Member of Crater Flat tuff, welded
Tfg	Fanglomerate
Pd	Paleozoic dolomite (Devonian)

Source: Scott and Bonk (1984)

Figure 4-10, continued.

Cross section B-B' in Scott and Bonk (1984) crosses the central part of Midway Valley and intersects the southern end of Exile Hill (Figure 4-11). Between the mapped Bow Ridge and Paintbrush Canyon faults, this cross section contains 25 unmapped and inferred normal faults that have down-on-the-west displacement; the faults are inferred based on geometric constraints. Such imbricate zones of complex faulting are inferred west of both the Bow Ridge and Paintbrush Canyon faults. The cross section shows a narrow imbricate zone and associated breccia zone at the inferred location of the postulated Midway Valley fault; the Midway Valley fault, however, is not depicted on Scott and Bonk's geologic map near cross section B-B'.

Neal (1986) constructed a cross section through Exile Hill and the site of the prospective surface facilities based on surface mapping and data from the UE-25 RF boreholes (Figure 4-12). This cross section shows seven faults east of the Bow Ridge fault. In the accompanying text, Neal (1986) states that extensive fracturing observed in cores from bore holes UE-25 RF #3, #9, #10, and #11 support the hypotheses of closely spaced normal faults across Midway Valley postulated by Scott and Bonk (1984; cross section B-B'). Because of the high density of fracturing observed in cores and because of the low seismic velocities reported by Reynolds and Associates (1985) (see Appendix B), Neal (1986) also concludes that the subsurface in this area may contain more faults than indicated by Scott and Bonk (1984).

The cross sections reviewed above address the near-surface geology of Midway Valley based on geologic mapping, shallow borehole data, and conservative interpretations of limited geophysical data. They do not address directly the down-dip geometry and kinematic interaction at depth of faults observed at the surface in Midway Valley. Instead, conjecture about the crustal-scale structure of the Midway Valley area and the origin and evolution of the observed tectonic features has relied on the application of generic models of crustal-scale continental extension.

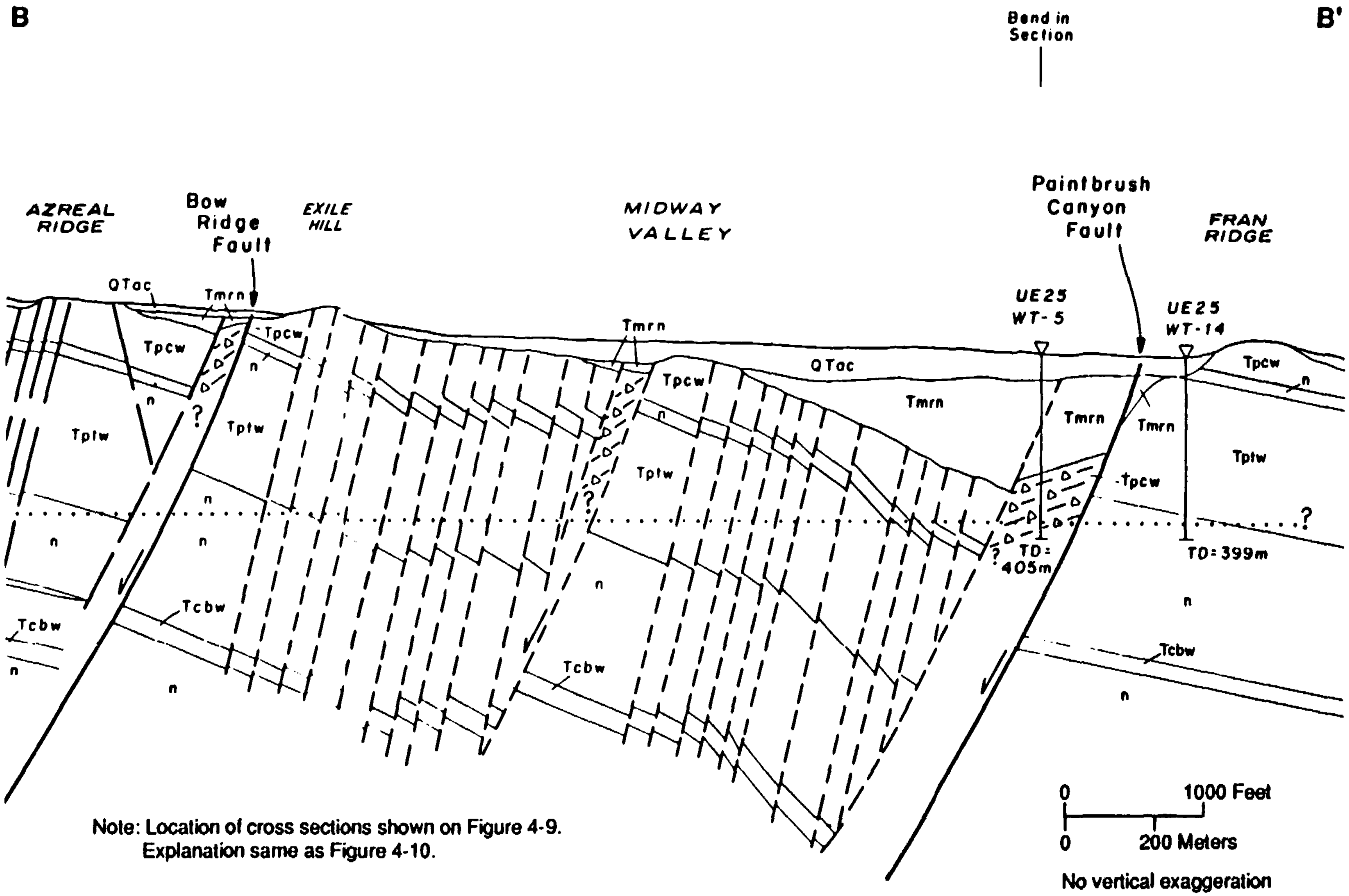

Note: Location of cross sections shown on Figure 4-9.
Explanation same as Figure 4-10.

Figure 4-11. Part of geologic cross section B-B' from Scott and Bonk (1984).

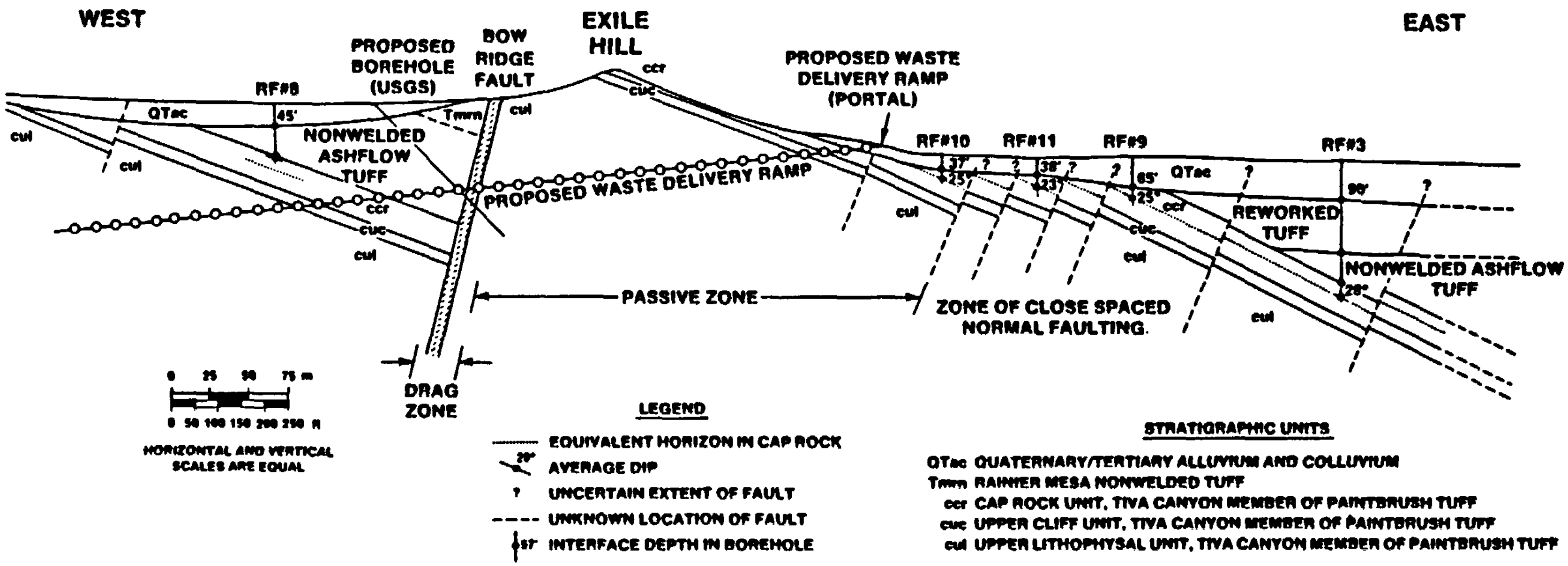

Note: location of cross section shown on Figure 4-9.

Figure 4-12. Geologic cross section from Neal (1986).

Kinematic Models. The nature of the interaction between the north-south, extensional Basin and Range style of faulting and the strike-slip style of deformation associated with the Walker Lane belt is not well understood. Consequently, there is considerable debate concerning the kinematics of late Cenozoic faulting in the Yucca Mountain region.

Models for crustal-scale continental extension and the kinematic evolution of normal fault systems fall into two primary categories: listric normal fault systems, and planar rotational (domino-style) normal fault systems (Wernicke and Burchfiel, 1982; McClay and Ellis, 1987). A listric normal fault system contains curved (concave up) normal faults that merge at depth with a subhorizontal detachment fault (Gibbs, 1983; Ramsay and Huber, 1987). A domino-style fault system contains planar normal faults that are linked kinematically; in the simplest system, all faults move together, and both the faults and the blocks rotate to a shallower dip during progressive deformation (Ransome et al., 1910, as cited in Jackson and White, 1989; Wernicke and Burchfiel, 1982; Ramsay and Huber, 1985).

Cenozoic extension in the Basin and Range province has been attributed to both listric normal faulting (Anderson, 1971; Wernicke and Burchfiel, 1982; Smith and Bruhn, 1984; Scott, 1984; Maldonado, 1990) and domino-style normal faulting (Ransome et al., 1910, as cited in Jackson and White, 1989; Wernicke and Burchfiel, 1982; Smith and Bruhn, 1984; Jackson and White, 1989; Maldonado, 1990). Models that incorporate characteristics of both styles of faulting also have been proposed (Proffett, 1977; Gans et al., 1985).

Scott (1984) cites the minor, closely spaced normal faults (imbricate zones) mapped by Scott and Bonk (1984) on the east side of fault blocks near Yucca Mountain as evidence for concave-up curvature at depth on major range-front normal faults (i.e., listric fault geometry). According to Scott (1984), faults within the imbricate zone originate as vertical tension gashes in the hanging wall and become secondary, west-dipping normal faults that allow the intervening "...narrow slices (to) drop..." into the void created between the hanging wall and the footwall when the primary listric fault moves.

Alternatively, the imbricate zones observed by Scott and Bonk (1984) may be interpreted as evidence for block rotation about a horizontal axis during domino-style faulting along planar rotational normal faults. In this model, the vertical tension gashes cited by Scott (1984) develop into synthetic (west-dipping) minor faults, an interpretation consistent with the field mapping of Scott and Bonk (1984). Recent seismological evidence (Jackson and White, 1989; Doser and Smith, 1989) and geodetic evidence (Stein and Barrientos, 1985) indicate that rupture on planar normal faults is the dominant mechanism for extension in the Basin and Range province. This evidence, combined with data from the detailed geologic mapping by Scott and Bonk (1984), suggests that domino-style normal faulting should be considered a possible kinematic model for the Midway Valley area.

The map-view geometry of the fault systems and the block rotations observed in the southern Walker Lane belt may be related in the neotectonic setting by a simple model for progressive kinematic development of a brittle, right-lateral shear couple superimposed on a normal fault system. A major northwest-trending, subvertical, right-lateral shear zone and a regional subhorizontal detachment at depth beneath the Yucca Mountain area are the primary tectonic elements of this model. The subvertical shear zone controls the lateral component of subsidiary deformation that is expressed at the surface as strike-slip faulting and attendant clockwise block rotation. The normal faulting that is responsible for regional physiography is the result of west-northwest-directed extension above a subhorizontal detachment (Maldonado, 1990). The mechanics and timing of this interaction, even if the model is accurate in a geometric sense, are still poorly understood, and the details of the relationship between crustal extension and transform motion are unresolved. A regional vertical shear zone, however, could be consistent with a regional subhorizontal detachment: both may operate simultaneously and maintain a stable kinematic geometry. This model, which is in agreement with the regional and local stress field, considers the southern

Walker Lane belt to be an extensional system overprinted and subsequently kinematically controlled by strike-slip tectonics.

The style, rate, and location of deformation predicted by the listric and the domino-style fault models differ greatly (Wernicke and Burchfiel, 1982). In assessing which style applies to past and future deformation in the Midway Valley area, it is important that the analysis be sufficiently flexible to encompass the most appropriate kinematic models, and that the model chosen agree with the observed data. Such care is particularly necessary for assessing Quaternary faulting in Midway Valley, where the goal is to characterize activity on faults that have limited or no outcrop exposure. These models are further complicated by the fact that the relative amounts and timing of activity on transform and extensional fault systems are not well understood. The relative contributions of these fault systems and the contribution from the different tectonic regimes that control them remain uncertain and can be resolved only by detailed analysis of their expression and activity in the most recent geologic materials.

4.3 DISPLACEMENT HISTORY AND SLIP RATES ON THE PAINTBRUSH CANYON AND BOW RIDGE FAULTS

Estimated amounts of displacement for Tertiary and Quaternary geologic units that are displaced by the Paintbrush Canyon and Bow Ridge faults are shown in Tables 4-1 and 4-2 and on Figure 4-13 of this report (Figure 4 in Gibson et al., 1990). Uncertainty about the type and amount of slip, the locations along the faults where these data were obtained, and the ages of the displaced units affect the assessment of long-term slip rates. However, an overall decreasing rate of displacement from the Tertiary into the Quaternary clearly is indicated by the data for the Paintbrush Canyon and Bow Ridge faults (Figure 4-13).

Gibson et al. (1990) do not address uncertainties in the amount of vertical separation of displaced units. Table 4-2 presents the differences in stratigraphic dip separation derived from previous studies. These differences may reflect changes in dip separation along the

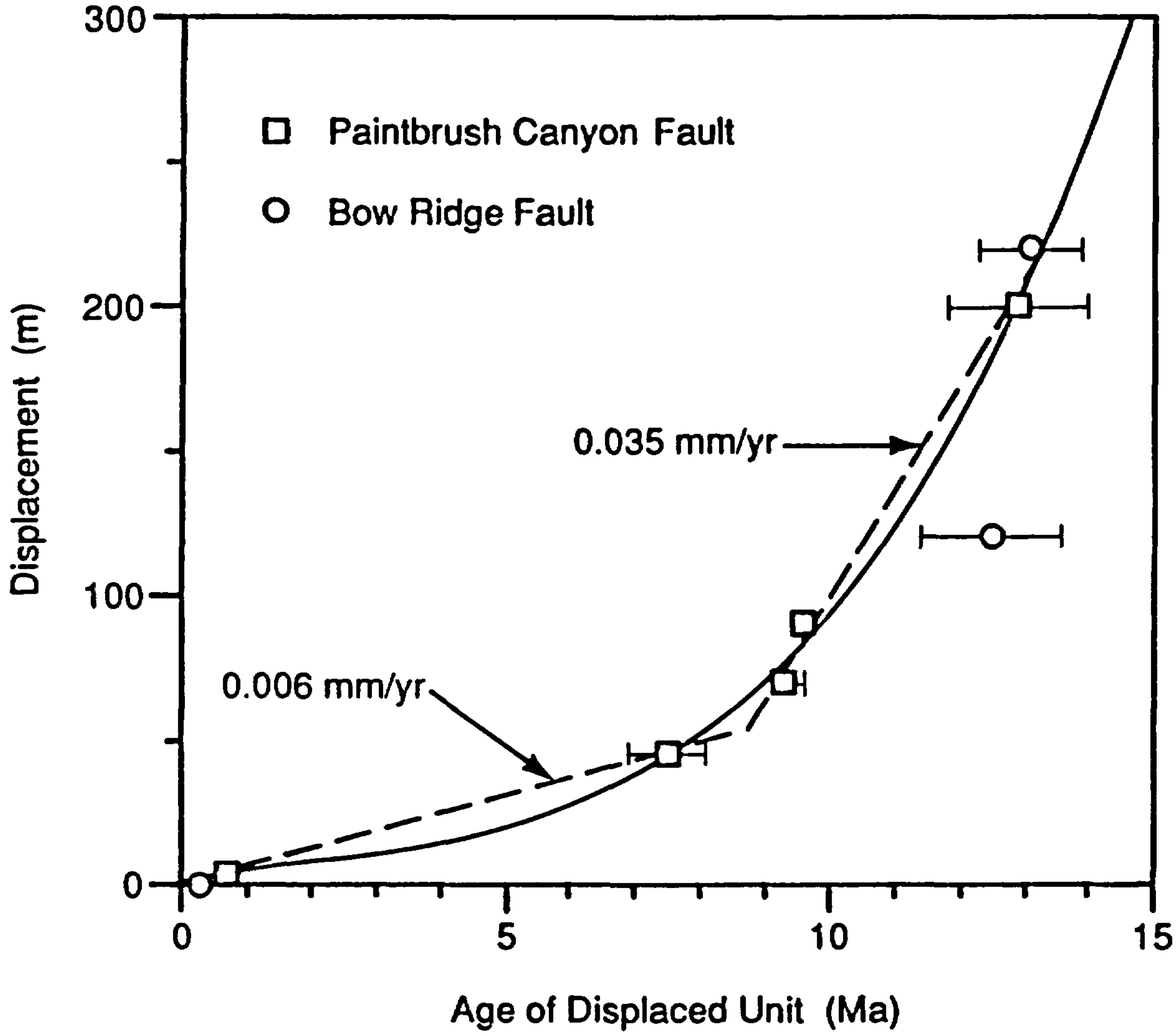

Source: Gibson and others (1990)

Figure 4-13. Graph showing displacement versus age of displaced unit for the Paintbrush Canyon and Bow Ridge faults. Lines are drawn through Paintbrush Canyon fault data points. See text for discussion and Table 4-1 for data and references.

strike of the fault, differences in the amount and quality of data used to calculate the dip separations, and/or differences in interpretation. In addition, the possibility of lateral slip on the Paintbrush Canyon and Bow Ridge faults largely has been ignored. These considerations were not addressed directly by Gibson et al. (1990).

The age estimates given in Table 4-1 are based on a variety of techniques, including potassium-argon dating of volcanic rocks, tephrachronology of volcanic ashes, and uranium-series and uranium-trend dating of calcic soils. The reliability of these techniques varies. Where reported, the range of uncertainty in the age of a displaced horizon is indicated in Table 4-1 and on Figure 4-13.

To evaluate changes in the displacement rate over time for the Bow Ridge and Paintbrush Canyon faults, Gibson et al. (1990) plot displacement versus age of the displaced unit using the data in Table 4-1 (Figure 4-13). Because the data are limited, a curve was developed from visual inspection only. Despite the uncertainties in the ages and amounts of displacement, Gibson et al. (1990) argue for an overall decrease in the rate of fault activity during the late Cenozoic. They further suggest that the data allow for either (1) a gradual decrease in the rate of fault activity during the past 10 to 15 Ma (solid line) or (2) an abrupt decrease at 8 to 9 Ma (dashed line). An abrupt change at 8 to 9 Ma (Gibson et al., 1990) may correlate with the marked decrease in regional silicic volcanic activity at about 7 Ma (Carr, 1984). However, more recent age determinations of the ryholites of Fortymile Canyon (Warren et al., 1988; Byers et al., 1989; Tables E-1 and E-2 in Appendix E) suggest that the slowing of fault activity was significantly earlier than 7 Ma.

In addition to potentially large uncertainties in the ages and amounts of fault displacement, there also are uncertainties in the temporal behavior of the Bow Ridge and Paintbrush Canyon faults during the Quaternary. At present, data on the Bow Ridge fault are insufficient to assess whether it has a displacement history similar to that of the Paintbrush Canyon fault. Data are insufficient to evaluate whether the two faults record a history of uniform slip or a temporal clustering of paleoseismic events.

5.0 SUMMARY AND RECOMMENDATIONS

Yucca Mountain and Midway Valley lie in a region that is influenced by two different tectonic regimes: the Walker Lane belt dominated by northwest-trending, right-lateral strike-slip faults; and the Basin and Range province, a region of extensional tectonics characterized by north-trending normal faults. The complex pattern of late Cenozoic faulting in the Yucca Mountain region reflects the interaction of these tectonic regimes and their influence on older Tertiary and pre-Tertiary structures in the bedrock.

The dominant tectonic features in Midway Valley are the north-trending, westward-dipping normal faults along the margins of the valley: the Bow Ridge fault on the west, and the Paintbrush Canyon fault on the east. The maximum apparent vertical stratigraphic separation on these faults is approximately 220 and 515 m, respectively, but the net slip is not well constrained. Both faults displace Quaternary sediments, but the ages of the most recent displacements are unknown.

The regional tectonic setting and structural models for the Yucca Mountain area indicate that lateral displacements have occurred concurrently with the extensional normal faulting during the late Cenozoic, particularly along northwest- and northeast-trending faults. No reported evidence suggests Quaternary faulting along any of the northwest-trending faults in the Midway Valley area.

The evidence for normal faulting concealed beneath the alluvial cover within Midway Valley is sufficient to warrant further subsurface investigation. Several lines of evidence suggest that a zone of normal faulting similar to the faults along the east flank of Yucca Mountain may exist in the Tertiary strata beneath Midway Valley. The existing borehole and geophysical data are inadequate to constrain the location and geometry of faulting beneath the Quaternary/Tertiary fill in Midway Valley. No data suggest that the inferred faults beneath Midway Valley displace Quaternary strata, but the available data are inadequate to preclude small displacements. Additional data are needed to define the structure of the Tertiary strata beneath Midway Valley and to characterize Quaternary deposits, soils, and geomorphic surfaces that can help constrain the age of faulting. Both types of data are needed to assess confidently the potential for significant Quaternary faulting in Midway Valley.

5.1 LOCATION AND GEOMETRY OF FAULTS

Faulting in Midway Valley must be characterized through a combination of several geologic and geophysical techniques. Each technique carries its own set of limitations in terms of horizontal and vertical resolution, depth of penetration, and environmental impact. Several surveys will have to be correlated to obtain an integrated picture of the tectonic and geologic environment within Midway Valley.

The resistivity/geoelectric surveys conducted in Midway Valley have detected variations in lateral resistivity that correlate with the Bow Ridge and Paintbrush Canyon faults; evidence for the postulated Midway Valley fault is equivocal. To date, the seismic reflection and refraction surveys conducted in Midway Valley have produced no reliable data. Despite the failure of seismic surveys to image the location and geometry of faulting in Midway Valley (see Appendix B), the use of new geophysical techniques and improved techniques, combined with a drilling program, offers the greatest potential for resolving Tertiary structure. Intermediate-depth seismic data perhaps can be acquired by using strong sources and innovative receiver arrays; such data might prove useful. Stronger acoustic contrasts between layers at depth might support more reliable interpretations. If high-quality seismic data can be acquired, future surveys should cover a larger area of Midway Valley than has been surveyed.

Shallow geophysical and borehole surveys also might prove valuable in constraining Quaternary faulting and corroborating results from geologic studies. Ground penetrating radar (GPR) surveys, identification of helium anomalies, inversion of crosshole seismic data (or seismic tomography), and acquisition of additional geophysical well logs through gravimetric or magnetic surveys may provide useful information and may facilitate correlation of shallow geologic data. GPR surveys are particularly attractive because of their minimal impact on the environment and the potential for three-dimensional imaging of the subsurface. This geophysical remote-imaging technique, which penetrates to a maximum depth of 10 to 30 m depending on the wavelength, could provide a means of correlating trench and borehole data. Deeper targets, such as the alluvial and volcanic strata below the terminations of trenches, could be interpreted and correlated with shallow and intermediate-depth seismic information where possible. A detailed discussion of past geophysical surveys and recommendations for future surveys is provided in Appendix B of this report.

5.2 QUATERNARY GEOLOGIC STUDIES

As described in Section 3.0, various approaches have been used to differentiate the surficial geology in the NTS area. Several techniques, some still in experimental stages, have been used to date the geomorphic surfaces, soils, and Quaternary deposits. Comparing the work of Hoover et al. (1981) and Hoover (1989) to that of Peterson (1988) illustrates the problems inherent in differentiating map units and making temporal correlations in an area that includes several complex geomorphic systems that cannot be related easily without oversimplifying the stratigraphic model.

The present landscape is the product of a complex history of constructional and erosional processes. The land surface can be characterized by describing the nature of the surface, the soils associated with the surface, and/or the nature of the underlying deposits. However, each element usually reflects a different aspect of the geologic history. The sediments represent the depositional phase; the surface represents the end of deposition or the end of a subsequent period of erosion; and the soil reflects a period of relative landscape stability during which weathering and soil-forming processes overshadowed erosional and depositional processes. At any given time, all these processes operate concurrently in different parts of the landscape. Differentiating and correlating Quaternary features is complicated further by temporal and spatial variations in climate and tectonic processes that can produce differential changes in the rates of surficial processes. The complex interrelations among deposits, soils, and geomorphic surfaces that are used to characterize the Quaternary geology make it difficult to develop consistent criteria for defining map units. Most of the criticisms concerning historical approaches to mapping the NTS area, and many of the problems concerning interpretation of age determinations, primarily reflect the failure to discriminate clearly between the age of the deposit and the ages of the associated geomorphic surface and soil.

Other sources of confusion stem from: (1) the mapping scale; (2) the fact that maps of surficial materials are, for the most part, two-dimensional representations of geology; and (3) differences in the intended purpose of the mapping, which may necessitate different mapping approaches. Except on very large-scale maps of local areas, some generalization and lumping of surficial features is unavoidable. In many places, geologic interpretations can be significantly affected because it proves impossible accurately to portray complex local features. Hence, it is important to provide comprehensive map descriptions and accompanying text to elaborate on features too small to map.

Where surficial deposits are very thin, considerable history may be recorded within only a few meters of the surface. How thin should a deposit be before it is considered "transparent" and is included only as part of the unit descriptions? This is an especially important question when the mapping is intended to support subsurface investigations. Conversely, if the mapping is intended to support photogeologic interpretations (e.g., photolineament analyses), the age of the surface may be the most important consideration.

The published Quaternary geologic maps of the NTS area (e.g., Swadley and Hoover, 1983) utilize "correlation characteristics" that combine parameters from various geologic elements (deposits, soils, and surface characteristics). This approach has created some confusion concerning the assigned ages of surficial geologic units. The primary focus of such work has been to delineate Quaternary map units that reflect the lithology and age of the deposits. In contrast, Peterson (1988) focuses on delineating geomorphic surfaces based on their near-surface (soil) and surface characteristics (cation ratio dates on rock varnish).

Historically, numerical dating methods have been problematic in desert environments in which datable organic materials are scarce. New methods for dating calcium carbonate, rock varnish, cosmogenic radionuclides, and fine-grained detrital material are still being calibrated and/or developed. Cation ratio, radiocarbon, and U-series dating of rock varnish appear promising, but problems related to the influences of geomorphic processes on desert pavements, sampling methodology (e.g., Wells and McFadden, 1987), and analytic procedures and precision (e.g., Harrington et al., 1989; Bierman and Gillespie, 1990) require cautious application of these experimental methods.

Thermoluminescence dating (TL) is a promising technique that also requires further calibration and testing. Future studies should address pedology and sedimentology of the Av soil horizon and other fine-grained deposits and the dose rate measured in the field.

Age-dating methods must be integrated with detailed geomorphic and soil stratigraphic studies to achieve reliable interpretations. To the extent possible, multiple methods should be used to obtain corroborating evidence for numerical ages. This is particularly true for VCR and TL techniques, which generally are considered experimental.

The techniques and approaches used in Quaternary geologic mapping of arid environments have changed markedly during the past 10 to 15 years. Although there is no universally accepted approach, standard practices are emerging. The objectives and site-specific nature of the Quaternary geologic mapping of Midway Valley require that it be based on a comprehensive understanding of the stratigraphic and sedimentological characteristics of the deposits and the relations of these deposits to the associated soils and geomorphic surfaces.

Because the mapping will be used to support trenching studies in Midway Valley, it must reflect the three-dimensional nature of the Quaternary deposits. The importance of trenches and soil test pits in providing the necessary vertical control cannot be overemphasized. In describing the various map units, it is essential that the distinction between deposits, soils, and geomorphic surfaces be stated clearly and that these geologic elements be characterized based on accepted state-of-the-art practices supported by multiple quantitative numerical and relative dating techniques.

5.3 CONCLUDING REMARKS

Based on this review of available geologic and geophysical data, evidence for concealed faulting beneath the alluvial cover within Midway Valley is sufficient to warrant further investigation. Additional data are needed to evaluate the potential for future fault displacements near the prospective surface facilities in terms of the sense and amount of displacement and the likelihood of displacement occurring during the preclosure period. The following elements are needed to accomplish the program objectives with the required high level of confidence:

- acceptable regulatory criteria to define potentially hazardous faults
- detailed knowledge of the structural geology beneath Midway Valley
- knowledge of the distribution and ages of the Quaternary deposits, soils, and geomorphic surfaces within Midway Valley that can be used to assess the location and deformational history of faults near the prospective surface facilities
- an understanding of the implications of the alternative tectonic and structural models on the assessment of the potential for future displacements on any identified faults.

The results of this study (SCP Study 8.3.1.17.4.2, Location and Recency of Faulting Near Prospective Surface Facilities) will be used in conjunction with other site characterization activities to support the siting of surface facilities and to assess the potential effects of surface faulting on the design of the surface facilities.

6.0 REFERENCES

Albers, J.P., 1967, Belt of Sigmoidal Bending and Right-Lateral Faulting in the Western Great Basin: Geological Society of America, v. 78, p. 143-156. (NNA.870406.0077)

Anderson, R.E., 1971, Thin-Skin Distension in Tertiary Rocks of Southeastern Nevada: Geological Society of America Bulletin, v. 82, p. 43-58. (HQS.880517.1041)

Anstey, N.A., 1986, Whatever Happened to Ground Roll: Geophysics: The Leading Edge of Exploration, v. 5, no. 3, p. 40-45. (NNA.910123.0028)

Antevs, E., 1955, Geological-Climatic Dating in the West: American Antiquity, v. 20, p. 317-335. (NNA.910123.0005)

Bath, G.D., and Jahren, C.E., 1985, Investigation of an Aeromagnetic Anomaly on West Side of Yucca Mountain, Nye County, Nevada: U.S. Geological Survey Open-File Report 85-459. (NNA.870326.0123)

Bierman, P.R., and Gillespie, A., 1990, Varnish Cation-Ratio Dates--How Precise Can They Be? (abs): Geological Society of America, Abstracts with Programs, Cordilleran Section, v. 22, p. 8. (NNA.910123.0017)

Birkeland, P.W., 1974, Pedology, Weathering, and Geomorphological Research: Oxford University Press, New York, p. 3-51; 247-273. (NNA.910123.0031)

Birkeland, P.W., 1984, Soils and Geomorphology: Oxford University Press, New York, 372 p. (NNA.910128.0129)

Brocker, T.M., and Hart, P.E., 1988, Direct Comparison of Dynamite and Vibroseis Methods for Deep Crustal Seismic Reflection Studies in the Southwestern Basin and Range, Nevada, U.S.A.: Eos, v. 69, no. 44, p. 1313. (NNA.910123.0029)

Bull, W.B., 1984, Tectonic Geomorphology: Journal of Geological Education, v. 32, p. 310-324. (HQS.880517.1097)

Bull, W.B., and Ku, T.L., 1975, Age Dating of the Late Cenozoic Deposits in the Vicinity of the Vidal Nuclear Generating Station Site: Southern California Edison Company, Appendix 2.5G. (NNA.910412.0008)

Burchfiel, B.C., 1965, Structural Geology of the Specter Range Quadrangle, Nevada, and its Regional Significance: Geological Society of America Bulletin, v. 76, p. 175-192. (HQS.880517.1099)

Byers, F.M., Jr., Carr, W.J., and Orkild, P.P., 1989, Volcanic Centers of Southwestern Nevada: Evolution of Understanding, 1960 - 1988: Journal of Geophysical Research, v. 94, no. B5, p. 5908-5924. (NNA.900403.0407)

Byers, F.M., Jr., Carr, W.J., Orkild, P.P., Quinlivan, W.D., and Sargent, K.A., 1976, Volcanic Suites and Related Cauldrons of Timber Mountain-Oasis Valley Caldera Complex, Southern Nevada: U.S. Geological Survey Professional Paper 919. (NNA.870406.0239)

Carr, W.J., 1984, Regional Structural Setting of Yucca Mountain, Southwestern Nevada, and Late Cenozoic Rates of Tectonic Activity in Part of the Southwestern Great Basin, Nevada and California: U.S. Geological Survey Open-File Report 84-854. (NNA.870325.0475)

Carr, W.J., Byers, F.M., Jr., and Orkild, P.P., 1986, Stratigraphic and Volcano-Tectonic Relations of Crater Flat Tuff and Some Older Volcanic Units, Nye County, Nevada: U.S. Geological Survey Professional Paper 1323. (HQS.880517.1115)

Christiansen, R.L., and Lipman, P.W., 1965, Geologic Map of the Topopah Spring NW Quadrangle, Nye County, Nevada: U.S. Geological Survey Map GQ-444. (HQS.880517.1118)

Christiansen, R.L., Lipman, P.W., Carr, W.J., Byers, F.M., Jr., Orkild, P.P., and Sargent, K.A., 1977, Timber Mountain-Oasis Valley Caldera Complex of Southern Nevada: Geological Society of America Bulletin, v. 88, p. 943-959. (NNA.870406.0166)

Crowe, B.M., 1986, Chapter 16: Volcanic Hazard Assessment for Disposal of High-Level Radioactive Waste, in Active Tectonics: Impacts on Society: National Academy Press, Washington, D.C., p. 247-260. (NNA.890501.0156)

Crowe, B.M., and Carr, W.J., 1980, Preliminary Assessment of the Risk of Volcanism at the Proposed Nuclear Waste Repository in the Southeastern Great Basin: U.S. Geological Survey Open-File Report 80-357. (NNA.870407.0400)

Crowe, B.M., Harrington, C., Turrin, B., Champion, D., Wells, S., Perry, F., McFadden, L., and Renault, C., 1989, Volcanic Hazard Studies for the Yucca Mountain Project: Waste Management 89, Volume 1 - High Level Waste and General Interest, p. 485-491. (NNA.901130.0017)

DePolo, C.M., Bell, J.W., and Ramelli, A.R., 1990, Estimating Earthquake Sizes in the Basin and Range Province, Western North America: Perspectives Gained From Historical Earthquakes: Proceedings of the International Topical Meeting, High Level Radioactive Waste Management, April 8-12, v. 1, p. 117-123. (NNA.910328.0044)

Dohrenwend, J.C., Wells, S.G., and Turrin, B.D., 1986, Degradation of Quaternary Cinder Cones in the Cima Volcanic Field, Mojave Desert, California: Geological Society of America Bulletin, v. 97, p. 421-427. (NNA.810123.0018)

Dorn, R.I., 1983, Cation-Ratio Dating: A New Rock Varnish Age-Determination Technique: Quaternary Research, v. 20, p. 49-73. (HQS.880517.1755)

Dorn, R.I., 1988, A Critical Evaluation of Cation-Ratio Dating of Rock Varnish, and an Evaluation of its Application to the Yucca Mountain Repository by the Department of Energy and its Subcontractors, in Bell, J.W., ed., Quaternary Geology and Active Faulting at and Near Yucca Mountain: Final Report to DOE by the Nevada Bureau of Mines and Geology. (NNA.910412.0009)

Dorn, R.I., and Oberlander, T.M., 1981a, Rock Varnish Origin, Characteristics, and Usage: Zeitschrift für Geomorphologie, v. 25, p. 420-436. (NNA.910123.0006)

Dorn, R.I., and Oberlander, T.M., 1981b, Microbial Origin of Desert Varnish: Science, v. 213, p. 1245-1247. (NNA.910123.0020)

Dorn, R.I., and Oberlander, T.M., 1982, Rock Varnish: Progress in Physical Geography, v. 6, p. 317-367. (NNA.910123.0007)

Dorn, R.I., and others, 1986, Cation-Ratio and Accelerator Radiocarbon Dating of Rock Varnish on Mojave Artifacts and Landforms: Science, v. 231, p. 830-833. (NNA.910123.0006)

Doser, D.I., and Smith, R.B., 1989, An Assessment of Source Parameters of Earthquakes in the Cordillera of the Western United States: Bulletin of the Seismological Society of America, v. 79, no. 5, p. 1383-1409. (NNA.910123.0009)

Ekren, E.B., 1968, Geologic Setting of the Nevada Test Site and Nellis Air Force Range, in Eckel, E.B., ed., Nevada Test Site: Geological Society of America Memoir 110, p. 11-19. (HQS.880517.1179)

Fitterman, D.V., 1982, Magnetometric Resistivity Survey Near Fortymile Wash, Nevada Test Site, Nevada: U.S. Geological Survey Open-File Report 82-401, 27 p. (HQS.880517.2674)

Flanigan, V.J., 1981, A Slingram Survey at Yucca Mountain on the Nevada Test Site: U.S. Geological Survey Open-File Report 81-980, 38 p. (HQS.880517.2675)

Fleck, R.J., 1970, Age and Possible Origin of the Las Vegas Valley Shear Zone, Clark and Nye Counties, Nevada: Geological Society of America Abstracts with Programs, v. 2, p. 333. (HQS.880517.1210)

Forman, S.L., 1988, Assessment of the Applicability of the Thermoluminescence (TL) Dating Technique to Natural Hazard Evaluations at the High-Level Nuclear Waste Repository Site, Yucca Mountain, Nevada, in Bell, J.W., ed., Quaternary Geology and Active Faulting at and Near Yucca Mountain: Final Report to DOE by the Nevada Bureau of Mines and Geology. (NNA.910412.0010)

Fox, K.F., Jr., and Carr, M.D., 1989, Neotectonics and Volcanism at Yucca Mountain and Vicinity, Nevada: in Laul, J.C., Van Luik, A.E., and Alexander, D.H., eds., Radioactive Waste Management and the Nuclear Fuel Cycle, v. 13 (1-14), p. 37-50. (NNA.900614.0534)

Frischnecht, F.C., and Raab, P.V., 1984, Time-Domain Electromagnetic Soundings at the Nevada Test Site, Nevada: Geophysics, v. 49, no. 7, p. 981-992. (HQS.880517.2676)

Frizzell, V.A., Jr., and Shulters, J., 1990, Geologic Map of the Nevada Test Site, Nevada: U.S. Geological Survey Miscellaneous Investigations Map I-2046. (NNA.901130.0020)

Frizzell, V.A., Jr., and Zoback, M.L., 1987, Stress Orientation Determined From Fault Slip Data in Hampel Wash Area, Nevada, and its Relation to Contemporary Regional Stress Field: Tectonics, v. 6, no. 2, p. 89-98. (HQS.880517.2677)

Gans, P.B., Miller, E.L., McCarty, J., and Ouldcott, M.L., 1985, Tertiary Extensional Faulting and Evolving Ductile-Brittle Transition Zones in the Northern Snake Range and Vicinity: New Insights From Seismic Data: Geology, v. 13, no. 3, p. 189-193. (HQS.880517.1221)

Gianella, V.P., and Callaghan, E., 1934, The Earthquake of December 20, 1932, at Cedar Mountain, Nevada, and its Bearing on the Genesis of Basin Range Structure: Journal of Geology, v. 42, p. 1-22. (HQS.880517.1230)

Gibbs, A.D., 1983, Balanced Cross Section Construction From Seismic Sections in Areas of Extensional Tectonics: Journal of Structural Geology, v. 5, p. 153-160. (NNA.910328.0061)

Gibson, J.D., Shephard, L.E., Swan, F.H., Wesling, J.R., and Kerl, F.A., 1990, Synthesis of Studies for the Potential of Fault Rupture at the Proposed Surface Facilities, Yucca Mountain, Nevada: Proceedings of International Topical Meeting, High Level Radioactive Waste Management, April 8-12, v. 1, p. 109-116. (NNA.910221.0069)

Gile, L.H., and Grossman, R.B., 1979, The Desert Project Soil Monograph: Soil Conservation Service, U.S. Department of Agriculture, 984 p. (NNA.910128.0138)

Gile, L.H., Peterson, F.F., and Grossman, R.B., 1965, The K-Horizon: A Master Soil Horizon of Carbonate Accumulation: Soil Science, v. 99, no. 2, p. 74-82. (NNA.910128.0139)

Gile, L.H., Peterson, F.F., and Grossman, R.B., 1966, Morphological and Genetic Sequences of Carbonate Accumulation in Desert Soils: Soil Science, v. 101, no. 5, p. 347-360. (HQS.880517.2684)

Harden, J.W., 1982, A Quantitative Index of Soil Development From Field Descriptions: Examples From a Chronosequence in Central California: Geoderma, v. 28, no. 1, p. 1-28. (HQS.880517.1253)

Harrington, C.D., Raymond, R., Jr., and Krier, D.J., 1989, Barium Concentrations in Rock Varnish: Implications for Calibrated Rock Varnish Dating Curves (abs.): Geological Society of America Abstracts with Programs, v. 21, no. 6, p. 343. (NNA.910328.0051)

Harrington, C.D., Reneau, S.L., Raymond, R., Jr., and Krier, D.J., 1990, Incorporation of Volcanic Ash Into Rock Varnish, and Implications for Geochronologic and Paleoenvironmental Research (abs.): Eos, v. 71, no. 43, p. 1341. (NNA.900927.0107)

Harrington, C.D., and Whitney, J.W., 1987, Scanning Electron Microscope Method For Rock-Varnish Dating: Geology, v. 15, p. 967-970. (HQS.880517.2703)

Harris, R.N., and Ponce, D.A., 1988, High-Precision Gravity Network to Monitor Temporal Variations in Gravity Across Yucca Mountain, Nevada: U.S. Geological Survey Open-File Report 88-243. (NNA.890424.0174)

Hasbrouck, W.P., 1987, Hammer-Impact, Shear-Wave Studies, in Danborn, S.H., and Domenico, S.N., eds., Shear Wave Exploration, Geophysical Development Series, v. 2: Society of Exploration Geophysicists, p. 97-121. (NNA.910123.0013)

Hasbrouck, W.P., 1988, Five Shallow Seismic Feasibility Surveys; Expanded Abstracts: Society of Exploration Geophysicists 58th Annual International Meeting, Oct. 30 - Nov. 3, p. 286-289. (NNA.910412.0015)

Haynes, C.V., 1967, Quaternary Geology of the Tule Springs Area, Clark County, Nevada, in Wormington, H.M., and Ellis, D. (eds), Pleistocene Studies in Southern Nevada, p. 1-128: Nevada State Museum of Anthropology Paper Number 13. (HQS.880517.2139)

Healey, D.L., Harris, R.N., Ponce, D.A., and Oliver, H.W., 1987, Complete Bouguer Gravity Map of the Nevada Test Site and Vicinity, Nevada: U.S. Geological Survey Open-File Report 87-506. (NNA.890424.0175)

Ho, D.M., Sayre, R.L., and Wu, C.L., 1986, Suitability of Natural Soils for Foundations for Surface Facilities at the Prospective Yucca Mountain Nuclear Waste Repository: Sandia National Laboratories, SAND85-7107. (NNA.890327.0053)

Holmes and Narver, Inc., 1988, Yucca Mountain Project Site Atlas: Work Performed Under Contract No. DE-AC08-87NV10576 for the U.S. Department of Energy, Nevada Operations Office, Las Vegas, Nevada. (NNA.890428.0364)

Hoover, D.L., 1989, Preliminary Description of Quaternary and Late Pliocene Surficial Deposits at Yucca Mountain and Vicinity, Nye County, Nevada: U.S. Geological Survey Open-File Report 89-359, 45 p. (NNA.900403.0406)

Hoover, D.L., Chornack, M.P., and Broker, M.M., 1982, E-Field Ratio Telluric Traverses Near Fortymile Wash, Nevada Test Site, Nevada: U.S. Geological Survey Open-File Report 82-1042, 14 p. (NNA.900703.0117)

Hoover, D.L., and Morrison, J.N., 1980, Geology of the Syncline Ridge Area Related to Nuclear Waste Disposal, Nevada Test Site, Nye County, Nevada: U.S. Geological Survey Open-File Report 80-942, 70 p. (NNA.870406.0220)

Hoover, D.L., Swadley, W.C., and Gordon, A.J., 1981, Correlation Characteristics of Surficial Deposits With a Description of Surficial Stratigraphy in the Nevada Test Site Region: U.S. Geological Survey Open-File Report 81-512, 27 p. (HQS.880517.1270)

Izett, G.A., 1982, The Bishop Ash Bed and Some Older Compositionally Similar Ash Beds in California, Nevada, and Utah: U.S. Geological Survey Open-File Report 82-582. (HQS.880517.1280)

Izett, G.A., and Naeser, C.W., 1976, Age of the Bishop Tuff of Eastern California as Determined by the Fission-Track Method: Geology, v. 4, p. 587-590. (NNA.910328.0052)

Jackson, J.A., and White, N.J., 1989, Normal Faulting in the Upper Continental Crust: Observations From Regions of Active Extension: Journal of Structural Geology, v. 11, no. 1/2, p. 15-36. (NNA.910123.0010)

Jenny, H., 1980, The Soil Resource: Ecological Studies, v. 37, Springer-Verlag, New York, 377 p. (NNA.910128.0148)

Jones, G.M., Blackey, M.E., Rice, J.E., Murphy, V.J., Levine, E.N., Fisk, P.S., and Bromery, R.W., 1987, Survey of Geophysical Techniques for Site Characterization in Basalt, Salt and Tuff: Weston Geophysical Corporation for Division of Waste Management, Office of Nuclear Material Safety and Safeguards, NUREG FIN D1003, NUREG/CR-4957. (NNA.910123.0003)

Kane, M.F., and Bracken, R.E.,1983, Aeromagnetic Map of Yucca Mountain and Surrounding Regions, Southwest Nevada: U.S. Geological Survey Open-File Report 83-616. (HQS.880517.1290)

Kelson, K.I., Swan, F.H., and Wesling, J.R., 1990, Late Quaternary Displacements on the Meers Fault, Southern Oklahoma (abs): Geological Society of America Abstracts with Programs, v. 22, no. 1, p. 10-11. (NNA.910328.0053)

Kistler, R.W., 1968, Potassium-Argon Ages of Volcanic Rocks in Nye and Esmeralda Counties, Nevada, in Eckel, E.B., ed., Nevada Test Site: Geological Society of America Memoir 110, p. 251-262. (HQS.880517.2006)

Knauss, K.G., and Ku, T.L., 1980, Desert Varnish: Potential for Age Dating Via Uranium-Series Isotopes: Journal of Geology, v. 88, p. 95-100. (NNA.910328.0054)

Krier, D.J., Harrington, C.D., Raymond, R., Jr., and Reneau, S.L., 1990, Pitfalls in the Construction of Rock Varnish Cation-Ratio Dating Curves for Young Volcanic Fields: Examples From the Cima Volcanic Field, CA (abs.): Eos, v. 71, no. 43, p. 1341-1342. (NNA.900927.0109)

Ku, T.L., 1988, Radiometric Dating With U- and Th-Series Isotopes in the Nevada Test Site Region - A Review, in Bell, J.W., ed., Quaternary Geology and Active Faulting at and Near Yucca Mountain: Final Report to DOE by the Nevada Bureau of Mines and Geology. (NNA.910412.0011)

Ku, T.L., Bull, W.B., Freeman, S.T., and Knauss, K.G., 1979, Th^{230} - U^{234} Dating of Pedogenic Carbonates in Gravelly Desert Soils of Vidal Valley, Southeastern California (abs): Geological Society of America Bulletin, Part I, v. 90, p. 1063-1073, doc. no. 91108. (NNA.910123.0021)

Lipman, P.W., and McKay, E.J., 1965, Geologic Map of the Topopah Spring SW Quadrangle, Nye County, Nevada: U.S. Geological Survey Map GQ-439. (NNA.900720.0032)

Maldonado, F., 1985, Geologic Map of the Jackass Flats Area, Nye County, Nevada: U.S. Geological Survey Map I-1519. (HQS.880517.1925)

Maldonado, F., 1990, Structural Geology of the Upper Plate of the Bullfrog Hills Detachment Fault System, Southern Nevada: Geological Society of America Bulletin, v. 102, p. 992-1006. (NNA.910123.0022)

Maldonado, F., and Koether, S.L., 1983, Stratigraphy, Structure and Some Petrographic Features of Tertiary Volcanic Rocks at the USW G-2 Drill Hole, Yucca Mountain, Nye County, Nevada: U.S. Geological Survey Open-File Report 83-732, 83 p. (HQS.880517.1329)

Marvin, R.F., Byers, F.M., Jr., Mehnert, H.H., Orkild, P.P., and Stern, T.W., 1970, Radiometric Ages and Stratigraphic Sequence of Volcanic and Plutonic Rocks, Southern Nye and Western Lincoln Counties, Nevada: Geological Society of America Bulletin, v. 81, p. 2657-2676. (HQS.880517.1334)

McClay, K.R., and Ellis, P.G., 1987, Geometries of Extensional Fault Systems Developed in Model Experiments: Geology, v. 15, p. 341-344. (NNA.910328.0055)

McFadden, L.D., Ritter, J.B., and Wells, S.G., 1989, Use of Multiparameter Relative-Age Methods for Age Estimation and Correlation of Alluvial Fan Surface on a Desert Piedmont, Eastern Mojave Desert, California: Quaternary Research, v. 32, p. 276-290. (NNA.910123.0011)

McFadden, L.D., Wells, S.G., Dohrenwend, J.C., and Turrin, B.D., 1984, Cumulic Soils Formed in Eolian Parent Materials on Flows of the Cima Volcanic Field, Mojave Desert, California, in Surficial Geology of the Eastern Mojave Desert, California: Geological Society of America Guidebook to Fieldtrip 14, p. 134-149. (NNA.910412.0012)

McFadden, L.D., Wells, S.G., and Jercinovich, M.J., 1987, Influences of Eolian and Pedogenic Processes on the Origin and Evolution of Desert Pavements: Geology, v. 15, p. 504-508. (NNA.910123.0023)

McGovern, T.F., 1983, Evaluation of Seismic Reflection Studies in the Yucca Mountain Area, Nevada Test Site: U.S. Geological Survey Open-File Report 83-912. (NNA.870518.0072)

McKay, E.J., and Sargent, K.A., 1970, Geologic Map of the Lathrop Wells Quadrangle, Nye County, Nevada: U.S. Geological Survey Map GQ-883. (NNA.910128.0140)

Molinari, M.P., 1984, Late Cenozoic Geology and Tectonics of the Stewart and Monte Cristo Valleys, West-Central Nevada: M.S. Thesis, University of Nevada, Reno, 124 p. (HQS.880517.2764)

Morrison, R.B., 1967, Principles of Quaternary Soil Stratigraphy: Quaternary Soils, Proceeding of the International Association of Quaternary Research 7th Congress, v. 9, p. 1-69. (NNA.910123.0037)

Muhs, D.R.,Whitney, J.W., Shroba, R.R., Taylor, E.M., and Bush, C.A., 1990, Uranium-Series Dating of Secondary Carbonates Near Yucca Mountain, Nevada: Applications to Tectonic, Paleoclimatic, and Paleohydrologic Problems: Proceedings of the First Annual International Topical Meeting on High Level Radioactive Waste Management, ISBN 0-87262-751-9, p. 924-929. (NNA.900523.0227)

Muller, D.C., and Kibler, J.E., 1984, Preliminary Analysis of Geophysical Logs From Drill Hole UE-25p#1, Yucca Mountain, Nye County, Nevada: U.S. Geological Survey Open-File Report 84-649, 14 p. (HQS.880517.1353)

Neal, J.T., 1985, Location Recommendation for Surface Facilities for the Prospective Yucca Mountain Nuclear Waste Repository: Sandia National Laboratories, SAND 84-2015, Albuquerque, New Mexico, 54 p. (NNA.870406.0061)

Neal, J.T., 1986, Preliminary Validation of Geology at Site for Repository Surface Facilities, Yucca Mountain, Nevada: Sandia National Laboratories, SAND85-0815, Albuquerque, New Mexico. (NNA.870824.0060)

Nelson, A.R., and Taylor, E.M., 1985a, Automated Calculation of Soil Profile Development Indices Using a Microcomputer and Integrated Spreadsheet: Geological Society of America Abstracts with Programs, v. 17, no. 4, p. 258. (NNA.910123.0024)

Noble, D.C., McKee, E.H., and Weiss, S.I., 1988, Nature and Timing of Pyroclastic and Hydrothermal Activity and Mineralization at the Stonewall Mountain Volcanic Center, Southwestern Nevada: Isochron West, v. 51, p. 25-28. (NNA.910412.0016)

Noble, D.C., Vogel, T.A., Weiss, S.I., Erwin, J.W., McKee, E.H., and Younker, L.W., 1984, Stratigraphic Relations and Source Areas of Ash Flow Sheets of the Black Mountain and Stonewall Mountain Volcanic Centers, Nevada: Journal of Geophysical Research, v. 89, p. 8593-8602. (NNA.910328.0056)

Oliver, H.W., Hardin, E.L., and Nelson, P.H., eds., 1990, Status of Data, Major Results, and Plans for Geophysical Activities, Yucca Mountain Project - final draft, prepared for the U.S. Department of Energy, Nevada Operations Office: U.S. Geological Survey and Science Applications International Corporation. (NNA.900621.0221)

Orkild, P.P., 1965, Paintbrush Tuff and Timber Mountain Tuff of Nye County, Nevada: Changes in Stratigraphic Nomenclature by the U.S. Geological Survey: U.S. Geological Survey Bulletin 1224-1, p. A44-A51. (HQS.880517.2039)

Orkild, P.P., and O'Connor, J.T., 1970, Geologic Map of the Topopah Spring Quadrangle, Nye County, Nevada: U.S. Geological Survey Map GQ-849. (NNA.891222.0002)

Ortiz, T.S., Williams, R.L., Nimick, F.B., Whittet, B.C., and South, D.L., 1984, A Three-Dimensional Model of Reference Thermal/Mechanical and Hydrological Stratigraphy at Yucca Mountain, Southern Nevada: Sandia National Laboratories, SAND84-1076, 76 p. (NNA.890315.0013)

Palmer, D.I., 1980, The Generalized Reciprocal Method of Seismic Refraction Interpretation: Society of Exploration Geophysicists, Tulsa, Oklahoma. (NNA.910128.0155)

Pankrantz, L.W., 1982, Reconnaissance Seismic Refraction Studies at Calico Hills, Wahmonie, and Yucca Mountain, Southwest Nevada Test Site, Nye County, Nevada: U.S. Geological Survey Open-File Report 82-478. (HQS.880517.1375)

Peterson, F.F., 1988, Appendix B, Consultant's Report: Soil-Geomorphology Studies in the Crater Flat, Nevada, Area, in Bell, J.W., Quaternary Geology and Active Faulting at and Near Yucca Mountain: Final Report to DOE by the Nevada Bureau of Mines and Geology. (NNA.910412.0013)

Ponce, D.A., Harris, R.N., and Oliver, H.W., 1988, Isostatic Gravity Map of the Nevada Test Site and Vicinity, Nevada: U.S. Geological Survey Open-File Report 88-664, Scale 1:100,000. (NN1.881206.0029)

Potter, R.M., and Rossman, G.R., 1977, Desert Varnish: The Importance of Clay Minerals: Science, v. 196, p. 1446-1448. (NNA.910123.0025)

Potter, R.M., and Rossman, G.R., 1979, The Manganese- and Iron-Oxide Mineralogy of Desert Varnish. Chemical Geology: v. 25, p. 79-94. (NNA.910123.0026)

Proffett, J.M., 1977, Cenozoic Geology of the Yerington District, Nevada, and Implications for the Nature of Basin and Range Faulting: Geological Society of America Bulletin, v. 88, p. 247-266. (HQS.880517.3160)

Quade, J., and Pratt, W.L., 1989, Late Wisconsin Groundwater Discharge Environments of the Southwestern Indian Springs Valley, Southern Nevada: Quaternary Research, v. 31, p. 351-370. (NNA.910123.0012)

Ramelli, A.L., Bell, J.W., and DePolo, C.M., 1988, Evidence for Distributive Faulting at Yucca Mountain, Nevada: Proceedings of Geological Society of America Annual Meeting October 31-November 3, 1988, Denver, Colorado, v. 20, no. 7, p. A383. (NNA.900720.0058)

Ramsay, J.G., and Huber, M.I., 1987, Modern Structural Geology, Volume 2: Folds and Fractures: Academic Press, Inc., London. (NNA.910406.0027)

Reynolds, C.B., and Associates, 1985, 1985 Repository Surface Facility Seismic Survey, Yucca Mountain Area, NTS, Nye County, Nevada: Sandia National Laboratories Final Report, 35 p. (NNA.900223.0120)

Rogers, A.M., Harmsen, S.C., Carr, W.J., and Spence, W., 1983, Southern Great Basin Seismological Data Report for 1981 and Preliminary Data Analysis: U.S. Geological Survey Open-File Report 83-669, 240 p. (HQS.880517.2842)

Rogers, A.M., Harmsen, S.C., and Meremonte, M.E., 1987, Evaluation of the Seismicity of the Southern Great Basin and its Relationship to the Tectonic Framework of the Region: U.S. Geological Survey Open-File Report 87-408, 195 p. (HQS.880517.1409)

Rosenbaum, J.G., Hudson, M.R., and Scott, R.B., 1991, Paleomagnetic Constraints on the Geometry and Timing of Deformation at Yucca Mountain, Nevada: Journal of Geophysical Research, paper no. 90JB01966. (NNA.910612.0003)

Saltus, R.W., and Ponce, D.A., 1988, Aeromagnetic Map of Nevada, Las Vegas Sheet: Nevada Bureau of Mines and Geology, Map 95, Scale 1:250,000; Includes Merged Aeromagnetic Map, Scale 1:1,000,000. (NNA.900108.0132)

Scott, R.B., 1984, Internal Deformation of Blocks Bounded by Basin and Range-Style Faults: Geological Society of America Abstracts with Programs, v. 16, p. 649. (HQS.880517.1441)

Scott, R.B., 1988, Tectonic Setting of Yucca Mountain, Southwest Nevada: Geological Society of America Abstracts with Programs, v. 20, no. 3, p. 229. (NNA.890713.0232)

Scott, R.B., Bath, G.D., Flanigan, V.J., Hoover, D.B., Rosenbaum, J.G., and Spengler, R.W., 1984, Geological and Geophysical Evidence of Structures in Northwest-Trending Washes, Yucca Mountain, Southern Nevada, and Their Possible Significance to a Nuclear Waste Repository in the Unsaturated Zone: U.S. Geological Survey Open-File Report 84-567, 23 p. (HQS.880517.1447)

Scott, R.B., and Bonk, J., 1984, Preliminary Geologic Map of Yucca Mountain, Nye County, Nevada, With Geologic Section: U.S. Geological Survey Open-File Report 84-494. (HQS.880517.1443)

Scott, R.B., and Castellanos, M., 1984, Stratigraphic and Structural Relations of Volcanic Rocks in Drill Holes USW GU-3 and USW G-3, Yucca Mountain, Nye County, Nevada: U.S. Geological Survey Open-File Report 84-491. (NNA.890804.0017)

Scott, R.B., and Rosenbaum, J.G., 1986, Evidence of Rotation About a Vertical Axis During Extension at Yucca Mountain, Southern Nevada: Eos, v. 67, p. 358. (HQS.880517.1445)

Scott, R.B., and Whitney, J.W., 1987, The Upper Crustal Detachment System at Yucca Mountain, SW Nevada: Geological Society of America, Abstracts with Programs, v. 19, no. 5, p. 332-333. (HQS.880517.2863)

Senterfit, R.M., Hoover, D.B., and Chornack, M.P., 1982, Resistivity Sounding Investigation by the Schlumberger Method in the Yucca Mountain and Jackass Flats Area, Nevada Test Site, Nevada: U.S. Geological Survey Open-File Report 82-1043. (HQS.880517.2865)

Sheriff, R.E., and Gledart, L.P., 1982, Exploration Seismology: Cambridge University Press, Melbourne, Australia, v. 1. (NNA.910328.0127)

Smith, C., and Ross, H.P., 1982, Interpretation of Resistivity and Induced Polarization Profiles With Severe Topographic Effects, Yucca Mountain Area, Nevada Test Site, Nevada: U.S. Geological Survey Open-File Report 82-182. (HQS.880517.1464)

Smith, R.B., and Bruhn, R.L., 1984, Intraplate Extensional Tectonics of the Eastern Basin-Range: Inferences on Structural Style From Seismic Reflection Data, Regional Tectonics, and Thermal-Mechanical Models of Brittle-Ductile Deformation: Journal of Geophysical Research, v. 89, no. B7, p. 5733-5762. (HQS.880517.3188)

Snyder, D.B., and Carr, W.J., 1982, Preliminary Results of Gravity Investigations at Yucca Mountain and Vicinity, Southern Nye County, Nevada: U.S. Geological Survey Open-File Report 82-701. (HQS.880517.1481)

Soil Survey Staff, 1951, Soil Survey Manual: U.S. Department of Agriculture Handbook no. 18. (NNA.891222.0028)

Soil Survey Staff, 1975, Soil Taxonomy, A Basic System of Soil Classification for Making and Interpreting Soil Surveys: U.S. Department of Agriculture Handbook No. 436, 754 p. (NNA.910412.0014)

Spaulding, W.G., 1985, Vegetation and Climates of the Last 45,000 Years in the Vicinity of the Nevada Test Site, South-Central Nevada: U.S. Geological Survey Professional Paper 1329, 83 p. (HQS.880517.1484)

Spengler, R.W., Byers, F.M., and Warner, J.B., 1981, Stratigraphy and Structure of Volcanic Rocks in Drill Hole USW G-1, Yucca Mountain, Nye County, Nevada: U.S. Geological Survey Open-File Report 81-1349. (HQS.880517.1492)

Spengler, R.W., and Chornack, M.P., 1984, Stratigraphic and Structural Characteristics of Volcanic Rocks in Core Hole USW G-4, Yucca Mountain, Nye County, Nevada, With a Section on Geophysical Logs by Muller, D.C., and Kibler, J.: U.S. Geological Survey Open-File Report 84-789. (NNA.870519.0105)

Spengler, R.W., Muller, D.C., and Livermore, R.B., 1979, Preliminary Report on The Geology and Geophysics of Drill Hole UE25A-1, Yucca Mountain, Nevada Test Site: U.S. Geological Survey Open-File Report 79-1244. (HQS.880517.1491)

Stein, R.S., and Barrientos, S.E., 1985, Planar High Angle Faulting in the Basin and Range: Geodetic Analysis of the 1980 Borah Peak, Idaho, Earthquake: Journal of Geophysical Research, v. 90, p. 11,355-11,366. (HQS.880517.1494)

Stewart, J.H., 1980, Regional Tilt Patterns of Late Cenozoic Basin-Range Fault Blocks, Western United States: Geological Society of America Bulletin, v. 91, p. 460-464. (HQS.880517.1500)

Stewart, J.H., Albers, J.P., and Poole, F.G., 1968, Summary of Regional Evidence for Right-Lateral Displacement in the Western Great Basin: Geological Society of America Bulletin, v. 79, no. 10, p. 1407-1413. (HQS.880517.1507)

Stock, J.M., and Healy, J.H., 1988, Stress Field at Yucca Mountain, Nevada, in Carr, M.D., and Yount, J.C., eds., Geologic and Hydrologic Investigations of a Potential Nuclear Waste Disposal Site at Yucca Mountain, Southern Nevada: U.S. Geological Survey Bulletin 1790, p. 87-93. (NN1.881128.0011)

Stock, J.M., Healy, J.H., Hickman, S.H., and Zoback, M.D., 1985, Hydraulic Fracturing Stress Measurements at Yucca Mountain, Nevada, and Relationship to the Regional Stress Field: Journal of Geophysical Research, v. 90, no. B10, p. 8691-8706. (HQS.880517.1509)

Swadley, W.C., 1983, Map Showing Surficial Geology of the Lathrop Wells Quadrangle, Nye County, Nevada: U.S. Geological Survey Miscellaneous Investigations Map I-1361, Scale 1:48,000. (HQS.880517.1513)

Swadley, W.C., and Carr, W.J., 1987, Geologic Map of the Quaternary and Tertiary Deposits of the Big Dune Quadrangle, Nye County, Nevada, and Inyo County, California: U.S. Department of Energy, U.S. Geological Survey Map I-1767. (NNA.900618.0080)

Swadley, W.C., and Hoover, D.L., 1983, Geology of Faults Exposed in Trenches in Crater Flat, Nye County, Nevada: U.S. Geological Survey Open-File Report 83-608, 15 p. (HQS.880517.1514)

Swadley, W.C., Hoover, D.L., and Rosholt, J.N., 1984, Preliminary Report on Late Cenozoic Faulting and Stratigraphy in the Vicinity of Yucca Mountain, Nye County, Nevada: U.S. Geological Survey Open-File Report 84-788, 42 p. (HQS.880517.1515)

Swadley, W.C., and Parrish, L.D., 1988, Surficial Geologic Map of the Bare Mountain Quadrangle, Nye County, Nevada: U.S. Geological Survey Map I-1826, Scale 1:48,000. (NNA.900618.0081)

Szabo, B.J., Carr, W.J., and Gottschall, W.C., 1981, Uranium-Thorium Dating of Quaternary Accumulations in the Nevada Test Site Region, Southern Nevada: U.S. Geological Survey Open-File Report 81-119, 35 p. (HQS.880517.1908)

Taylor, E.M., 1986, Impact of Time and Climate on Quaternary Soils in the Yucca Mountain Area of the Nevada Test Site: M.S. Thesis, University of Colorado, Boulder. (HQS.880517.1520)

Taylor, E.M., 1988, Instructions for the Soil Development Index Template -- Lotus 1-2-3 U.S. Geological Survey, Denver, Colorado, program diskette no. 88-233B. (NNA.880512.0028)

Taylor, E.M., and Huckins, H.E., 1986, Carbonate and Opaline Silica Fault-Filling on the Bow Ridge Fault, Yucca Mountain, Nevada - Deposition From Pedogenic Processes or Upwelling Ground Water: Geological Society of America Abstracts with Programs, v. 18, no. 5, p. 418. (HQS.880517.1846)

URS/John A. Blume & Associates, 1986, Ground Motion Evaluations at Yucca Mountain, Nevada, With Applications to Repository Conceptual Design and Siting: Sandia National Laboratories, SAND 85-7104, Albuquerque, New Mexico, 140 p. (NNA.871204.0008)

U.S. Department of Energy (DOE), 1988, Site Characterization Plan: DOE/RW-0199, Office of Civilian Radioactive Waste Management, Washington, D.C. (HQO.881201.0002)

U.S. Geological Survey, 1984, A Summary of Geologic Studies Through January 1, 1983, of a Potential High-Level Radioactive Waste Repository Site at Yucca Mountain, Southern Nye County, Nevada: U.S. Geological Survey Open-File Report 84-792. (HQS.880517.1538)

Vetter, U.R., 1990, Variation of the Regional Stress Tensor at the Western Great Basin Boundary From the Inversion of Earthquake Focal Mechanisms: Tectonics, v. 9, no. 1, p. 63-79. (NNA.910123.0032)

Warren, R.G., McDowell, F.W., Byers, F.M., Jr., Broxton, D.E., Carr, W.J., and Orkild, P.P., 1988, Episodic Leaks From Timber Mountain Caldera: New Evidence From Rhyolite Lavas of Fortymile Canyon, SW Nevada Volcanic Field, Geological Society of America Abstracts with Programs, v. 20, no. 3, p. 241. (NNA.900308.0333)

Wells, S.G., and Dohrenwend, J.C., 1985, Relict Sheetflood Bed Forms on Late Quaternary Alluvial-Fan Surfaces in the Southwestern United States: Geology, v. 13, p. 512-516. (NNA.910123.0027)

Wells, S.G., and McFadden, L.D., 1987, Comment and Reply on "Isotopic Evidence for Climatic Influence on Alluvial-Fan Development in Death Valley, California": Geology, v. 15, p. 1178. (NNA.910328.0057)

Wells, S.G., McFadden, L.D., Dohrenwend, J.C., Bullard, T.F., Feilberg, B.F., Ford, R.L., Grimm, J.P., Miller, J.R., Orbock, S.M., and Pickle, J.D., 1984, Late Quaternary Geomorphic History of the Silver Lake Area, Eastern Mojave Desert, California: An Example of the Influence of Climatic Change on Desert Piedmonts, in Dohrenwend, J.D., ed., Surficial Geology of the Eastern Mojave Desert: Geological Society of America Guidebook to Fieldtrip 14, p. 69-87. (HQS.880517.2244)

Wells, S.G., McFadden, L.D., Renault, C.E., and Crowe, B.M., 1990a, Geomorphic Assessment of Late Quaternary Volcanism in the Yucca Mountain Area, Southern Nevada: Implications for the Proposed High-Level Radioactive Waste Repository: Geology, v. 18, p. 549-553. (NNA.90113.0030)

Wells, S.G., McFadden, L.D., and Ritter, J.B., 1990b, Reply to R. LeB. Hookes's Discussion of "Use of Multiparameter Relative-Age Methods for Age Estimation and Correlation of Alluvial Fan Surface on a Desert Piedmont, Eastern Mojave Desert, California": Quaternary Research, v. 34, p. 263-265. (NNA.910328.0129)

Wernicke, B., and Burchfiel, B.C., 1982, Modes of Extensional Tectonics: Journal of Structural Geology, v. 4, p. 105-115. (HQS.880517.1565)

Whitney, J.W., Shroba, R.R., Simonds, R.W., and Harding, S.T., 1986, Recurrent Quaternary Movement on the Windy Wash Fault, Nye County, Nevada: Geological Society of America Abstracts with Programs, v. 18, p. 787. (HQS.880517.1572)

Winograd, I.J., 1981, Radioactive Waste Disposal in Thick Unsaturated Zones: Science, v. 212, no. 4502, p. 1457-1464. (HQS.880517.2584)

Winograd, I.J., and Doty, G.C., 1980, Paleohydrology of the Southern Great Basin, With Special Reference to Water Table Fluctuations Beneath the Nevada Test Site During the Late(?) Pleistocene: U.S. Geological Survey Open-File Report 80-569, 97 p. (NNA.870518.0073)

Yilmaz, O., 1987, Seismic Data Processing Series: Investigations in Geophysics, v. 2: Society of Exploration Geophysicists, Tulsa, Oklahoma. (NNA.910128.0131)

Zoback, M.L., and Zoback, M.D., 1980, State of Stress in the Conterminous United States: Journal of Geophysical Research, v. 85, p. 6113-6156. (HQS.880517.1587)

Zumberge, M.A., Harris, R.N., Oliver, H.W., Sasagawa, G.S., and Ponce, D.A., 1988, Preliminary Results of Absolute and High-Prediction Gravity Measurements at the Nevada Test Site and Vicinity, Nevada: U.S. Geological Survey Open-File Report 88-242. (NNA.880926.0079)

APPENDIX A

STRUCTURAL MODEL FOR WESTERN MIDWAY VALLEY BASED ON RF DRILLHOLE DATA AND BEDROCK OUTCROPS

APPENDIX A

STRUCTURAL MODEL FOR WESTERN MIDWAY VALLEY BASED ON RF DRILLHOLE DATA AND BEDROCK OUTCROPS

by

Wilfred J. Carr

The structural model of the Midway Valley area proposed in this appendix is based on UE-25 RF, or so-called RF, exploratory drillholes and on outcrops of volcanic bedrock. In 1984 and 1985, 12 RF drillholes were constructed in Midway Valley to obtain subsurface information about sites being considered for repository surface facilities. Lithologic logs of these drillholes, prepared from analyses of cored intervals, are included in this appendix. Interpretations of drillholes in this appendix differ from those of Neal (1985, 1986) (Table 2-2; Section 2.0).

A cross section of the west-central part of Midway Valley was prepared based on data from five RF drillholes near Exile Hill: UE-25 RF #3, #8, #9, #10, and #11 (Figures A-1 and A-2). Stratal dips measured in cores from these five drillholes are summarized in Table A-1. Stratal dips were measured by recording the inclinations of flattened pumice fragments in welded tuff and of bedding in air-fall and reworked tuffs and other sediments. Strike orientation is assumed to be similar to that of the Tiva Canyon Member of the Paintbrush Tuff exposed on Exile Hill and on Alice Ridge. Measurements of the dip of flattened pumice are not precise; figures given are probably within $\pm$ 5° of true dip. Dips in bedded units are variable in some intervals (see Table A-1). The drillholes penetrated alluvium and colluvium as much as 27.4 m (90 ft) thick and penetrated from 7.3 to 64.3 m (24 to 211 ft) of Tertiary tuff beneath the alluvium. Only one of the five drillholes, RF #3, produced core that contained faults; however, small faults could occur in the short drillhole intervals from which no core was recovered. Cores from RF #3 contain a zone of small faults and fractures from between 65.8 m (216 ft) and the bottom of the hole at 91.7 m (301 ft). These faults are represented by a single fault on the cross section in Figure A-2. The most

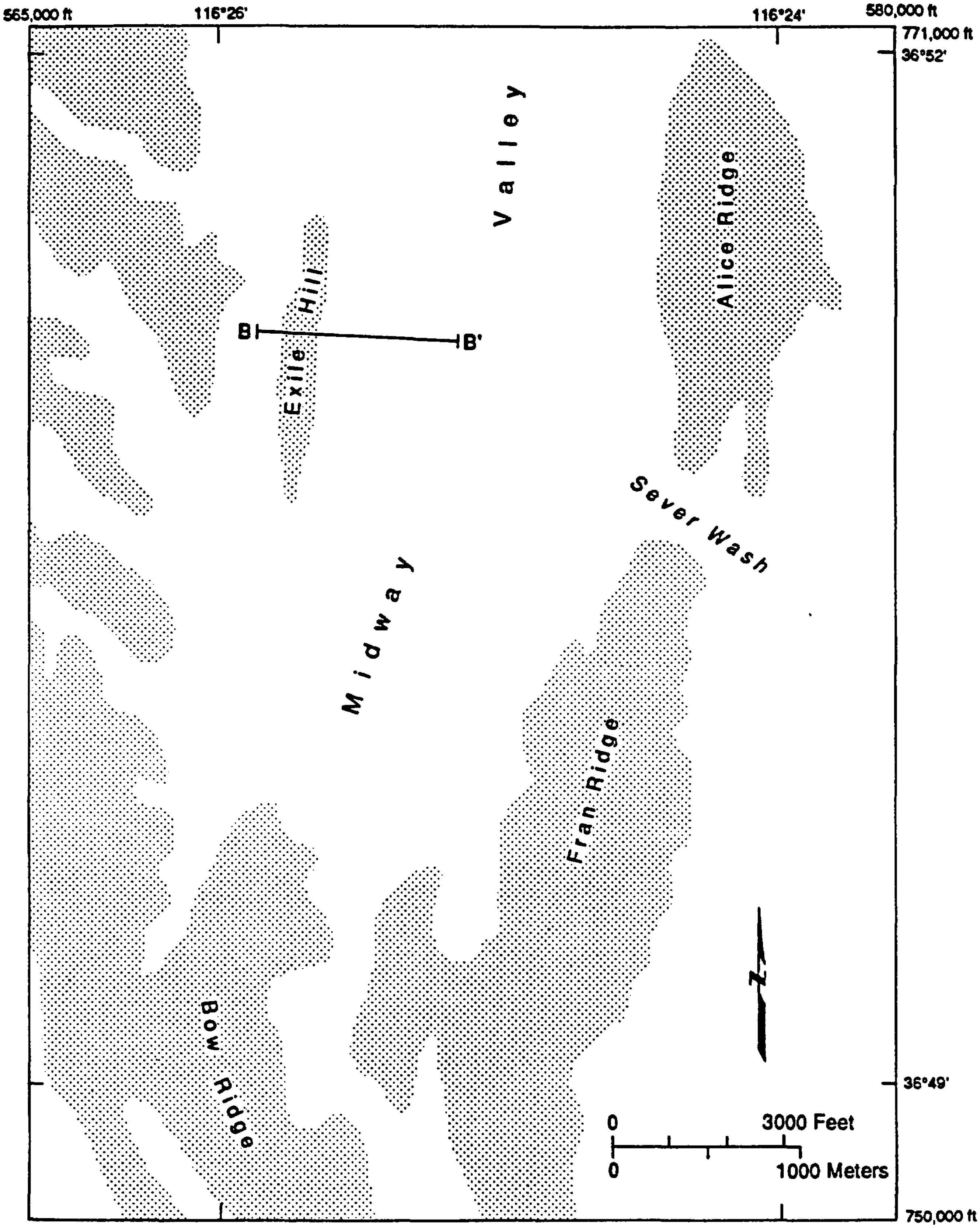

Figure A-1. Location of cross section shown in Figure A-2. Screened areas indicate the location of Tertiary silicic volcanic rocks. Unscreened areas indicate the location of Tertiary to Quaternary alluvial, fluvial, and eolian sediments.

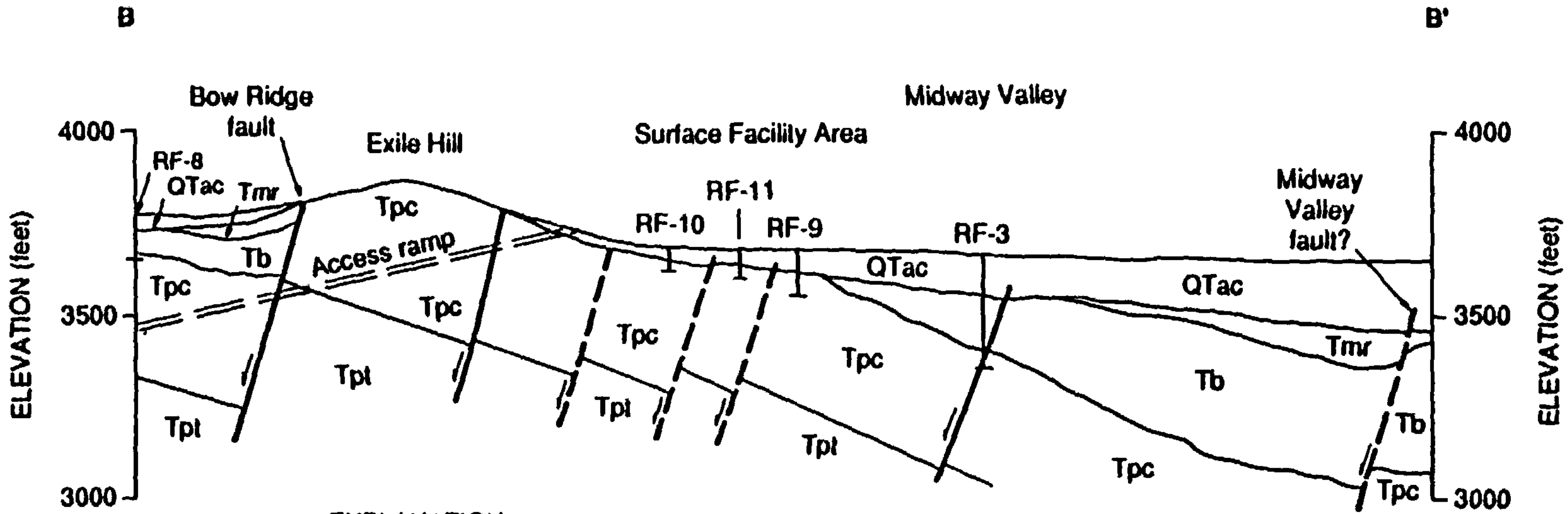

EXPLANATION

Fault or fault zone; solid where exposed at the surface or in cores; dashed where inferred from dips and apparent offsets of lithologic units in cores; arrows indicate relative displacement.

RF-3 Borehole

Stratigraphic Units

Tertiary and Quaternary

QTac Alluvium and colluvium

Tertiary

Tmr Rainier Mesa Member of the Timber Mountain Tuff

Tb Tuff and tuffaceous sediments

Tpc Tiva Canyon Member of the Paintbrush Tuff

Tpt Topopah Spring Member of the Paintbrush Tuff

Note: Location of cross section shown on Figure A-1; drillholes RF-9 and RF-10 projected into line of section

0 1000 Feet
0 300 Meters

No vertical exaggeration

Figure A-2. Geologic cross section near Exile Hill.

prominent faults occur in a narrow zone between 71.6 and 79.9 m (235 and 262 ft), which is equivalent to a fault zone about 3.7 m (12 ft) wide, assuming an average dip of 65°. Measured fault dips were (from shallower to deeper well depths): 70°, 45°, 80°, 40°, 55°, 65°, 60°, 65°, 80°, 70°, and 45°; faults that have shallower dips (i.e., 40° to 55°) appear to be largely antithetic, as they are truncated by faults that have steeper dips.

Five faults are shown on the cross section between the Bow Ridge fault and the inferred Midway Valley fault (Figure A-2). Two of these faults are exposed at the ground surface or in drillholes, and three are inferred; the latter are required by the repetition of Tiva Canyon Member subunits, based on stratal dips observed in cored intervals (Table A-1). The average of the measured stratal dips is 22°, which is steeper than most dips in the Yucca Mountain region west of Midway Valley. A dip of as much as 50° that occurs in a reworked tuff in core from the RF #3 drillhole appears to be unrepresentative of the average dip; the underlying Tiva Canyon Member has a dip of 20° to 25°. This range is consistent with the average dip measured from other cored intervals, suggesting that the 50° dip may be the result of deposition on a scoured or slumped surface, rather than a rotation caused entirely by faulting.

Except for the zone of faults in the lower part of drillhole RF #3, cores from the RF holes provide no indication that a closely spaced fault pattern characterizes the rocks below the alluvium in west-central Midway Valley. The presence of faults in areas between these boreholes, however, cannot be precluded. Insufficient subsurface information is available to verify any structural model. The thin, young deposits in Midway Valley (i.e., the fact that there is no deep basin that has a thick sedimentary fill) support the premise of relative stability in the area during the past 10 m.y. (Carr, 1984) despite Quaternary faulting.

TABLE A-1

STRATAL DIPS MEASURED IN CORES FROM
DRILLHOLES ALONG CROSS SECTION (FIGURE 4-7)

Drillhole	Unit	Approximate Depth,m (ft)	Dip
RF #3	Tuff, reworked	37.2 (122)	20°
	Tuff, reworked	40.8 (134)	25°
	Sandstone	44.2 (145)	20°
	Sandstone	50.3 (165)	10° - 35°
	Tuff	79.6 (261)	25°
	Tuff, reworked	80.2 (263)	50°[1]
	Tiva Canyon Member	82.9 (272)	20° - 25°
RF #8	Tiva Canyon Member	35.1 (115)	15° - 20°
RF #9	Tiva Canyon Member	32.0 (105)	20° - 25°
RF #10	Tiva Canyon Member	15.2 (50)	22°
RF #11	Tiva Canyon Member	21.3 (70)	20° - 25°

[1] Maximum dip present

LITHOLOGIC LOGS FOR APPENDIX A
RF DRILLHOLES
MIDWAY VALLEY STUDY AREA, NEVADA
Logged by W.J. Carr

Original measurements were given in feet rounded to the nearest 0.5 foot.

Elevations and Nevada Plane Coordinates are taken from Holmes and Narver, Inc. (1988)

UE-25 RF #1
N 232375 m (762190 ft); E 174007 m (570890 ft); Elevation 1124.3 m (3688.5 ft);
Cored Intervals: 3.0-3.7 m (10-12 ft); 6.7-6.8 m (22-22.2 ft); 9.1-9.5 m (30-31 ft); 15.2-15.7 m (50.0-51.5 ft); 35.1-36.0 m (115-118 ft); 37.2-38.7 m (122-127 ft); 42.7-44.2 m (140-145 ft).

Stratigraphic Unit - Lithology	Depth, m (ft)	Interval Thickness, m (ft)
Alluvium, bouldery; clasts of Tiva Canyon welded tuff more than 6 in. across. Carbonate coatings.	0.0 - ± 36.6 (0.0 - ± 120.0)	± 36.6 (± 120.0)
Tiva Canyon Member Ashflow tuff, moderately welded, light gray. Gray and white vesicular vapor-phase altered pumice. Phenocrysts 5% to 10%, mostly biotite and feldspar. Carbonate and silica minerals along irregular fractures and a small fault dipping 55° at 37.6 m (123.5 ft). Dip of flattened pumice 20° to 25°.	± 36.6 - 44.2 (± 120.0 - 145.0) T.D.	± 7.6 (± 25.0)

UE-25 RF #2
N 231282 m (758800 ft); E 173838 m (570335 ft); Elevation 1114.7 m (3656.8 ft);
Cored Intervals: 3.0-3.5 m (10-11.5 ft); 9.1-9.4 m (30.0-30.8 ft); 12.5-15.5 m (41-51 ft).

Stratigraphic Unit - Lithology	Depth, m (ft)	Interval Thickness, m (ft)
Alluvium, welded tuff fragments in fine, sandy, silty tan matrix.	0.0 ± 10.1 (0.0 ± 35.0)	± 10.1 (± 35.0)
Tiva Canyon Member Ashflow tuff, densely welded, light gray. 5% phenocrysts, mostly feldspar and biotite. A few fractures having calcite coatings at about 50 ft. Dip of pumice 20°. A few large lithophysal cavities having vapor-phase mineral coatings.[1]	± 10.1 - 15.5 (± 35.0 - 51.0) T.D.	± 4.9 (± 16.0)

[1] The other RF holes generally bottom in the upper part of the caprock zone of the Tiva Canyon Member. This Tiva Canyon appears to be somewhat lower in the section, probably the lowest part of the caprock of Scott and Bonk (1984).

UE-25 RF #3
N 233347 m (765575 ft); E 174071 m (571100 ft); Elevation 1114.9 m (3657.7 ft); Continuous Core.

Stratigraphic Unit - Lithology	Depth, m (ft)	Interval Thickness, m (ft)
Alluvium, light orange-brown, slightly clayey, sandy matrix containing some carbonate; abundant angular clasts of welded tuff, including Tiva Canyon Member caprock facies.	0.3 - 2.4 (1.0 - 8.0)	2.1 (7.0)
Colluvium, light gray, blocks and fragments of welded tuff and rhyolite lava in tuffaceous, silty, sandy, and gravelly matrix having soft carbonate cement. Clasts are Paintbrush Tuff and rhyolites of Fortymile Canyon.	2.4 - 27.4 (8.0 - 90.0)	25.0 (82.0)
Sandstone and Alluvium, tuffaceous, very light gray or tan to white, clayey, calcareous. Contains a few volcanic clasts 2.5 to 5.1 cm (1 to 2 in) in diameter, but mostly pebble- to sand-size fragments that are clay- and carbonate-coated. Lower part is mostly tan to very light yellowish-gray.	27.4 - 34.0 (90.0 - 111.5)	6.6 (21.5)
Sandstone,[1] tuffaceous, very light tan, containing abundant clasts of pumiceous light-colored tuff in a matrix of rather uniform, fine-grained tan sand, weakly cemented by carbonate and clay. Pumice clasts are 0.3 to 1.9 cm (0.125 to 0.75 in) in diameter. At about 34.1 m (112 ft) is a 2.5-cm-thick (1-in) irregular layer of white chalky opal with a little admixed calcite. Sand is mostly rock grains containing some quartz, biotite, and feldspar. A 0.15 m (0.5-ft) concentration of small rock fragments, of pebble to sand size, occurs at base of unit.	34.0 - 35.1 (111.5 - 115.0)	1.1 (3.5)

Stratigraphic Unit - Lithology	Depth, m (ft)	Interval Thickness, m (ft)
Sandstone,[2] tuffaceous, light tan, massive to crudely sorted, except for a few thin (2.5 to 5.0 cm [1 to 2 in]) zones that are distinctly bedded, especially at base. Contains reworked (?) white to light gray pumice fragments, mostly 0.3 to 0.8 cm (0.125 to 0.33 in), but a few as large as 3.8 cm (1.5 in) across. Pumice has less than 2% phenocrysts and generally is altered to clay. Matrix contains silt- to sand-size mineral and rock grains similar to those in unit above.	35.1 - 37.0 (115.0 - 121.5)	2.0 (6.5)
Tuff, reworked, grading down into siltstone that is tuffaceous, light tan, massive. 2.5 cm (1-in) layer of siltstone at base, dipping 20°.	37.0 - 37.2 (121.5 - 122.0)	0.2 (0.5)
Tuff, reworked, very light gray to light tan, massive to crudely sorted; scattered yellowish, pinkish, and white pumice altered to clay. Matrix contains noticeable sand-size rock grains, increasing in size from 0.3 to 0.6 cm (0.125 to 0.25 in) in some zones near base of unit. Crystal fragments, which also increase downward to 25%, consist of quartz, feldspar, and biotite. Lower contact abruptly gradational.	37.2 - 40.1 (122.0 - 131.5)	2.9 (9.5)
Tuff,[3] reworked, or tuff breccia; light tan, coarse-grained with about 5% crystals of quartz, feldspar, and biotite; 20% perlitic colorless glass fragments; and 25% rock grains and fragments as large as 5 cm (2 in) across, mostly light gray silicic lava containing few phenocrysts; hornblende and sphene noted. Basal contact dips 25° and is sharp and scoured.	40.1 - 40.8 (131.5 - 134.0)	0.8 (2.5)
Sandstone, tuffaceous, tan, well sorted, mostly fine and medium grained; thin zones 1.3 to 2.5 cm ([0.5 to 1 in]) of reworked white pumice fragments. Dip of stratification 20°. Biotite, quartz, and feldspar grains. Pumice fragments are coarser toward base--as much as 5 cm (2 in) across; pumice is not vitric, contains sphene and hornblende.	40.8 - 46.0[6] (134.0 - 151.0)	5.2 (17.0)

UE-25 RF #3 (continued)

Stratigraphic Unit - Lithology	Depth, m (ft)	Interval Thickness, m (ft)
Sandstone, tuffaceous, tan, massive to crudely interbedded with white pumice fragment zones; otherwise similar to overlying unit. Dip of well-developed fine stratification from 10° to 35°. Occasional light brown fine siltstone or clay layers. Contacts, especially lower one, gradational. Pumice is mostly vitric and phenocryst-poor.	46.0 - 54.9 (151.0 - 180.0)	8.8 (29.0)
Tuff,[3] highly pumiceous, very light tan, with interbedded intervals 0.3 to 0.9 m (1 to 3 ft) thick of reworked, mostly massive tuffaceous sandstone, as in overlying units. Pumice white to light yellow, similar to overlying units, diameter mostly about 2.0 cm (0.75 in) not vitric. Contacts gradational.	54.9 - 57.2 (180.0 - 187.5)	2.3 (7.5)
Sandstone, tuffaceous, tan, fine- to medium-grained, mostly massive with a few zones of gray and purplish-brown lava fragments; a few gray fragments are vitric, average about 0.6 cm (0.25 in) across. Scattered white pumice altered to clay. Contacts gradational.	57.2 - 62.5 (187.5 - 205.0)	5.3 (17.5)
Tuff, unit "x",[4] ashflow, very light gray, highly pumiceous, nonwelded; zeolitic, vesicular pumice. Probably originally a vapor-phase zone. 10% lithic fragments of mostly purplish-gray lava. A 2.5-cm-(1-in) -thick ash parting at 63.0 m (207 ft), and 1.3 cm (0.5 in) siltstone layer at 64.0 m (209.5 ft). Phenocrysts about 5%; include sphene, hornblende, minor biotite, and quartz. Phenocrysts decrease downward. Irregular parting at 64.0 m (209.5 ft). Clay-coated small fault or tension fracture at about 66.0 m (216 ft), dipping 70°; fault is filled with about 6.4 cm (2.5 in) of pale pinkish-tan pumiceous tuff containing only a few lithic fragments.	62.5 - 76.5 (205.0 - 251.0)	14.0 (46)

UE-25 RF #3 (continued)

Stratigraphic Unit - Lithology	Depth, m (ft)	Interval Thickness, m (ft)
Tuff, unit "x" (continued)		
Rock is slightly iron-stained in footwall. Irregular blobs of iron staining between 66.0 and 66.5 m (216 and 218 ft). Two small faults at 70.5 m (231.5 ft): one dips 45°, has clay coating and down-dip slickensides; the other dips 80° and truncates the first one. Another tight fault occurs at 71.0 m (232.5 ft), dips 40°; no brecciation. A parting or small fault at 72.5 m (238 ft) dips 55°. Two tight faults occur at 73.0 m (239 ft), one dipping 65° and truncating the other, which dips 60°; both have clay coating; first fault has slightly oblique slickensides. Parting or fracture containing fine silt or clay at 75.0 m (245.5 ft). Other faults with clay at 75.0 m (246.5 ft) dip 65°, and at 75.5 m (248.5 ft) dip about 80°; latter fault widens downward to a zone about 2 in. wide, where it leaves the hole at 76.0 m (250 ft). Faults have no breccia and little opening, seem to be primarily fractures filled by tuffaceous silt and clay. Crudely sorted zone at 76.5 m (251 ft) marks basal contact of an ashflow unit.		
Tuff, white to tan, crudely bedded, some fine sand-size sorted layers 2.5 to 7.5 cm (1 to 3 in) thick; abundant small lithic fragments in more massive parts, some clayey coarse pumice in lower part. Subtle unbrecciated fault at 77.5 m (255 ft) dips about 70°; unit is broken and clayey below the fault, which is the lower contact of unit.	76.5 - 77.7 (251.0 - 255.0)	1.2 (4.0)
Tuff, ashflow, nonwelded, pumiceous, pale pinkish-tan to light gray, zeolitic. Scattered sparse lithic fragments of tuff and lava, mostly less than 0.6 cm (0.25 in) across, but a few as large as 3.2 cm (1.25 in) across. 5% to 10% phenocrysts of feldspar, biotite, green pyroxene, biotite, and sparse quartz; biotite more abundant than in overlying units.	77.7 - 79.2 (255.0 - 260.0)	1.5 (5.0)

UE-25 RF #3 (continued)

Stratigraphic Unit - Lithology	Depth, m (ft)	Interval Thickness, m (ft)
Tuff,[5] crudely bedded to massive, light gray, pumiceous zeolitic; a few thin sorted layers of finer pumice dip 25°. Some pumice is pale pink. Phenocrysts same as in overlying unit. Fault marks base, dips 45°, has clay coating and no breccia.	79.2 - 79.9 (260.0 - 262.0)	0.6 (2.0)
Tuff, crudely bedded, reworked, light yellowish-gray; phenocryst-poor; alternating coarse- and fine-grained layers that dip as much as 50°. Base of unit rests on scoured surface that dips 30° to 50°.	79.9 - 80.6 (262.0 - 264.5)	0.8 (2.5)
Tiva Canyon Member		
Ashflow tuff, nonwelded pumiceous, tan grading down to brownish-purple; vapor-phase zone, devitrified, zeolitic and/or clayey; minor biotite and feldspar, but phenocryst content increases downward from less than 5% at top to 10% in lower part. Pumice 0.6 to 2.5 cm (0.25 to 1.0 in), yellow and brown. Lower contact gradational.	80.6 - 81.4 (264.5 - 267.0)	0.8 (2.5)
Ashflow tuff, slightly welded at top, grading abruptly down into densely welded, light purplish-brown to purplish-brown, devitrified. High-angle fracture containing 0.6 cm (0.25 in) layer of indurated ash at 82.0 m (270 ft).	81.4 - 82.6 (267.0 - 271.0)	1.2 (4.0)
Ashflow tuff, densely welded, purplish to grayish-brown, vitrophyric; partly vitric gray groundmass containing yellowish-brown pumice. Phenocrysts 10%, mostly biotite and feldspar with minor quartz and clinopyroxene. Pumice foliation dips 20° to 25°. Contacts gradational.	82.6 - 83.8 (271.0 - 275.0)	1.2 (4.0)
Ashflow tuff, moderately welded at top to slightly welded at base, devitrified, purplish-brown; phenocrysts 5%, mostly bronze biotite; a few high-angle fractures. Contacts gradational.	83.8 - 86.6 (275.0 - 284.0)	2.7 (9.0)

Stratigraphic Unit - Lithology	Depth, m (ft)	Interval Thickness, m (ft)
Ashflow tuff, slightly to moderately welded in lower part, light purplish-brown (lower caprock zone); 5% to 10% small gray pumice. Phenocrysts 5% to 10%, include biotite, feldspar, minor quartz, and clino-pyroxene. Several small faults and fractures have clay filling; unit very rubbly and clayey from 87.5 to 88.5 m (288 to 290 ft) and 89.0 to 91.5 m (292 to 301 ft). Irregular fractures and small faults especially common in lower part. Irregular high-angle fracture as much as 3.8 cm (1.5 in) wide from 91.4 to 91.7 m (300 to 301 ft), filled with clayey pumiceous tuff containing about 5% phenocrysts of sphene and feldspar and some hornblende, quartz, and biotite, as well as a few small lithic fragments; fracture filling probably derived from units above the Tiva Canyon Member.	86.6 - 91.7 (284.0 - 301.0) T.D.	5.2 (17.0)

[1] A sample of the core at 34.5 m (113 ft) in drillhole RF #3 was studied by J.R. Connolly, Department of Geology, University of New Mexico. The following is his petrologic characterization of that sample, as reported in a memorandum of September 25, 1985, to F.B. Nimick of Sandia National Laboratories.

Sample Description - The core sample is light brown to brownish-buff in color, tuffaceous, and very fine-grained except for rare white fragments (up to a few millimeters) and frothy altered pumice (up to one centimeter). Thin section study indicates that the rock is a fine-grained, well-sorted tuffaceous volcaniclastic siltstone with a predominance of fragments composed of altered (zeolitized) glass. Almost all fragments (including feldspars) show a thin (30 microns or less) rim of clay alteration, and many shards have been leached and partially replaced by zeolites. The sample is not welded, and shards are generally undeformed with preserved pumice bubbles and delicate shard shapes present locally.

UE-25 RF #3 (continued)

Most crystalline fragments are angular broken phenocrysts. Except for rare feldspars up to 1 mm in size, most are under 100 microns across, and in the same general size range as shards and other matrix material. Phenocrysts compose 9% of the mode, and are chiefly alkali feldspar, plagioclase, and quartz. All other phenocrysts comprise less than 1% of the mode. These include biotite, typically showing pale brown to greenish-brown pleochroism (rarely dark brown and oxidized), as the dominant mafic phenocryst, with rare titanium/iron oxides and pale green clinopyroxene, and trace amounts of strongly pleochroic hornblende, chevkinite/perrierite, and zircon. No sphene was noted in any of the sections.

About 2% of the mode is composed of devitrified volcanic lithic fragments. The fine grain size makes identification difficult, but most seem to be spherulitic to granophyric fragments of welded ashflow tuff.

Secondary (alteration-related) minerals include birefringent clays rimming phenocryst and shard fragments, finely crystalline tabular zeolites replacing glass, and iron/manganese oxide with prominent colloform textures forming primarily around phenocryst Fe/Ti oxide nuclei. The tabular zeolite morphology, best developed in leached glass shards, suggests heulandite/clinoptilolite composition.

Interpretation of Origin and Tentative Correlations - Sample RF #3, 34.5 m (113 ft), is too well sorted to have originated as an ashflow, yet contains too many delicate structures (e.g., pumice bubbles and delicate shard forms) to have been extensively reworked. The rimming of glassy and crystalline fragments by clays strongly suggests that transport occurred in an environment of active clay formation. Zeolite crystallization from glass followed clay formation, and since zeolites act as a cement, must have largely crystallized after deposition.

Without information on lithologic variability within the unit, it is difficult to evaluate its origin. The good sorting in the sample suggests origin as a pyroclastic fall deposit. A sequence of pyroclastic fall deposits should show some grain size variability between layers, with good sorting within layers. Pulsed eruptions from the fluidized cloud may show thin intercalated, poorly sorted ashflow beds within the well sorted fall deposits. The active clay alteration during transport suggests hydrous conditions (as might be expected when hot ash comes in contact with water, producing an explosive phreatic eruption).

The mineralogy of the sample suggests a genetic affinity with the Rainier Mesa Member of the Timber Mountain Tuff. The Rainier Mesa Member phenocryst assemblage consists of alkali feldspar, plagioclase, and quartz with subordinate biotite and minor clinopyroxene, hornblende, and Fe/Ti oxides.

[2] A sample (RF #3-115.2) of the core at the top of this unit was examined by petrographic and microprobe analysis by F.M. Byers, Jr., and R.G. Warren of Los Alamos National Laboratory, New Mexico. Their results were reported to J.T. Neal of Sandia National Laboratories in a letter (TWS-ESS-1 of October 21, 1986). They characterize the mineral chemistry of the sample as "Typical of lower Rainier Mesa (Member) (tmrl) petrologic zone." They also state that "except for the presence of sphene, the combined petrographic characteristics and feldspar chemistry for sample RF #3-115.2 are uniquely and distinctively those of (petrologic zone) tmrl, although the lithology is atypical."

[3] Samples at 40.8 m and 56.7 m (134.0 and 185.9 ft) were described by Byers and Warren (see Note 2 above) as having "petrochemical characteristics typical for reworked tuff of the Pool petrologic zone (tnp), which is defined from work by Warren at Pahute Mesa to include all post Tpc (Tiva Canyon Member), pre Tmr (Rainier Mesa Member) reworked tuff. These samples have low contents of generally altered biotite relative to other mafic minerals (clinopyroxene and hornblende) and relatively high contents of both metamorphic minerals (such as epidote and garnet) and plagioclase. Much of the plagioclase is highly Ca-rich. Felsic phenocrysts have been highly comminuted by substantial subaerial transport. Sanidine compositions, however, indicate derivation primarily from the underlying unit (tphb) (hornblende rhyolite related to Paintbrush Tuff, referred to as tuff unit "x" in these drillhole logs).

[4] A sample of unit "x" from 67.7 m (222.2 ft) was examined by Byers and Warren (see Note 2 above), who reported that it "matches petrography and mineral chemistry with sample TR 14A-5, which occurs as a pyroclastic fill or dike in the Bow Ridge fault zone" in trench 14-A on the west side of Exile Hill.

[5] A sample of this unit from 79.6 m (261.0 ft), examined by Byers and Warren (see Note 2 above), has petrographic characteristics similar to those of sample TR14A-1 collected from trench 14A on the west side of Exile Hill. Byers correlated this tuff with the tuff of Chocolate Mountain, a thick ashflow sequence inside the Claim Canyon cauldron, 10 km northwest of Midway Valley. The tuff of Chocolate Mountain is intracaldera Tiva Canyon Member.

[6] According to depth markings on blocks in core box, as much as 1.5 m (5 ft) of core may be missing from this interval; blocks marked 40.7 m (133.6 ft) and 43.0 - 46.0 m (141.0 - 151.0 ft) are only 0.6 m (2 ft) apart.

UE-25 RF #3b
N 233384 m (765695 ft); E 174061 m (571066 ft); Elevation 1115.9 m (3661.1 ft)
Core: 27.4-29.0 m (90 - 95 ft); 32.3 - 33.8 m (106 - 111 ft).

Stratigraphic Unit - Lithology	Depth, m (ft)	Interval Thickness, m (ft)
Alluvium, probably similar to that found in hole RF #3.	0.0 - 27.4 (0.0 - 90.0)	27.4 (90.0)
Alluvium, light tan, tuffaceous sandy matrix, moderately indurated; lenses of subangular volcanic clasts; calcareous cement and thin calcitic layers.	27.4 - ± 32.0 (90.0 - ± 105.0)	± 4.6 (± 15.0)
Sandstone, light tan, tuffaceous, containing 1.3- to 2.5-cm (0.5- to 1.0-in) white pumice fragments; sphene and horn-blende; sparse volcanic clasts; minor carbonate in matrix. Correlates with 34.0 to 35.0 m (111 to 115 ft) in hole RF #3.	± 32.0 - 33.8 (± 105.0 - 111.0) T.D.	± 1.8 (± 6.0)

UE-25 RF #4
N 232285 m (762091 ft); E 174365 m (572063 ft); Elevation 1108.5 m (3636.8 ft)
Intermittent Core.

Stratigraphic Unit - Lithology	Depth, m (ft)	Interval Thickness, m (ft)
Alluvium, bouldery, and tuffaceous sandstone. Clasts as much as 20.3 cm (8 in) across, nearly all of which are Tiva Canyon Member. Lower part of unit consists almost entirely of welded tuff clasts.	0.0 - ±45.7[1] (0.0 - ±150.0)	±45.7 (±150.0)
Tuff, Unit "x", ashflow, nonwelded, very light gray to white, containing sparse fine-grained, pale orange pumice fragments as much as 3.2 cm (1.25 in) across, and pale yellow to pink pumice. Lithic fragments 10%, phenocrysts less than 5%. Contacts not cored. Correlates with unit 62.5 to 76.5 m (205 to 251 ft) in hole RF #3.	±45.7 - ±80.8 (±150.0 - ±265.0	±35.1 (±115.0)
Tiva Canyon Member		
Tuff, ashflow, nonwelded, light reddish- to purplish-brown, gray vesicular pumice in lower part. Pumice as large as 3.8 cm (1.5 in) across. Vapor-phase alteration; phenocrysts 2%. Contacts gradational.	±80.8 - 88.7 (±265.0 - 291.0)	±7.9 (±26.0)
Tuff, ashflow, slightly welded, light vapor phase, varicolored pumice; phenocrysts 5%, increasing downward to 15%. Contacts gradational.	88.7 - 91.4 (291.0 - 300.0)	2.7 (9.0)
Tuff, ashflow, moderately welded, light pinkish- to brownish-gray; vapor-phase crystallization; gray, brown, and white pumice. Phenocrysts 20%, mostly feldspar. Pumice lineation dips 25° at 91.5 m (300 ft).	91.4 - 93.3 (300.0 - 306.0) T.D.	1.8 (6.0)

[1] Contact based on cuttings that do not match well with cored interval.

UE-25 RF #5

N 231404 m (759199 ft); E 173156 m (568098 ft); Elevation 1162.4 m (3813.7 ft)

Cored Intervals: 1.8-2.7 m (6.0-9.0 ft); 6.4-7.2 m (21.0-23.5 ft);12.2-13.1 m (40.0-43.0 ft); 24.4-25.6 m (80.0-84.0 ft); 31.1-32.6 (102.0-107.0 ft); 34.1-37.2 (112.0-122.0 ft).

Stratigraphic Unit - Lithology	Depth, m (ft)	Interval Thickness, m (ft)
Alluvium, bouldery; clasts as large as 15 cm (6 in) in diameter in sandy tan calcareous matrix. Lower contact sharp.	0.0 - 31.2 (0.0 - 102.5)	31.2 (102.5)
Tuff, unit "x", ashflow, very light gray. A few white to gray vitric pumice and angular clayey pale orange pumice fragments; 5% small lithic fragments as large as 1.3 cm (0.5 in) in diameter. A few small black to colorless perlitic glass fragments. Phenocrysts less than 5%: quartz, feldspar, biotite, and sparse sphene.	31.2 - 37.2 (102.5 - 122.0) T.D.	5.9 (19.5)

UE-25 RF #7
N 234331 m (768804 ft); E 174093 m (571171 ft); Elevation 1144.9 m (3756.1 ft)
Cored Intervals: 9.1-10.0 m (30.0-33.0 ft); 18.3-19.2 m (60.0-63.0 ft); 27.4-28.7 m (90.0-94.0 ft); 36.6-38.1 m (120.0-125.0 ft); 42.7-45.7 m (140.0-150.0 ft).

Stratigraphic Unit - Lithology	Depth, m (ft)	Interval Thickness, m (ft)
Alluvium, bouldery; clasts to at least 25.5 cm (10 in) in diameter, including several of rhyolite lava, in matrix of calcareous, clayey tan sand.	0.0 - 45.7 (0.0 - 150.0) T.D.	45.7 (150.0)

UE-25 RF #7A
N 234320 m (768768 ft); E 173818 m (570269 ft); Elevation 1144.8 m (3755.9 ft.)
Cored Intervals: 9.1-9.8 m (30-32 ft); 18.3-18.9 m (60-62 ft); 26.5-27.4 m (87-90 ft); 36.6-37.3 m (120-122.5 ft); 45.7-46.6 m (150-153 ft).

Stratigraphic Unit - Lithology	Depth, m (ft)	Interval Thickness, m (ft)
Alluvium, bouldery, carbonate-cemented clayey sand matrix. Clasts as large as 0.5 m (1.5 ft) in diameter. Some rhyolite lava clasts.	0.0 - ±38.1 (0.0 - ±125.0)	±38.1 (±125.0)
Colluvium, coarse fragments and blocks of densely welded Paintbrush Tuff.	±38.1 - 46.6 (±125.0 - 153.0) T.D.	±8.5 (±28.0)

UE-25 RF #8
N 233364 m (765631 ft); E 173367 m (568790 ft); Elevation 1154.6 m (3787.9 ft)
No core from 0-8.5 m (0-28 ft) and 9.8-15.2 m (32-50 ft).

Stratigraphic Unit - Lithology	Depth, m (ft)	Interval Thickness, m (ft)
Alluvium, tan, tuffaceous, sandy, containing cobble-sized clasts of welded tuff. Calcareous cement. Less indurated and more tuffaceous downward.	0.0 ± 13.7[1] (0.0 - ±45.0)	±13.7 (±45.0)
Tuff, white, massive, but possibly reworked; 15% small lithic fragments. Lower contact gradational.	13.7 - 17.1 (45.0 - 56.0)	3.4 (11.0)
Tuff, unit "x", ashflow, nonwelded, white, pumicous; some vitric pumice, pale gray, with a few orange clayey fragments. Phenocrysts 5%, biotite and feldspar with trace of quartz, sphene, and hornblende. 5 to 10% 0.6 to 1.2 cm (0.25 to 0.50 in) lithic fragments, some of which are perlitic gray to black glass; fragments of pumice and lithics increase downward. Thin sorted zones of reworked material 2.5 to 5.0 cm (1 to 2 in) thick at about 28.0 and 28.5 m (92 and 93.5 ft). Similar to unit from 62.5 to 76.5 m (205 to 251 ft) in hole RF #3.	17.1 - 28.5 (56.0 - 93.5)	11.4 (37.5)
Tuff, poorly sorted to crudely bedded; white, coarse, pumiceous. A few lithic fragments.	28.5 - 29.1 (93.5 - 95.5)	0.6 (2.0)
Sandstone, tuffaceous, tan, poorly sorted; scattered white tuff fragments increasing downward; 25% small volcanic rock grains. Lower contact gradational.	29.1 - 29.6 (95.5 - 97.0)	0.5 (1.5)
Tuff, ashflow, white to light gray, pumiceous; pumice mostly white, vitric. A few clasts of black glass. 10% biotite and feldspar, with minor quartz, hornblende, and sphene. Probably the same as interval 62.5 to 76.5 m (205 to 251 ft) in hole RF #3. Similar to unit "x", but has more phenocrysts and pumice.	29.6 - 30.3 (97.0 - 99.5)	0.8 (2.5)

---

[1] Contact based on cuttings that do not match well with cored interval.

UE-25 RF #8 (concluded)

Stratigraphic Unit - Lithology	Depth, m (ft)	Interval Thickness, m (ft)
Tuff, bedded lapilli, tan, poorly indurated.	30.3 - ±30.5 (99.5 - ±100.0)	±0.2 (±0.5)
Tiva Canyon Member		
Tuff, ashflow, caprock, nonwelded to slightly welded; hole ends in zone of gray vesicular pumice. Dip of pumice 15° to 20°. Low-angle calcite-coated fracture at about 33.0 m (108 ft).	±30.5 - 39.0 (±100.0 - 128.0) T.D.	±8.5 ±28.0

UE-25 RF #9
N 233460 m (765945 ft); E 173932 m (570643 ft); Elevation 1119.8 m (3674.0 ft).
Continuous Core

Stratigraphic Unit - Lithology	Depth, m (ft)	Interval Thickness, m (ft)
Colluvium, coarse, bouldery, cemented with calcareous tuffaceous sand. Boulders, as large as 0.5 m (1.5 ft) in diameter, are gray to purplish-gray Paintbrush Tuff and rhyolite lava. Latter is gray to pinkish-gray, flow-banded, and contains 5% to 10% biotite, quartz, feldspar, and probably hornblende. Lava boulders and cobbles more abundant in lower part of unit, where they represent about one-third of the clasts.	0.0 - 19.8 (0.0 - 65.0)	19.8 (65.0)
Tiva Canyon Member		
Tuff, ashflow, mostly devitrified, nonwelded, pale purplish-pink, shardy; lower part has gray vesicular pumice showing vapor-phase crystallization. Phenocrysts 5% to 10%, mostly bronze-colored biotite. Interval, badly broken and crumbly, has several carbonate-coated fractures. Lower contact gradational.	19.8 - 22.3 (65.0 - 73.0)	2.4 (8.0)
Tuff, ashflow, slightly welded, light grayish-purple with gray vesicular pumice. Pumice and degree of welding increase downward. Phenocrysts about 5%, mostly feldspar and biotite. Botryoidal chalcedony in cavities. Contacts gradational.	22.3 - 25.9 (23.0 - 85.0)	3.7 (12.0)
Tuff, ashflow, slightly to moderately welded in lower part, purplish-gray; gray vesicular pumice as much as 6.4 cm (2.5 in) long, but average about 1.3 cm (0.5 in). Phenocrysts 10%, mostly feldspar and subordinate biotite. Some chalcedony in cavities. Contacts gradational. Lithology at 26.0 m (85 ft) matches that at 19.0 m (62 ft) in hole RF #11.	25.9 - 30.5 (85.0 - 100.0)	4.6 (15.0)
Tuff, ashflow, moderately welded, light gray pumice as in overlying unit. A few fractures having clay coatings. Dip of flattened pumice 20° to 25°.	30.5 - 32.3 (100.0 - 106.0) T.D.	1.8 (6.0)

UE-25 RF #10
N 233266 m (765308 ft); E 173806 m (570230 ft); Elevation 1118.5 m (3669.7) ft.
Core from 9.1-18.3 m (30.0 - 60.0 ft).

Stratigraphic Unit - Lithology	Depth, m (ft)	Interval Thickness, m (ft)
Alluvium, cored part light brown calcareous sandstone and siltstone containing scattered welded tuff fragments and numerous thin layers of white to light tan calcium carbonate.	0.0 - 10.8 (0.0 - 35.0)	10.8 (35.5)
Tiva Canyon Member Ashflow tuff, nonwelded to slightly welded, grayish-purple, light and dark pumice, some as large as 5.0 cm (2 in) across, all devitrified with some vapor-phase alteration. Phenocrysts 5%, biotite and feld-spar. Near top of unit are fractures that have carbonate filling. Grades downward to light purplish-gray and becomes moderately welded near bottom of hole. Pumice dips about 22°. One fracture at about 13.0 m (43 ft).	10.8 - 18.3 (35.5 - 60.0) T.D.	7.5 (24.5)

UE-25 RF #11
N 233362 m (765622 ft); E 173869 m (570435 ft); Elevation 1117.2 m (3665.4 ft)
Core Intervals: 0-0.6 m (0-2.0 ft); 10.7-12.2 m (35.0-40.0 ft).

Stratigraphic Unit - Lithology	Depth, m (ft)	Interval Thickness, m (ft)
Alluvium, coarse, bouldery; clasts of Tiva Canyon welded tuff in calcareous, friable tan sandstone; carbonate seams common.	0.0 - 12.0 (0.0 - 39.5)	12.0 (39.5)
Tiva Canyon Member		
Tuff, ashflow, nonwelded, light purplish-pink, poorly indurated; broken, crumbly, clay alteration, carbonate along seams and fractures. Less than 5% phenocrysts, mostly biotite and feldspar.	12.0 - 15.4 (39.5 - 50.5)	3.4 (11.0)
Tuff, ashflow, slightly welded, light purplish-gray; some large 5.0-cm (2-in) light and dark pumice with vapor-phase alteration. Phenocrysts 5% to 10%, biotite, feldspar (same as uppermost Tiva Canyon unit in hole RF #10).	15.4 - 18.6 (50.5 - 61.0)	2.9 (9.5)
Tuff, ashflow, slightly to moderately welded in lower part, light gray with gray and white pumice; vapor-phase alteration. Open fracture at about 19.5 m (64 ft), dipping 75°, chalcedony-coated. Dip of flattened pumice 20° to 25°. Lithology at 19.0 m (62 ft) matches lithology at 26.0 m (85 ft) in hole RF #9.	18.6 - 23.3 (61.0 - 76.5) T.D.	4.7 (15.5)

APPENDIX B

GEOPHYSICAL SURVEYS IN THE MIDWAY VALLEY STUDY AREA

APPENDIX B

GEOPHYSICAL SURVEYS IN THE MIDWAY VALLEY STUDY AREA

Available reports on geophysical surveys in Midway Valley were reviewed to obtain information to help evaluate the thickness of the Quaternary alluvial cover and to identify and assess the geologic structure of the underlying Tertiary bedrock. The reports reviewed below were identified and briefly described in the Oliver et al. (1990) report, "Status of Data, Major Results, and Plans for Geophysical Activities, Yucca Mountain Project." This report "describes past and planned geophysical activities associated with the Yucca Mountain Project and is intended to serve as a starting point for integration of geophysical activities" (Oliver et al., 1990, p. 1-1). The various geophysical techniques and their applications to site characterization in the volcanic tuff of the Yucca Mountain area are described by Jones et al. (1987); relevant conclusions from these analyses are presented below.

Geophysical surveys in Midway Valley described here include seismic reflection surveys, seismic refraction surveys, resistivity/geoelectric surveys, gravity surveys, and magnetic surveys. Summaries of survey results and recommendations for additional work are provided at the end of each section. Suggestions for additional geophysical surveys in support of the study objectives are addressed in Section 5.0.

B-1. Seismic Reflection Surveys

Seismic reflection data obtained in the Yucca Mountain area can be divided into three categories based on depth of penetration: (1) shallow, high-resolution reflection data that image between 0.3 and 1.0 seconds or, typically, depths of 0.15 to 1.5 km (within which the upper 50 to 150 m of sediments generally are not well imaged); (2) intermediate-depth surveys that image structures from 0.3 to 10.0 km and generally fall between 0 and 5 seconds on the seismic time sections; and (3) deep-reflection profiles that image structures up to 15 seconds on the time sections, or depths to 30 km. Neither intermediate- nor deep-reflection profiles cross Midway Valley or the immediately adjacent area.

McGovern (1983) reviewed three studies commissioned by the USGS that cross Midway Valley: the first was conducted in 1980 by the Colorado School of Mines (CSM), the second was conducted in 1981 by Birdwell, and the third was conducted in 1982 by Seisdata (Plate 4). Survey lines from the three studies reviewed by McGovern (1983) are shown on Plate 4. Signal-to-noise ratios are low, even in the 1982 Seisdata 3-D survey. The three surveys produced no interpretable data.

Hasbrouck (1987 and 1988) performed two shear-wave tests in the Yucca Mountain region. The two tests employed a sledgehammer source and closely spaced (6 m apart), three-component geophone receiver arrays. The first line, located near the entrance to Drill Hole Wash, imaged a coherent set of reflections from a depth ranging to about 200 m. The second line is an east-west profile on the west flank of Fran Ridge. This line displays changes in frequency content, reduced amplitude, and time delays related to fracturing. Arrivals could be detected down to 36 m below the source, and signals generally were strongly attenuated. A fault, which was identified by differences in phase velocity between radial-radial and transverse-transverse methods, is interpreted beneath these profiles; the location of this fault within Midway Valley is not described.

Reynolds and Associates (1985) conducted an integrated survey using reflection, P-wave refraction, and S-wave refraction in an area near the prospective surface facilities; survey lines are shown on Plate 4. A weight drop consisting of a leather bag filled with bird shot served as the source. Five lines were recorded near Exile Hill using six groups of geophones spaced 20 m apart. Generally, one to three drops were summed at each drop point. Table B-1 below shows the range of values for P- and S-wave velocities taken from seismic lines and adjacent RF-series wells.

TABLE B-1

RANGE OF VALUES FOR SEISMIC VELOCITIES
IN MIDWAY VALLEY

	Alluvium	Tuff, Tiva Canyon Member
Vp*	0.76 to 1.17 km/sec	1.1 to 1.6 km/sec
Vs*	0.42 to 0.63 km/sec	0.60 to 0.81 km/sec
Vp+	0 to 1.0 km/sec	1.3 to 2.8 km/sec

* Reynolds and Associates (1985) (means) ft/sec.
\+ Pankrantz (1982) (line C)

Based on these values, the potential exists for some overlap of velocities between the alluvium/reworked tuff and tuff of the Tiva Canyon Member (Reynolds and Associates, 1985). The boundaries between these two layers may exhibit small velocity contrasts and local velocity inversions.

From borehole and seismic velocity information, Reynolds and Associates (1985) interpret rocks on the west side of Exile Hill to be less weathered and fractured than those on the east. This interpretation was derived from mapped zones that showed velocities greater than 1219.2 m/sec (4000 ft/sec). Whether these velocities represent a single lithologic layer is questionable. Additional interpretations for these mapped zones of alternating high and low velocities, as noted by Reynold and Associates (1985), include local structural highs and lows and "zones of varying alluvial composition" and/or thickness. The Bow Ridge fault on the west side of Exile Hill was recognized on both survey lines that crossed it (Plate 4). Reflection data suggest an unfaulted 182.9-m-wide (600-foot-wide) block in the northeastern section of the survey.

Unlike in previous surveys, coherent reflectors were interpreted down to one second by Reynolds and Associates (1985). Whether these reflectors are geologic, however, is questionable. The data were so rigorously processed and filtered (using frequency-wave number [f-k] filters) that many events may be artifacts of aliasing. Indeed, Oliver et al. (1990) note that severe attenuation of signals would be expected given the low alluvium velocities in the region, so interpreted horizons at one second may be suspect.

Conclusions from Seismic Reflection Data

Shallow seismic reflection surveys conducted in the Midway Valley area to date have not provided reliable data. Two major contributors to the low signal-to-noise ratios in the seismic data are the lack of well-defined bedding contrasts and the side-scattering of seismic energy by large boulders, caliche layers, and sides of eroded channels. Abrupt variations in the degree of welding and fracturing in the tuff also may disrupt reflections.

The seismic reflection lines shot and processed by Reynolds and Associates (1985) likely contain artifacts that could be misinterpreted as geologic structures. Because this is the only seismic reflection survey from which geologic interpretations have been made, some cautionary observations on the acquisition, processing, and interpretation of the data are made below.

The "soft" dropped-weight source used in the Reynolds survey has the advantage of deforming the earth in a nearly elastic manner, in contrast to explosive sources. A trade-off of using a dropped weight, however, is that the source output is not as impulsive as a shot record, theoretically decreasing the useful frequency range of the source. Reynolds and Associates (1985) state that the bandwidth of the source is from 5 to 140 Hz, which they believe is sufficient to acquire high-resolution seismic data. Another limitation to using a dropped-weight source is that a precursor appears on the record due to the vibration of the truck when the weight is released.

As mentioned above, artifacts resulting from artificial smoothing and aliasing of data may have occurred during processing of the Reynolds and Associates data. Spatial aliasing of steeply dipping events in the f-k domain causes poor performance of both the f-k filter and migration processing steps. The threshold frequency, or the frequency above which aliasing occurs, can be calculated from the equation $f = v/(4\ dx \cdot \sin \theta)$, where v = median velocity, θ = dip of events from the horizontal, and dx = trace interval (Yilmaz, 1987). Given a trace interval of 20 m, dip of 20° (see Appendix A) and range of alluvium and tuff velocities of from 762 to 1614 m/sec, the threshold frequencies range from 28 to 59 Hz. These frequencies are well within the range of recorded frequencies. Spatial aliasing generally can be avoided by selecting a sufficiently small trace spacing (dx).

Oliver et al. (1990) point out that f-k filtering also can introduce an artificial line-up of random events. This smearing of data is further compounded by migration and the application of a nonlinear dip filter to increase the amplitude of coherent events having dips as great as 20°. These processing steps, although they suppress the effects of side-scattered and coherent noise, probably accentuate the artifacts created by aliasing and clipping (loss of data above a certain amplitude) (Oliver et al., 1990).

Coherent noise such as ground roll can be attenuated more effectively if an appropriate source and receiver array are used. Anstey (1986) suggests a stack array in which the source interval is equal to the group interval. The low-frequency, low group velocity, strong-amplitude noise is thus eliminated without having to resort to dip filters during processing.

The receiver cable system used by Reynolds and Associates (1985) also may have contributed to spurious results. Their survey employed reflection "land streamer" cables having gimbal-mounted, self-oriented drag geophones that usually were allowed to lie unburied on the surface. A geophone not coupled to the earth is less likely to follow the motion of the surface of the earth (Sheriff and Geldart, 1982). The response becomes contaminated with air and guided wave noise that propagates along the free surface.

Despite the poor results obtained to date by shallow seismic reflection surveys, useful information may be obtained if different array designs, such as the stack array discussed above, are used. More accurate velocity information in the form of additional well logs would improve processing results. Oliver et al. (1990) suggest that surveys using short-spread and nonexplosive (low-energy) sources such as the minisosie method would be successful in an area where thick alluvium overlies bedrock, if the sources were placed at an adequate distance from major structures that could introduce side-scattering. Reynolds and Associates (1985) suggest that, in conjunction with future high-resolution reflection surveys, a gravity survey and extensive drilling program be performed in the Exile Hill region so that basement structures can be resolved better and velocities can be more tightly constrained.

Another attempt at a 3-D (swath) survey would be helpful if high-quality reflection data could be obtained on test lines. Currently there is an interpretational bias toward north-trending faults parallel to the axis of Midway Valley. A swath survey of the valley would delineate faults and fractures trending in all directions. Future surveys should also extend the length of the valley. Liberal interpretations of lines over limited areas, such as the Reynolds and Associates (1985) survey, can then be avoided.

Intermediate reflection profiles along or across Midway Valley would be most useful if high-quality data could be acquired. Identification of faults at depth on higher-quality lines could then be continued upward toward the surface to assess recency of movement. No such data has been acquired to date in the Midway Valley area. Studies by Brocher and Hart (1988) in the Amargosa Desert showed that reflectivity in the lower crust is much greater than in the upper crust, making fault delineation more reliable at depth. If this is the case at Midway Valley, it may be possible to confidently relate any identified Quaternary faults to tectonic features at depth.

B-2. Seismic Refraction Surveys

Seismic refraction survey data collected in the Midway Valley area can be used to map shallow-velocity structure; to provide velocity information for processing seismic reflection sections; and to study upper, middle, and lower crustal structure, as well as the Moho (Oliver et al., 1990). When possible, interpreted velocity information is correlated to nearby borehole velocity surveys.

Pankrantz (1982) summarizes a survey composed of three reversed-shallow refraction profiles acquired in the Yucca Mountain area. The locations of the three lines are shown on Plate 4. The first line trends northwest and extends from Drill Hole Wash southeast into Midway Valley. The second line crosses Midway Valley between the southern end of Exhile Hill and the northern end of Fran Ridge. The third line crosses the eastern part of the valley by following Sever Wash from the northern end of Exile Hill to the southern end of Alice Hill.

High-velocity explosive sources were used in the Pankrantz (1982) survey; receiver arrays were comprised of 24 geophones spaced 120 m apart. A large explosive charge was used, possibly because of the strong attenuation of seismic energy in the weathered layers. Maximum penetration was 600 m. The refraction lines located along Drill Hole Wash and in the eastern part of Midway Valley provided interpretable data; the third line across central Midway Valley produced no interpretable data. Significant discrepancies exist between the refraction velocities derived from the first line shot along Drill Hole Wash and the well velocities measured from well UE-25a #1. Although further work is needed to assess the discrepancies in velocities, Pankrantz (1982, p. 19) suggests four possible factors: "(1) poor signal-to-noise ratios...; (2) occurrences of undetected low-velocity layers giving rise to errors in travel time curve analysis; (3) the occurrence of a major vertical discontinuity between materials of contrasting velocity...; or (4) the presence of a strong anisotropy of acoustical impedance." Subsurface structure appears to be complex (Pankrantz, 1982). Faulting, both subparallel and oblique to the axis of Midway Valley, can be interpreted on the refraction lines. From data obtained along the line in the eastern part of Midway Valley, Pankrantz (1982) interprets what may be either a major fault covered by Tertiary and Quaternary alluvium or an erosional feature in the center of the horst block that contains Fran Ridge and Alice Hill. Based on a zone of anomalously low velocities within the Topopah Spring Member, the interpreted fault appears to offset strata east of the Paintbrush Canyon fault, implying a "strand" or "zone" of faulting at the base of Fran Ridge. More data are needed to substantiate the existence and characteristics of this fault.

Reynolds and Associates (1985) acquired P-wave and S-wave seismic refraction data as part of their integrated seismic study near the prospective surface facilities. Ten P-wave refraction lines were recorded on the east side of Exile Hill using the same weight-drop source as for the reflection profiles (Plate 4). The depth of resolution for the eight 91.4-m (300-foot) and two 182.9-m (600-foot) spreads comprised of six geophones was less than 30.5 m (100 feet). Because wind noise was prevalent for this part of their survey, the geophones generally were buried, unlike for the reflection survey. The velocity information acquired from these surveys is comparable to the earlier USGS refraction surveys (e.g., Pankrantz, 1982) and is considered by Reynolds and Associates (1985) to be reliable (see Table B-1). The time-depth solutions, however, could not reliably map a consistent, continuous reflector because of large differences in reciprocal times between lines shot in opposite directions. Reynolds and Associates (1985) note that these differences may be the result of greater attenuation of first-arrival energy from one direction than from the other. Undulating refractors or lateral velocity variation commonly are responsible for this phenomenon (Palmer, 1980). Alluvium, especially in fan sequences, may act as an unfaulted discontinuous reflector.

Three shear-wave lines having spread lengths of 91.4 m (300 feet) were shot on the east side of Exile Hill. The shear-wave source was created by striking the side of a bulkhead attached to two trucks. Reynolds and Associates (1985) believed that some of the shear-wave data were incompatible with the primary wave data and thus did not include them in the study. Results of the integrated seismic survey by Reynolds (1985) include:

1) No continuous refractor exists above a depth of at least 30.5 m (100 feet).

2) Very low velocities within beds that also contain rocks having velocities that are as much as 610 m/sec (2000 ft/sec) higher than surrounding velocities suggest that the rocks are highly fractured and weathered, especially the tuffs of the Tiva Canyon Member.

3) Poisson's ratio values are indicative of noncoherent, loose material.

4) Rocks on the west side of Exile Hill appear to be much less fractured and weathered than those on the east side.

5) Tectonic disturbance in the northern part of Exile Hill may be quite old (i.e., pre-Quaternary), as there is no seismic evidence for faulting.

6) Lateral variations in refraction velocities east of Exile Hill suggest the existence of buried horsts and grabens, variations in fracturing, or an alluvial composition.

<u>Conclusions from Seismic Refraction Data</u>

Faulting can be indicated clearly by refraction data; however, downdip geometries and variation of displacement with depth are better imaged on reflection sections (Sheriff and Geldart, 1982). Generally, only structural information is obtained reliably from refraction techniques. Thus, if used in conjunction with trenching investigations in Midway Valley, seismic refraction data could be valuable in detecting and characterizing Quaternary faults.

Realistically, refraction data are limited to the interpretation of at most three to four layers and to depths of approximately one-third the spread length. Thin, weathered, low-velocity layers commonly are undetected, creating time-depth plots that indicate discontinuous layers. The result is a shingling effect whereby layer boundaries are subparallel to each other but are offset in such a manner that they can be misinterpreted to represent units offset by faulting. The fractured layers in the Midway Valley region therefore may create difficulties in the identification of faulting. The scattering of energy within the fractured tuff will further degrade the quality of the data. Refraction data recorded from small arrays should be used in conjunction with reflection data to verify the presence and nature of faulting. Unfortunately, the quality of the reflection data, such as that acquired by Reynolds and Associates (1985), commonly is suspect.

An additional complication in acquiring good refraction data for the Midway Valley area is the small contrast in layer velocities between the alluvium and the Tiva Canyon tuff (see Table B-1). Empirically, velocity contrasts between refractors ideally should vary by a factor of approximately four or five to obtain a dependable image of the subsurface (personal communication, Jim Applegate of Jim Applegate and Associates, 1990). The ratio of velocities between the alluvium and Tiva Canyon tuff, based on the data acquired by Pankrantz, is between 1.3 and 2.8. Conceivably, given significant margins of error and complicated stratigraphy, the ratio could be 1.0 or less. Velocity inversions are not incorporated in seismic refraction analysis.

Future studies should cover a larger area of Midway Valley than has been surveyed to date. The seismic refraction data obtained by Pankrantz (1982) could be reevaluated using information obtained from additional wells that have been drilled in the area since the 1982 survey. None of the UE-25 RF boreholes (see Section 2.2) ties directly with the existing refraction data, nor do any provide velocity information. However, nearby wells for which lithologic data are available (see Appendix A) include UE-25 series RF #7A, RF #7, RF #2, and RF #1. Acquiring geophysical data from these wells would enable comparison with refraction velocities.

B-3. <u>Resistivity/Geoelectric Surveys</u>

Resistivity contrasts that correspond to major features such as structural and lithologic contacts (e.g., the depth to basement) can be delineated by various geoelectric surveys. In the Yucca Mountain area, these surveys have been used to accomplish shallow exploration objectives, including detecting faults and delineating and estimating the thickness of alluvium. The principal objective of the resistivity surveys in the region has been to characterize deep structure (Oliver et al., 1990).

Resistivity surveys have been performed within Midway Valley using several methods, including Schlumberger soundings, time-domain electromagnetic (TDEM) soundings, and magnetometric soundings (Oliver et al., 1990). These studies have approximate depth ranges of 1 m to 20 km. Surveys that crossed Midway Valley near the prospective surface facilities are described by Frischknecht and Raab (1984), Senterfit et al. (1982), Hoover et al. (1982), Smith and Ross (1982), Fitterman (1982), and Flanigan (1981). The locations of survey lines are shown on Plate 4.

Frischknecht and Raab (1984) used short-offset (near-zone), time-domain electromagnetic (TDEM) techniques to evaluate structural discontinuities such as faults in Midway Valley. The anomalies identified in this study have been confirmed by other researchers using different geophysical techniques, demonstrating that TDEM techniques can be applied effectively in geologically complex areas such as the Yucca Mountain region. TDEM line 1 consisted of 17 stations oriented east-west across Midway Valley near the southern end of Exile Hill (Plate 4). The resistivity cross section prepared along this line is interpreted by Frischknecht and Raab to contain a major fault or fault zone in the central part of the line. They state that the fault appears to displace a lower conductive layer about 400 m downward on the west. The location of the interpreted fault coincides with the postulated Midway Valley fault zone. Another possible discontinuity, marked by a decrease in upper-layer resistivity, is interpreted by Frischknecht and Raab a few hundred meters to the east. Near the eastern end of the line, the TDEM data indicate a major discontinuity that Frischknecht and Raab (1984) suggest probably is related to the Paintbrush Canyon fault.

Senterfit et al. (1982) conducted a Schlumberger resistivity survey in the Midway Valley area and showed resistivity variations on three geoelectric cross sections. Two of these cross sections cross Midway Valley near the prospective surface facilities (Plate 4): cross section B-B' is oriented north-northwest, and cross section C-C' is oriented northwest. Significant lateral variations in rock resistivity along these cross sections are indicated by areas of high and low resistivity between the ground surface and a depth of about 300 m. These variations "are attributed to differences in fracturing, faulting, and lithology of the tuffs throughout the area and to varying amounts of clay and other fine-grained materials in the alluvium" (Senterfit et al., 1982). Inferred faults along the C-C' cross section are attributed to Lipman and McKay (1965); faults along the B-B' cross section presumably are interpreted from the resistivity data. A fault on the B-B' cross section line is located in the center of Midway Valley, in the approximate area of the postulated Midway Valley fault (Plate 4). Another mapped fault on the B-B' cross section could represent the Paintbrush Canyon fault. Faults are also interpreted along the strike of Yucca Wash on line B-B'. The orientations of these faults cannot be evaluated from survey data.

Hoover et al. (1982) used electrical (E)-field ratio telluric traverses across Fortymile Wash to better define fault locations. (This method refers to measuring differences in the earth's electric field using a receiving array of three electrodes spaced equidistant and in line, creating, in effect, two colinear dipoles that share a common electrode.) Two of these lines extend east-west from near the proposed repository boundary across Midway Valley to Fortymile Wash (Plate 4). Telluric data for the two lines indicate several prominent short-wavelength anomalies that extend north-south. Hoover et al. (1982) interpret the anomalies to be fault zones that have a low resistivity because of increased fracture porosity. One of the interpreted faults, located along the western edge of Fran Ridge, coincides with the Paintbrush Canyon fault. The telluric data provide no evidence of a low-resistivity zone near the postulated Midway Valley fault.

Smith and Ross (1982) use dipole-dipole resistivity/induced-polarization (IP) data combined with topography in a 2-D model that shows resistivity contrasts related to faults and lithologic variation. Line B', based on 1000-foot dipoles, contains prominent vertical resistivity contrasts coincident with the Bow Ridge fault and the postulated Midway Valley fault (Plate 4).

Several other electromagnetic methods have been tested in the Midway Valley area to assess their effectiveness in locating concealed faults. The Paintbrush Canyon fault was delineated by Flanigan (1981) using a slingram survey (a moving-source electromagnetic profiling method) and by Fitterman (1982) using a magnetometric resistivity survey (magnetic variation of field from 1 Hz line source) (Plate 4). The slingram traverse lines did not extend into the postulated Midway Valley fault zone. Although electromagnetic conductors on other slingram traverses may be related to fracturing and faulting, Flanigan (1981) states that independent geologic and geophysical evidence is necessary to confirm whether the conductors are fault zones. The Turam method (magnetic variation of fields related to different magnetic sources), electromagnetic measurements, and the very-low-frequency measurements made by Flanigan (1981) provided no conclusive data that indicate fault zones. In the magnetometric resistivity survey conducted by Fitterman (1982), an interpreted contact between a high-conductivity zone on the west and a low-conductivity zone on the east is approximately coincident with the Paintbrush Canyon fault. The western edge of the high-conductivity zone possibly coincides with the location of the postulated Midway Valley fault as mapped by Lipman and McKay (1965).

Conclusions from Resistivity/Geoelectric Data

Resistivity/geoelectric surveys conducted within Midway Valley have detected variations in lateral resistivity that correlate with the Bow Ridge, Paintbrush Canyon, and postulated Midway Valley faults. Five of the six studies described above detected anomalies approximately coincident with the Paintbrush Canyon fault; two detected anomalies approximately coincident with the Bow Ridge fault; and three detected anomalies approximately coincident with the postulated Midway Valley fault. An additional study, by Fitterman (1982), also may have detected anomalies associated with the postulated Midway Valley fault. Anomalies interpreted to coincide with the postulated Midway Valley fault are widely distributed across the valley (Plate 4) and probably represent more than one structural feature. Survey coverage in four of the studies was inadequate to identify additional faults; the Bow Ridge fault was not identified by Frischknecht and Raab (1984) or Senterfit et al. (1982), although a wide zone containing sharp resistivity changes was noted east of this fault in the latter study. Future surveys conducted across other parts of Midway Valley could produce additional useful data on fault locations.

B-4. Gravity Surveys

Gravity investigations have been conducted in the Midway Valley study area to detect and characterize faults and other structural features. Gravity data do not permit development of a unique model of the subsurface; thus gravity information typically is used in conjunction with other geophysical data. Gravity maps that include the Yucca Mountain study area include a residual gravity map at a scale of 1:48,000 (Snyder and Carr, 1982); a Bouguer gravity map at a scale of 1:100,000 (Healey et al., 1987); and an isostatic gravity map at a scale of 1:100,000 (Ponce et al., 1988).

Snyder and Carr (1984, 1982) conducted a regional gravity study and prepared a residual gravity map of the Yucca Mountain area. The study is based on more than 2500 Bouguer gravity measurements, 100 surface rock samples, and three borehole gamma-gamma logs. Gravity effects attributable to topography have been eliminated, and an isostatic correction was applied to remove effects of variations in lateral density. The prospective surface facilities are approximately within the area of the 6 and 8 milligal contours. Locally, the gradients are moderate, and the contours obliquely intersect the Bow Ridge and Paintbrush Canyon faults. A large gravity low, which includes parts of the summit of Yucca Mountain and Crater Flat, exists west of the prospective surface facilities. Snyder and Carr (1984) interpret this gravity low to represent a large depression or older caldera that contains at least 4000 m of tuffaceous fill.

Absolute and high-precision gravity measurements have been made in the Midway Valley area to provide base-line information (Zumberge et al., 1988; Harris and Ponce, 1988). Repeatable high-precision gravity surveys provide a method for monitoring temporal variations in the gravity field. Changes in subsurface densities and dilatancy associated with tectonic strain may be interpreted from these temporal variations. In the event of a future major earthquake, vertical movements of as little as 5 cm in subsurface layers could be detected by remeasuring the survey points (Harris and Ponce, 1988).

Conclusions from Gravity Data

Gravimetric techniques could be used to investigate both shallow and deep structures beneath Midway Valley. Jones et al. (1987) suggest that high-resolution data that indicate near-surface faulting can be obtained if additional gravity stations are established to create a detailed grid and if highly accurate data corrections are applied. Reynolds and Associates (1985) state that a detailed gravity survey should be conducted in conjunction with additional seismic and drilling work on the east side of Exile Hill to help delineate possible faults within Midway Valley. The existing gravity data appears best suited for evaluating large-scale regional features.

B-5. Magnetic Surveys

Aeromagnetic, ground magnetic, paleomagnetic, and magnetic property measurements have been made in the Yucca Mountain area to help assess subsurface structure and volcanic history. Compilations of regional aeromagnetic data are displayed on maps of several scales, including 1:48,000 (Kane and Bracken, 1983); 1:62,500 (USGS, 1984); and 1:1,000,000 (Saltus and Ponce, 1988). Linear anomalies having steep gradients that could be interpreted as faults do not appear on these maps in the area of the prospective surface facilities in Midway Valley. Local anomalous lows may indicate thicker units of alluvium.

The feasibility of using magnetic methods for locating concealed faults and possible intrusions in the Yucca Mountain area was tested by Bath and Jahren (1984). Both air and ground magnetic surveys were made. Techniques used at Yucca Mountain were developed by studying magnetic characteristics of displaced volcanic rocks along the Yucca fault in the relatively simple volcanic terrain of Yucca Flat, about 50 km northeast of Yucca Mountain. Eleven major faults were interpreted in the Yucca Mountain area from aeromagnetic anomaly trends. In Midway Valley, anomaly trends correlate with the Bow Ridge, Paintbrush Canyon, and Yucca Wash faults. There are no continuous linear trends indicative of faulting within Midway Valley between the Bow Ridge and Paintbrush Canyon faults. Bath and Jahren (1984) identify the possibility of an east-west structure beneath Yucca Mountain along a latitude that approximately aligns with the northern end of Bow Ridge.

Kane and Bracken (1983) investigated the causes of magnetic anomalies in the Yucca Mountain area. Along the southern end of Midway Valley, they identified an east-west discontinuity in the anomaly pattern that they interpret as a fault. No magnetic anomalies were recognized by Kane and Bracken in the area of the proposed repository or the prospective surface facilities.

Conclusions from Magnetic Data

Bath and Jahren (1984) used aeromagnetic anomaly trends to interpret the Bow Ridge and Paintbrush faults; evidence for the postulated Midway Valley fault was not detected. Jones et al. (1987) recommend that a new aeromagnetic survey, flown at a constant altitude over the Yucca Mountain region and using rigorously processed survey data, would yield data having improved quality and resolution. Computer programs are available that can correlate gravity and magnetic data to produce a model based on both sets of data.

APPENDIX C

AERIAL PHOTOGRAPHS THAT INCLUDE THE MIDWAY VALLEY AREA

APPENDIX C

AERIAL PHOTOGRAPHS THAT INCLUDE THE MIDWAY VALLEY AREA

Aerial photographs of the Yucca Mountain region have been made by the Nevada Bureau of Mines and Geology, U.S. Geological Survey, U.S. Department of Energy, and Sandia National Laboratories (SNL). Coverage of the Midway Valley area is provided by black and white, color, and false color infrared photographs taken under conditions that ranged from both morning and evening low-sun-angle illumination to midday high-sun-angle conditions. Photographic scales are approximately 1:6000, 1:12,000, and 1:60,000. Aerial photographs relevant to this study were compiled, and index maps indicating photograph centers were prepared; these index maps appear as Figures C-1 through C-9 in this appendix.

In accordance with the quality assurance technical procedures, each aerial photograph used in this study carries a unique identifier. The format of this identifier is AAAA/mm-dd-yy/BBBB/CCC, where: (1) AAAA identifies the source of the photograph (e.g., USGS = U.S. Geological Survey, SNL = Sandia National Laboratories, NBMG = Nevada Bureau of Mines and Geology); (2) mm-dd-yy gives the month (mm), day (dd), and year (yy) that the photograph was taken; (3) BBBB is the flight line, if applicable (NA = no flight line designation); and (4) CCC is the frame number of the photograph.

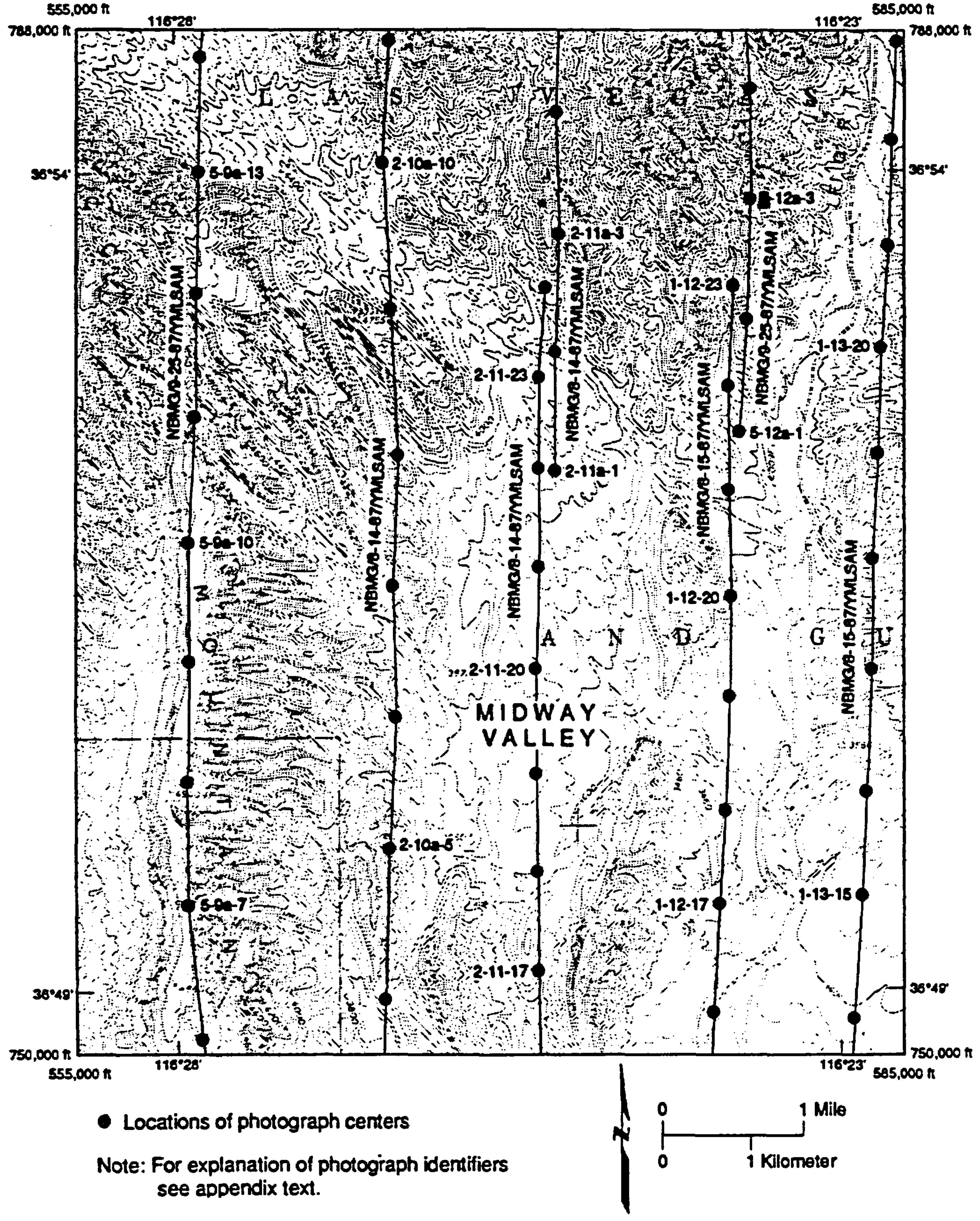

● Locations of photograph centers

Note: For explanation of photograph identifiers see appendix text.

Figure C-1. Aerial photographs of the Midway Valley area: scale ≈ 1:12,000, morning low sun angle photographs taken by Nevada Bureau of Mines and Geology.

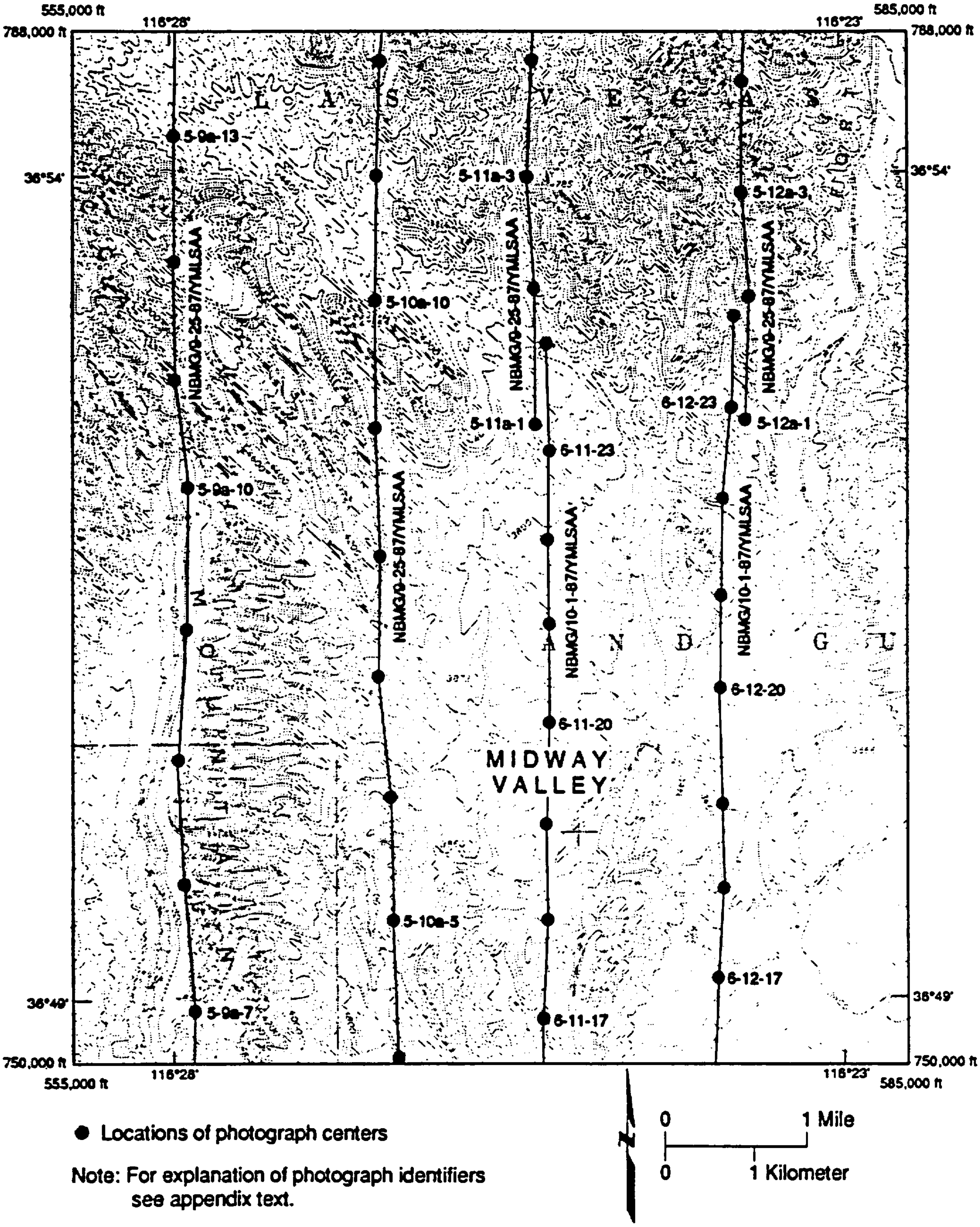

● Locations of photograph centers

Note: For explanation of photograph identifiers see appendix text.

Figure C-2. Aerial photographs of the Midway Valley area: scale = 1:12,000, afternoon low sun angle photographs taken by Nevada Bureau of Mines and Geology.

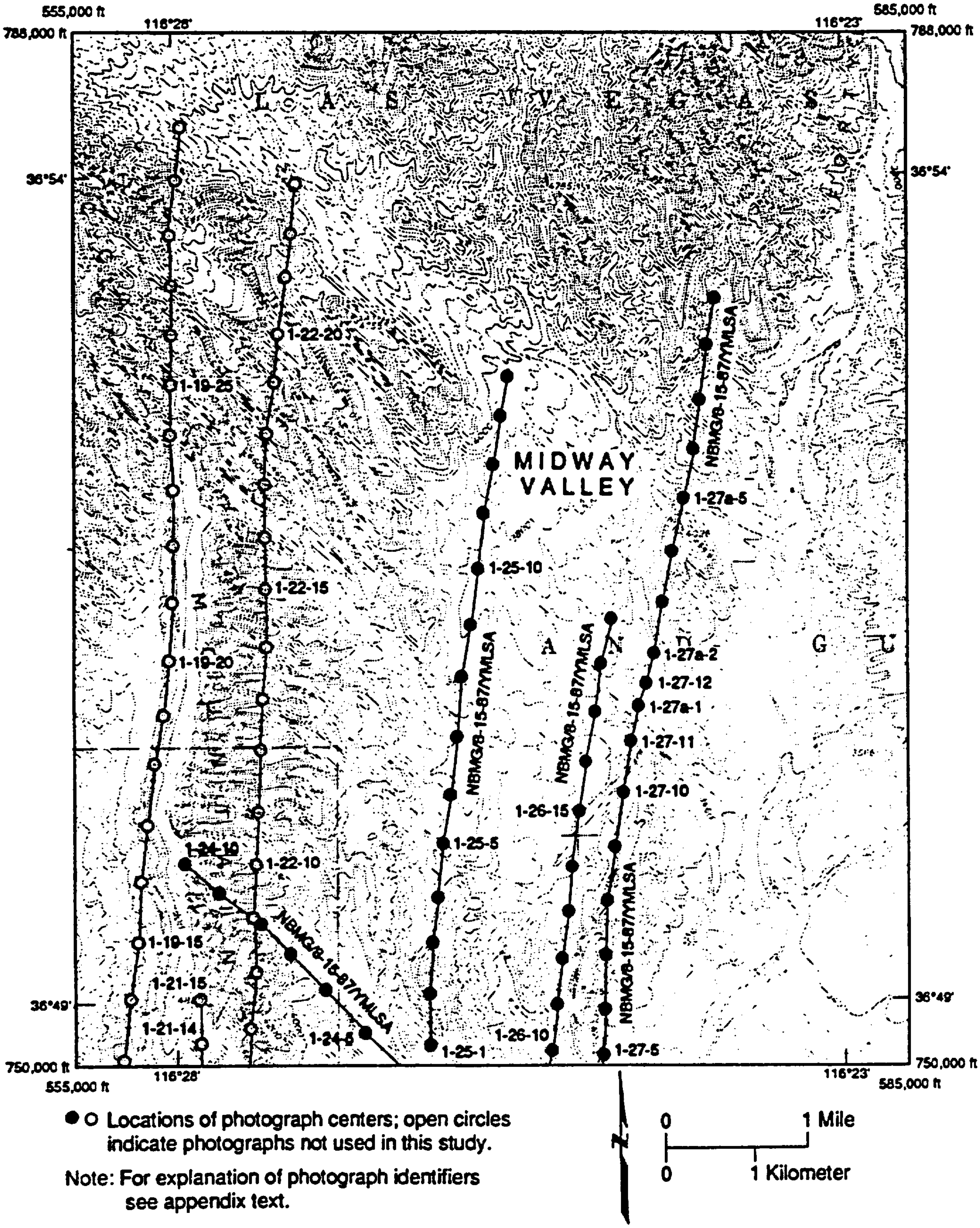

Figure C-3. Aerial photographs of the Midway Valley area: scale ≈ 1:6,000, morning low sun angle photographs taken by Nevada Bureau of Mines and Geology.

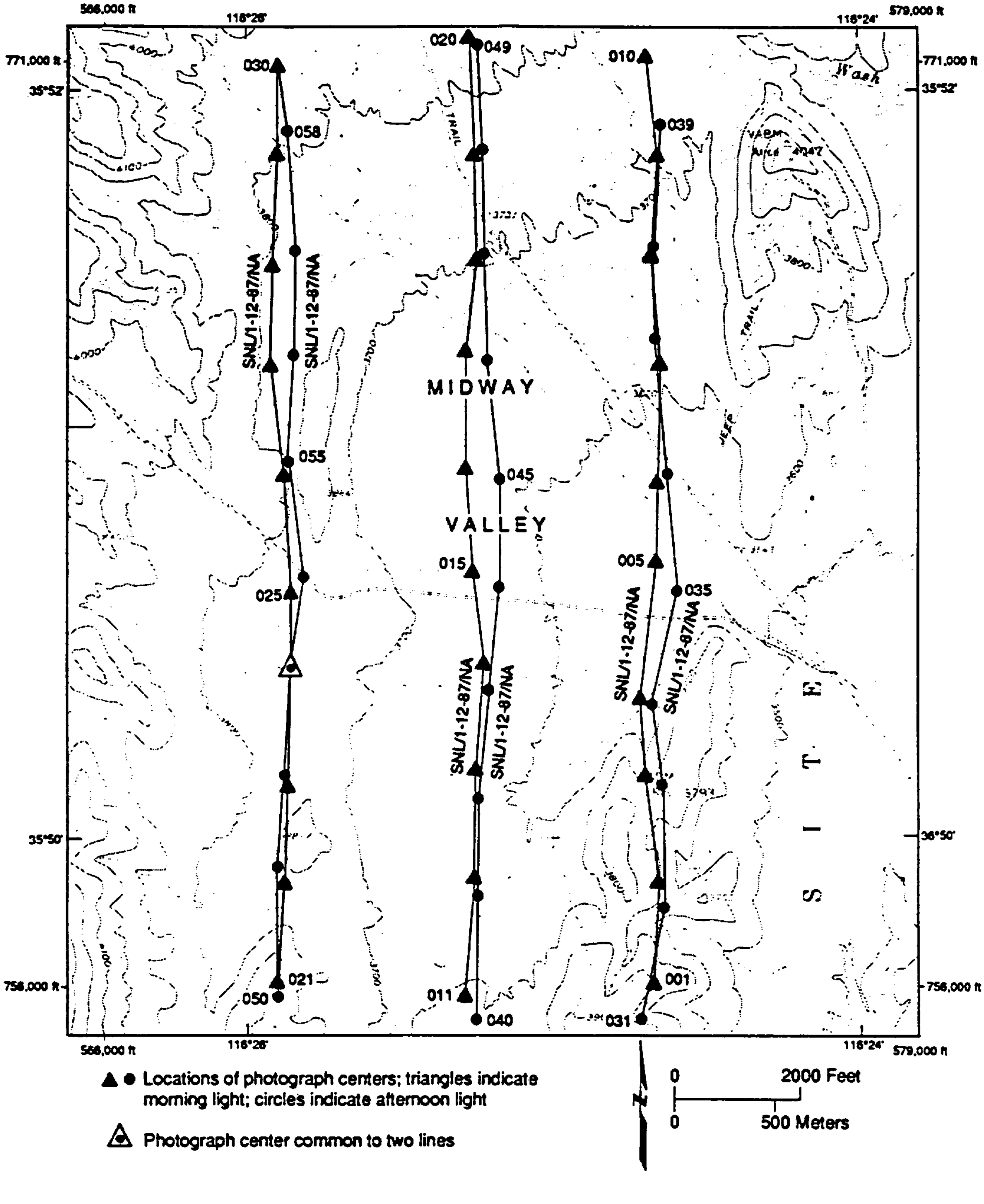

Figure C-4. Aerial photographs of the Midway Valley area: scale ≅ 1:6,000, morning and low sun angle photographs taken by Sandra National Laboratories.

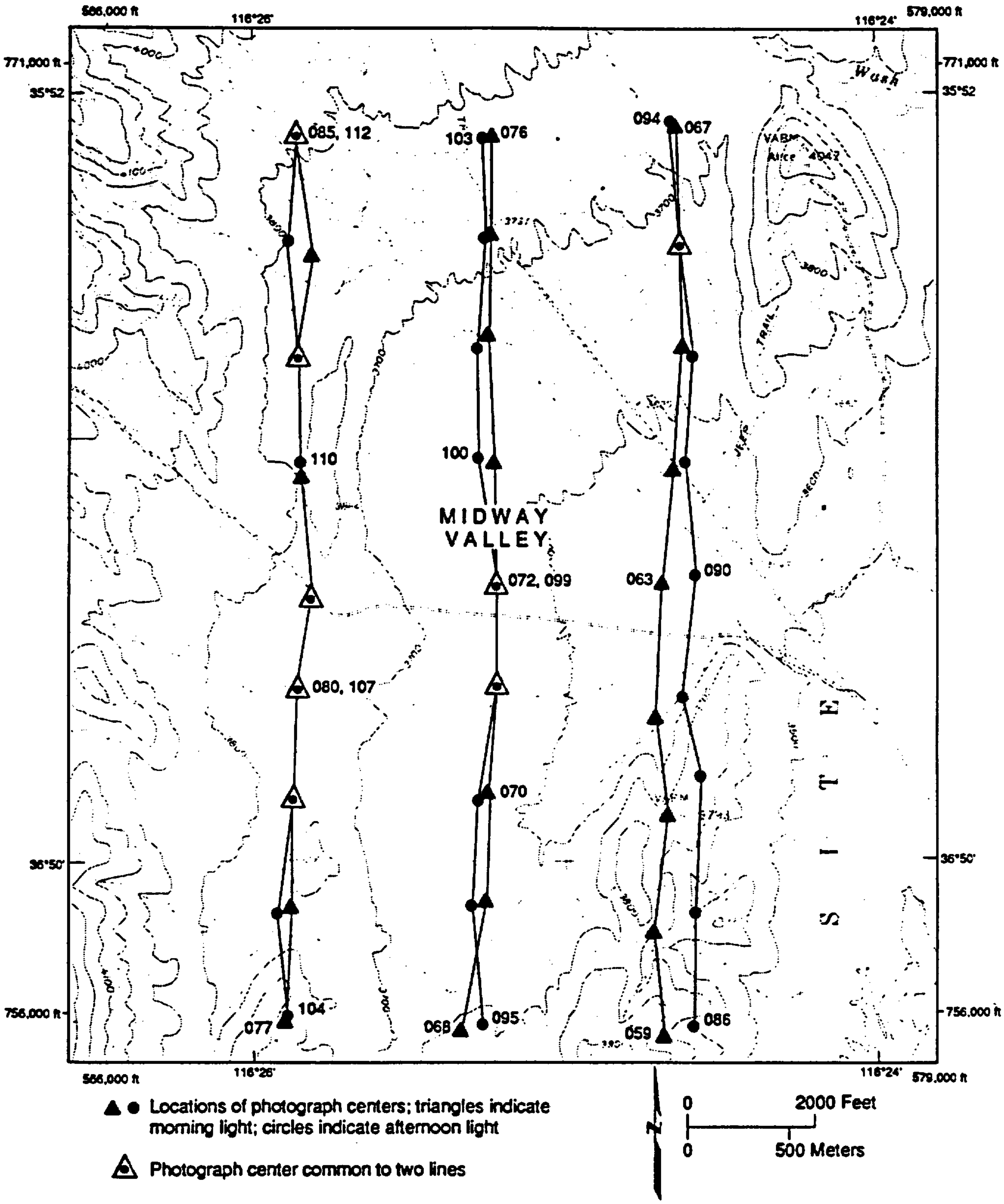

Figure C-5. Aerial photographs of the Midway Valley area: scale ≅ 1:6,000, morning and low sun angle photographs taken by Sandra National Laboratories.

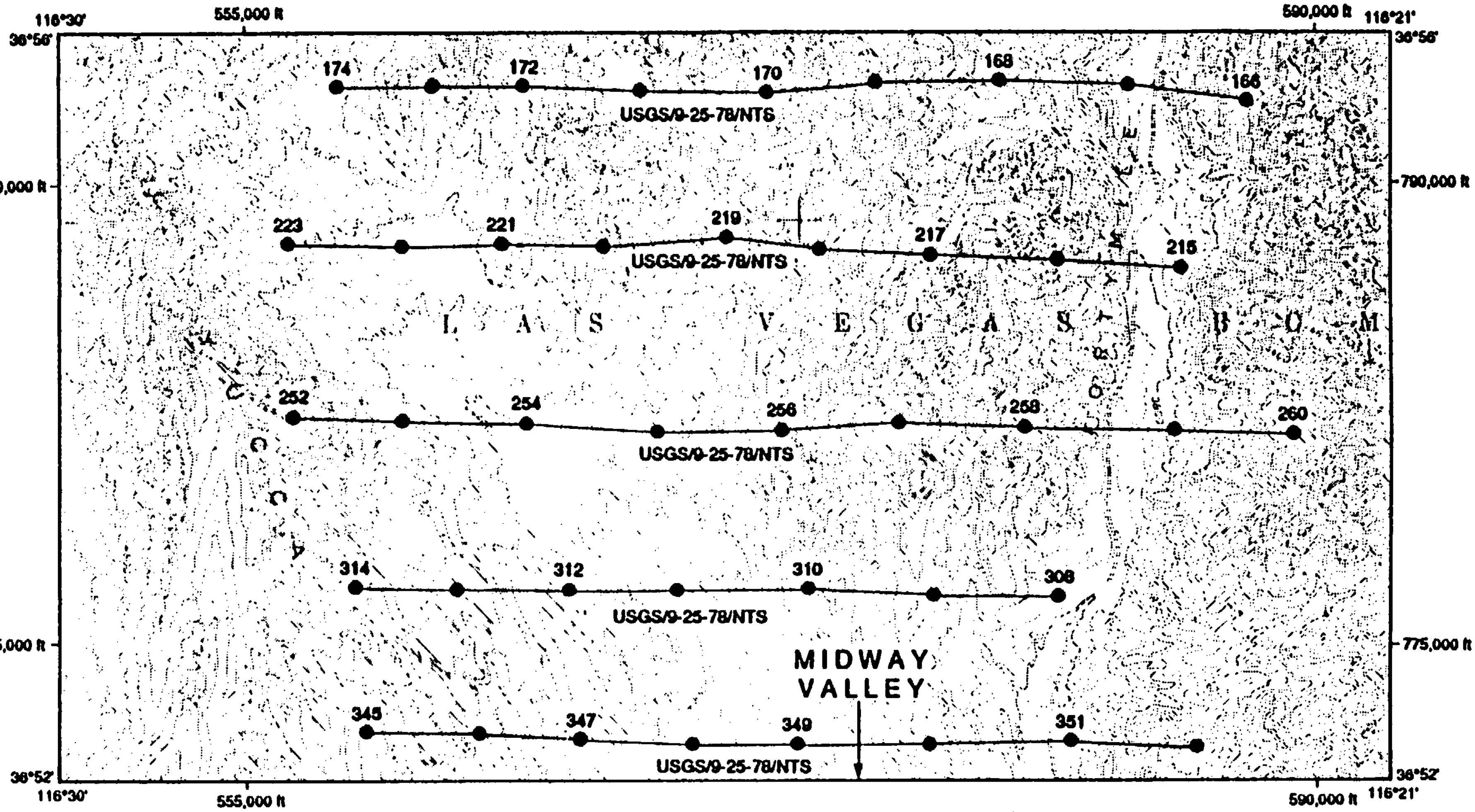

● Locations of photograph centers

Note: For explanation of photograph identifiers see appendix text.

N

0 1 Mile

0 1 Kilometer

Figure C-6. Aerial photographs of the Midway Valley area: scale = 1:12,000, photographs taken by US Geological Survey.

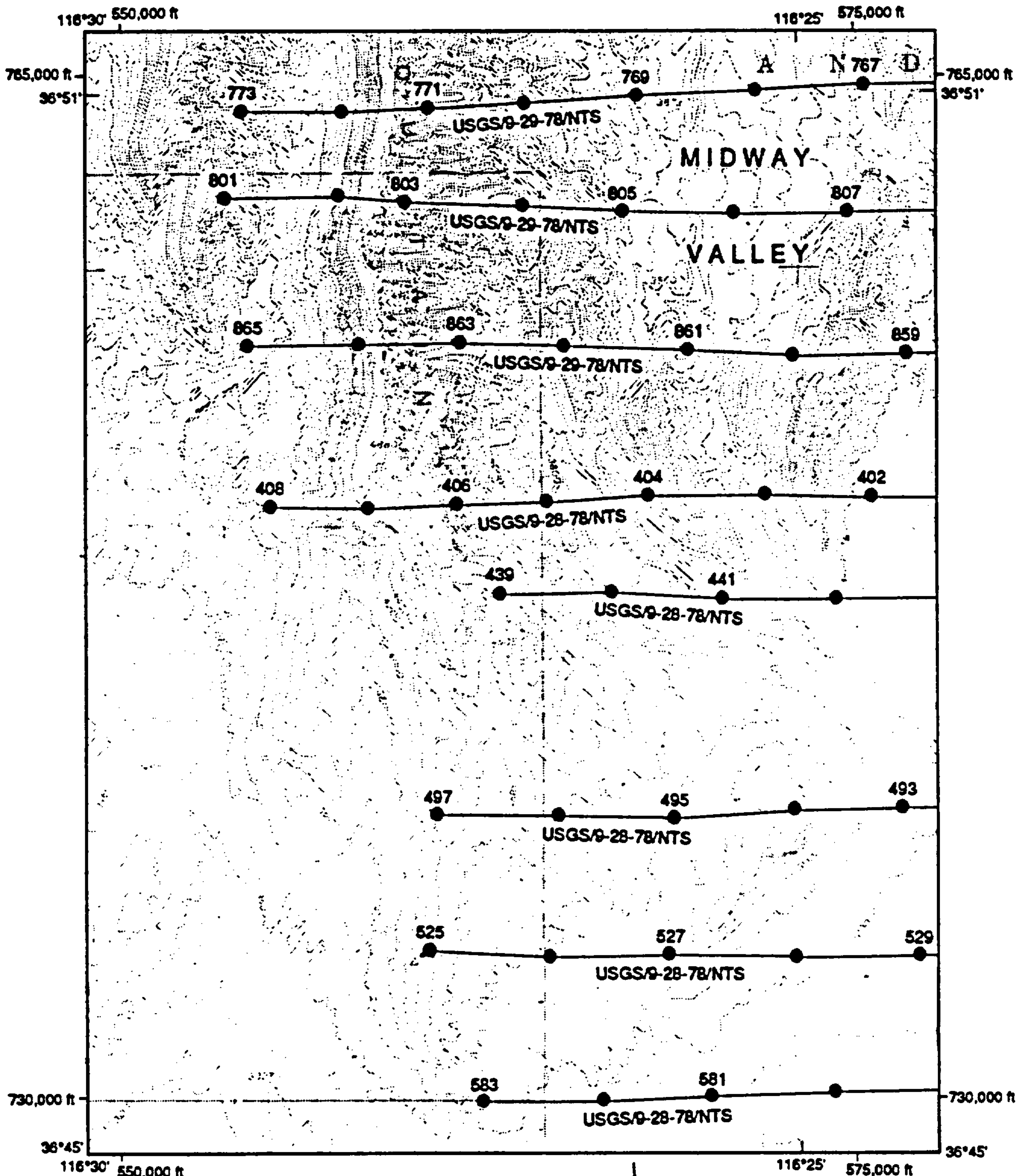

● Locations of photograph centers

Note: For explanation of photograph identifiers see appendix text.

N

0 1 Mile

0 1 Kilometer

Figure C-7. Aerial photographs of the Midway Valley area: scale = 1:12,000, photographs taken by US Geological Survey.

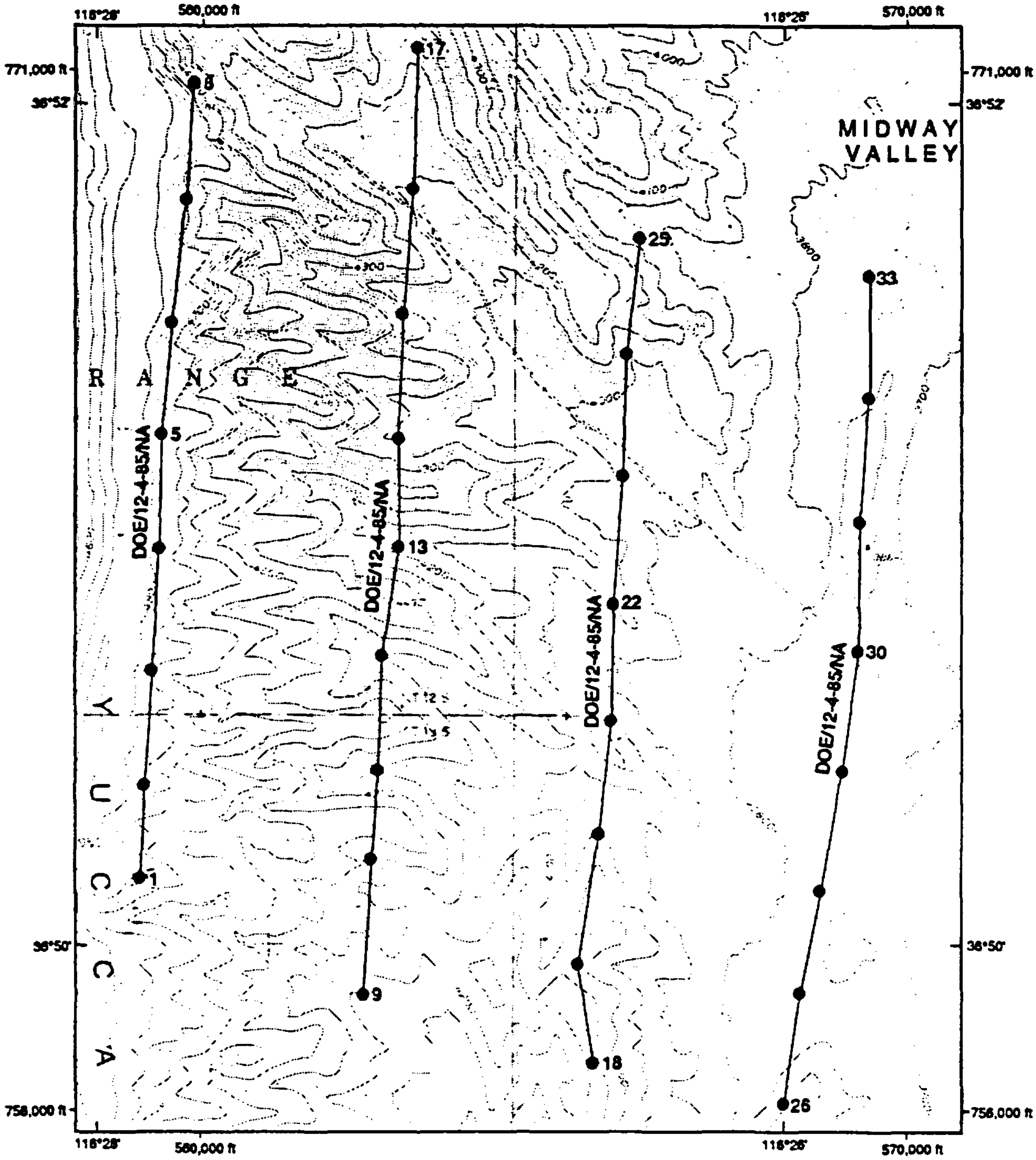

● Location of photograph centers

Note: For explanation of photograph identifiers see appendix text

0 2000 Feet
0 500 Meters

Figure C-8. Geologic cross section near Exile Hill.

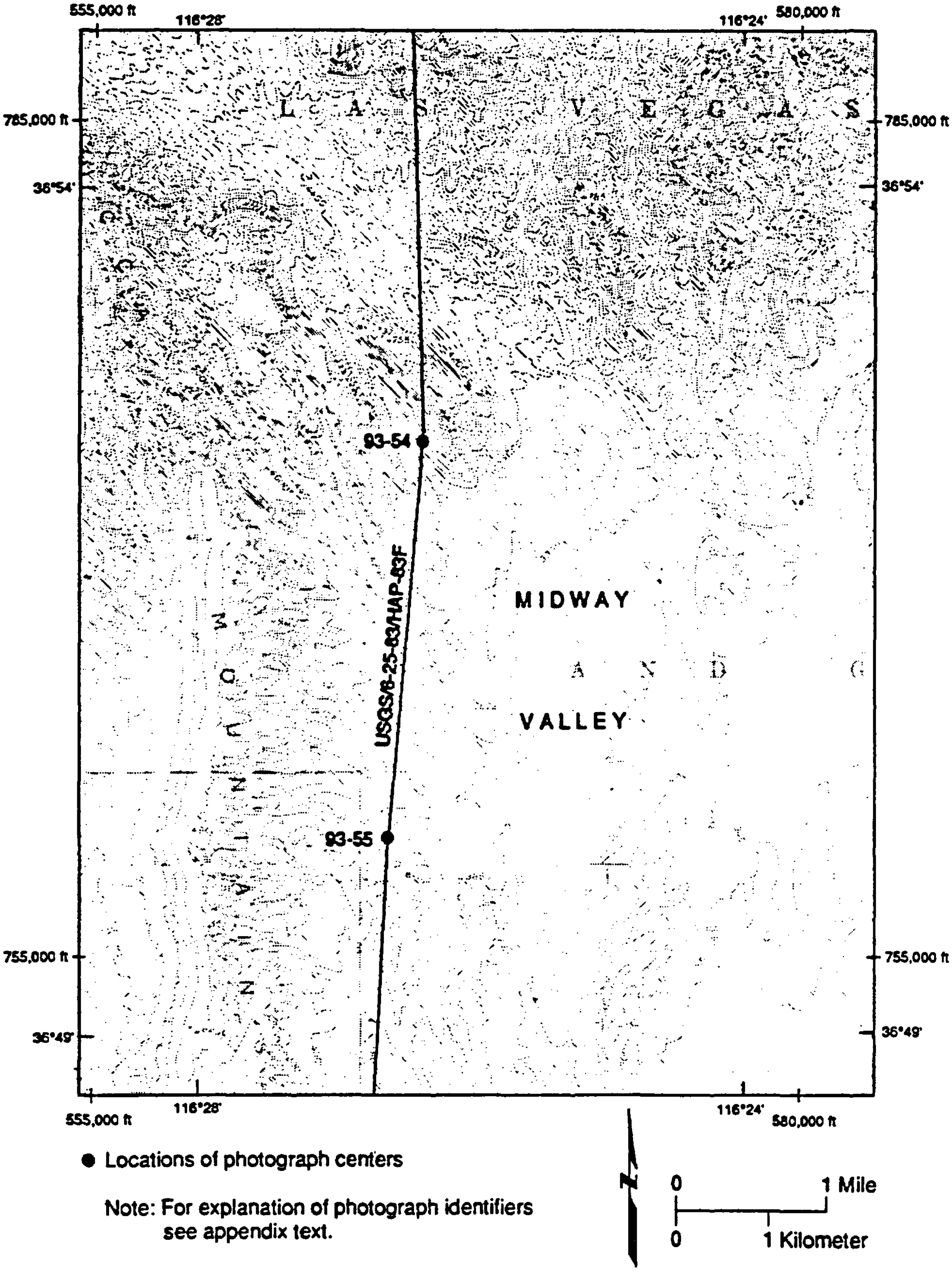

Figure C-9. 1:60,000-scale, false-color infrared aerial photographs of the Midway Valley area used in the lineament study. Photographs acquired from the U.S. Geological Survey.

APPENDIX D

SOIL DATA OF TAYLOR (1986)

APPENDIX D

SOIL DATA OF TAYLOR (1986)

Twenty-two soil profiles were described along Yucca and Fortymile washes by Taylor (1986) using the terminology of the Soil Survey Staff (1951) and Birkeland (1984). Soil descriptions from this work are listed in Table D-1. See Plate 3 for the locations of soil trench locations. A key to the abbreviations in Table D-1 follows the table.

Laboratory analyses were run by Taylor (1986) on selected soil samples. The results of analyses of particle size, bulk density, carbonate content, gypsum content, and soluble salt content are listed in Table D-2. Table D-3 contains the results of analyses of organic carbon and organic matter content, loss on ignition, pH, dithionite extractable iron, oxalate extractable iron, and secondary silica.

TABLE D-1

SOIL DESCRIPTIONS OF TAYLOR
(1986, p. 105 - 111)

Map Unit, Elev (m) (m > stream)	Sample Number	Horizon	Basal Depth (cm)	Lower Boundary	Color dry	Color moist	Texture 1/	% Gravel	Structure	pH	Consistence Dry	Consistence Moist	Consistence Wet	$CaCO_3$	Clay Films	SiO_2	Parent Material
Qlb	FW-7	Ak	1.5	--	10YR7/2	10YR4/2	S	18	1 vt pl	7.75	so		so,po	0	0	0	eolian & overbank
		Cox	18	--	10YR6.5/2	10YR3/3	S	12	m	7.80	lo		so,po	0	0	0	eolian & overbank
1030		2Ckox	100+	--			S	63	sg	8.15	lo		so,po	weak 1	0	0	fluvial gravel
(0.6)														diss			
Qlc	FW-4	Ak	3	as	10YR6/3	10YR4/3	LS	5	1 t pl	7.30	so		so,vps	0, e in places		0	overbank fines mixed
									2° 2 f sbk								w/ gravel component
1006		Btj	9	aw	10YR7/2.5	10YR5/4	LS	7	I m pl	7.35	sh		so,ps	I, cw	3 n br	0	"
(1.2)									2° 2 f-m								
									sbk-sbk								
	2/	2Btk	60	gi	10YR7/3	10YR5/4	SL	28	3 co-vco sbk	7.60	sh		ss,ps	ev I I-	0	0	fluvial gravel
		2Cuk	100+	--	10YR6.5/3	10YR5/4	LS	67	sg	7.80	lo		so,po	I+	0	0	fluvial gravel
Qlc	FW-17	A	6	ci	10YR6/3	10YR4/3	LS	40	I t pl	7.50	so		so,po	0	0	0	pebbly overbank sand
									2° I m-c sbk								
1079		Bwk	24	cw	10YR7/3	10YR4.5/3	LS	40	m in places	8.00	so		so,po	0	0	0	pebbly overbank sand
(1.8)									2° I m-c sbk								
		2Cuk	120+	--	10YR7/3	10YR5/3	S	75	sg	8.10	lo		so,po	e	0	0	fluvial gravel
Qlc	YW-13	A	9	cw	10YR5/2	10YR3/2	LS	53	3m gr, 2° sg	6.80	so		so,po	0	0	0	pebbly overbank sand
		Bw	21	cw	10YR6/2	10YR4/2	SL	33	I f-m sbk	7.10	so		so,po	0	0	0	pebbly overbank sand
1266									2° sg								
(0.9)		2Bqj	73	aw	10YR6/3	10YR4.5/3	S	48	sg	7.40	so		so,po	0	0	0	fluvial gravel
		2Ckqn	138+	--	10YR6/1	10YR5/2	S	67	sg	7.60	lo		so,po	I+, cw	0	I-	fluvial gravel
Qlc	YW-15	A	18		10YR5/2	10YR4/2	LS	55	2 m gr	7.20	so		so,ps	0	0	0	fluvial gravel
		Bw	46		10YR6/3	10YR3.5/3	LS	62	2 m gr	7.30	so-sh		so-ss,	0	0	0	fluvial gravel
1378		(46 - 108 & 108-170)											ps				
(1.2)		2Bqk	170		7.5YR6.5/4	7.5YR4/4	SL	78	sg	7.60	sh		so,po	I+, cw	0	I+	fluvial gravel
		2Cuk	220+	--	7.5YR6.5/4	7.5YR5/4	LS	63	sg	7.95	so		so,po	lenses I	0	0	fluvial gravel

TABLE D-1

SOIL DESCRIPTIONS OF TAYLOR (1986, p. 105 - 111)

Map Unit, Elev (m) (m > stream)	Sample Number	Horizon	Basal Depth (cm)	Lower Boundary	Color dry	Color moist	Texture 1/	% Gravel	Structure	pH	Consistence Dry	Consistence Moist	Consistence Wet	$CaCO_3$	Clay Films	SiO_2	Parent Material
Q2b	FW-3 2/ 3/	Avk	5	as	10YR7/2.5	10YR4/3	L	10	2 c pl 2° 2 co sbk	7.75	so-sh		ss,ps	e-es in places	0	0	eolian and sheetwash
1012 (4.6)		Btk	12	aw	10YR7/3	10YR4/3.5	L	33	2 m-co sbk	7.65	sh		s,p	e I	I mk pf & po	0	eolian and sheetwash
	2/	2Btk	45	cw	7.5YR6/4	7.5YR4/4	SL	82	sg 2° 1 m sbk	7.65	sh		s,p	I	3 n po & br	I	fluvial gravel
		2Bqmkl	83	cw	7.5-10YR7/5 7.5YR5/5	7.5-10YR5/6 7.5YR4/4	LS (grav)	81	m	7.60	h		so,po	e, I+ in veins	3n gr	II	fluvial gravel
	3/ 4a/	2Bqmk2	107	gw	10YR7/4	7.5YR5/6	S	83	m	7.60	h		so,po	I, pods of II	1-2 n gr	II ~3mm thick on bottom of clasts	fluvial gravel
	4b/	2Ckqa	210+	--	10YR5/2	10YR3/2	S	80	sg	7.90	lo		so,po	I	0	I	fluvial gravel
Q1c and	YW-21	Avk	4	as	10YR7/3	10YR4/3	SL+	19	3 co sbk	8.00	so-sh		ss,p	ev	2 n po	0	eolian, sheetwash
Q2b over Q2c		Bijk	15	aw	10YR6/3	10YR4/3	SL+	17	2 t pl 2° 1 f sbk	7.50	sh		ss,ps	ev	3 mk br	0	and gravel
		Bk	33	di	10YR6.5/3	10YR4/3	SL	47	sg	7.45	so		so,ps	II es diss	0	0	channel gravel
1173 (12.8)		2Btqkbl	55	ci	10YR5.5/3	10YR3.5/3	SL	54	2 m sbk	7.50	h		ss,ps	I, matrix 0	3 n gr & br	III	channel gravel
		2Btqmkbl	144	as	10YR6/4	10YR4/4	SL	59	m	8.10	eh		so,po-ps	lenses III, none in places	1 n gr	III	channel gravel
		3Bqmkb2	186	cw	7.5YR-10YR 7/4	7.5YR-10YR 4/4	LS	48	m	7.35	eh		so,po	I, matrix 0	I n gr	III	fluvial gravel
	4b/	3Ckqnb2	233+	--			S	79	sg	7.30	sh-so		so,po	0	0	I	fluvial gravel

TABLE D-1

SOIL DESCRIPTIONS OF TAYLOR
(1986, p. 105 - 111)

Map Unit, Elev (m) (m >stream)	Sample Number	Horizon	Basal Depth (cm)	Lower Boundary	Color dry	Color moist	Texture 1/	% Gravel	Structure	pH	Consistence Dry	Consistence Moist	Consistence Wet	$CaCO_3$	Clay Films	SiO_2	Parent Material
Q2b	YW-11	Av	4	as	10YR6/3	10YR4/3	LS	40	3 m pl 2° 2 m sbk	7.00	so		ss,ps	0	0	0	sheetwash & eolian
1274		Bt1	15	as	10YR6/3	10YR4/3	SL	27	1 m sbk	7.20	so		ss,ps	0	0	0	sheetwash & eolian
(7.3)		2Bt2	42	aw	10YR6/4	10YR4/4	SL	39	2 m sbk	7.05	h		ss,ps	0	1 n gr	0	sheetwash & eolian
		2Btqmk	90	cb	10YR6.5/4 10YR8/2	10YR4/4 10YR6/4 (pf)	SL	48	m in place 2° 2 f-m sbk	7.90	eh		s,ps	I+, gr pf matrix 0	2 n br & po	II & III	channel gravel
		2Bkq	150	si-b	10YR7/4	10YR5/4	SL	75	m-sg	7.95	lo		so,po	II	1 n br	I	channel gravel
	4a/	2Kqmk	170+	–	10YR8/2 10YR7/3	10YR6/4 10YR5/6 (SiO_2)	SL	73	m	8.00	eh		so,po	III	0	0	debris flow
Qlc over	YW-12	Av1	4	as	10YR6/3	10YR3.5/3	SL	35	1-2 vt-t pl	7.20	so		so,ps	0	0	0	sheetwash & eolian
Q2b		Av2	14	cw	10YR6/3	10YR4/3	SL	25	1-2 t pl 2° 2 co sbk	7.80	so		so,ps	0	0	0	sheetwash & eolian
1283		Bt	47	ci	10YR6.5/3	10YR4/3	SL	26	3 m-co sbk	7.50	sh		s,ps	0	0	0	sheetwash & eolian
(6.1)		2Bk1	105	gw	10YR7/2 10YR6/3	10YR4.5/3 10YR4/3	SL-	56	2 m-co sbk 2° 2 f sbk	7.80	sh-h		ss,ps	II+ pf & grav	2 n po & br	0	channel gravel
		2Bk2	120	aw	10YR6/4	10YR4/4	LS	10	sg	8.00	so		so,po	II, cw	2 n po & br	III	channel gravel
		2Bqmkb	130		10YR6/4	10YR4/6	S	66	3 m sbk	7.95	eh		so,po	e- & gr	2 n pf	IV-	channel gravel
			144	cw	10YR8/2	10YR7/3	LS-		3 m sbk		eh		so,po	III in places	0	0	cemented gravel
		2Bqkb	200+	–			LS	80	sg	7.85			so,po	e diss, I	0	I	channel gravel
Qlc over	YW-14	A	8	cs	10YR7/3	10YR4/3	SL	32	2 vf pl	7.15	so		so,ps	0	0		eolian & sheetwash
Q2b(?)		Bt	28	gw	10YR6/3	10YR4/3	SL	24	1 co-vco sbk	7.15	so		ss-so, ps	0	0		eolian & sheetwash
1369		2Bk	54	gw	10YR6/3	10YR4/3	SL	35	2 m sbk	7.80	so		ss,ps	eI+ diss	0	0	colluvium
(12.2)		2Bkq	107	cw	10YR7/3	10YR4.5/3	SL	42	sg	8.05	lo		ss,ps	evII diss	0	I	colluvium
		3Bkjb	121	aw	20YR5.5/3	10YR3/3.5	SL-	19	2 m sbk	8.05	sh-h		so,po	ea pf I 0 in ped	2n gr	0	fluvial gravel

TABLE D-1

SOIL DESCRIPTIONS OF TAYLOR
(1986, p. 105 - 111)

Map Unit, Elev (m) (m > stream)	Sample Number	Horizon	Basal Depth (cm)	Lower Boundary	Color dry	Color moist	Texture 1/	% Gravel	Structure	pH	Consistence Dry	Consistence Moist	Consistence Wet	$CaCO_3$	Clay Films	SiO_2	Parent Material
		3Bqmk1b	152	gw	10YR6/3	10YR3/3	SL	30	m, 2° 3 f-vf abk	8.00	eh		so,po	I, III in veins	1 n pf	III	fluvial gravel
		4Bqmk2b	221	cw	10YR6/3	10YR4/3	SL-	63	m-sg	8.00	vh		ss,ps	es I & gr	1 n pf	III	fluvial gravel
		4Bkjb	230+	--	7.5YR5/4	7.5YR4/4	SL-LS	80	sg	8.50	lo		so,po	I diss	2 mk pf	I	fluvial gravel
Q2b(?)	YW-20	Av	8	cs	10YR6/3	10YR3/4	SL	38	1 m-co abk	6.90	sh		ss,po	0	0	0	sheetwash & eolian
		Bt1	19	cs	10YR	10YR4/3.5	SL	24	3 co-vco abk	6.90	sh		ss,ps	0	3 mk po	0	sheetwash & eolian
1373		Bt2	42	gw	10YR6/4	7.5YR4/4	L	39	2 m-co abk	6.75	sh	fr	ss,ps	0	0	I	sheetwash & eolian
(10.7)		2Bq	64	gw	7.5YR5/4	7.5YR4/4	SL	84	1-2 m abk	7.30	sh		ss,po	0	2 n br	I	fluvial gravel
		2Bqk1	76	ab	7.5YR5/4	7.5YR4/4	SL	84	1-2 m abk	7.80	sh		ss,po	I+ - II	1 n gr	I-III	fluvial gravel
		2Bqk2-1	114		7.5YR5/4	7.5YR4/4	SL	68	m-sg	7.95			so,po	diss	2 n br	III	bedded fluvial
		2Bqk2-2	152		7.5YR6/4	7.5YR4/4	SCL-	89		8.00				II	0	I-II	gravel
		2Bqk2-3	190+		7.5YR6/4	7.5YR4/4	SL	89		8.00				I, diss	0	II	
Qlc over Q2c	FW-5 3/	A	5	as	7.5YR7/3	7.5YR4/3	S	25	1 vt pl 2° vf-f abk	7.55	so		so,po	0	0	0	sheetwash
		AB	20	aw	10YR6/3	10YR3/3	S	9	1 m abk	7.30	so-sh		so,po	0	1 n gr	0	sheetwash
1021		Btk	45	aw-b	10-7.5YR7/2	10YR4/3	SL	14	m, 2° 1co abk	7.45	sh		so,po	II-ev cw	1 n gr	I	sheetwash
(13.4)		2Btkb	56	as-d	7.5YR5.5/4	7.5YR4/4	SL	18	3 m sbk pf & po	7.55	h		so,ps	0	2 mk-k pf & po	I	fluvial gravel
		2Btqmkb	106	cw	7.5YR6/4	7.5YR5/6	SL	60	m	7.50	vh		so,po	II pf	2 mk br	III	fluvial gravel
		2Kqb	164	aw	7.5YR7/4 7.5YR8/2	7.5YR5/6 7.5YR7/4	S ($CaCO_3$)	71	m, 2° 2m sbk	7.60	vh (ca) sh (SiO_2)		so,po	lenses of III 5-7 cm thick	3 n br	I+	fluvial gravel
		2Cqn	263+		10YR6/1	10YR4/2	S	72	sg	7.50	lo		so,po	0 & lenses of I	0	II	fluvial gravel
Q2c over QTa	FW-18	Avk	11	as	10YR7/3	10YR4.5/3	L	13	3 co abk 2° 1 co-vc pl	8.10	sh		ss,ps	e diss		0	sheetwash & eolian
		Ak	33	cs	10YR7/3	10YR4.5/3	SL	24	sg	8.00	lo		so,vps	ev diss	0	0	sheetwash & eolian
1085		Btkj	40	cw	10YR6/4	10YR4/4	SL	30	2 m-co pl				ss,ps	e diss	2 mk po	0	sheetwash & eolian

TABLE D-1

SOIL DESCRIPTIONS OF TAYLOR
(1986, p. 105 - 111)

Map Unit, Elev (m) (m >stream)	Sample Number	Horizon	Basal Depth (cm)	Lower Boundary	Color dry	Color moist	Texture 1/	% Gravel	Structure	pH	Consistence Dry	Consistence Moist	Consistence Wet	$CaCO_3$	Clay Films	SiO_2	Parent Material
(21.3)		2Btqkj1	66	cw	7.5-10YR6/4	7.5YR4/4	SL-	53	2° 1 f sbk 1 co pl 2° 3 vc sbk	7.55	h		so,po	I pf	2 k po & br, lt pf	I-II	fluvial gravel
		2Btqkj2	120	aw	10YR6/3	10YR4/4	LS	72	m	7.25	h		so,po	II+ lenses	2 k br	II	fluvial gravel
	4a/	3Kb	160+	–	white 6/	10YR8/4	S	76	m	7.20	eh			III	0	0	fluvial gravel
Q2a over Q2c	YW-8	Av	11	cw	10YR6/3	10YR4/3	L	13	3 co ssbk	7.40	sh	fr	ss,p	0	3 k po 3 n br	0	eolian & sheetwash
1198		Bt1	21	cw	7.5YR4/4	5YR4/6	C	13	2 f pr 2_o 2 f sbk	7.30	so		vs,vp	0	4 k pf	0	eolian & reworked gravel
(18.0)		2Bt2b	35	cw	7.5YR7/6	7.5YR5/6	SL	27	3 m-co abk	7.45	vh		so,po	0 4 k pf	pods of	0	fluvial gravel
		2Kqmb	68	as	7.5YR7/6	7.5YR6/6	LS	18	2 co-vco abk 3 vco pl in places	7.90	vh		so,po	II-III	3 mk br & gr	III	fluvial gravel
		2Kb	100	ci	10YR8/2 ($CaCO_3$)	7.5YR7.5/6	S	52	1 f pl 3 f-co sbk	8.15	h		so,po	III in lenses	0	0	fluvial gravel
		2Cukb	210+	–	10YR7/3	10YR4/3	S	62	sg	7.75	lo		so,po	II	0	0	fluvial gravel
Q2a over Q2c	YW-16	Av	13	as	10YR5/3	10YR3/3	SL		1 m sbk	7.05	lo		s,p	0	ln gr & po	0	eolian
		Bt1	30	aw	10YR5.5/4	10YR4/4	L		1 m sbk	7.55	so		s,p	0	ln gr	0	eolian
1311		Bt2	43	aw	7.5-10YR5/4	7.5-10YR4/4	SL		2 vco sbk to abk	7.60	so		s,p	0	3n gr	0	eolian
(10.7)		2Btqkb	58	ai	7.5YR7/5	7.5YR5/6	SL	44	1 c pl 2° 2 m sbk	7.70			s,ps	II	3 mk pf	III	fluvial gravel
		2Kqb	100	cw	7.5YR8/2 white 6/ ($CaCO_3$)	7.5YR7/7	LS	57	m	7.90	eh		so,po	III+	0	IV	fluvial gravel
		2Bqmkb	150	cw	7.5-10YR6/4	7.5YR4/4	LS	70	m 2° 2 f sbk	7.65	h-vh		so,po	lenses III	0	III	fluvial gravel

TABLE D-1

SOIL DESCRIPTIONS OF TAYLOR
(1986, p. 105 - 111)

Map Unit, Elev (m) (m >stream)	Sample Number	Horizon	Basal Depth (cm)	Lower Boundary	Color dry	Color moist	Texture 1/	% Gravel	Structure	pH	Consistence Dry	Consistence Moist	Consistence Wet	$CaCO_3$	Clay Films	SiO_2	Parent Material
		2Ckqnb	207+	–	10YR6/4 white 6/ ($CaCO_3$)	10YR3.5/4	S	71	sg	7.90	lo-sh		so,po	lenses III	0	II	fluvial gravel
Qlc over Q2c	YW-IW	A	10	cs	10YR6/3	10YR4/2	SL	27	1 m-c sbk 2° sg	7.25	so		ss,ps		1 n gr		eolian & sheetwash
1317		Bt	25	c-aw	10YR5.5/3	10YR4/3	SL+	15	1 m sbk 2° 2 f-m sbk	7.20	so		ss,ps		0		eolian & sheetwash
(12.5)	2/	2Btqkjlb	42	as	7.5YR5/4	10YR4/3	C-	47	2 co sbk	7.30	sh	fi	s,p		2n-k pf	II	eolian & fluvial gravel
		2Btqkj2b	56	cw	7.5YR5/4	7.5YR4/4	C-	30	2 co sbk	7.40	sh	vfi	s,p		2 k pf	II	eolian & fluvial gravel
		3Kb	70+	cw	7.5YR6/4	7.5YR5/4	C-	46	1 c pl	7.70	h	vfi	s,po	III-IV-	0		eolian & fluvial gravel
Qlc over	YW-1E	Spoil	30														
Q2c		2Btkjqb	50		7.5YR6/6	7.5YR5/4	C-	32	1-2 m sbk	7.60	h	vfr	s,p	0	0	II	colluvium
		2Btqmkb	56	aw	7.5YR7/4-5	7.5YR4/4	C-	38	1-2 m pl 2° 1 m sbk	8.10	v-eh	fi	so,po	0	0	IV	colluvium
(con't 1W)	4a/	3Kqmlb	70	cw	10YR8/2	10YR7/2	SCL+	50	2 vc pl	8.15	eh	fr	ps,po	IV-	0	IV	debris flow
1317		4Kqm2b	115	cw			SCL	61	m	8.40	vh	fr	so,po	III-IV-	0	III	debris flow
(12.5)		5Bkb	167	dw	7.5YR7/6		SL	66	sg	8.10				lenses IV-	0		fluvial gravel
		5Cnkb	195	dw	7.5YR7/4	7.5YR5/4	SL	70	sg	8.40	lo	lo	so,po	diss	0		fluvial gravel
		5Cnb	290+	–	7.5YR7/4 7.5YR6/2-3	7.5YR5/4	LS+	67	sg	8.40	lo	lo	so,po	diss	0		fluvial gravel
QTa	FW-19	Avk1	4	as	10YR7/2	10YR3.5/3	L		3 m-co sbk	8.45	so	fr	ss, ps	es	0	0	sheetwash
		Avk2	9	aw	10YR	10YR4/3	SL	5	3 co sbk	8.45	h		s,ps	es	1 n po	0	sheetwash
1093		Bk	13	aw	7.5YR7/4	7.5YR5/4	L	13	1 m sbk	8.15	so		s,ps	ev cw	0	0	sheetwash
(28.0)		Btk	17	as	7.5YR6.5/4	7.5YR4/4	L	3	1 f-vf sbk 1 f pl	7.80			so,po	0	0	0	sheetwash
		Btqmkj	29	cw	7.5YR6.5/4	7.5YR5/5	L	11	3 n pl	7.70	eh		so,po	II on pf	3 n br	III+	fluvial gravel

TABLE D-1

SOIL DESCRIPTIONS OF TAYLOR
(1986, p. 105 - 111)

Map Unit, Elev (m) (m >stream)	Sample Number	Horizon	Basal Depth (cm)	Lower Boundary	Color dry	Color moist	Texture 1/	% Gravel	Structure	pH	Consistence Dry	Consistence Moist	Consistence Wet	$CaCO_3$	Clay Films	SiO_2	Parent Material
	4a/	2Kqm1	47	cw	10YR8/2	7.5YR7/3	L		3 vc pl	7.30	eh		so,po	III	3-4k pf	III	fluvial gravel
					7.5YR7/4	7.5YR5/6	L		2° 3 c abk								debris flow?
	4a/	2Kqm2	72	cw	10YR8/3	7.5YR7/6	L	34	m	7.40	vh		so,po	III	0	III	fluvial gravel
									2° 2 f-vf abk & vf pl								
	4a/	2Kqm3	150+	--	10YR7/4	10YR5/6	SL	40	m	7.60	vh		ss,po	III	0	III	fluvial gravel
QTa	YW-6	Avk	6	cs		10YR4/3	L	24	3 vco abk	7.70	fr		ss,ps	e diss	0	0	eolian & sheetwash
	5/	Btk	10	as		7.5YR5/6	L	14	2 m abk	7.60	fr		s,p	e diss	2 n pf	0	eolian & sheetwash
1170	4a/	2Kmq	52	as	7.5YR7/6	7.5YR6/6	SL		3 vco pl	7.75			so,po	IV	0	IV	fluvial gravel
(19.8)					7.5YR8/2	white 6/ ($CaCO_3$)											
		3Kqm	101	gw	7.5YR7/4	7.5YR5/6	S	59	m	7.80	eh		so,po	III	0	II	fluvial gravel
					white 6/ $CaCO_3$)									lenses			
		3Kqy	153	gw	10YR8/2	10YR6/3	S	67	sg	7.60	so		so,po	II with	0	II	fluvial gravel
														lenses of III			
		3Bkq	230	--	7.5YR7/4	10YR4/3	S	63	sg	7.60	lo		so,po	I	0	II	fluvial gravel
		3Ckqn	250+				S	41		7.70							
QTa	YW-2W	Avk	3	as	10YR7/3	10YR4/3	L	6	3 co abk	7.95	sh		ss,p	ev	0	0	eolian & sheetwash
		Ak	10	cw	10YR7/4	10YR3.5/3	L	9	1 m abk-sg	7.95	so		ss,p	e	0	0	eolian & sheetwash
1180		Bty	19	ai	10YR5.5/3	10YR3/4	L	12	2 vf abk-sg	7.60	so		s,p	e	0	0	eolian & sheetwash
(21.3)	2/ 4a/	2Btqmky	34	ci	10YR7/4	10YR3/3	L-	23	3 co pl	7.50	eh			1-2 mm	2 n gr	III	fluvial gravel
					7.5YR6/6	7.5YR4/4								lenses	& br		
					(SiO_2)									II on pf top			
		2Btqmy	70+	--	7.5YR5.5/6	7.5YR4/4	L-	33	2 co pl	7.50	eh		so,po-	lenses	4 n pf	III	fluvial gravel
									2° f-m abk				ps	on pf top			
QTa	YW-2E	Spoil	4														
		Btk	19		7.5YR6/4	7.5YR4/4	CL	13	2 m-co abk	8.20	so		ss,p	ev	2 n gr		eolian & sheetwash
1180	3/ 4a/	2Ktqm	52		7.5YR8/6	7.5YR7/6	C	39	3 vco pl	8.20	eh		so,po	III-IV	1 n gr	IV	fluvial gravel
(21.3)					(internal peds)									coats peds	2 mk pf		
					10YR8/4	10YR7/6											

TABLE D-1

SOIL DESCRIPTIONS OF TAYLOR
(1986, p. 105 - 111)

Map Unit, Elev (m) (m > stream)	Sample Number	Horizon	Basal Depth (cm)	Lower Boundary	Color dry	Color moist	Texture 1/	% Gravel	Structure	pH	Consistence Dry	Consistence Moist	Consistence Wet	$CaCO_3$	Clay Films	SiO_2	Parent Material
		2Kqm	114		pf white 6/ (CaCO3) white 6/ (CaCO3)		SCL-	48	2 vco pl	8.00	h-eh		so,po	IV in places	1 n gr & br	IV	fluvial gravel (debris flow?)
		3Kq	197+	–	10YR8/2	10YR6/3	SL	76	m	7.55	so		so,po	III, veiny on pebbles			fluvial gravel
QTa	<u>YW-22</u>	Avk	10	aw	10YR7/3	10YR5/3	CL	5	2 vco sbk 2° 1 m-co pl	8.50	so-sh		s,ps	e	1 n po	0	eolian & sheetwash
1209		Btk	21	aw	7.5YR5.5/6	7.5YR4/4	CL+	20	2 f-m sbk	8.00	so		s,p	e	2 mk br & gr	0	eolian & reworked gravel
(19.2)	4a/	Kqm	62	as	7.5YR8/4	7.5YR7/6	SCL	42	2 vo pl & m	7.90	eh		so,po	IV	0	IV	eolian & reworked gravel
		2Kmq	92	cw	10YR8/3 white 6/ (CaCO3)	7.5YR6.5/6	SL	54	m	7.65	eh		so,po	III	0	III?	fluvial gravel
		2Bkqm	184+	–	7.5YR7/4	7.5YR5/4	SL	52	1 m sbk	7.65	h		so,po	II	0	II	fluvial gravel

KEY TO TABLE D-1

SOIL DESCRIPTION OF TAYLOR (1986, p. 105-111)

Horizon Boundary

	Distinctness		Topography
va	very abrupt	s	smooth
a	abrupt	w	wavy
c	clear	i	irregular
g	gradual	b	broken
d	diffuse		

Soil Texture

co	coarse	S	sand	SCL	sandy clay loam
f	fine	LS	loamy sand	CL	clay loam
vf	very fine	SL	sandy loam	SiCL	silty clay loam
		L	loam	SC	sandy clay
		SiL	silt loam	C	clay
		Si	silt	Sic	silty clay

Soil Structure

	Grade		Size		Type
m	massive	vf	very fine (v thin)	gr	granular
sg	single grained	f	fine (thin)	pl	platey
1	weak	m	medium	pr	prismatic
2	moderate	co	coarse (thick)	cpr	columnar
3	strong	vco	very coarse	abk	angular blocky

KEY TO TABLE D-1

SOIL DESCRIPTION OF TAYLOR (1986, p. 105-111)

			(v thick)	sbk	subangular blocky

If two structures - listed as primary and secondary (2°)

Soil Consistence

	Dry		Moist		Wet
lo	loose	lo	loose	so,po	non-sticky or plastic
so	soft	vfr	very friable	ss,ps	slightly sticky or plastic
sh	slightly hard	fr	friable	s,p	sticky or plastic
h	hard	fi	firm	vs,vp	very sticky or plastic
vh	very hard	vfi	very firm		
eh	ex hard	efi	extremely firm		

Clay Films

	Frequency		Thickness		Morphology
vf	very few	n	thin	pf	ped face coating
1	few	mk	moderately thick	br	bridging grains
2	common	k	thick	po	pore linings
3	many			gr	gravel coats

$CaCO_3$

Effervescence on matrix

O - none in matrix.

KEY TO TABLE D-1

SOIL DESCRIPTION OF TAYLOR
(1986, p. 105-111)

diss	-	disseminated, discontinuous.
e	-	slightly, bubbles are readily observed.
es	-	strongly, bubbles form a low foam.
ev	-	violently, thick foam "jumps" up.

* For more information, see Soil Survey Staff 1951 and 1975

1/ Texture is based on lab analyses
2/ Sampled for phytolith and pollen analyses
3/ Sampled for U-trend dating
4a/ Soil ped thin section
4b/ Rock thin section
5/ Sampled for ^{36}Cl analyses
6/ White carbonate is whiter than 10YR8/0

TABLE D-2

SOIL PROFILE LABORATORY DATA OF TAYLOR (1986, p. 184-187) INCLUDING PARTICLE SIZE, BULK DENSITY, CARBONATE, GYPSUM, AND SOLUBLE SALTS

						Depth (cm)		% Total by Summation			Density	$CaCO_3$	(Gypsum)		(Soluble Salts)	
Surface	Profile	Elevation (ft)	Soil	No.	Horizon	Top	Base	Sand	Silt	Clay	(od) gm/cc	(%)	EC mho/cm	%	EC mho/cm	%
Qla	FWA-1		FWA-1					94.37	4.52	1.11	1.35	0.43				
	FWA-2		FWA-2					84.78	13.22	2.00	1.31	0.51				
	FWA-3		FWA-3					98.55	0.85	0.60	1.40	0.34				
	FWA-4		FWA-4					95.63	2.76	1.61	*1.32	0.31				
Qla	YWA-1		YWA-1					99.16	0.42	0.42	1.35	0.15				
	YWA-2		YWA-2					98.30	0.94	0.77	1.35	0.16				
Qlb	FW-7	3380		7.01	Ak	0	2	93.37	4.92	1.71	*1.35	0.40				
				7.02	Cox	2	18	90.83	6.53	2.64	*1.33	0.19				
				7.03	2Ckox	18	100	95.42	3.24	1.34	*1.35	0.72				
Qlc	FW-4	3300		4.01	Ak	0	3	86.55	9.37	4.08	1.45	0.44	0.00000	0.00	0.00008	0.03
				4.02	Bqj	3	9	81.75	10.64	7.60	1.36	0.90	0.00002	0.01	0.00009	0.03
				4.03	2Btk	9	60	71.42	16.97	11.61	1.48	2.34	0.00003	0.02	0.00012	0.04
				4.04	2Cuk	60	100	82.03	13.88	4.08	*1.42	1.59	0.00004	0.02	0.00010	0.03
Qlc	FW-17	3540		17.01	A	0	6	70.07	25.06	4.87	*1.35	0.07				
				17.02	Bwk	6	24	76.19	19.32	4.50	1.50	0.27				
				17.03	2Cuk	24	120	92.73	5.00	2.27	*1.42	0.24				
Qlc	YW-13	4155		13.01	A	0	9	81.75	13.78	4.47	1.42	0.14				
				13.02	Bw	9	21	80.57	13.46	5.96	*1.42	0.12				
				13.03	2Bqj	21	73	87.56	8.18	4.26	1.61	0.15				
				13.04	2Ckqn	71	138	93.15	4.91	1.94	1.81	0.22				
Qlc	YW-15	4520		15.01	A	0	18	78.36	16.06	5.58	*1.40	0.02				
				15.02	Bw	18	46	79.88	13.88	6.25	*1.40	0.09				
				15.03	2Bqk	46	170	70.98	18.64	10.38	*1.48	0.13				
				15.06	2Bqk(1)	46	108	80.46	11.96	7.58	*1.42	0.21				
				15.04	2Bqk(2)	108	170	61.35	25.77	12.88	*1.40	0.20				
				15.05	2Cuk	170	220	85.35	7.33	7.33	*1.60	0.24				

TABLE D-2

SOIL PROFILE LABORATORY DATA OF TAYLOR (1986, p. 184-187) INCLUDING PARTICLE SIZE, BULK DENSITY, CARBONATE, GYPSUM, AND SOLUBLE SALTS

Surface	Profile	Elevation (ft)	Soil No.	Horizon	Depth (cm) Top	Depth (cm) Base	% Total by Summation Sand	Silt	Clay	Density (od) gm/cc	$CaCO_3$ (%)	(Gypsum) EC mho/cm	%	(Soluble Salts) EC mho/cm	%
Q2b	FW-3	3320	3.01	Avk	0	5	42.10	40.84	17.06	1.62	1.49	0.00003	0.01	0.00010	0.03
			3.02	Btk	5	12	35.11	39.29	25.60	1.72	0.85	0.00001	0.01	0.00011	0.03
			3.03	2Btk	12	45	76.96	14.16	8.87	*1.80	0.38	0.00000	0.00	0.00018	0.06
			3.04	2Bqmk1	45	83	85.71	9.58	4.72	1.94	0.54	0.00001	0.01	0.00016	0.05
			3.05	2Bqmk2	83	107	94.40	2.74	2.85	2.00	0.57	0.00001	0.01	0.00021	0.07
			3.06	2Ckqn	107	210	95.34	2.27	2.39	*1.80	0.70	0.00002	0.01	0.00017	0.05
Q1c and Q2B over Q2c	YW-21	3850	21.01	Avk	0	4	52.23	38.92	8.85	1.37	1.73				
			21.02	Btjk	4	15	54.58	34.11	11.31	1.39	1.03				
			21.03	Bk	15	33	67.17	23.71	9.12	1.52	3.32				
			21.04	2Btqkb1	33	55	64.23	16.82	18.95	1.71	0.79				
			21.05	2Btqmkb1	55	144	77.33	10.92	11.76	1.95	0.48				
			21.06	3Bqmkb2	144	186	84.28	11.48	4.24	1.79	0.24				
			21.07	3Ckqnb2	186	233	94.57	3.16	2.26	*1.80	0.36				
Q2b	YW-11	4180	11.01	Av	0	4	80.15	16.02	3.83	1.57	0.23				
			11.02	Bt1	4	15	72.12	18.23	9.65	1.59	0.18				
			11.03	2Bt2	15	42	66.71	19.25	14.04	1.54	0.20				
			11.04	2Btqmk	42	90	63.25	22.47	14.28	1.81	1.14				
			11.05	2Bkq	90	150	74.75	13.71	11.53	1.87	1.55				
			11.06	3Kqmk	150	170	66.38	11.37	22.25	1.82	2.13				
Q1c over Q2b	YW-12	4210	12.01	Av1	0	4	70.68	21.85	7.47	1.56	0.07				
			12.02	Av2	4	14	69.34	22.16	8.50	1.40	0.20				
			12.03	Bt	14	47	63.64	23.12	13.23	1.64	0.19				
			12.04	2Bk1	47	105	74.38	18.30	7.32	1.85	1.61				
			12.05	2Bk2	105	120	81.06	14.16	4.78	1.89	1.86				
			12.06	2Bqmkb	120	144	88.73	7.08	4.18	1.77	1.68				
			12.07	2Bqkb	144	200	85.51	9.81	4.68	*1.75	0.73				

TABLE D-2

SOIL PROFILE LABORATORY DATA OF TAYLOR (1986, p. 184-187) INCLUDING PARTICLE SIZE, BULK DENSITY, CARBONATE, GYPSUM, AND SOLUBLE SALTS

							% Total by Summation			Density	$CaCO_3$	(Gypsum)		(Soluble Salts)	
		Elevation			Depth (cm)					(od)		EC		EC	
Surface	Profile	(ft)	Soil No.	Horizon	Top	Base	Sand	Silt	Clay	gm/cc	(%)	mho/cm	%	mho/cm	%
Q1c over Q2b (?)	YW-14	4490	14.01	A	0	8	64.64	29.89	5.48	1.36	0.20				
			14.02	Bt	8	28	63.77	26.99	9.24	1.26	0.19				
			14.03	2Bk	28	54	61.10	29.35	9.55	1.39	0.92				
			14.04	2Bkq	54	107	65.99	26.61	7.39	1.65	2.98				
			14.05	3Bkjb	107	121	75.34	19.16	5.50	1.62	0.91				
			14.06	3Bqmk1b	121	152	63.14	27.60	9.26	1.83	1.53				
			14.07	4Bqmk2b	152	221	73.82	18.07	8.11	1.67	0.87				
			14.08	4Bkjb	221	230	76.91	15.56	7.52	*1.75	0.74				
Q2b (?)	YW-20	4505	20.01	Av	0	8	72.21	23.13	4.66	1.51	0.06				
			20.02	Bt1	8	19	58.08	29.22	12.70	1.53	0.09				
			20.03	Bt2	19	42	47.96	31.95	20.09	1.56	0.10				
			20.04	2Bq	42	64	69.00	14.36	16.64	*1.65	0.19				
			20.05	2Bqk1	64	76	66.79	16.72	16.49	1.96	3.31				
			20.06	2Bqk2-1	76	114	71.58	13.33	15.08	1.72	1.32				
			20.07	2Bqk2-2	114	152	56.63	22.04	21.33	*1.72	4.77				
			20.08	2Bqk2-3	152	190	75.16	13.29	11.55	*1.72	1.30				
Q1c over Q2c	FW-5	3350	5.01	A	0	5	88.53	7.80	3.67	1.51	0.29	0.00001	0.00	0.00006	0.02
			5.02	AB	5	20	87.07	8.82	4.11	1.44	0.13	0.00000	0.00	0.00005	0.02
			5.03	Btk	20	45	72.97	16.98	10.05	1.64	1.94	0.00003	0.01	0.00011	0.03
			5.04	2Btkb	45	56	68.16	22.67	9.17	1.66	0.39	0.00000	0.00	0.00009	0.03
			5.05	2Btkjmkb	56	106	69.98	19.10	10.92	1.78	1.18	0.00008	0.04	0.00051	0.16
			5.06	2Kqb	106	164	89.80	6.27	3.94	1.86	4.51	0.00016	0.08	0.00091	0.29
			5.07	2Cqn	164	263	98.07	0.67	1.25	*1.80	0.19	0.00006	0.03	0.00045	0.14
Q2c over QTa	FW-18	3560	18.01	Avk	0	11	39.27	45.10	15.63	1.72	2.34				
			18.02	Ak	11	33	64.13	27.34	8.53	1.69	1.61				
			18.03	Btkj	33	40	62.90	25.58	11.52	1.81	0.19				
			18.04	2Btqkj1	40	66	75.22	16.85	7.93	1.79	0.22				
			18.05	2Btqkj2	66	120	85.97	7.87	6.16	*1.80	0.17				
			18.06	3Kb	120	160	89.81	5.97	4.22	1.82	14.42				

TABLE D-2

SOIL PROFILE LABORATORY DATA OF TAYLOR (1986, p. 184-187) INCLUDING PARTICLE SIZE, BULK DENSITY, CARBONATE, GYPSUM, AND SOLUBLE SALTS

Surface	Profile	Elevation (ft)	Soil	No.	Horizon	Depth (cm) Top	Base	% Total by Summation Sand	Silt	Clay	Density (od) gm/cc	$CaCO_3$ (%)	(Gypsum) EC mho/cm	%	(Soluble Salts) EC mho/cm	%
Q2a over Q2c	YW-8	3930		8.01	Av	0	9	45.33	36.21	18.46	1.65	0.00				
				8.02	Bt1	9	21	25.44	28.88	45.67	1.52	0.07				
				8.03	2Bt2b	21	35	72.07	18.81	9.13	1.64	0.11				
				8.04	2Kqmb	35	68	83.24	10.36	6.40	1.56	19.41				
				8.05	2Kb	68	100	87.35	7.93	4.72	1.70	7.53				
				8.06	2Cukb	100	210	88.42	7.49	4.09	1.75	4.08				
Q2a over Q2c	YW-16	4300		16.01	Av	0	13	68.88	16.39	14.73	1.26	0.00	0.00001	0.01	0.00013	0.04
				16.02	Bt1	13	30	66.15	16.57	17.28	1.49	0.05	0.00000	0.00	0.00007	0.02
				16.03	Bt2	20	43	62.77	21.73	15.50	1.48	0.07	0.00001	0.01	0.00005	0.02
				16.04	2Btqkb	43	58	31.01	21.54	47.45	1.76	2.18	0.00010	0.05	0.00012	0.04
				16.05	2Kqb	58	100	42.93	24.88	32.18	1.48	22.93	0.00001	0.01	0.00014	0.04
				16.06	2Kqmb(nc)	100	150	69.16	14.68	16.17	1.70	0.19	0.00001	0.01	0.00016	0.05
				16.07	2Bqmkb	100	150	56.24	24.11	19.65	1.70	1.01	0.00000	0.00	0.00015	0.05
				16.08	2Ckqnb	150	207	82.16	12.31	5.53	1.84	0.07	0.00003	0.02	0.00008	0.02
Q1c/Q2c	YW-1W	4310		1.01	A	0	10	61.66	23.26	15.07	1.47	0.06				
				1.02	Bt	10	25	53.13	27.90	18.97	1.52	0.14				
				1.03	2Btqkj1b	25	42	33.66	21.23	45.11	1.40	0.22				
				1.04	2Btqkj2b	42	56	36.06	19.73	44.22	1.62	0.24				
				1.05	3Kb	56	70	41.99	18.70	39.30	1.32	0.40				
Q1c/Q2c	YW-1E	4310		1.06	2Btkjqb		50	41.14	18.60	40.26	1.47	0.25				
				1.07	2Btqmkb	50	56	34.28	19.69	46.03	1.49	1.52				
				1.08	3Kqm1b	56	70	46.16	20.77	33.07	1.64	6.79				
				1.09	4Kqm2b	70	115	61.61	17.40	20.99	1.48	20.05				
				1.10	5Bkb	115	167	73.98	12.58	13.45	1.71	8.58				
				1.11	5Ckn1b	167	195	70.56	16.43	13.01	1.75	2.51				
				1.12	5Ckn2b	195	290	80.36	8.98	10.66	*1.75	0.92				

TABLE D-2

SOIL PROFILE LABORATORY DATA OF TAYLOR (1986, p. 184-187) INCLUDING PARTICLE SIZE, BULK DENSITY, CARBONATE, GYPSUM, AND SOLUBLE SALTS

Surface	Profile	Elevation (ft)	Soil No.	Horizon	Depth (cm) Top	Base	% Total by Summation Sand	Silt	Clay	Density (od) gm/cc	$CaCO_3$ (%)	(Gypsum) EC mho/cm	%	(Soluble Salts) EC mho/cm	%
QTa	FW-19	3585	19.01	Avk1	0	9	41.49	41.07	17.45	1.61	3.30				
			19.03	Bk	9	13	62.61	20.38	17.01	1.75	2.96				
			19.04	Btk	13	17	29.46	17.46	53.08	1.24	1.12				
			19.05	Btqmkj	17	29	43.30	13.99	42.71	1.43	0.27				
			19.06	2Kqm1	29	47	46.57	20.77	32.67	1.59	8.99				
			19.07	2Kqm2	47	72	46.14	19.79	34.07	1.59	8.36				
			19.08	2Kqm3	72	150	53.85	18.16	27.98	1.72	16.33				
QTa	YW-6	3840	6.01	Avk	0	6	50.53	34.65	14.82	1.46	1.97	0.00002	0.01	0.00010	0.03
			6.02	Btk	6	10	43.47	34.66	21.86	1.31	0.95	0.00002	0.01	0.00010	0.03
			6.03	2Kmq	10	52	71.74	16.32	11.95	1.50	30.32	0.00004	0.02	0.00015	0.04
			6.04	3Kqm	52	101	87.81	8.22	3.97	1.60	19.58	0.00006	0.03	0.00058	0.18
			6.05	3Kqy	101	153	90.69	6.15	3.15	1.84	15.27	0.00080	0.43	0.00193	0.61
			6.06	3Bkq	153	230	92.03	5.54	2.43	1.73	6.18	0.00024	0.13	0.00120	0.58
			6.07	3Ckqn	230	250	93.15	4.57	2.28	1.77	2.01	0.00054	0.29	0.00165	0.52
QTa	YW-2W	3870	2.01	Avk	0	3	43.44	40.24	16.32	1.53	1.72				
			2.02	Ak	3	10	46.67	39.63	13.70	1.52	0.51				
			2.03	Bty	10	19	42.19	39.83	17.98	1.30	0.21				
			2.04	2Btqmky	19	34	48.92	32.32	18.76	1.80	0.29				
			2.05	2Btqmy	34	70	50.41	28.79	20.80	1.79	0.11				
QTa	YW-2E	3870	2.06	Btk	4	19	35.17	27.47	37.36	1.31	1.19				
			2.07	2Ktqm	19	52	22.57	27.33	50.10	1.36	5.64				
			2.08	2Kqm	52	114	66.21	17.18	16.61	1.63	12.90				
			2.09	3Kq	114	197	66.04	20.94	13.02	1.73	7.96				
QTa	YW-22	3965	22.01	Avk	0	10	42.81	30.61	26.58	1.58	5.26				
			22.02	Btk	10	21	44.88	21.30	33.82	1.37	0.88				
			22.03	Kqm	21	62	56.31	20.76	22.93	1.66	20.10				
			22.04	2Kmq	62	92	67.88	17.05	15.07	1.42	22.36				
			22.05	2Bkqm	92	184	73.63	15.00	11.37	*1.75	6.18				

TABLE D-3

SOIL PROFILE LABORATORY DATA OF TAYLOR (1986, p. 188-191) INCLUDING ORGANIC CARBON LOSS ON IGNITION, pH, DITHIONITE EXTRACTABLE IRON (Fe-d), OXALATE EXTRACTABLE IRON (Fe-o), AND SECONDARY SILICA

								(	Carbon	)	P		(	Iron	)	
Surface	Profile	Elevation (ft)	Soil	No.	Horizon	Depth (cm) Top	Base	% Org.	% oxid OM	%101	Pa mg %	pH 1:1H_2O	Fe-d %	Fe-o %	Feo/Fed %	SiO_2 % by wt
Qla	FWA-1		FWA-1					0.05	0.08	0.44		8.10				1.80
	FWA-2		FWA-2					0.17	0.30	0.67		7.75				3.11
	FWA-3		FWA-3					0.03	0.05	0.31		8.15				1.27
	FWA-4		FWA-4					0.07	0.11	0.44		8.70				2.09
Qla	YWA-1		YWA-1					0.01	0.02	0.32		7.75				0.49
	YWA-2		YWA-2					0.02	0.03	0.30		7.30				1.06
Qlb	FW-7	3380		7.01	Ak	0	2	0.18	0.31	0.30		7.75				2.02
				7.02	Cox	2	18	0.09	0.16	0.32		7.80				2.58
				7.03	2Ckox	18	100	0.10	0.17	0.25		8.15				2.14
Qlc	FW-4	3300		4.01	Ak	0	3	0.09	0.16	0.46		7.30				2.70
				4.02	Btj	3	9	0.25	0.43	0.42		7.35				2.95
				4.03	2Btk	9	60	0.11	0.20	0.48		7.60				6.26
				4.04	2Cuk	60	100	0.07	0.12	0.46		7.80				4.60
Qlc	FW-17	3540		17.01	A	0	6	0.35	0.61	0.54		7.50				4.37
				17.02	Bwk	6	24	0.18	0.31	0.40		8.00				2.70
				17.03	2Cuk	24	120	0.09	0.15	0.36		8.10				1.13
Qlc	YW-13	4155		13.01	A	0	9	0.61	1.05	0.48		6.80	0.48	0.023	0.05	6.16
				13.02	Bw	9	21	0.25	0.43	0.47		7.10	0.51	0.021	0.04	3.88
				13.03	2Bqj	21	73	0.12	0.20	0.35		7.40	0.45	0.019	0.04	2.68
				13.04	2Ckqn	73	138	0.06	0.10	0.25		7.60	0.42	0.017	0.04	2.18

TABLE D-3

SOIL PROFILE LABORATORY DATA OF TAYLOR (1986, p. 188-191) INCLUDING ORGANIC CARBON LOSS ON IGNITION, pH, DITHIONITE EXTRACTABLE IRON (Fe-d), OXALATE EXTRACTABLE IRON (Fe-o), AND SECONDARY SILICA

Surface	Profile	Elevation (ft)	Soil	No.	Horizon	Depth (cm) Top	Depth (cm) Base	(Carbon % Org.	% oxid OM	) %101	P Pa mg %	pH 1:1H_2O	(Iron Fe-d %	Fe-o %	Feo/Fed) %	SiO_2 % by wt
Q1c	YW-15	4520		15.01	A	0	18	0.56	0.96	0.71		7.20				4.48
				15.02	Bw	18	46	0.39	0.68	0.55		7.30				2.76
				15.03	2Bqk	46	170	0.21	0.36	0.75		7.55				3.49
				15.06	2Bqk (1)	46	108	0.14	0.25	0.40		7.75				3.08
				15.04	2Bqk (2)	108	170	0.29	0.51	0.76		7.65				4.56
				15.05	2Cuk	170	220	0.09	0.16	0.35		7.95				1.85
Q2b	FW-3	3320		3.01	Avk	0	5	0.08	0.14	0.47		7.75				6.61
				3.02	Btk	5	12	0.07	0.13	0.67		7.65				6.27
				3.03	2Btk	12	45	0.11	0.19	0.45		7.65				3.90
				3.04	2Bqmk 1	45	83	0.07	0.12	0.37		7.60				2.75
				3.05	2Bqmk 2	83	107	0.04	0.07	0.25		7.60				1.32
				3.06	2Ckqn	107	210	0.05	0.08	0.21		7.90				2.59
Q1c and Q2b over Q2c	YW-21	3850		21.01	Avk	0	4	0.11	0.19	0.32		8.00				6.08
				21.02	Btjk	4	15	0.13	0.22	0.40		7.50				5.74
				21.03	Bk	15	33	0.22	0.38	0.39		7.45				7.69
				21.04	2Btqkbl	33	55	0.07	0.11	0.38		7.50				20.62
				21.05	2Btqmkb1	55	144	0.03	0.05	0.34		8.10				20.19
				21.86	3Bqmkb2	144	186	0.06	0.10	0.34		7.35				5.61
				21.07	3Ckqnb2	106	233	0.03	0.05	0.22		7.30				2.63

TABLE D-3

SOIL PROFILE LABORATORY DATA OF TAYLOR (1986, p. 188-191) INCLUDING ORGANIC CARBON LOSS ON IGNITION, pH, DITHIONITE EXTRACTABLE IRON (Fe-d), OXALATE EXTRACTABLE IRON (Fe-o), AND SECONDARY SILICA

								(	Carbon	)	P		(	Iron	)	
Surface	Profile	Elevation (ft)	Soil	No.	Horizon	Depth (cm) Top	Base	% Org.	% oxid OM	%101	Pa mg %	pH 1:1H_2O	Fe-d %	Fe-o %	Feo/Fed %	SiO_2 % by wt
Q2b	YW-11	4180		11.01	Av	0	4	0.20	0.34	0.36		7.00				5.05
				11.02	Bt1	4	15	0.12	0.21	0.41		7.20				5.24
				11.03	2Bt2	15	42	0.19	0.33	0.57		7.05				6.46
				11.04	2Btqmk	42	90	0.07	0.12	0.76		7.90				18.70
				11.05	2Bkq	90	150	0.18	0.31	0.86		7.95				21.39
				11.06	3Kqmkb	150	170	0.07	0.13	0.75		8.00				29.38
Q1c over Q2b	YW-12	4210		12.01	Av1	0	4	0.58	0.99	0.73		7.20	0.61	0.040	0.07	6.43
				12.02	Av2	4	14	0.27	0.46	0.46		7.80	0.65	0.042	0.06	4.56
				12.03	2Bt	14	47	0.20	0.35	0.48		7.50	0.68	0.039	0.06	3.41
				12.04	2Bk1	47	105	0.23	0.39	0.41		7.80	0.54	0.023	0.04	3.69
				12.05	2Bk2	105	120	0.23	0.40	0.47		8.00	0.51	0.025	0.05	3.36
				12.06	2Bqmkb	120	144	0.14	0.24	0.57		7.95	0.46	0.030	0.07	7.80
				12.07	2Bqkb	144	200	0.11	0.19	0.42		7.85	0.47	0.027	0.06	3.27
Q1c over Q2b (?)	YW-14	4490		14.01	A	0	8	0.29	0.50	0.38		7.15				3.29
				14.02	Bt	8	28	0.22	0.37	0.45		7.15				4.32
				14.03	2Bt	28	54	0.26	0.45	0.59		7.80				5.25
				14.04	2Bkq	54	107	0.22	0.38	0.48		8.05				6.51
				14.05	3Bkjb	107	121	0.14	0.25	0.45		8.05				2.57
				14.06	3Bqmk1b	121	152	0.11	0.18	0.46		8.00				3.25
				14.07	4Bqmk2b	152	221	0.11	0.19	0.53		8.00				1.85
				14.08	4Bkjb	221	230	0.10	0.18	0.44		8.50				1.82

TABLE D-3

SOIL PROFILE LABORATORY DATA OF TAYLOR (1986, p. 188-191) INCLUDING ORGANIC CARBON LOSS ON IGNITION, pH, DITHIONITE EXTRACTABLE IRON (Fe-d), OXALATE EXTRACTABLE IRON (Fe-o), AND SECONDARY SILICA

Surface	Profile	Elevation (ft)	Soil	No.	Horizon	Depth (cm) Top	Base	(Carbon % Org.	% oxid OM	) %101	P Pa mg %	pH $1:1H_2O$	(Iron Fe-d %	Fe-o %	) Feo/Fed %	SiO_2 % by wt
Q2b (?)	YW-20	4505		20.01	Av	0	8	0.17	0.29	0.28		6.90				5.57
				20.02	Bt1	8	19	0.16	0.28	0.36		6.90				7.82
				20.03	Bt2	19	42	0.18	0.31	0.41		6.75				17.19
				20.04	2Bq	42	64	0.25	0.44	0.49		7.30				19.12
				20.05	2Bqk 1	64	76	0.27	0.47	0.44		7.80				24.86
				20.06	2Bqk 2-1	76	114	0.07	0.13	0.31		7.95				22.91
				20.07	2Bqk 2-2	114	152	0.34	0.59	0.56		8.00				27.45
				20.08	2Bqk 2-3	152	190	0.06	0.10	0.25		8.00				22.43
Q1c over Q2c	FW-5	3350		5.01	A	0	5	0.20	0.34	0.41		7.55				1.31
				5.02	AB	5	20	0.13	0.22	0.35		7.30				1.67
				5.03	Btk	20	45	0.13	0.22	0.33		7.45				3.74
				5.04	2Btkb	45	56	0.09	0.16	0.42		7.55				6.52
				5.05	2Btqmkb	56	106	0.05	0.09	0.46		7.50				7.71
				5.06	2Kqb	106	164	0.08	0.14	0.42		7.65				7.91
				5.07	2Cqn	164	263	0.02	0.03	0.22		7.50				0.55
Q2c over Q1a	FW-1B	3560		18.01	Avk	0	11	0.09	0.16	0.50		8.10				7.14
				18.02	Ak	11	33	0.10	0.18	0.36		8.00				3.96
				18.03	Btkj	33	40	0.08	0.13	0.38		7.55				4.53
				18.04	2Btqkj1	40	66	0.08	0.13	0.45		7.25				3.34
				18.05	2Btqkj2	66	130	0.06	0.11	0.48		7.20				2.27
				18.06	3Kb	120	160	0.17	0.29	0.64		7.90				19.21

TABLE D-3

SOIL PROFILE LABORATORY DATA OF TAYLOR (1986, p. 188-191) INCLUDING ORGANIC CARBON LOSS ON IGNITION, pH, DITHIONITE EXTRACTABLE IRON (Fe-d), OXALATE EXTRACTABLE IRON (Fe-o), AND SECONDARY SILICA

Surface	Profile	Elevation (ft)	Soil	No.	Horizon	Depth (cm) Top	Depth (cm) Base	(Carbon % Org.	Carbon % oxid OM	Carbon) %LOI	P Pa mg %	pH 1:1H_2O	(Iron Fe-d %	Iron Fe-o %	Iron) Feo/Fed %	SiO_2 % by wt
Q2a over Q2c	YW-8	3930		8.01	Av	0	9	0.14	0.24	0.49		7.40				3.38
				8.02	Bt1	9	21	0.20	0.34	0.91		7.30				8.93
				8.03	2Bt2b	21	35	0.16	0.28	1.20		7.45				7.39
				8.04	2Kqmb	35	68	0.27	0.47	0.92		7.90				22.70
				8.05	2Kb	68	100	0.10	0.18	0.52		8.15				13.32
				8.06	2Cukb	100	210	0.08	0.14	0.59		7.75				9.05
Q2a over Q2c	YW-16	4300		16.01	Av	0	13	0.38	0.66	0.47	20.8	7.05	0.55	0.038	0.07	8.28
				16.02	Bt1	13	30	0.26	0.45	0.38	12.7	7.55	0.58	0.037	0.06	5.38
				16.03	Bt2	30	43	0.23	0.39	0.45	11.3	7.60	0.55	0.36	0.07	5.68
				16.04	2Btqkb	43	58	0.19	0.32	0.64	9.0	7.70	0.51	0.028	0.05	37.47
				16.05	2Kqb	58	100	0.20	0.35	0.66	21.2	7.90	0.25	0.008	0.03	45.65
				16.06	2Bqmkb(nc)	100	150	0.03	0.05	0.37	6.8	7.65	0.37	0.020	0.05	32.74
				16.07	2Bqmkb	100	150	0.04	0.07	0.31	4.8	7.90	0.36	0.019	0.05	43.22
				16.08	2Ckqnb	150	207	0.02	0.03	0.21	6.9	7.90	0.42	0.024	0.06	6.27
Q1c/Q2c	YW-1W	4310		1.01	A	0	10	0.23	0.41	0.58		7.25	0.76	0.073	0.10	9.47
				1.02	Bt	10	25	0.21	0.35	0.60		7.20	0.96	0.163	0.17	8.84
				1.03	2Btqkj1b	25	42	0.30	0.51	0.85		7.30	0.74	0.037	0.05	23.68
				1.04	2Btqkj2b	42	56	0.27	0.47	1.14		7.40	0.68	0.035	0.05	26.30
				1.05	3Kb	56	70	0.26	0.45	1.11		7.70	0.72	0.028	0.04	28.38

TABLE D-3

SOIL PROFILE LABORATORY DATA OF TAYLOR (1986, p. 188-191) INCLUDING ORGANIC CARBON LOSS ON IGNITION, pH, DITHIONITE EXTRACTABLE IRON (Fe-d), OXALATE EXTRACTABLE IRON (Fe-o), AND SECONDARY SILICA

								(	Carbon	)	P		(	Iron	)	
		Elevation				Depth (cm)			% oxid		Pa	pH	Fe-d	Fe-o	Feo/Fed	SiO_2
Surface	Profile	(ft)	Soil	No.	Horizon	Top	Base	% Org.	OM	%101	mg %	1:1H_2O	%	%	%	% by wt
Q1c/Q2c	YW-1E	4310		1.06	2Btkjqb		50	0.19	0.32	0.98		7.60	0.66	0.036	0.05	23.42
				1.07	2Btqmkb	50	56	0.11	0.19	1.56		8.10	0.59	0.024	0.04	29.92
				1.08	3Kqm1b	56	70	0.18	0.32	1.93		8.15	0.42	0.017	0.04	33.18
				1.09	4Kqm2b	70	115	0.17	0.29	2.19		8.40	0.27	0.008	0.03	36.25
				1.10	5Bkb	115	167	0.10	0.17	1.24		8.10	0.37	0.014	0.03	28.20
				1.11	5Cnkb	167	195	0.02	0.04	0.85		8.40	0.60	0.017	0.03	25.97
				1.12	5Ckn2b	195	290	0.01	0.02	0.43		8.40	0.55	0.016	0.03	20.10
Q1a	FW-19	3585		19.01	Avk1	0	9	0.08	0.14	0.46		8.45				7.86
				19.03	Bk	9	13	0.07	0.12	0.29		8.15				5.92
				19.04	Btk	13	17	0.09	0.16	1.04		7.80				26.80
				19.05	Btqmkj	17	29	0.08	0.15	0.68		7.70				29.92
				19.06	2Kqm1	29	47	0.20	0.35	0.94		7.30				31.15
				19.07	2Kqm2	47	71	0.17	0.29	0.87		7.40				31.49
				19.08	2Kqm3	72	150	0.15	0.26	0.80		7.60				36.59
Q1a	YW-6	3840		6.01	Avk	0	6	0.10	0.17	0.49		7.70				7.65
				6.02	Btk	6	10	0.08	0.14	1.78		7.60				8.57
				6.03	2Kmq	10	52	0.42	0.72	0.64		7.75				25.61
				6.04	3Kqm	52	101	0.13	0.22	0.37		7.80				19.01
				6.05	3Kqy	101	153	0.06	0.10	0.25		7.60				16.39
				6.06	3Bkq	158	230	0.04	0.07	0.25		7.60				8.68
				6.07	3Ckqn	230	250	0.02	0.04	0.26		7.70				4.64

TABLE D-3

SOIL PROFILE LABORATORY DATA OF TAYLOR (1986, p. 188-191) INCLUDING ORGANIC CARBON LOSS ON IGNITION, pH, DITHIONITE EXTRACTABLE IRON (Fe-d), OXALATE EXTRACTABLE IRON (Fe-o), AND SECONDARY SILICA

								(	Carbon	)	P		(	Iron	)	
		Elevation				Depth (cm)			% oxid		Pa	pH	Fe-d	Fe-o	Feo/Fed	SiO_2
Surface	Profile	(ft)	Soil	No.	Horizon	Top	Base	% Org.	OM	%101	mg %	$1:1H_2O$	%	%	%	% by wt
Qla	YW-2W	3870		2.01	Avk	0	3	0.04	0.08	0.58		7.95				9.09
				2.02	Ak	3	10	0.04	0.07	0.32		7.95				9.19
				2.03	Bty	10	19	0.04	0.07	0.29		7.60				25.06
				2.04	2Btqmky	19	34	0.07	0.13	0.32		7.50				25.12
				2.05	2Btqmy	34	70	0.04	0.07	0.33		7.50				26.26
QTa	YW-2E	3870		2.06	Btk	4	19	0.26	0.44	0.50		8.20				31.28
				2.07	2Ktqm	19	52	0.26	0.45	0.66		8.20				42.20
				2.08	2Kqm	52	114	0.10	0.18	0.32		8.00				39.95
				2.09	3Kq	114	197	0.07	0.12	0.36		7.55				37.81
QTa	YW-22	3965		22.01	Avk	0	10	0.17	0.30	0.73		8.50				18.50
				22.02	Btk	10	21	0.24	0.41	0.87		8.00				19.38
				22.03	Kq	21	62	0.22	0.37	1.05		7.90				35.01
				22.04	2Kmq	62	92	0.13	0.23	0.96		7.65				35.73
				22.05	2Bkqm	92	184	0.08	0.13	0.67		7.65				25.47

APPENDIX E

DESCRIPTION OF TERTIARY STRATIGRAPHIC UNITS IN THE MIDWAY VALLEY AREA

APPENDIX E

DESCRIPTION OF TERTIARY STRATIGRAPHIC UNITS IN THE MIDWAY VALLEY AREA

The stratigraphic sequence of volcanic rocks in the Midway Valley area is summarized in Table 2-1 (from Byers et al., 1989) and described below; the geology of the area as mapped by Scott and Bonk (1984) is shown in Plate 1. The exposed volcanic rocks are principally rhyolitic ashflow tuffs, with smaller amounts of dacitic lava flow and flow breccias and minor amounts of rhyolitic lavas, tuffaceous sedimentary rocks, and air-fall tuffs. Only the widespread and important welded tuff units have been assigned formational names. Bedded and minor ashflow tuffs that generally are only a few meters thick occur between formally designated units; there are important differences between the physical and chemical properties of these rocks and the flow rock units (USGS, 1984; Scott and Bonk, 1984). The thermal/mechanical properties of the rocks at Yucca Mountain were evaluated by Ortiz et al. (1985).

Paintbrush Tuff

The Paintbrush Tuff (Orkild, 1965) consists of widespread and voluminous rhyolitic to quartz latitic tuffs that issued cogenetically from the Claim Canyon Caldron and the Oasis Valley caldera complex located to the north and northwest of Midway Valley (Byers et al., 1976; Christiansen et al., 1977). The Paintbrush Tuff is the most extensively exposed volcanic unit near Midway Valley. It consists of four members, from oldest to youngest: Topopah Spring, Pah Canyon, Yucca Mountain, and Tiva Canyon. Each of these members has been divided into several mappable units by Scott and Bonk (1984).

The Topopah Spring Member is 287 to 359 m thick near the repository site (USGS, 1984) and contains the horizon that is being considered as the potential host rock for the repository in Yucca Mountain. It crops out primarily in the Yucca Wash and Fortymile Canyon areas to the north and northeast of Midway Valley, at the south end of Fran Ridge in the Dune Wash area to the south, and in Solitario Canyon to the west. The Topopah Spring Member is a compound cooling unit. At Yucca Mountain, the member is characterized by four distinct zones, from top to bottom: a nonwelded to densely welded, generally vitric tuff; a moderately to densely welded, devitrified tuff that accounts for most of the total thickness of the member and is the potential host rock for the repository; a basal vitrophyre; and a vitric tuff that grades downward from welded to nonwelded. The member is phenocryst-poor except for the caprock unit, which contains about 15 percent crystals that are primarily feldspar, biotite, and pyroxene. Several prominent lithophysal zones occur in the thick, densely welded portion of the member.

The Pah Canyon and Yucca Mountain members crop out near Yucca Wash and Fortymile Canyon and in a few canyons in the northwestern part of Yucca Mountain. The Pah Canyon Member ranges in thickness from 0 to about 71 m, and the Yucca Mountain Member from 0 to 29 m (USGS, 1984). Both members are simple cooling units that primarily are nonwelded but locally are moderately welded. Both have sparse phenocrysts; the Pah Canyon Member contains feldspar, biotite, and minor quartz; the Yucca Mountain Member contains only feldspar.

The Tiva Canyon Member is exposed over most of Yucca Mountain; it is also present in a few places north of Yucca Wash. The Tiva Canyon Member is about 69 to 148 m thick near the proposed repository (USGS, 1984). The member has a moderately to densely welded devitrified central portion underlain by a less densely welded vitric zone. It is a compound cooling unit, compositionally zoned from rhyolite in the lower and middle parts to quartz latite near the top. The Tiva Canyon Member is similar in appearance to the Topopah Spring Member.

Timber Mountain Tuff

This ashflow sequence consists of several formal units; only the Rainier Mesa Member crops out in the Midway Valley region. The largest outcrop is along Dune Wash; other exposures occur on the west side of Exile Hill and Fran Ridge (Plate 1). In the Yucca Mountain area, the Rainier Mesa Member has a maximum thickness of about 46 m (USGS, 1984) and occurs only on the downthrown side of large faults. The Rainier Mesa Member is a nonwelded to moderately welded ashflow tuff that contains 10 to 15 percent phenocrysts of feldspar, quartz, and biotite.

Rhyolites of Fortymile Canyon

The rhyolites of Fortymile Canyon include at least eight individual lava flows and domes, each associated with a sequence of bedded tuffs or other pyroclastic rocks. The rhyolites are petrochemically and structurally related to volcanism of the Timber Mountain center. None of the rhyolites in this group are known to occur beneath the surface in Midway Valley; all exposures are along or north of Yucca Wash. Data on the stratigraphic positions and ages of these rhyolites may provide additional information on the amount and timing of displacement on the Paintbrush Canyon fault. The ages of the rhyolites of Fortymile Canyon and their positions within the Tertiary stratigraphic succession in the Yucca Mountain area are summarized by Wilfred J. Carr and presented in Tables E-1 and E-2.

Research conducted during the past few years indicates that most of the rhyolites were deposited before the Rainier Mesa Member was deposited (Warren and others, 1988). The two oldest lavas, the rhyolites of Delirium Canyon and Black Glass Canyon, occur temporally between the Yucca Mountain and Pah Canyon Members of the Paintbrush Tuff (Table 2-1). Others, including the rhyolites of Vent Pass, Comb Peak, Waterpipe Butte, Windy Wash, and Pinnacles Ridge, were deposited in the time interval between the Paintbrush Tuff and Timber Mountain Tuffs. Another lava is assigned to the interval between the Rainier Mesa and Ammonia Tanks members. The two youngest lavas, which are younger than the Timber Mountain Tuff, occur to the north of Fortymile Canyon, inside the Timber Mountain caldera.

TABLE E-1

STRATIGRAPHIC SUCCESSION AND AGE OF RHYOLITES OF FORTYMILE CANYON AND OTHER IMPORTANT VOLCANIC UNITS OF THE FORTYMILE CANYON/YUCCA MOUNTAIN AREA

by

Wilfred J. Carr

Unit (Underlined units are formal stratigraphic names.)	K-Ar Age Ma	Interpolated or Adjusted Age, Ma
Thirsty Canyon Tuff	8.0[1]	--
basalt of Dome Mountain	--	9.5
rhyolite of "Comb Peak"[7]	10.7[2]	10.5
rhyolite of Chukar Canyon[8]	10.6[2]	10.7
Ammonia Tanks Member	11.4[3,4]	--
rhyolite of Buried Canyon	11.4[2]	11.5
Rainier Mesa Member	11.6[5]	--
rhyolite of Pinnacles Ridge	11.3[2]	11.6
rhyolite of Windy Wash	12.7[2]	12.0
rhyolite of Waterpipe Butte	12.6[2]	12.2
rhyolite of Comb Peak	12.1[2]	12.4
rhyolite of Vent Pass	12.5[2] 13.4[2]	12.7
Tiva Canyon Member[9]	12.9[5]	--
Yucca Mountain Member	--	13.0
rhyolite of Black Glass Canyon	--	13.1
rhyolite of Delirium Canyon	12.6[2]	13.1

TABLE E-1 (concluded)

STRATIGRAPHIC SUCCESSION AND AGE OF RHYOLITES OF FORTYMILE CANYON AND OTHER IMPORTANT VOLCANIC UNITS OF THE FORTYMILE CANYON/YUCCA MOUNTAIN AREA
by
Wilfred J. Carr

Unit (Underlined units are formal stratigraphic names.)	K-Ar Age Ma	Interpolated or Adjusted Age, Ma
Pah Canyon Member	--	13.2
Topoah Spring Member	13.2[6]	13.3
tuffs and rhyolite lavas of Calico Hills	13.8[3]	13.4
Prow Pass Member	--	13.5
Bullfrog Member	13.5[5]	13.5
Tram Member	--	13.7

---

1 R.J. Fleck, U.S. Geological Survey, written communication, 1980. (NNA.911009.0010)

2 Determination by F.W. McDowell, University of Texas, Austin; written communication from R.G. Warren, Los Alamos National Laboratory, 1990. (NNA.911009.0011)

3 Kistler, R.W., 1968, Potassium-argon ages of volcanic rocks in Nye and Esmeralda counties, Nevada; in Nevada Test Site, E.B. Eckel (ed.), Geological Society of America Memoir 110, pp. 251-262. (HQS.880517.2006)

4 Average of 17 determinations (Kistler, 1968) on several phases of the Ammonia Tanks Member.

5 Marvin, R.F., Byers, F.M., Jr., Mehnert, H.H., Orkild, P.P., and Stern, T.W., 1970, Radiometric ages and stratigraphic sequence of volcanic and plutonic rocks, southern Nye and western Lincoln counties, Nevada: Geological Society of America Bulletin, v. 81, pp. 2657-2676. (HQS.880517.1334)

6 Kistler, 1968; Marvin et al., 1970. Average of five determinations.

7 Quartz-bearing rhyolite lava inside Timber Mountain caldera, originally mapped as rhyolite of Comb Peak.

8 Rhyolite lava inside Timber Mountain caldera, originally mapped as rhyolite of Vent Pass.

9 Includes the intracaldera tuff of Chocolate Mountain.

Note: All ages are corrected for modern constants.

TABLE E-2

LOCATION, ANALYTICAL DATA, AND POTASSIUM-ARGON AGES
OF RHYOLITE LAVAS OF FORTYMILE CANYON
by
Wilfred J. Carr

Determinations by F.W. McDowell,
University of Texas

Sample No.	Location Nevada State Coord. North(m)	East(m)	Unit	Mineral	%K	% Ar^{40}	Ar^{40} ($x10^{-6}$ scc/gm)	Age, m.y. (±1r)
FB-29 a-3	244606	178766	rhyolite of "Comb Peak"	Sanidine	5.410 5.440	77 81 63	2.148 2.307 2.344	10.7 ± 0.5
FB-30 a-1	248451	179685	rhyolite of Chukar Canyon	Sanidine	7.884 7.970	62 60	3.299 3.269	10.6 ± 0.2
FB-29 a-4	244822	179348	rhyolite of Buried Canyon	Sanidine	6.378 6.272	53 68	2.845 2.758	11.4 ± 0.2
FB-PP-8	242771	170868	rhyolite of Pinnacles Ridge	Sanidine	7.992 8.082	63 64	3.525 3.582	11.3 ± 0.2
POG 2b-11	243306	164271	rhyolite of Windy Wash	Sanidine	5.514 5.655	60 66	2.944 2.596	12.7 ± 1.1
RW 29a-12	240978	179637	rhyolite of Waterpipe Butte	Sanidine	2.779 2.779	18	1.370	12.6 ± 0.3
CS-1-86A	238053	173750	rhyolite of Comb Peak	Plagio-clase	2.895 2.870	50 48	1.373 1.352	12.1 ± 0.3
FB-29a-1	243670	178692	rhyolite of Vent Pass	Sanidine	6.156 5.987	77 83	2.863 3.055	12.5 ± 0.6
TF 30a-4	243598	174347	rhyolite of Vent Pass	Sanidine	5.980 6.176	64 71	3.295 3.074	13.4 ± 0.7
FB 29a-2	243877	178814	rhyolite of Delerium Canyon	Sanidine	4.778 4.614	54 64	2.320 2.291	12.6 ± 0.3

Decay constants K^{40}: $_{\beta} = 4.963 \times 10^{-10} yr^{-1}$; $e + e^{1} = 0.581 \times 10^{-10} yr^{-1}$

Abundance: $K^{40}/K = 1.167 \times 10^{-4}$

APPENDIX F

RELEVANT YUCCA MOUNTAIN PROJECT DATA AND INFORMATION BASES

Information from the Reference Information Base Used in this Report

This report contains no information from the Reference Information Base.

Candidate Information for the Reference Information Base

This report contains no candidate information for the Reference Information Base.

Candidate Information for the Site & Engineering Properties Data Base

This report contains no candidate information for the Site and Engineering Properties Data Base.

DISTRIBUTION LIST

1 J. W. Bartlett, Director (RW-1)
Office of Civilian Radioactive Waste Management
U.S. Department of Energy
1000 Independence Avenue, S.W.
Washington, DC 20585

1 F. G. Peters, Deputy Director (RW-2)
Office of Civilian Radioactive Waste Management
U.S. Department of Energy
1000 Independence Avenue, S.W.
Washington, DC 20585

1 T. H. Isaacs (RW-4)
Office of Strategic Planning and International Programs
Office of Civilian Radioactive Waste Management
U.S. Department of Energy
1000 Independence Avenue, S.W.
Washington, DC 20585

1 J. D. Saltzman (RW-5)
Office of External Relations
Office of Civilian Radioactive Waste Management
U.S. Department of Energy
1000 Independence Avenue, S.W.
Washington, DC 20585

1 Samuel Rousso (RW-10)
Office of Program and Resources Management
Office of Civilian Radioactive Waste Management
U.S. Department of Energy
1000 Independence Avenue, S.W.
Washington, DC 20585

1 J. C. Bresee (RW-10)
Office of Civilian Radioactive Waste Management
U.S. Department of Energy
1000 Independence Avenue, S.W.
Washington, DC 20585

1 C. P. Gertz (RW-20)
Office of Geologic Disposal
Office of Civilian Radioactive Waste Management
U.S. Department of Energy
1000 Independence Avenue, S.W.
Washington, DC 20585

1 S. J. Brocoum (RW-22)
Analysis and Verification Division
Office of Civilian Radioactive Waste Management
U.S. Department of Energy
1000 Independence Avenue, S.W.
Washington, DC 20585

1 J. Roberts, Acting Assoc. Dir. (RW-30)
Office of Systems and Compliance
Office of Civilian Radioactive Waste Management
U.S. Department of Energy
1000 Independence Avenue, S.W.
Washington, DC 20585

1 J. Roberts (RW-33)
Director, Regulatory Compliance Division
Office of Civilian Radioactive Waste Management
U.S. Department of Energy
1000 Independence Avenue, S.W.
Washington, DC 20585

1 G. J. Parker (RW-332)
Office of Civilian Radioactive Waste Management
U.S. Department of Energy
1000 Independence Avenue, S.W.
Washington, DC 20585

1 R. A. Milner (RW-40)
Office of Storage and Transportation
Office of Civilian Radioactive Waste Management
U.S. Department of Energy
1000 Independence Avenue, S.W.
Washington, DC 20585

1 S. Rousso, Acting Assoc. Director (RW-50)
Office of Contract Business Management
Office of Civilian Radioactive Waste Management
U.S. Department of Energy
1000 Independence Avenue, S.W.
Washington, DC 20585

1 Trudy Wood (RW-52)
Director, M&O Management Division
Office of Civilian Radioactive
Waste Management
U.S. Department of Energy
1000 Independence Avenue, S.W.
Washington, DC 20585

1 D. U. Deere, Chairman
Nuclear Waste Technical Review Board
1100 Wilson Blvd. #910
Arlington, VA 22209-2297

1 Dr. Clarence R. Allen
Nuclear Waste Technical Review Board
1000 E. California Blvd.
Pasadena, CA 91106

1 Dr. John E. Cantlon
Nuclear Waste Technical Review Board
1795 Bramble Dr.
East Lansing, MI 48823

1 Dr. Melvin W. Carter
Nuclear Waste Technical Review Board
4621 Ellisbury Dr., N.E.
Atlanta, GA 30332

1 Dr. Donald Langmuir
Nuclear Waste Technical Review Board
109 So. Lookout Mountain Cr.
Golden, CO 80401

1 Dr. D. Warner North
Nuclear Waste Technical Review Board
Decision Focus, Inc.
4984 El Camino Real
Los Altos, CA 94062

1 Dr. Dennis L. Price
Nuclear Wast Technical Review Board
1011 Evergreen Way
Blacksburg, VA 24060

1 Dr. Ellis D. Verink
Nuclear Waste Technical Review Board
4401 N.W. 18th Place
Gainesville, FL 32605

5 C. P. Gertz, Project Manager
Yucca Mountain Site Characterization
Project Office
U.S. Department of Energy
P.O. Box 98608--MS 523
Las Vegas, NV 89193-8608

1 C. L. West, Director
Office of External Affairs
DOE Field Office, Nevada
U.S. Department of Energy
P.O. Box 98518
Las Vegas, NV 89193-8518

12 Technical Information Officer
DOE Nevada Field Office
U.S. Department of Energy
P.O. Box 98518
Las Vegas, NV 89193-8518

1 P. K. Fitzsimmons, Technical
Advisor
Office of Assistant Manager for
Environmental Safety and Health
DOE Field Office, Nevada
U.S. Department of Energy
P.O. Box 98518
Las Vegas, NV 89193-8518

1 D. R. Elle, Director
Environmental Protection Division
DOE Nevada Field Office
U.S. Department of Energy
P.O. Box 98518
Las Vegas, NV 89193-8518

1 Repository Licensing & Quality
Assurance
Project Directorate
Division of Waste Management
U.S. Nuclear Regulatory Commission
Washington, DC 20555

1 Senior Project Manager for Yucca
Mountain
Repository Project Branch
Division of Waste Management
U.S. Nuclear Regulatory Commission
Washington, DC 20555

1 NRC Document Control Desk
Division of Waste Management
U.S. Nuclear Regulatory Commission
Washington, DC 20555

1 P. T. Prestholt
NRC Site Representative
301 E. Stewart Ave., Room 203
Las Vegas, NV 89101

1 E. P. Binnall
Field Systems Group Leader
Building 50B/4235
Lawrence Berkeley Laboratory
Berkeley, CA 94720

1 Center for Nuclear Waste
Regulatory Analyses
6220 Culebra Road
Drawer 28510
San Antonio, TX 78284

3 W. L. Clarke
Technical Project Officer for YMP
Attn: YMP/LRC
Lawrence Livermore National
Laboratory
P.O. Box 5514
Livermore, CA 94551

4 R. J. Herbst
Technical Project Officer for YMP
N-5, Mail Stop J521
Los Alamos National Laboratory
P.O. Box 1663
Los Alamos, NM 87545

1 H. N. Kalia
Exploratory Shaft Test Manager
Los Alamos National Laboratory
Mail Stop 527
101 Convention Center Dr., Suite 820
Las Vegas, NV 89109

1 J. F. Divine
Assistant Director for
Engineering Geology
U.S. Geological Survey
106 National Center
12201 Sunrise Valley Dr.
Reston, VA 22092

6 L. R. Hayes
Technical Project Officer
Yucca Mountain Project Branch--MS 425
U.S. Geological Survey
P.O. Box 25046
Denver, CO 80225

1 V. R. Schneider
Asst. Chief Hydrologist--MS 414
Office of Program Coordination
& Technical Support
U.S. Geological Survey
12201 Sunrise Valley Drive
Reston, VA 22092

1 J. S. Stuckless
Geological Division Coordinator
MS 913
Yucca Mountain Project
U.S. Geological Survey
P.O. Box 25046
Denver, CO 80225

1 D. H. Appel, Chief
Hydrologic Investigations Program
MS 421
U.S. Geological Survey
P.O. Box 25046
Denver, CO 80225

1 E. J. Helley
Branch of Western Regional Geology
MS 427
U.S. Geological Survey
345 Middlefield Road
Menlo Park, CA 94025

1 R. W. Craig, Chief
Nevada Operations Office
U.S. Geological Survey
101 Convention Center Drive
Suite 860, MS 509
Las Vegas, NV 89109

1 D. Zesiger
U.S. Geological Survey
101 Convention Center Dr.
Suite 860 - MS 509
Las Vegas, NV 89109

1 R. V. Watkins, Chief
Project Planning and Management
U.S. Geological Survey
P.O. Box 25046
421 Federal Center
Denver, CO 80225

1 A. L. Flint
U.S. Geological Survey
MS 721
P.O. Box 327
Mercury, NV 89023

1 D. A. Beck
U.S. Geological Survey
1500 E. Tropicana, Suite 201
Las Vegas, NV 89119

1 P. A. Glancy
U.S. Geological Survey
Federal Building, Room 224
Carson City, NV 89701

1 Sherman S. C. Wu
Branch of Astrogeology
U.S. Geological Survey
2255 N. Gemini Dr.
Flagstaff, AZ 86001

1 J. H. Sass
Branch of Tectonophysics
U.S. Geological Survey
2255 N. Gemini Dr.
Flagstaff, AZ 86001

1 DeWayne A. Campbell
Technical Project Officer for YMP
U.S. Bureau of Reclamation
Code D-3790
P.O. Box 25007
Denver, CO 80225

1 K. W. Causseaux
NHP Reports Chief
U.S. Geological Survey
421 Federal Center
P.O. Box 25046
Denver, CO 80225

1 W. R. Keefer
U.S. Geological Survey
913 Federal Center
P.O. Box 25046
Denver, CO 80225

1 J. H. Nelson
Technical Project Officer for YMP
Science Applications International Corp.
101 Convention Center Dr.
Suite 407
Las Vegas, NV 89109

2 SAIC-T&MSS Library
Science Applications International Corp.
101 Convention Center Dr.
Suite 407
Las Vegas, NV 89109

2 L. D. Foust
Nevada Site Manager
TRW Environmental Safety Systems
101 Convention Center Drive
Suite 540, MS 423
Las Vegas, NV 89109

1 C. E. Ezra
YMP Support Project Manager
EG&G Energy Measurements, Inc.
MS V-02
P.O. Box 1912
Las Vegas, NV 89125

1 R. E. Jackson, Program Manager
Roy F. Weston, Inc.
955 L'Enfant Plaza, Southwest
Washington, DC 20024

1 Technical Information Center
Roy F. Weston, Inc.
955 L'Enfant Plaza, Southwest
Washington, DC 20024

1 D. Hedges, Vice President, Quality Assurance
Roy F. Weston, Inc.
4425 Spring Mountain Road, Suite 300
Las Vegas, NV 89102

1 D. L. Fraser, General Manager
Reynolds Electrical & Engineering Co.
Mail Stop 555
P.O. Box 98521
Las Vegas, NV 89193-8521

1 R. F. Pritchett
Technical Project Officer for YMP
Reynolds Electrical & Engineering Co.
MS 408
P.O. Box 98521
Las Vegas, NV 89193-8521

1 B. W. Colston
President/General Manager
Las Vegas Branch
Raytheon Services Nevada
MS 416
P.O. Box 95487
Las Vegas, NV 89193-5487

1 R. L. Bullock
Technical Project Officer for YMP
Raytheon Services Nevada
Suite P250, MS 403
101 Convention Center Dr.
Las Vegas, NV 89109

1 R. E. Lowder
Technical Project Officer for YMP
MAC Technical Services
101 Convention Center Drive
Suite 1100
Las Vegas, NV 89109

1 Paul Eslinger, Manager
PASS Program
Pacific Northwest Laboratories
P.O. Box 999
Richland, WA 99352

1 A. T. Tamura
Science and Technology Division
Office of Scientific and Technical Information
U.S. Department of Energy
P.O. Box 62
Oak Ridge, TN 37831

1 Carlos G. Bell, Jr.
Professor of Civil Engineering
Civil and Mechanical Engineering Department
University of Nevada, Las Vegas
4505 South Maryland Parkway
Las Vegas, NV 89154

1 C. F. Costa, Director
Nuclear Radiation Assessment Division
U.S. Environmental Protection Agency
Environmental Monitoring Systems Laboratory
P.O. Box 93478
Las Vegas, NV 89193-3478

1 ONWI Library
Battelle Columbus Laboratory
Office of Nuclear Waste Isolation
505 King Avenue
Columbus, OH 43201

1 T. Hay, Executive Assistant
Office of the Governor
State of Nevada
Capitol Complex
Carson City, NV 89710

3 R. R. Loux, Jr.
Executive Director
Nuclear Waste Project Office
State of Nevada
Evergreen Center, Suite 252
1802 North Carson Street
Carson City, NV 89710

1 C. H. Johnson
Technical Program Manager
Nuclear Waste Project Office
State of Nevada
Evergreen Center, Suite 252
1802 North Carson Street
Carson City, NV 89710

1 John Fordham
Water Resources Center
Desert Research Institute
P.O. Box 60220
Reno, NV 89506

1 Dr. Martin Mifflin
Water Resources Center
Desert Research Institute
2505 Chandler Avenue, Suite 1
Las Vegas, NV 89120

1 Eric Anderson
Mountain West Research-Southwest Inc.
2901 N. Central Ave. #1000
Phoenix, AZ 85012-2730

1 Department of Comprehensive Planning
Clark County
225 Bridger Avenue, 7th Floor
Las Vegas, NV 89155

1 Planning Department
Nye County
P.O. Box 153
Tonopah, NV 89049

1 Lincoln County Commission
Lincoln County
P.O. Box 90
Pioche, NV 89043

5 Judy Foremaster
City of Caliente
P.O. Box 158
Caliente, NV 89008

1 Economic Development Department
City of Las Vegas
400 East Stewart Avenue
Las Vegas, NV 89101

1 Community Planning & Development
City of North Las Vegas
P.O. Box 4086
North Las Vegas, NV 89030

1 Director of Community Planning
City of Boulder City
P.O. Box 367
Boulder City, NV 89005

1 Commission of the European
Communities
200 Rue de la Loi
B-1049 Brussels
BELGIUM

2 M. J. Dorsey, Librarian
YMP Research and Study Center
Reynolds Electrical & Engineering
Co., Inc.
MS 407
P.O. Box 98521
Las Vegas, NV 89193-8521

1 Amy Anderson
Argonne National Laboratory
Building 362
9700 So. Cass Ave.
Argonne, IL 60439

1 Steve Bradhurst
P.O. Box 1510
Reno, NV 89505

1 Phillip Niedzeilski-Eichner
13013 Lee Jackson Highway
Fairfax, VA 22033

1 Vernon Poe
P.O. Box 1026
Hawthorne, NV 89415

1 Jason Pitts
Lincoln County Courthouse
Pioche, NV 89043

1 Michael L. Baughman
35 Clark Road
Fiskdale, MA 01518

1 Glenn Van Roekel
Director of Community Development
P.O. Box 158
Caliente, NV 89008

1 Ray Williams, Jr.
P.O. Box 10
Austin, NV 89310

1 Leonard J. Fiorenzi
P.O. Box 257
Eureka, NV 89316

1 Brad Mettam
P.O. Box 539
Goldfield, NV 89013

1 Bjorn Selinder
190 W. First St.
Fallon, NV 89406

1 Charles Thistlethwaite, AICP
Associate Planner
Planning Department
Drawer L
Independence, CA 93526

1 Dr. Roger Kasperson
CENTED
Clark University
950 Main Street
Worcester, MA 01610

1 Robert E. Cummings
Engineers International, Inc.
P. O. Box 43817
Tucson, AZ 85733-3817

1 Dr. Jaak J. K. Daemen
University of Nevada
Mackay School of Mines
Reno, NV 89557-0139

1 Department of Comprehensive Planning
Clark County
225 Bridger Avenue, 7th Floor
Las Vegas, NV 89155

1 Economic Development Department
City of Las Vegas
400 East Stewart Avenue
Las Vegas, NV 89109

1 Planning Department
Nye County
P. O. Box 153
Tonopah, NV 89049

1 Director of Cummunity Planning
City of Boulder City
P. O. Box 367
Boulder City, NV 89005

1 Commission of the European Communities
200 Rue de la Loi
B-1049 Brussels, Belgium

1 Lincoln County Commission
Lincoln County
P. O. Box 90
Pioche, NV 89043

1 Community Planning & Development
City of Las Vegas
P. O. Box 4086
North Las Vegas, NV 89030

1 City Manager
City of Henderson
Henderson, NV 89015

1 ONWI Library
Battelle Columbus Laboratory
Office of Nuclear Waste Isolation
505 King Avenue
Columbus, OH 43201

1 Librarian
Los Alamos Technical Associates, Inc.
P. O. Box 410
Los Alamos, NM 87544

1 Loren Lorig
Itasca Consulting Group, Inc.
1313 5th Street SE, Suite 210
Minneapolis, MN 55414

1 James K. Lein
Department of Geography
122 Clippinger Laboratories
Ohio University
Athens, OH 45701-2979

20 Geomatrix Consultants, Inc.
100 Pine Street, Suite 1000
San Francisco, CA 94111

1	6300	D. E. Miller
10	6301	J. D. Gibson
1	6302	T. E. Blejwas
1	6312	F. W. Bingham
1	6313	L. S. Costin
1	6316	R. P. Sandoval
2	6318	R. J. Macer for 100/1232842/SAND90-2491/QA
1	6319	R. R. Richards
5	3141	S. A. Landenberger
8	3145	Document Processing for DOE/OSTI
3	3151	G. C. Claycomb
20	6341	WMT Library
1	6410	D. A. Dahlgren
1	8523-2	Central Technical Files

THIS PAGE IS AN OVERSIZED DRAWING OR FIGURE,

THAT CAN BE VIEWED AT THE RECORD TITLED:

PLATE 1

"PRELIMINARY GEOLOGIC MAP OF THE MIDWAY VALLEY AREA FROM SCOTT AND BONK, 1984"

WITHIN THIS PACKAGE

D-01A (IMAGE 1 OF 2)
D-01B (IMAGE 2 OF 2)

THIS PAGE IS AN OVERSIZED DRAWING OR FIGURE,

THAT CAN BE VIEWED AT THE RECORD TITLED:

PLATE 2

"Surficial Deposits in the Midway Valley Area from Swadley, Hoover, and Rosholt, 1984"

WITHIN THIS PACKAGE..

D-02

THIS PAGE IS AN OVERSIZED DRAWING OR FIGURE,

THAT CAN BE VIEWED AT THE RECORD TITLED:

PLATE 3

"Drillhole and Trench Locations in the Midway Valley Area from Holmes & Narver, Inc., 1988"

WITHIN THIS PACKAGE..

D-03

THIS PAGE IS AN OVERSIZED DRAWING OR FIGURE,

THAT CAN BE VIEWED AT THE RECORD TITLED:

PLATE 4

"Geophysical Survey Lines and Features Interpreted from Geophysical Data in Midway Valley"

WITHIN THIS PACKAGE..

D-04

SAND90-2491

The number in the lower right-hand corner is an accession number used for Office of Civilian Radioactive Waste Management purposes only. It should not be used when ordering this publication.

NNA.910709.0001

Org.	Bldg.	Name	Rec'd by	Org.	Bldg.	Name	Rec'd by

Sandia National Laboratories